Exploring gold glyconanoparticles as multivalent carrier for specific molecules involved in HIV-1 infection

Paolo Di Gianvincenzo

2013

Exploring gold glyconanoparticles as multivalent carrier for specific molecules involved in HIV-1 infection

Paolo Di Gianvincenzo

Glyco-Nanotechnology Laboratory, Biofuntional Nanomaterials Unit, CIC biomaGUNE

2013

AUTORIZACION DEL/LA DIRECTOR/A DE TESIS

PARA SU PRESENTACION

Prof. Soledad Penadés Ullate con N.I.F.02683273R como Directora de la Tesis Doctoral: Exploring gold glyconanoparticles as multivalent carrier for specific molecules involved in HIV-1 infection, realizada en el Glyconanotechnology Laboratory en el Centro de Investigacíon Cooperativa en Biomateriales (CIC biomaGUNE) por el Doctorando Don Paolo Di Gianvincenzo, autorizo la presentación de la citada Tesis Doctoral, dado que reúne las condiciones necesarias para su defensa.

En _____ a _____ de _____ de _____

EL/LA DIRECTOR/A DE LA TESIS

Fdo.: Soledad Penadés Ullate

Universidad **Euskal Herriko**
del País Vasco **Unibertsitatea**

CONFORMIDAD DEL DEPARTAMENTO

El Consejo del Departamento de Ciencia y tecnologia de Polimeros en reunión celebrada el día ____de _____ de 2013 ha acordado dar la conformidad a la admisión a trámite de presentación de la Tesis Doctoral titulada: Exploring gold glyconanoparticles as multivalent carrier for specific molecules involved in HIV-1 infection, dirigida por Prof. Soledad Penadés Ullate y presentada por Don Paolo Di Gianvincenzo ante este Departamento.

En _____a ____de _____de ____

Vº Bº DIRECTOR/A DEL DEPARTAMENTO   SECRETARIO/A DEL DEPARTAMENTO

Fdo.: _____   Fdo.: _____

ACTA DE GRADO DE DOCTOR O DOCTORA
ACTA DE DEFENSA DE TESIS DOCTORAL

DOCTORANDO DON Paolo Di Gianvincenzo

TITULO DE LA TESIS: Exploring gold glyconanoparticles as multivalent carrier for specific molecules involved in HIV-1 infection

El Tribunal designado por la Subcomisión de Doctorado de la UPV/EHU para calificar la Tesis Doctoral arriba indicada y reunido en el día de la fecha, una vez efectuada la defensa por el doctorando y contestadas las objeciones y/o sugerencias que se le han formulado, ha otorgado por_____la calificación de:

    unanimidad ó mayoría

APTO o NO APTO

Idioma/s de defensa (en caso de más de un idioma, especificar apartados o porcentaje defendido en cada idioma): _____

En _____a _____de _____de _____

       EL/LA PRESIDENTE/A,   EL/LA SECRETARIO/A,

Fdo.:   Fdo.:

Dr/a: _____   Dr/a: _____

VOCAL 1º,   VOCAL 2º,   VOCAL 3º,

Fdo.:   Fdo.:   Fdo.:

Dr/a: _____ Dr/a:_____ Dr/a:_____

EL/LA DOCTORANDO/A,

Fdo.: _____

AUTORIZACION DEL PONENTE DE TESIS

PARA SU PRESENTACION

Prof. Dr/a. Isabel Goñi Echave, como Ponente de la Tesis Doctoral: Exploring gold glyconanoparticles as multivalent carrier for specific molecules involved in HIV-1 infection, realizada en el realizada en el Glyconanotechnology Laboratory en el Centro de Investigacíon Cooperativa en Biomateriales (CIC biomaGUNE) por el Doctorando Don Paolo Di Gianvincenzo, y dirigida por la Prof. Soledad Penadés Ullate autorizo la presentación de la citada Tesis Doctoral, dado que reúne las condiciones necesarias para su defensa.

En _____ a _____ de _____ de _____

EL PONENTE DE LA TESIS

Fdo.: _____

ABSTRACT

The infection of the human immunodeficiency virus (HIV) is the cause of AIDS and is one of the greatest infectious diseases ever seen. HIV infects cells of the human immune system such as helper T cells (specifically $CD4^+$ T cells), macrophages, and dendritic cells. The HIV membrane is decorated with proteins spikes. The envelope glycoprotein (Env) spikes are formed by three transmembrane gp41 non-covalently bound to three gp120, a highly glycosilated protein. The Env spikes initiate infection of host cells and are targets for vaccine development. The molecular mechanism of the entry process, where CD4 receptor, CCR5/CXCR4 co-receptors and the viral envelop glycoprotein gp120 are involved, is still not well understood, however, it was demonstrated that HIV entry is characterized by binding of multiple copies of Env, CD4 and CCR5 or CXCR4. In this thesis we use gold nanoparticles, biofunctionalized with carbohydrates (glyconanoparticles, GNPs) to mutimerize selected molecules that may interfere with concrete steps of HIV infection. Three different families of GNPs were prepared. Sulphated gold glyconanoparticles (SO_4-GNPs), able to bind positive charged amino acids of gp120, were prepared and characterized. We demonstrate that depending on the sulphate ligand density, these nanoparticles can bind gp120 with high affinity as shown in SPR-based experiments and neutralize the *in vitro* HIV infection of T-lymphocytes in the nanomolar range. A miniprotein that mimics the CD4 receptor (miniCD4) and inhibits the HIV entry process was multimerized on GNPs (miniCD4-GNPs). The conformation of miniCD4 did not change once linked to the GNPs as showed by circular dichroism (CD) experiments. However, the multivalent presentation of miniCD4 on GNP did not increase the activity of miniCD4. Indeed, HIV-1 neutralization assays did not show improved IC50 values for the miniCD4-GNPs respect to the free miniCD4, probably because the distance between the miniCD4 on the GNPs do not perfectly match the distance between CD4 binding site on HIV Env. An important peptide of gp120, the V3 variable loop, was also multimerized on GNPs. We found that GNPs bearing only glucose and carboxylic ending linkers are able to modulate the conformation of V3 peptide (random coil) to obtain V3-GNP constructs with well defined conformations (α-helix or β-strand) as showed by CD. Studies by SPR showe that only the V3β-GNP are able to bind mAb the specific anti-V3 antibody 447-52D. HIV neutralization experiments show that V3-GNP were active only at high concentration (100 ug/ml). However, a preliminary immunization study with V3β-GNP on mice shows that mAb contained in mice sera are able to recognize V3β-GNP. A more extensive immunization study will be performed immunizing rabbits with different kind of V3-GNP.

RESUMEN TESIS

El síndrome de inmunodeficiencia adquirida (SIDA), es una enfermedad del sistema inmunológico humano causada por el virus de la inmunodeficiencia humana (VIH). La respuesta inmune natural contra el VIH casi nunca es eficaz. Los medicamentos contra el VIH han prolongado la vida de millones de personas, pero la epidemia sigue su curso y, todavía no se entienden por completo los mecanismos que conducen a la patogénesis del SIDA.

La membrana viral está decorada con proteínas de la envoltura (Env) que inician la infección de las células huésped, y son dianas para el desarrollo de vacunas. La Env del VIH es una de las estructuras más N-glicosiladas que se encuentran en la naturaleza. Alrededor del 50% de su peso corresponde a glicanos de tipo "high mannose" ($Man_{5-9}GlcNAc_2$). La Env está formada por seis glicoproteínas: tres transmembranales gp41 unidas de forma no covalente a tres gp120.

El VIH infecta principalmente las células del sistema inmune humano, tales como células auxiliares T (concretamente células T CD4+), macrófagos, y células dendríticas. El VIH consigue entrar en las células huésped mediante el uso de proteínas de la envoltura (Env) que decoran la membrana viral. El cambio conformacional de gp120 inducido por la unión a los receptores CD4 el péptido V3, uno de las regiones variables de la gp120, para interaccionar con los co-receptores CCR5 o CXCR4. CCR5 y CXCR4 son receptores acoplados a la proteína G (GPCR) y son responsables de la transmisión del VIH-1 en los primeros años de la infección, y en las etapas finales de la infección, respectivamente. La unión al co-receptor V3 induce un segundo cambio conformacional en la gp120 que conduce a la inserción de la gp41 en la membrana de la célula diana y que permite la fusión de la membrana viral con la celular. Los fenómenos de fusión y formación de poros entre las dos membranas son aún poco conocidos.

Otros mecanismos de infección utilizan la unión de la proteína gp120 del VIH a la lectina DC-SIGN, expresada en células dendríticas, a los dominios de glicoesfingolipidos que contienen β-galactosilceramida (β-GalCer), y al heparán sulfato de los proteoglicanos de la membrana celular (HSPGs). Estas interacciones facilitan el reclutamiento inicial del virus a las células diana. El VIH también puede utilizar una vía endocítica alternativa para entrar en las células huésped.

Esta tesis se ha centrado en el proceso de entrada del VIH, en el cual están involucrados el receptor CD4, los co-receptores CCR5/CXCR4 y la proteina de envoltura viral gp120. Cualquier enfoque con el objetivo de controlar y detener la entrada del virus debería tener en cuenta estas biomoléculas y las que el propio virus utiliza para interaccionar con ellas. Una cuestión importante a tener en cuenta en el estudio de la infección por VIH es el número de Env, CD4 y co-receptores CCR5/CXCR4 que están involucrados en el proceso de entrada del VIH. Existen evidencias de que la unión del complejo de gp120/gp41 a CD4 y los co-receptores es cooperativa y requiere de múltiples CCR5, tres eventos de unión CD4 y el conjunto de múltiple de gp120/gp41 (de 5 a 8) para formar un poro de fusión de forma efectiva. Esta tesis se ha centrado en (i) tirosinas sulfato del co-receptor implicado en la unión con el peptido V3, (ii) en los receptores CD4 y (iii) en el peptido V3 como objetivos para desarrollar herramientas polivalentes basadas en nanoparticulas de oro capaces de interferir con el proceso de entrada del VIH. Estas nanoparticulas de oro se han recubierto con grupos sulfato (mimetizando las tirosinas sulfato del co-receptor) o miniproteínas que mimetizan el receptor CD4 (miniCD4) para neutralizar el virus, y el péptido V3 para bloquear la interacción del virus con el co-receptor CCR5 o CXCR4. Se espera contribuir a la comprensión del papel de la presentación multivalente de las moléculas seleccionadas en la infección por el VIH con el fin de combatirlo más eficazmente.

En la ultima década se han preparado muchos sistemas multivalentes sintéticos, y algunos de ellos han sido estudiados como agentes anti-VIH o como inmunógenos del VIH. Se han multimerizado péptidos, hidratos de carbono y fármacos mediante el uso de plataformas con más de dos sitios de anclaje. También se ha sugerido que la presentación repetitiva de un epítopo en el inmunógeno puede inducir una respuesta inmune más fuerte, probablemente porque tales inmunógenos pueden desencadenar oligomerización de los receptores de células B que reconocen el epítopo.

La nanotecnología ha ampliado las posibilidades de crear nuevas plataformas multivalentes y, hoy en día, juega un papel clave en el campo de la biomedicina. El diagnóstico, tratamiento, administración de fármacos y la ingeniería de tejidos son las principales áreas biomédicas en las que la nanotecnología ofrece potenciales beneficios para la salud. Las nanopartículas metálicas presentan propiedades únicas magnéticas, eléctricas, ópticas, mecánicas y químicas, que pueden ser modificadas mediante el control del tamaño, la forma y la variación de los materiales del núcleo.

Estas propiedades únicas y la utilidad de las nanopartículas se deben a una serie de atributos que incluyen su tamaño similar a biomoléculas (proteínas y ácidos polinucleicos).

Desde el año 2000, nuestro laboratorio ha desarrollado nanopartículas metálicas, biofuncionalizadas con carbohidratos (gliconanopartículas, GNP) para estudiar las interacciónes mediadas por carbohidratos y explorar sus posibles aplicaciones en el área emergente de la nanomedicina. Las GNPs consisten en un núcleo metálico con monocapas auto-ensambladas de glicoconjugados unidos covalentemente. Las GNPs y la metodología desarrollada para prepararlas (Gliconanotecnología) han llevado al desarrollo de GNPs de oro multivalentes, biocompatibles y multifuncionales. Han demostrado ser herramientas polivalentes de gran utilidad, para estudiar las interacciones mediadas por hidratos de carbono. Las GNPs son nanoclusteres de oro biofuncionales y solubles en agua con una composición bien definida que pueden presentar un gran número de glicanos sobre su superficie (100 moléculas sobre un núcleo de oro de 2 nm de diámetro) y permitir la combinación de diferentes moléculas de una manera controlada. Las GNPs recubiertas con oligomanosidos de los glicanos de la gp120 han demostrado ser capaces de inhibir la infección de células T que ocurre a través de las células dendriticas infectadas (infección en trans).

Por tanto, las GNPs representan una interesante herramienta multivalente en el estudio de las bases moleculares de la infección por VIH:
i) Se ha demostrado que la mayor parte de las uniónes relacionada con la Env (DC-SIGN, CD4, CCR5/CXCR4) son multivalentes,
ii) Las GNPs pueden ser recubiertas con diferentes moléculas (péptidos, hidratos de carbono, fármacos, etc...) que pueden interferir con etapas concretas de la infección por VIH. Estas moléculas pueden actuar en conjunto de forma sinérgica en un mismo fenómeno de unión o pueden tener diferentes funciones en pasos secuenciales biológicos (por ejemplo, dirigiéndose a células específicas y en la posterior liberación de los compuestos activos).
En este trabajo hemos diseñado y preparado GNPs oro que incorporan otras moléculas capaces de interferir con el ciclo de vida del VIH-1.

Hemos seleccionado moléculas (derivados sulfatados y miniCD4) que se prevé reduzcan la entrada del VIH en las células huésped mediante el bloqueo de determinadas regiones de la gp120, mientras que otras como el péptido V3 bloquea dominios de unión de HIV a co-receptores. Se espera que la multimerización de estas

moléculas sobre las GNPs aumente su actividad. Otro aspecto de este trabajo se relaciona con la respuesta inmune de las GNPs. El péptidos V3 de la gp120 es capaz de provocar la producción de anticuerpos anti-V3 ampliamente neutralizantes. Por este motivo pensamos que varias copias del V3 sobre las GNPs serían también capaces de provocar anticuerpos contra el V3.

Cada capítulo de esta tesis está dedicado a la preparación de GNPs con cada una de las moléculas seleccionadas (sulfatos, miniCD4 y V3) y a la exploración de sus propiedades antivirales e imunogenicas.

En el capítulo 1, se prepararon y caracterizaron gliconanopartículas de oro sulfatadas (SO_4-GNP), capaces de unirse a los aminoácidos de carga positiva del V3. La interacción de SO_4-GNP con gp120 fue estudiada por resonancia de plasmón de superficie (SPR). Para investigar la captación celular de SO_4-GNP se llevó a cabo un estudio preliminar con células Raji y gliconanopartículas de oro recubiertas con grupos sulfato y marcadas con fluoresceína (SO_4-GNP-FITC). Se realizaron experimentos de neutralización de VIH-1 en colaboración con el Dr. Alcamí, (Unidad Inmunopatogénesis SIDA, Instituto de Salud Carlos III (ISCIII), Madrid), socio del proyecto CHAARM. Dependiendo de la densidad de ligandos, estas GNPs se pueden unir a la gp120 con elevada afinidad, tal y como se muestra en los experimentos de SPR, y pueden neutralizar el VIH en la infección directa in vitro de los linfocitos T en concentraciones nanomolares. Se ha demostrado que un 50% de densidad de ligandos sulfatados sobre nanopartículas de ~ 2 nm es suficiente para conseguir actividad anti-VIH y que esta actividad es comparable con la actividad obtenida con GNPs completamente recubiertas con ligandos sulfatados, abriendo la posibilidad de anclar otras moléculas anti-VIH en el mismo clúster de oro.

En el capítulo 2, se prepararon GNPs que contienen péptidos miniCD4 (proporcionado por el Dr. Loic Martin). Estos péptidos mimetizan el receptor CD4 de las celulas T. Se espera que las miniCD4-GNPs se unan a la gp120 del VIH y compitan con la unión de gp120 a los receptores celulares CD4. Se prepararon tres miniCD4-GNPs diferentes: sólo con miniCD4, con miniCD4 y colesterol (miniCD4-GNP-Chol) y con miniCD4 y ligandos sulfatados (miniCD4-GNP-SO_4). Se estudió la estructura del miniCD4 en las tres GNPs por dicroísmo circular (DC). La conformación del miniCD4 no cambió una vez unido a las GNPs según demostraron los experimentos de DC. Sólo se encontró una ligera desviación en el espectro de DC de las miniCD4-GNP-SO_4. También se llevaron a cabo experimentos de SPR para estudiar la unión de miniCD4-GNPs a gp120. Los miniCD4 en las GNPs se unen a la gp120. Por otra parte, los experimentos

de neutralización del VIH, que se realizaron en el laboratorio de la Dra. Elisa Vicenzi (Hospital San Raffaele (HSR) Milán, Italia), con las miniCD4-GNPs no dieron mejores valores de IC50 con respecto a los miniCD4 libres. Todos estos resultados demuestran claramente que el miniCD4 ha sido anclado con éxito a las GNPs sin ninguna pérdida de su actividad. Desafortunadamente, no se observó ningúna mejora de su actividad antiviral debida al efecto multivalente. El problema radica probablemente en que la distancia entre los miniCD4 sobre las GNPs no coinciden perfectamente con la distancia entre los sitios de la Env del VIH unión CD4. Los estudios futuros podrían estar dirigidos a la preparación de miniCD4-GNPs multivalente con ligandos de distinta longitud.

En los primeros dos capítulos se presentan GNPs que tienen a la gp120 como diana. Una estrategia alternativa es preparar GNPs que se unan y bloqueen los receptores o co-receptores del VIH en la célula huésped. En el capítulo 3, se presenta la preparación y caracterización de las GNPs que presentan el péptido V3 (V3-GNPs). Hemos demostrado que GNPs funcionalizadas con glucosa y ligandos terminados en grupo carboxílicos (GNP1), son capaces de modular la conformación del péptido V3. Dependiendo de las condiciones experimentales, el péptido V3 (que presenta una conformacion esencialmente aleatoria) en presencia de las GNP1 adopta una conformación predominante de α-hélice (V3α-GNP1) o β-strand (V3β-GNP1), según lo observado por dicroísmo circular (DC). Las V3-GNPs también se caracterizaron por ^{1}HRMN, electroforesis, y Z-potencial. Se estudió la interacción de V3-GNPs con el anticuerpo anti-V3 447-52D por SPR y se observó que sólo V3β-GNPs son capaces de unirse a dicho anticuerpo. Se prepararon también GNPs funcionalizadas con glucosa, ligandos terminados en grupo carboxílicos y disacárido de mannosa (V3β-GNP2). Las V3β-GNP1 y las V3β-GNP2 mostraron una unión similar con el anticuerpo 447-52D. Experimentos de neutralización del VIH con V3-GNP1 y GNP1 mostraron actividad de neutralización sólo en una concentración elevada (100 μg/ml). Por otra parte, a esta concentración, la inhibición por parte de V3-GNP1 es comparable a GNP1, concluyendo que las V3-GNPs no son un buen sistema para bloquear la entrada del VIH. Sin embargo, resultados mas esperanzadores se estan obteniendo en un estudio preliminar de inmunización de ratones con V3β-GNP1. En este estudio se ha observado que anticuerpos obtenidos del suero de los ratones inmunizados, reconocen V3β-GNP1, aunque con el fin de entender el papel desempeñado por GNP1 se necesitan nuevos experimentos de inmunización. Futuros experimentos de inmunización en conejos proporcionaran una mayor cantidad de suero que permitirá un estudio más amplio de los anticuerpos presentes.

LIST OF ABBREVIATIONS

AcOH	acetic acid
AIDS	Acquired immunodeficiency syndrome
APC	antigen-presenting cells
bNAb	broadly neutralizing antibody
BSA	Bovine serum albumin
CD4	cluster of differentiation 4
CHAARM	Combined Highly Active Anti-Retroviral Microbicides
CLR	C-type lectin receptors
CRA	chemokine receptor antagonist
CTB	cholera toxin B
DC	dendritic cell
DC-SIGN	Dendritic Cell-Specific Intercellular adhesion molecule-3-Grabbing Non-integrin
DMAP	4-dimethylaminopyridine
DNA	Deoxyribonucleic acid
EDC	ethyl-3-(3-(dimethylamino)-propyl)carbodiimide
EMPRO	European Microbicides Project
Env	HIV envelope glycoprotein
ELISA	Enzyme-Linked ImmunoSorbent Assay
EtOH	Ethanol
Fab	fragment antigen binding
GNP	glyconanoparticle
HAART	highly active antiretroviral therapy
HIV	human immunodeficiency virus
HPLC	High-performance liquid chromatography
HRP	horseradish peroxidase
IC_{50}	half maximal inhibitory concentration
Ig	immunoglobulin
K_D	Dissociation constant
KDa	kilodalton
LPE	ligand place exchange
MeOH	Methanol
MW	molecular weight
NHS	*N*-hydroxysuccinimide
NMR	Nuclear magnetic resonance

NNRTI	non-nucleoside RT inhibitor
PBL	peripheral blood leucocytes
PBMC	peripheral blood mononuclear cell
PBS	Phosphate buffered saline
PI	protease inhibitor
$PySO_3$	Pyridine sulphate
RNA	Ribonucleic acid
RT	reverse transcriptase
RU	response unit
SAM	self-assembled monolayer
SPR	Surface Plasmon Resonance
TEG	Tetraethylenglycol
TEM	Transmission electron microscopy
TMB	3,3′,5,5′-Tetramethylbenzidine
TRIS	Tris(hydroxymethyl)aminomethane buffered saline
UV	ultraviolet

CONTENTS

A mamma, papá, Silvia e Lander

ACKNOWLEDGEMENTS

I want to thank first my supervisor, Soledad, who gave me the opportunity to develop this research project. I would also like to thank all the present and former members of the laboratory of glyconanotechnology for their help. Thanks to all the scientific and no-scientific staff of CIC biomaGUNE.

I would also like to thank all other contributors to this thesis: Pepe Alcamí and Luismi Bedoya, from Instituto de Salud Carlos III (ISCIII) in Madrid and Elisa Vicenzi, Hospital San Raffaele (HSR), Milan, for HIV neutralization assays, Loic Martin, for the miniCD4 peptide and Stephan Grzesiek and Sébastien Morin for the SPR study with the coreceptor CCR5. An important part of this thesis wouldn't have been possible without their work.

Me gustaría agradecer especialmente a Lander su paciencia, buen humor y por estar a mi lado durante todos estos años. También quisiera agradecer de corazón a mis amigos de Donosti los buenos momentos que me han hecho pasar y el haberme aguantado pacientemente en las malas épocas.

Grazie a tutti i miei amici di Milano, a quelli che son passati da Donosti a salutarmi, e a quelli che verranno in futuro. Grazie perché tutte le volte che torno in Italia é come se non fossi mai partito. Un grazie speciale alla mia famiglia, per l'amore, la pazienza e i buoni consigli. Grazie per esserci sempre, anche da lontano, e per appoggiarmi in tutte le mie scelte. Questa tesi é anche vostra.

INTRODUCTION

INTRODUCTION

The story begins more than 25 years ago, when the initial clinical observations of a new alarming epidemic were made. In June 1981, clinicians in the United States first reported a number of cases of Pneumocystis carinii in homosexual men.[1] Subsequently, the first cases of what would later be known as AIDS were observed in France. At the time, I was working at the Institut Pasteur with Luc Montagnier and Jean-Claude Chermann. In December 1982, we were contacted by clinicians in France who provided us with a biopsy of a lymph node from an AIDS patient, with the aim of isolating the etiological agent causing the disease.

Francois Barré-Sonoussi, Nobel Lecture, 2009

The isolation of this new human retrovirus (at the time known as LAV, lymphoadenopathy-associated virus) was first reported and published in May 1983.[2] In 1984, Gallo and colleagues and Levy and co-workers published reports confirming the identification of the causative agent of the acquired immunodeficiency syndrome (AIDS).[3] [4] The infection of the human immunodeficiency virus (HIV) is the cause of AIDS and is one of the greatest infectious diseases ever seen.[5] Since the discovery of the virus, scientists have learnt that HIV infection is much more complex than they initially thought, and the mechanisms leading to AIDS pathogenesis are today still not entirely understood.[6]

In 2010 around 33 million people were living with HIV worldwide and every year around 2-3 million people become HIV-infected.[7]

---

[1] Gottlieb, M. S., Schroff, R., Schanker, H. M., Weisman, J. D., Fan, P. T., Wolf, R. A., Saxon, A., (1981). Pneumocystis carinii pneumonia and mucosal candidiasis in previously healthy homosexual men: evidence of a new acquired cellular immunodeficiency: *N. Engl. J. Med.*, **305**, 1425-1431.

[2] Barre-Sinoussi, F., Chermann, J. C., Rey, F., Nugeyre, M. T., Chamaret, S., Gruest, J., Dauguet, C., Axler-Blin, C., Zinet-Brun, F. V., Rouzioux, C., Rozenbaum, W., and Montagnier, L. (1983). Isolation of a T-lymphotropic retrovirus from a patient at risk for acquired immune deficiency syndrome (AIDS): *Science*, **220**, 868-871.

[3] Gallo, R. C., Salahuddin, S. Z., Popovic, M., Shearer, G. M., Kaplan, M., Haynes, B. F., Palker, T. J., Redfield, R., Oleske, J., Safai, B., White, G., Foster, P., and Markham, P. D. (1984). Frequent detection and isolation of cytopathic retroviruses HTLV-III, from patients with AIDS and at risk for AIDS: *Science*, **224**, 500-503.

[4] Levy, J. A., Hoffman, A. D., Kramer, S. M., Landis, J. A., Shimabukuro, J. M., and Oshiro, L. S. (1984). Isolation of lymphocytopathic retroviruses from San Francisco patients with AIDS: *Science*, **225**, 840-842.

[5] Fauci, A. S. (2003). HIV and AIDS: 20 years of science. *Nat. Med.* **9**, 839-843.

[6] Barré-Sinoussi, F. (2009). HIV: A discovery opening the road to novel scientific knowledge and global health improvement (Nobel Lecture). *Ang. Chem. Int. Ed.* **48**, 32, 5809-5814.

[7] http://www.who.int/hiv/data/fast_facts/en/index.html

HIV-1 and its life cycle

HIV-1 is a lentivirus (family of retrovirus) that can lead to AIDS, a condition in humans in which the immune system begins to fail, leading to life-threatening opportunistic infections. HIV is roughly spherical with a diameter of about 120 nm, around 60 times smaller than a red blood cell. In Figure 1 a schematic of HIV-1 is showed with the envelope glycoproteins, enzymes and proteins.[8]
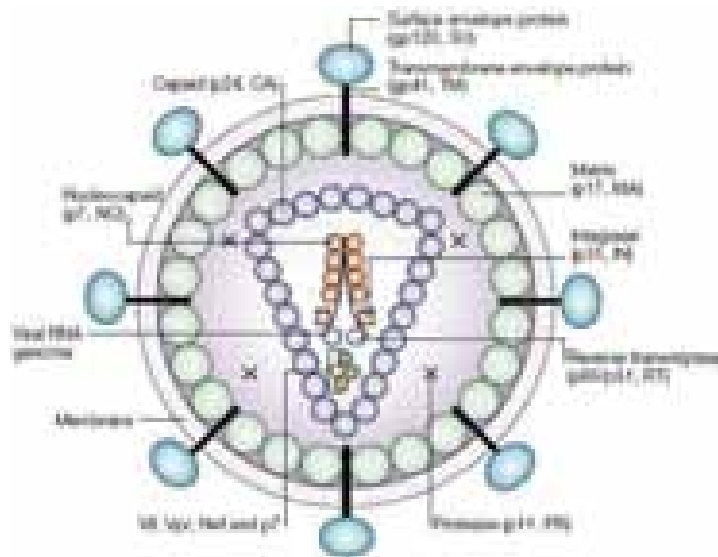

Figure 1. HIV-1. Cartoon of HIV-1 showing the envelope glycoproteins, structural proteins and enzymes.[8]

RNA virus transcribes the Gag, Env and Pol polyproteins. The Gag polyprotein is processed into the matrix protein (MA or p17), the capsid protein (CA or p24) and nucleocapsid protein (NC or p7), which form the inner core of the viral particle. The surface envelope protein glycoprotein 120 (gp120 or SU) and the transmembrane envelope glycoprotein 41 (gp41 or TM) come from the envelope (Env) polyprotein and are the outer membrane proteins of the virus. Processing of the polymerase (Pol) polyprotein yields the enzymes protease (PR), reverse transcriptase (RT) and integrase (IN), which are encapsulated in the core of the inner particle. Vif, Vpr and Nef are accessory proteins.

[8] Robinson, H. L. (2002). New hope for an AIDS vaccine. *Nat. Rev. Immunol.* **2**, 239-250.

The HIV-1 life cycle (Figure 2) begins with the attachment of the virus to the host cell.[9] The principal and the most studied entry pathway is driven by sequential interactions of HIV Env protein and host receptor, CD4, and co-receptor CCR5 or CXCR4 (step 1), followed by fusion of virus and cell membrane (step 2).
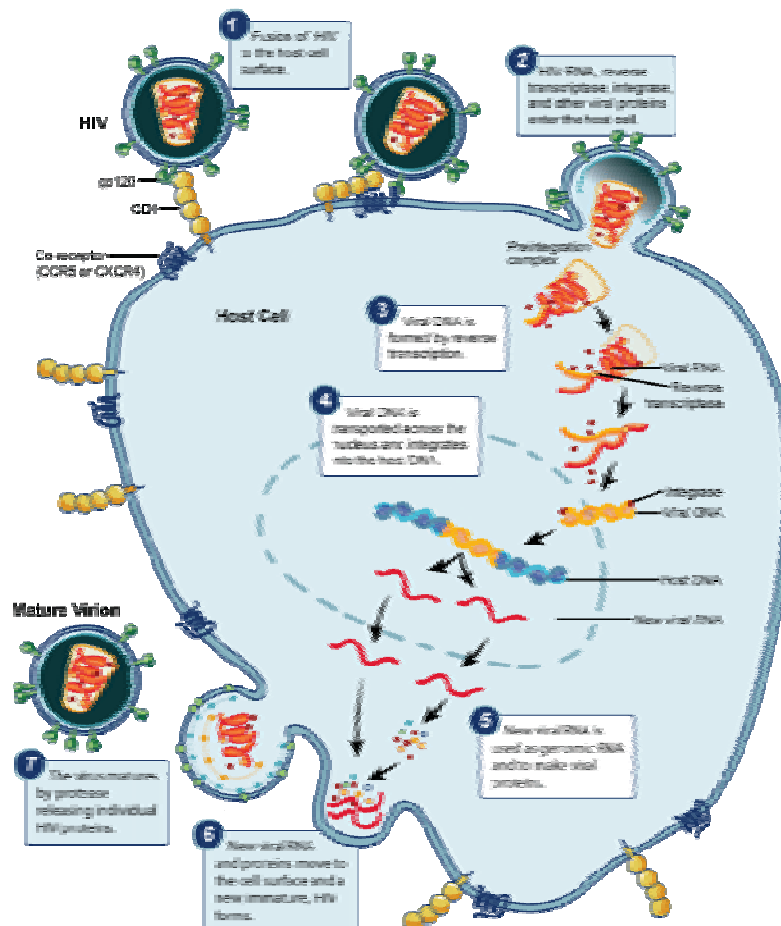
Figure 2. HIV-1 life cycle. 1) HIV first binds to CD4 receptor and a co-receptor on the cell surface and then fuse with the host cell. 2) Release of HIV genetic material into the cell. 3) An HIV enzyme called reverse transcriptase converts the viral RNA into a complementary strand of DNA. 4) Viral DNA is integrated into the host genome using the viral enzyme integrase. 5) New viral RNA and proteins are produced and move to the cell surface. 6) Assembly of new virion. 7) Virus budding and maturation (gag polyprotein is cleaved into matrix, capsid and nucleocapsid proteins).[10]

After membrane fusion, HIV RNA and various enzymes (reverse transcriptase, integrase, ribonuclease, and protease) are injected into the cell (step 3). Viral single-strand RNA is transcribed into double-strand DNA and integrates into the host chromosome (step 4). By using host-cell machineries viral DNA codify the production of

---

[9] Simon, V., and Ho, D. D. (2003). HIV-1 dynamics *in vivo*: implications for therapy. *Nat. Rev. Microbiol.* **1**, 181-190.

[10] http://www.niaid.nih.gov/topics/HIVAIDS/Understanding/Biology/pages/hivreplicationcycle.aspx

viral proteins (step 5). The Env polyprotein (gp160) is cleaved by a cellular protease to obtain gp41 and gp120 and transported to the host cell membrane. The viral proteins assemble at the cell membrane, and the immature viral particle containing the RNA genome and viral enzymes egresses the cell (step 6). After virion budding, proteolytic processing of gag polyproteins produce matrix, capsid and nucleocapsid proteins and leads to a structural rearrangement of the virion and generates a mature viral particle (step 7).

Among all the biochemical steps that characterize HIV-1 life cycle, the entry process (step 1) where CD4 receptor, co-receptors and the viral envelop glycoprotein are involved, have been the object of this thesis.

HIV envelope glycoprotein

Viral membrane is decorated with proteins spikes. Envelope glycoprotein (Env) spikes on HIV initiate infection of host cells and are targets for vaccine development. Env of HIV is one of the most highly N-glycosylated structures found in nature, indeed around 50% of weight are carbohydrates.[11] These oligosaccharides are mainly high-mannose type glycans ($Man_{5-9}GlcNAc_2$) and are conserved across primary isolates and geographically divergent clades (Figure 3).

---

[11] Doores, K. J., C. Bonomelli, D. J. Harvey, S. Vasiljevic, R. A. Dwek, D. R. Burton, M. Crispin, and C. N. Scanlan. (2010). Envelope glycans of immunodeficiency virions are almost entirely oligomannose antigens. *Proc. Natl. Acad. Sci. U.S A.* **107**,13800-13805.
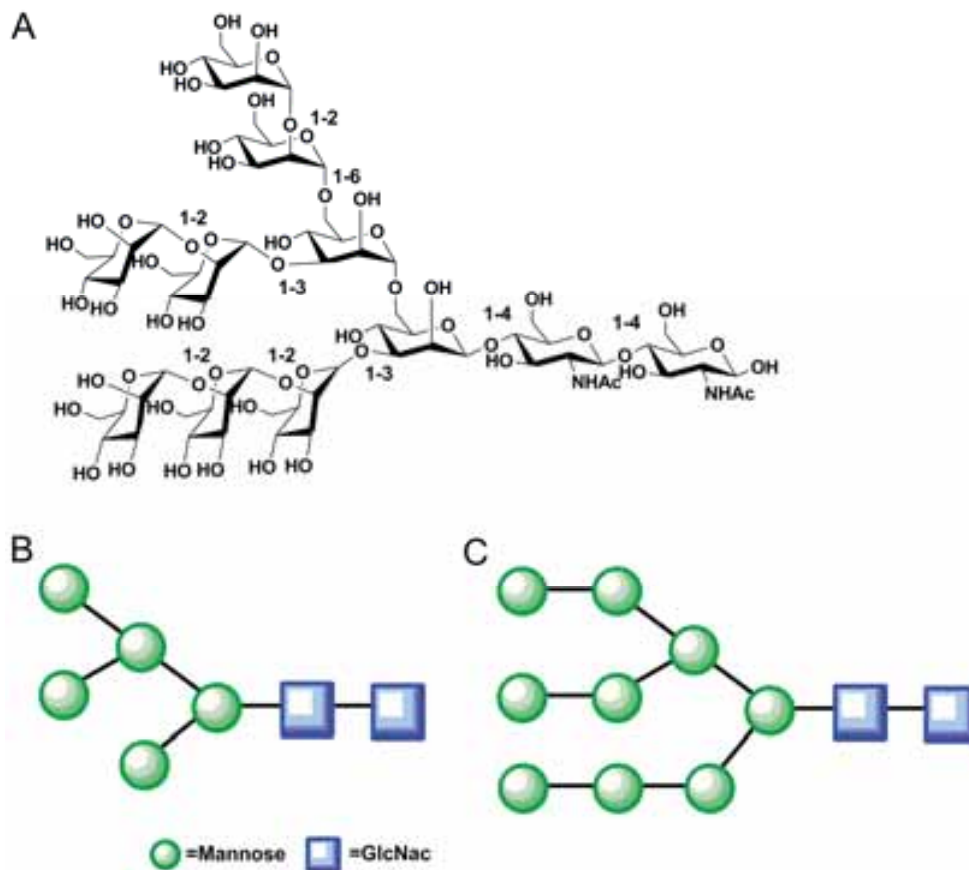
Figure 3. High-mannose type glycans, the most abundant N-glycans of gp120. A) Molecular structure of the undecaoligosaccharide $Man_9GlcNAc_2$. B) Schematic structure of $Man_5GlcNAc_2$ and C) of $Man_9GlcNAc_2$ oligosaccharides that compose the glycan shield of gp120.

Moreover, Manα1→2Man terminating glycans ($Man_{5-9}GlcNAc_2$) are 3-fold more abundant on the native envelope than on the recombinant gp120 monomer. Env protein is formed by three transmembrane gp41 non-covalently bound to three gp120. Both are glycoproteins and the number corresponds to the MW (KDa) of the subunit. Unfortunately, the X-ray crystal structure of complete Env is not available. However, the crystal structure of a deglycosylated gp120, lacking the third variable region, V3 loop, in complex with CD4 and antibody Fab 17b was described for the first time in 1998 (Figure 3A).[12] By using the similar strategy P. Kwong et al. in 2005 were able to crystallize the entire deglycosylated gp120 containing V3 loop (Figure 3B).[13]

---

[12] Kwong, P. D., Wyatt, R., Robinson, J., Sweet, R. W., Sodroski, J., and Hendrickson, W. A. (1998). Structure of an HIV gp120 envelope glycoprotein in complex with the CD4 receptor and a neutralizing human antibody. *Nature*. **393**, 648-659.

[13] Huang, C., Tang, M., Zhang, M., Majeed, S., Montabana, E., Stanfield, R. L., Dimitrov, D. S., Korber, B., Sodroski, J., Wilson, I. A., Wyatt, R., and Kwong, P. D. (2005). Structure of a V3-containing HIV-1 gp120 core. *Science*. **310**, 1025-1028.
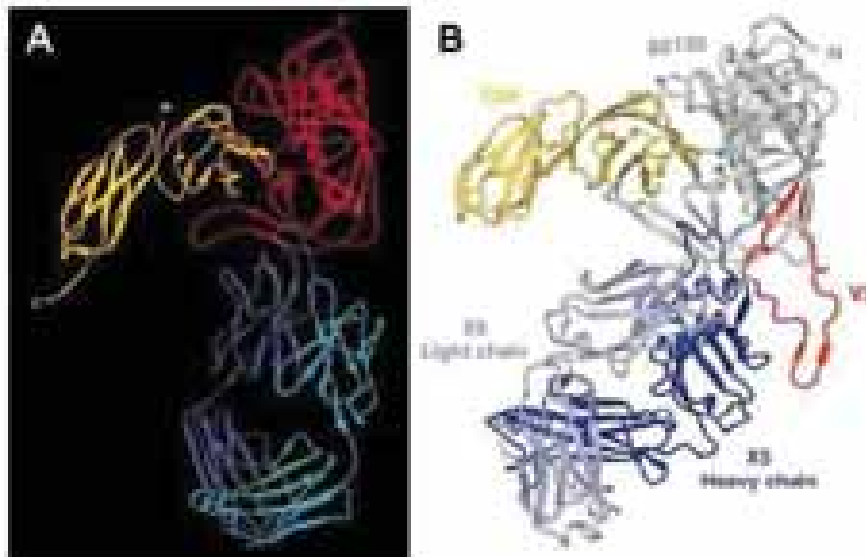
Figure 3. Crystal structure of gp120 core. A) X-ray crystal structure of deglycosylated gp120 core without V3 (red) in complex with the N-terminal two domains of CD4 (yellow) and the Fab of Ab 17b (blue). B) X-ray crystal structure of deglycosylated gp120 core (gray) with the complete V3 loop (red) in complex with two domains of the CD4 receptor (yellow) and the Fab portion of the X5 antibody (dark and light blue).[12, 13]

The gp120 core is composed of two domains, an inner and an outer domain. The domain names reflect the orientation of gp120 in the assembled envelope glycoprotein trimer: gp120 can be divided into *five conserved* (C1-C5) and *five variable* (V1-V5) regions. Conserved regions are located in the inner domain (C1 and C5) and in the hydrophobic gp120 core, while the variable regions are exposed on the glycosylated outer domain. Variables regions, with exception of V5, are bracketed with cysteine disulfide bonds and form four loops that emanates from the surface of the protein. Although the crystal structure of the complete Env is not still available, cryoelectron microscopy tomography was used to define ultrastructural details of spikes.[14] Virions of wild type HIV-1 contains around 14 spikes per virus particle with some cluster distribution. Authors were also able to measure the height of the spike and the diameter of the head, 13.7 and 10.5 nm, respectively.
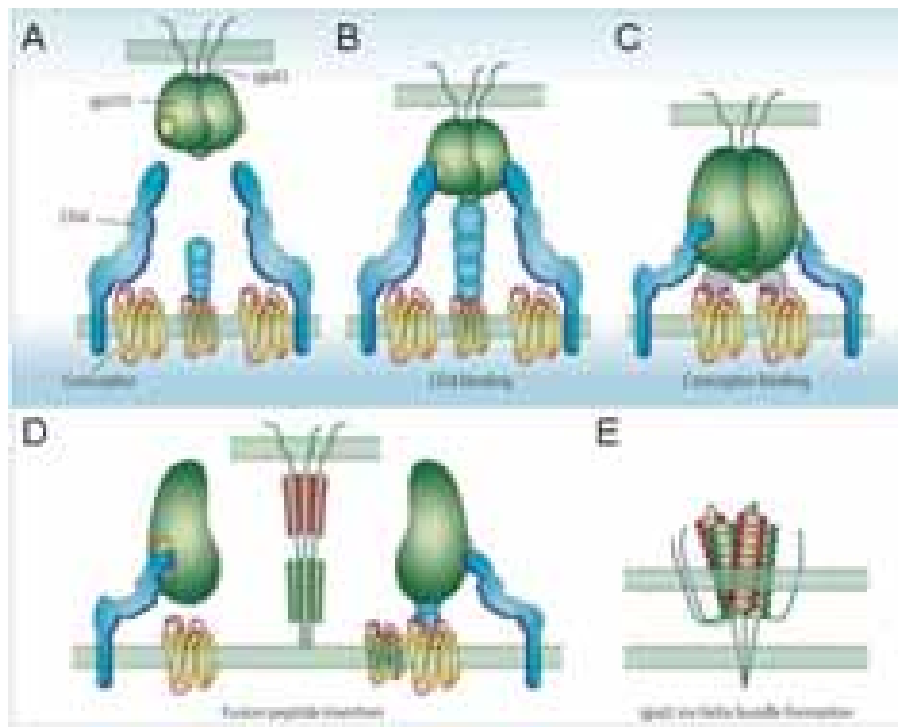
HIV entry process

HIV primarily infects cells of the human immune system such as helper T cells (specifically CD4$^+$ T cells), macrophages, and dendritic cells. The first, essential step

---

[14] Zhu, P., Liu, J., Bess, J., Jr., Chertova, E., Lifson, J.D., Grise, H., Ofek, G.A., Taylor, K.A., and Roux, K.H. (2006). Distribution and three-dimensional structure of AIDS virus envelope spikes. *Nature* **441**, 847–852.

for a mammalian virus to initiate a successful infection is to overcome the membrane barrier of the host cell, which separates it from the reproduction machinery located in the cytosol and nucleus. Enveloped viruses release their genome into the cytoplasm by fusing the viral envelope with the host membrane, which is initiated by interaction of viral fusion proteins with cellular receptors.[15] HIV virus gain entry into host cells by using *envelope proteins* (Env) that decorate the viral membrane (Figure 4). Conformational change of gp120 induced by the binding to *CD4 receptors* allows the interaction of the exposed V3 loop peptide with coreceptor *CCR5* or *CXCR4*. CCR5 and CXCR4 are G-protein coupled receptors (GPCR) and are responsible for HIV-1 transmission and early years of infection, and for late infection stages, respectively.[16,17]

Figure 4. HIV-1 entry process. A) By using Env protein (gp120/gp41) HIV infects CD4 and CCR5/CXCR4 expressing cells. B) CD4 binds to HIV gp120 and induces a conformational change that exposes V3 loop of gp120. C) The binding between V3 loop and CCR5 or CXCR4 co-receptors exposes gp41. D) and E) gp41 change its conformation and move HIV membrane close to cell membrane until fusion occur.[18]

---

[15] Melikyan, G. B. (2008). Common principles and intermediates of viral protein mediated fusion: the HIV-1 paradigm. *Retrovirology* **5**, 111.

[16] Wyatt, R., and Sodroski, J. (1998). The HIV-1 envelope glycoproteins: fusogens, antigens, and immunogens. *Science*, **280**, 1884-1888.

[17] Marsh, M., and Helenius, A. (2006) Virus entry: open sesame. *Cell.* **124**, 729-740.

[18] Esté, J. A., and Telenti, A. (2007). HIV entry inhibitors. *Lancet* **370,** 81–88.

The coreceptor binding to V3 induce a second conformational change in gp120 that lead to the insertion of gp41 into the membrane of target cell allowing the fusion of viral and cell membrane. The fusion event and the pore formation between the two membranes are still poorly understood.

Dendritic cells (DCs) can undergo HIV infection through CD4, CCR5 mechanism.[19] However, DCs also express a C-type lectin receptor (CLR) named DC-SIGN (DC specific ICAM3-grabbing non-integrin) that facilitate capture and infection of HIV-1 (Figure 5).[20]
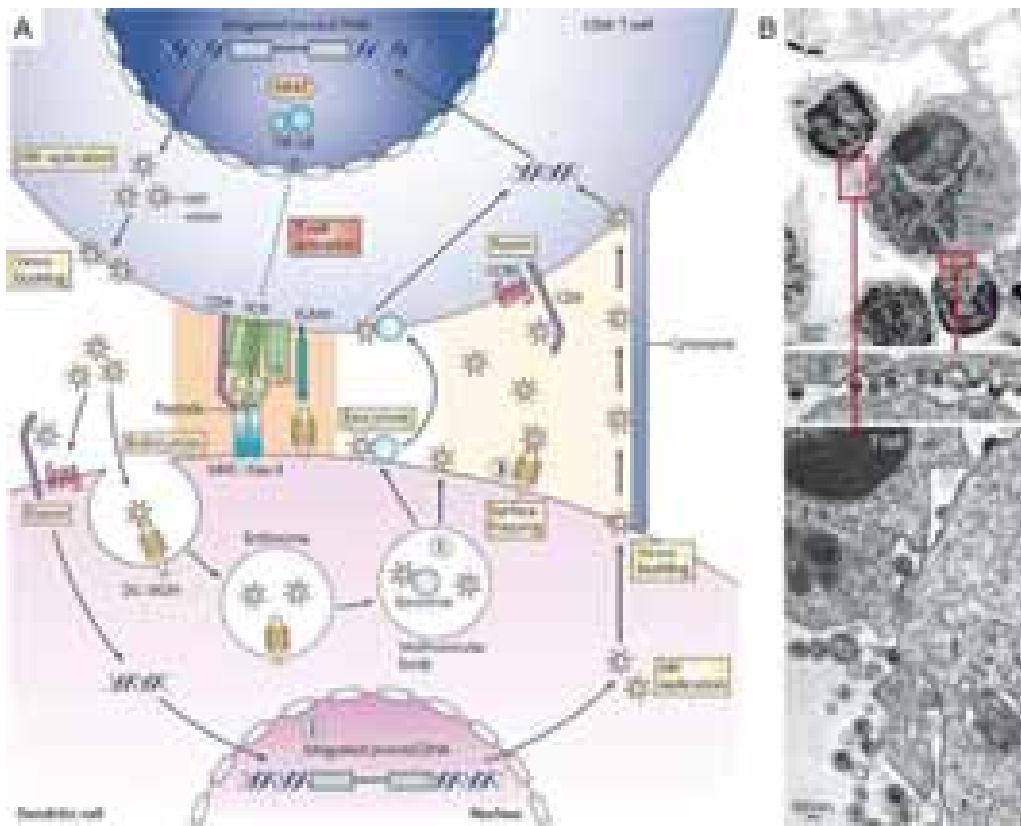
Figure 5. HIV-1 DCs infection and transmission to T-cells. A) DCs can store HIV-1 in three forms: (1) by endocytosis of intact virions in multivesicular bodies (2) by fusion and direct infection (3) by surface trapping of intact virions through DC-SIGN. B) Infectious-synapse formation between DCs and T cells in the human vagina.[20]

---

[19] Pope, M., and Haase, A. T. (2003). Transmission, acute HIV-1 infection and the quest for strategies to prevent infection. *Nat. Med.* **9**, 847-852.

[20] Hladik, F., and McElrath, M. J. (2008). Setting the stage: host invasion by HIV. *Nat. Rev. Immunol.* **8**, 447-457.

DC-SIGN is abundantly expressed on dendritic cells of mucosal tissues such as rectum, uterus, and cervix. DCs are able to capture HIV virus and deliver it to T cells in a process called trans-infection.[21] Crystal structures of carbohydrate-recognition domains of DC-SIGN bound to oligosaccharide, in combination with binding studies, reveal that this receptor selectively recognize high-mannose oligosaccharides on gp120.[22]

HIV can also use an alternative endocytic pathway to gain entry into host cells. Endocytosis of HIV-1 particles by clathrin-coated vesicles has been observed by electron and fluorescence microscopy but has generally been considered a dead-end pathway. However, recent results showed that dynamin-dependent, clathrin mediated uptake can lead to productive entry by HIV-1, suggesting this pathway as an alternative route of virus entry.[23] Several lines of evidence suggest that the formation and enlargement of a fusion pore are the most energy-intensive steps [15] that require the concerted action of several viral proteins. Considering the low number of Env per virion,[14] HIV-1 may not be able to sustain a fusion pore on its own without cellular partners. The ability of dynamin to regulate actin remodelling and/or to associate with membrane-bending proteins could provide an additional driving force to expand pores and permit the release of the HIV-1 core.[24]

Another controversial issue is the number of Env trimers (multivalence) that CD4 and co-receptor need for HIV infection. Several line of evidence demonstrated that the binding of gp120/gp41 complex to CD4 and coreceptors is cooperative, requiring multiple CCR5, three CD4 binding events and multiple cluster of gp120/gp41 (from 5 to 8) to effectively form a fusion pore (Figure 6).[25] [26] [27]

[21] Geijtenbeek, T. B., Kwon, D. S., Torensma, R., van Vliet, S. J., van Duijnhoven, G. C., Middel, J., Cornelissen, I. L., Nottet, H. S., KewalRamani, V. N., Littman, D. R., Figdor, C. G., and van Kooyk, Y. (2000). DC-SIGN, a dendritic cell-specific HIV-1-binding protein that enhances trans-infection of T cells. *Cell* **100**, 587–597.

[22] Feinberg, H., Mitchell, D. A., Drickamer, K., Weis, W. I. (2001). Structural basis for selective recognition of oligosaccharides by DC-SIGN and DC-SIGNR. *Science* **294**, 2163–2166.

[23] Daecke, J., Fackler, O. T., Dittmar, M. T., and Kräusslich, H. (2005). Involvement of clathrin-mediated endocytosis in human immunodeficiency virus type 1 entry. *J. Virol.* **79**, 1581-1594.

[24] Miyauchi, K., Kim, Y., Latinovic, O., Morozov, V., and Melikyan, G. B. (2009). HIV enters cells via endocytosis and dynamin-dependent fusion with endosomes. *Cell.* **137**, 433-444.

[25] Kuhmann, S. E., Platt, E. J., Kozak, S. L. and Kabat, D. (2000). Cooperation of multiple CCR5 coreceptors is required for infections by human immunodeficiency virus type 1. *J. Virol.* **74**, 7005-7015.

[26] Sougrat, R., Bartesaghi, A., Lifson, J. D., Bennett, A.E., Bess, J. W., Zabransky, D. J., and Subramaniam, S. (2007) Electron tomography of the contact between T cells and SIV/HIV-1: implications for viral entry. *PLoS Pathog* **3**, e63.
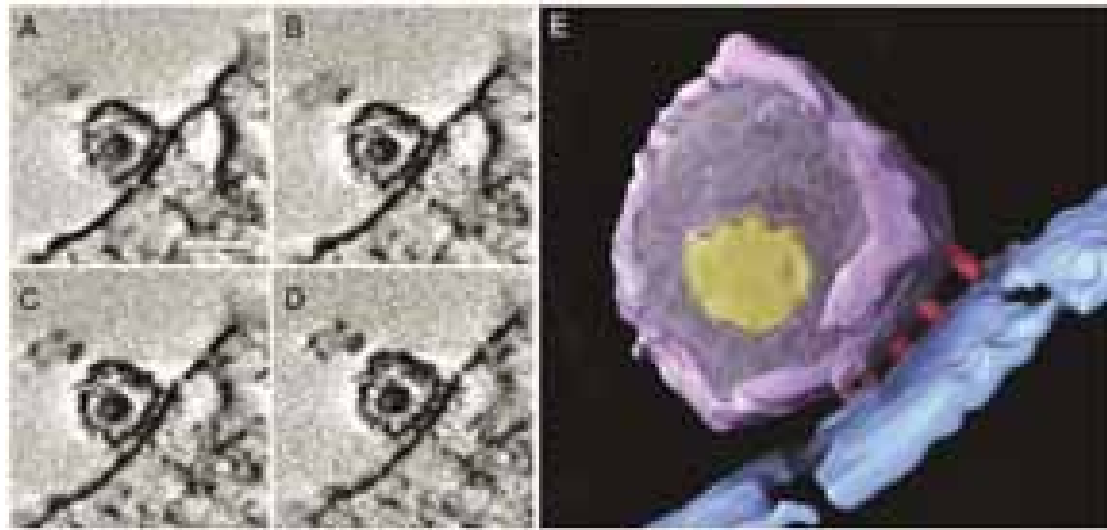
Figure 6. TEM images of the interaction between HIV-1 and T cells. A–D) Four slices at different depths of the contact between HIV-1 and T cells (scale bar is 100 nm). (E) Model 3-D of the contact region between HIV-1 and the T cell membrane (colours: envelope, magenta; contact rods, red; core, yellow; and cell membrane, blue). Note that there are almost no spikes on the virion surface away from the region of viral–cell contact.[26]

However, Yang and co-authors postulated that a single Env is probably enough to mediate virus entry.[28] Finally, Regoes *et al.* suggested that, based on our present knowledge of HIV entry, the stoichiometry of this process cannot be reliably estimated. But, can a single viral protein induce fusion? Probably viral proteins can promote hemifusion and create a small pore while relying on a host cell to carry out the energetically costly step of pore dilation.[15]

In addition to the cellular receptors DC-SIGN, CD4 and coreceptors CCR5 and CXCR4, other molecules seem to be involved in virus recruitment. The V3 loop also binds to β-galactosylceramide (β-GalCer) patches on cellular membrane and to cell surface heparan sulfate proteoglycans (HSPGs).[29, 30] These interactions facilitate the

[27] Klasse, P.J. (2007) Modeling how many envelope glycoprotein trimers per virion participate in human immunodeficiency virus infectivity and its neutralization by antibody. *Virology* **369**, 245-262.

[28] Yang, X., Kurteva, S., Ren, X., Lee, S., and Sodroski, J. (2005) Stoichiometry of envelope glycoprotein trimers in the entry of human immunodeficiency virus type 1. *J Virol* **79**, 12132-12147.

[29] Bhat, S., Spitalnik, S. L., Gonzalez-Scarano, F., and Silberberg, D. H. (1991). Galactosyl ceramide or a derivative is an essential component of the neural receptor for human immunodeficiency virus type 1 envelope glycoprotein gp120. *Proc. Nat. Acad. Sci. USA.* **88**, 7131–7134.

[30] Vivés, R. R., Imberty, A., Sattentau, Q. J., and Lortat-Jacob, H. (2005). Heparan sulfate targets the HIV-1 envelope glycoprotein gp120 coreceptor binding site. *J. Biol. Chem.* **280**, 21353–21357.

initial recruitment of virus to target cells. The region recognized by a synthetic water soluble analogue of β-GalCer corresponds to the conserved core V3 sequence Gly-Pro-Gly-Arg-Ala-Phe,[31] while a single conserved arginine (Arg-298) in the V3 region selectively binds 6-O sulphates of HSPGs.[32]

Any approach aiming at controlling and stopping virus entry should take into account these biomolecules. In this thesis, we have focused on (i) tyrosines sulphate of the co-receptor involved in the binding with V3 loop, (ii) on the receptor CD4 and (iii) on the V3 loop as targets to develop multivalent tools based on gold nanocluster able to interfere with HIV entry process. These gold nanoclusters will be coated with sulphate groups or miniprotein (miniCD4) to neutralize the virus, or with specific V3 loop to block the interaction of the virus with co-receptor CCR5 or CXCR4. We expected to contribute to the understanding of the role of multivalent presentation of selected molecules in HIV infection in order to fight more efficiently HIV.

How to fight HIV-1

Currently, there are mainly three different strategies to fight HIV infection. One of them (HAART) is well established and in clinical use, but the other two (microbicides and vaccines) are still a field of research.

Highly active antiretroviral treatment (HAART)
The first effective drug against HIV, zidovudine (AZT), was discovered in 1987. It was the first of 25 antiretroviral drugs that in these years have been formally licensed for clinical use.[33] Currently, six classes of antiretroviral agents exist in clinical use:
- Nucleoside reverse transcriptase inhibitors (NRTIs)
- Non-nucleoside reverse transcriptase inhibitors (NNRTIs)
- Protease inhibitors (PIs)
- Integrase inhibitors (IIs)
- Fusion inhibitors (FIs)
- Chemokine receptor antagonists (CRAs)

---

[31] Fantini, J., Hammache, D., Delezay, O., Yahi, N., Andre-Barres, C., Rico-Lattes, I., and Lattes, A. (1997). Synthetic soluble analogs of galactosylceramide (GALCER) bind to the V3 domain of HIV-1 gp120 and inhibit HIV-1-induced fusion and entry. *J. Biol. Chem.* **272**, 7245–7252.

[32] de Parseval, A., Bobardt, M. D., Chatterji, A., Chatterji, U., Elder, J. H., David, G., Zolla-Pazner, S., Farzan, M., Lee, T., and Gallay P. A. (2005). A highly conserved arginine in gp120 governs HIV-1 binding to both syndecans and CCR5 via sulfated motifs. J. Biol. Chem. 280, 21353–21357.

[33] De Clercq, E. (2010). Antiretroviral drugs. *Current Opinion in Pharmacology* **10**, 507–515.

These drugs are used in combination in the so called: highly active antiretroviral treatment (HAART). This therapy has drastically altered AIDS from a fatal disease to a chronic infection. However, research in anti-HIV drug discovery can not stop because rapid mutation confers drug resistance to HIV, and new and more effective molecular systems are needed to continue to fight viral infection.

HIV microbicides

In sub-Saharan Africa, the epicentre of HIV pandemic, prevention of sexual mucosal transmission, the principal route of acquisition, is needed to retain the number of HIV infected people.[34] Microbicides are compounds that can be applied directly to the vagina or rectum prior to sexual intercourse in order to prevent the transmission of HIV. They can come in the form of a gel, cream, or in a slow release device. Many different inhibitors were studied as vaginal microbicides including natural and synthetic polyanionic polymers (Carraguard, cellulose sulfate and the polynaphthalene sulfonate Pro2000), antibodies (b12, 2G12 and 2F5), chemokines analogues (PSC RANTES) and carbohydrate-binding proteins (Cyanovirin-N and soluble DC-SIGN).[35] Most of them are founded toxic in clinical trials. Only recently, The Centre for the AIDS Program of Research in South Africa (CAPRISA) 004 trial, assessed the effectiveness and safety of a 1% vaginal gel formulation of tenofovir, a nucleotide reverse transcriptase inhibitor, for the prevention of HIV acquisition in women.[36] Tenofovir gel reduced HIV acquisition by an estimated 39% overall, and by 54% in women with high gel adherence.

Since 2004 HIV microbicides have also been the focus of the European Microbicides Project (EMPRO), which was continued in 2008 under the name of CHAARM (Combined Highly Active Anti-Retroviral Microbicides). The purpose of this project is to develop combinations of new and existing microbicides, which can be applied topically to reduce transmission of HIV during sexual intercourse.[37]

---

[34] Haase, A. T. (2010). Targeting early infection to prevent HIV-1 mucosal transmission. *Nature* **464**, 217-223.

[35] Balzarini, J., and Van Damme, L. (2007). Microbicide drug candidates to prevent HIV infection. *Lancet*, **369**, 787–797.

[36] Karim, Q. A., Abdool Karim, S. S., Frohlich, J. A., Grobler, A. C., Baxter, C., Mansoor, L. E., Kharsany, A. B. M., Sibeko, S., Mlisana, K. P., Omar, Z., Gengiah, T. N., Maarschalk, S., Arulappan, N., Mlotshwa, M., Morris, L., *et. al* (2010). Effectiveness and safety of tenofovir gel, an antiretroviral microbicide, for the prevention of HIV infection in women. *Science* **329**, 1168-1174.

[37] http://chaarm.eu/microbicides/about-microbicides-against-hivaids

HIV vaccines

Despite almost 30 years of research, a protective vaccine against HIV-1 is still a challenge. A common feature of protective viral vaccine is their ability to elicit neutralizing antibodies (NAbs). HIV trimeric Env complex is the principal target for NAbs.[38] The sera of HIV infected individuals contain antibodies against gp120 and gp41, but they are not able to eradicate the infection. This problem is strictly related to important structural Env features. The outer domain of gp120 is heavily glycosylated and most carbohydrate moieties may appear as "self" to the immune system.[16] The gp120 glycoprotein elicits both virus-neutralizing and non-neutralizing antibodies during natural infection. Antibodies that lack neutralizing activity are often directed against the gp120 regions that are occluded on the assembled trimer and which are exposed only upon shedding.[39] Indeed, trimerization of the gp120-gp41 structure can shield vulnerable epitopes that are better exposed in the monomeric subunit.[40] Moreover, during HIV replication, viral RNA has to be converted into a duble-stranded DNA. This process, mediated by the viral reverse transcriptase (RT), is extremely error-prone and it is during this step that mutations occur.[41] However, to replicate, HIV-1 must interact with its receptors on target cells. As a consequence, part of the surface of gp120 has to be both exposed and conserved or semiconserved.[42] The challenge in HIV vaccine design is to identify immunogens able to elicit antibodies that neutralize a broad range of HIV primary isolates: the so-called broadly neutralizing antibodies (bNAb). A small panel of broadly neutralizing Ab has been identified in HIV infected individuals.[43] Antibody b12 recognizes the CD4 binding site of gp120,[44] 2F5 and 4E10 bind the

---

[38] Pantophlet, R., and Burton. D. R. (2006). gp120: Target for neutralizing HIV-1 antibodies. *Annu. Rev. Immunol.* **24**, 739-769.

[39] Wyatt, R., Kwong, P. D., Desjardins, E., Sweet, R. W., Robinson, J., Hendrickson, W. A., and Sodroski, J. G. (1998). The antigenic structure of the HIV gp120 envelope glycoprotein. *Nature* **393**, 705-711.

[40] Burton, D. R., Desrosiers, R. C., Doms, R. W., Koff, W. C., Kwong, P. D., Moore, J. P., Nabel, G. J., Sodroski, J., Wilson I. A., and Wyatt R. T. (2004). HIV vaccine design and the neutralizing antibody problem. *Nat. Immunol.* **5**, 233-236.

[41] Johnson, W. E., and Desrosiers, R. C. (2002). Viral persitance: HIV's strategies of immune system evasion. *Annu. Rev. Med.* **53**, 499-518.

[42] Poignard, P., Ollmann Saphire, E., Parren, P. W., and Burton, D. R. (2001). gp120: Biologic aspects of structural features. *Annu. Rev. immunol.* **19**, 253-274.

[43] Burton, D. R., Stanfield, R. L., and Wilson, I. A. (2005). Antibody vs. HIV in a clash of evolutionary titans. *PNAS*. **102**, 14943-14948.

[44] Saphire., E. O., Parren, P. W. H. I., Pantophlet, R., Zwick, M. B., Morris, G. M., Rudd. P. M., Dwek, R. A., Stanfield, R. L., Burton., D. R., and Wilson, I. A. (2001). Crystal structure of a neutralizing human IgG against HIV-1: a template for vaccine design. *Science* **293**, 1155-1159.

membrane proximal region (MPER) of gp41,[45] antibody 2G12 recognizes clusters of oligomannosides on gp120 [46] and antibody 447-52D bind the relatively conserved GPGR region of V3 loop.[47] Very recently a new potent and broad NAb was discovered.[48] This bNAb recognizes two conserved oligomannosides as well as a short β-strand segment of the gp120 V3 loop. Naturally occurring bNAb confirm that it could be possible to stimulate human immune system to produce these antibodies. Structural studies of bNAb complexed with gp120 or gp41 give very important informations on the preparations of immunogenic molecules.

It is also possible to enhance immunogenicity of HIV-1 antigens by in vivo targeting dendritic cells. DCs, the most potent antigen presenting cells (APCs), have a pivotal role in the initiation and maintenance of immune responses against viruses.[49] Promising results showed the ability of vaccines based on dendritic cells to reduce viral load in a significant number of patients.[50] In that work, *ex vivo* pulsed autologous monocyte-derived DCs with inactivated autologous virus induce a prolonged reduction of HIV RNA in a substantial number of patients. Recently, very promising results were obtained with a therapeutic vaccine made of autologous monocyte-derived dendritic cells (MD-DCs) pulsed with autologous heat-inactivated whole HIV.[51] These results highlighted the potential of immunotherapy strategies targeting HIV antigens to DCs in HIV infected patients.

---

[45] Cardoso, R. M., Zwick, M. B., Stanfield, R. L., Kunert, R., Binley, J. M., Katinger, H., Burton, D. R., and Wilson, I. A. (2005). Broadly neutralizing anti-HIV antibody 4E10 recognizes a helical conformation of a highly conserved fusion-associated motif in gp41. *Immunity* **22**, 163–173.

[46] Calarese, D. A., Scanlan, C. N., Zwick, M. B., Deechongkit, S., Mimura, Y., Kunert, R., Zhu, P., Wormald, M. R., Stanfield, R. L., Roux, K. H., Kelly, J. W., Rudd, P. M., Dwek, R. A., Katinger, H., Burton, D. R., and Wilson, I. A. (2003). Antibody Domain Exchange Is an Immunological Solution to Carbohydrate Cluster Recognition. *Science* **300**, 2065-2071.

[47] Stanfield, R. L., Gorny M. K., Williams, C., Zolla-Pazner, S., and Wilson, I. A. (2004). Structural rational for the broad neutralizion of HIV-1 by human monoclonal antibody 447-52D. *Structure*, **12**, 193-204.

[48] Pejchal, R., Doores, K. J., Walker, L. M., Khayat, R., Huang, P. S., Wang, S. K., Stanfield, R. L., Julien, J. P., Ramos, A., Crispin, M., Depetris, R., Katpally, U., Marozsan, A., Cupo, A., Maloveste, S., Liu, Y., McBride, R., Ito, Y., Sanders, R. W., Ogohara, C., Paulson, J. C., Feizi, T., Scanlan, C. N., Wong, C. H., Moore, J. P., Olson, W. C., Ward, A. B., Poignard, P., Schief, W. R., Burton, D. R., and Wilson, I. A. (2011). A potent and broad neutralizing antibody recognizes and penetrates the HIV glycan shield. *Science* **334**, 1097-1103.

[49] Knight, S.C., and Stagg, A.J. (1993). Antigen-presenting cell types. *Curr. Opin. Immunol.* **5**, 374–382

[50] Lu, W., Arraes L. C., Ferreira W. T., and Andrieu J. M. (2004). Therapeutic dendritic- cell vaccine for chronic HIV-1 infection. *Nat. Med.* **10**, 1359–1365.

[51] García, F., Climent, N., Guardo, A. C., Gil, C., León, A., Autran, B., Lifson, J. D., Martínez-Picado, J., Dalmau, J., Clotet, B., Gatell, J. M., Plana, M., and Gallart, T. (2013). A dendritic cell–based vaccine elicits T cell responses associated with control of HIV-1 replication. *Sci. Transl. Med.* **5**, 166ra2.

Multivalent synthetic systems against HIV

As the HIV-1 Env is displayed as a trimeric complex, multimerization of Env binding molecules is expected to enhance antiviral activity or immunogenicity, respectively. Many multivalent synthetic systems were prepared in the last decade and some of them were studied as anti HIV agents or as HIV immunogens. Peptides, carbohydrates and drugs were multimerized by using scaffold with more than two anchoring sites. It has also been suggested that repetitive presentation of an epitope on the immunogen can induce a stronger immune response, probably because such immunogens can trigger oligomerization of B-cell receptors recognizing the epitope.[52, 53]

Multivalent peptides based system

Many efforts were made to prepare peptides that mimic CD4 receptors with the same binding site of natural CD4 but lower MW. These CD4 miniproteins are able to bind gp120 in the same way as native human CD4; however, their small size and constrained structure give them better access to the CD4-binding site on the viral gp120. In addition, these peptides are stable in strong denaturing conditions, including acidic pH. Li *et al.* prepared a series of trivalent CD4-mimetic miniprotein with different scaffold and spacers between miniproteins (Figure 7).[54] Triazacyclododecane (Figure 7B), Kemp's triacid (Figure 7C) and trimesic acid (Figure 7D) were used as scaffolds. Polyethylen glycol and aliphatic chains were used as spacers. Antiviral assays revealed that most of the trivalent miniproteins showed enhanced anti-HIV activity over the monomer, indicating the gain of affinity through multivalent interactions. The compound that possesses a hydrophobic linker (compound 9b) showed an anti HIV activity 140-fold more potent than the monovalent miniCD4.

---

[52] Cruz, L. J., Iglesias, E., Aguilar, J. C., Cabrales, A., Reyes, O., and Andreu, D. (2004). Different immune response of mice immunized with conjugates containing multiple copies of either consensus or mixotope version of the V3 loop peptide from human immunodeficiency virus type 1. *Bioconjug. Chem.* **15**, 1110-1117.

[53] Totrov, M., Jiang, X., Kong, X., Cohen, S., Krachmarov, C., Salomon, A., Williams, C., Seaman, M. S., Cardozo, T., Gorny, M. K., Wang, S., Lu, S., Pinter, A., and Zolla Pazner, S. (2010). Structure-guided design and immunological characterization of immunogens presenting the HIV-1 gp120 V3 loop on a CTB scaffold. *Virology* **405**. 513–523.

[54] Li, H., Guan, Y., Szczepanska, A., Moreno-Vargas, A. J., Carmona, A. T., Robina, I., Lewisa, G. K., and Wang L. (2007). Synthesis and anti-HIV activity of trivalent CD4-mimetic miniproteins. *Bioorganic & Medicinal Chemistry* **15**, 4220–4228.
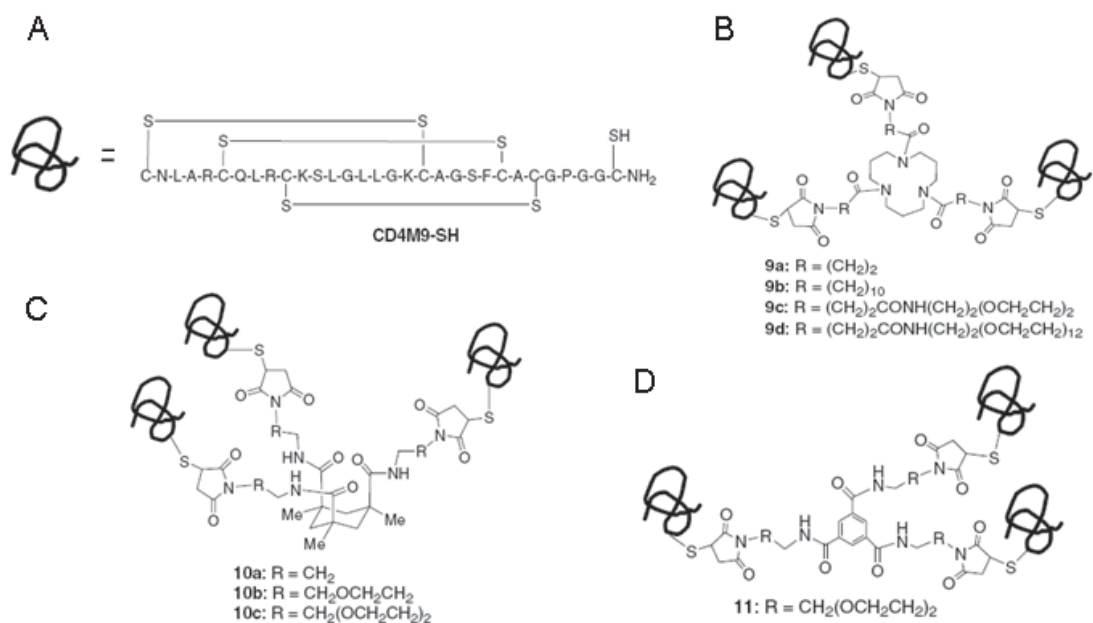
Figure 7. Multimerization of miniCD4 (CD4M9-SH). A) Peptide sequence of miniCD4 (CD4M9-SH) B) Trimeric miniCD4 derivative of triazacyclododecane. C) Trimeric miniCD4 derivative of Kemp's triacid. D) Trimeric miniCD4 derivative of trimesic acid. Adapted from reference 52.

By using a different CD4-mimetic miniprotein[55] and a different scaffold with longer spacers, the group of L. Martin prepared di- and tetravalent miniCD4 conjugates (Figure 8). Dimeric (Figure 8A) and tetrameric (Figure 8B) miniCD4 miniproteins (M48) were prepared with different polyethylene glycol spacer lengths of 30, 50 or 100 Å within each group. They found that the increase in antiviral activity of the dimeric compounds was limited and all tetrameric analogues showed decreased anti HIV activity in comparison with mono and dimeric structures.[56]

[55] Vita, C., Drakopoulou, E., Vizzavona, J., S., Rochette, Martin, L., Ménez, A., Roumestand, C., Yang, Y., Ylisastigui, L., Benjouad, A., and Gluckman, J. C. (1999). Rational engineering of a miniprotein that reproduces the core of the CD4 site interacting with HIV-1 envelope glycoprotein. *Proc. Natl. Acad. Sci. USA* **96**, 13091-13096.

[56] Van Herrewege, Y., Morellato, L., Descours, A., Aerts, L., Michiels, J., Heyndrickx, L., Martin, L., and Vanham, G. (2008). CD4 mimetic miniproteins: potent anti-HIV compounds with promising activity as microbicides. *J. Antimicrobial Chemotherapy* **61**, 818-826.
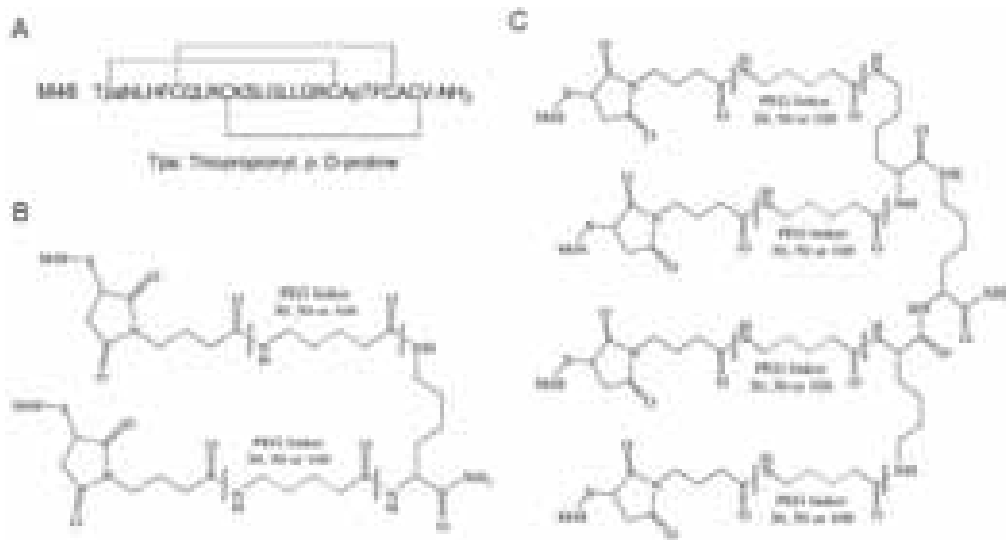
Figure 8. Multimerized miniCD4 structures. A) Peptide sequence of M48 mimetic CD4 miniprotein. B) Dimeric CD4 miniprotein with different length of PEG linkers. C) Tetrameric CD4 miniproteins with different length of PEG linkers. Adapted from reference 54.

In 2003 Wang et al. prepared a multivalent structure composed by gp41 peptides on a carbohydrate scaffold as HIV vaccines and viral membrane fusion inhibitors.[57]
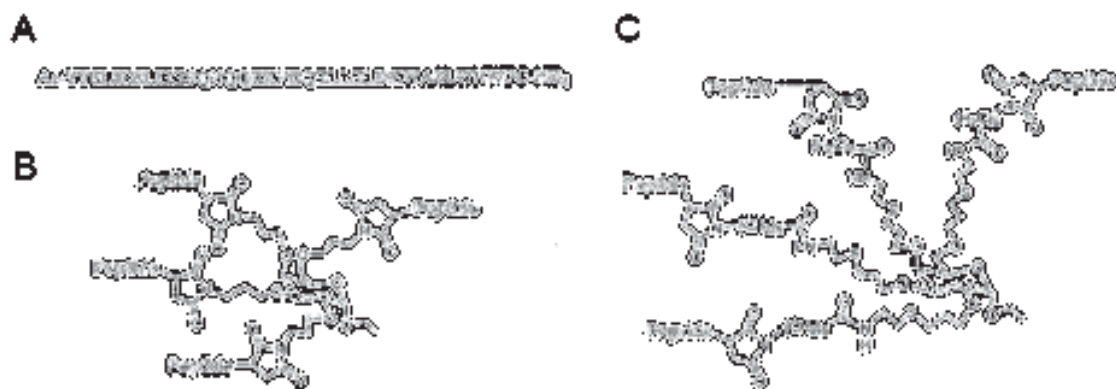
Figure 8. Multimerized gp41 peptide on a carbohydrate scaffold. A) Peptide sequence of gp41 peptide. B) Tetrameric gp41 peptide on a carbohydrate scaffold (short linker). C) Tetrameric gp41 peptide on a carbohydrate scaffold (long linker). Adapted from reference 55.

Immunization studies indicated that while the gp41 peptide alone was poorly immunogenic, the tetravalent peptide gave high titers of antibodies in mice that recognize not only gp41 peptide, but also the native HIV-1 glycoprotein gp41.[58]

---

[57] Wang, L., Ni, J., and Singh, S. (2003) Carbohydrate-centered maleimide cluster as a new type of templates for multivalent peptide assembling: synthesis of multivalent HIV-1 gp41 peptides. *Bioorg. Med. Chem.* **11**, 159-166.

V3 peptide is a very important region of gp120, crucial for HIV-1 entry process. V3 was studied in monovalent and multivalent presentation as HIV entry inhibitor and as immunogen. More detailed discussion can be found in chapter 3. A multimeric V3-lysine dendrimers (Figure 9A) and a multivalent V3 peptide-cholera toxin B (Figure 9B) have been prepared and studied as HIV immunogen.[53, 59]
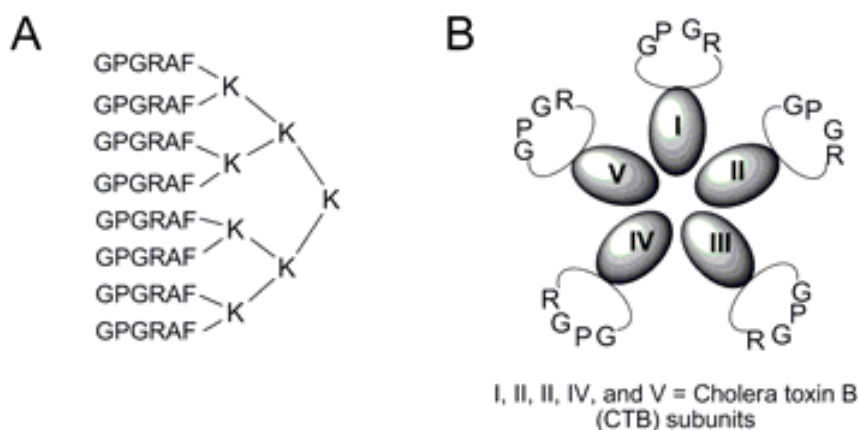
Figure 9. Multimeric form of V3 peptides. A) Short V3 peptides on a lysine dendrimer scaffold. B) V3 peptides on a multimeric form of cholera toxin B. Adapted from reference 57 and 51.

Although these constructs are able to induce an immune response in animals, the sera neutralize only T-cell line adapted virus or narrow range of primary isolates.

Multivalent oligosaccharides systems

A dense shield of high-mannose type glycans (Figure 3) protects gp120 from exposure to the immune response of the host. Nevertheless, the broadly neutralizing monoclonal antibody 2G12 can target a cluster of high-mannose oligosaccharides of HIV gp120.[60] Moreover, new broadly neutralizing antibodies that are also carbohydrate-directed have been isolated recently from patients.[61] Mimicking the cluster presentation of

[58] Ni, J., Powell, R., Baskakov, I. V., DeVico, A., Lewis, G. K., and Wang, L., (2004). Synthesis, conformation, and immunogenicity of monosaccharide-centered multivalent HIV-1 gp41 peptides containing the sequences of DP178. *Bioorg. Med. Chem.* **12**, 3141-3148.

[59] Hewer, R., and Meyer, D. (2003). Peptide immunogens based on the envelope region of HIV-1 are recognized by HIV/AIDS patient polyclonal antibodies and induce strong humoral immune responses in mice and rabbits. *Mol. Immunol.* **40**, 327-335.

[60] Scanlan, C. N., Pantophlet, R., Wormald, M. R., Saphire, E. O., Stanfield, R., Wilson, I. A., Katinger, H., Dwek, R. A., Rudd, P. M., and Burton, D. R. (2002). The broadly neutralizing anti-human immunodeficiency virus type 1 antibody 2G12 recognizes a cluster of α1→2 mannose residues on the outer face of gp120. *J. Virol.*, **76**, 7306–7321.

[61] Pejchal, R., Doores, K. J., Walker, L. M., Khayat, R., Huang, P., Wang, S., Stanfield, R. L., Julien, J., Ramos, A., Crispin, M., Depetris, R., Katpally, U., Marozsan, A., Cupo, A., Maloveste, S., Liu, Y., Mcbride,

oligomannosides expressed at the HIV-1 surface is a strategy for eliciting a vaccine response. Several groups, including those of Wang,[62][63] Wong,[64][65] Danishefsky,[66] and Rappuoli,[67] have multimerized high-mannose type oligosaccharides on synthetic and natural scaffolds in order to mimic the carbohydrate epitope of 2G12 (Figure 10).
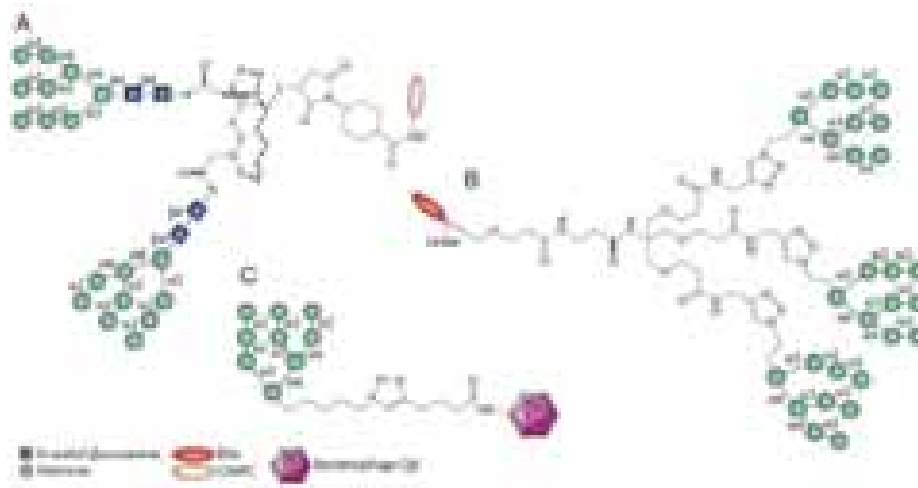
Figure 10. Multimeric high-mannose glycoconjugate immunogens prepared for HIV vaccine studies. A) GlcNAc$_2$Man$_9$ divalent glycopeptide OmPC (outer membrane protein complex, derived from *Neisseria meningitidis*) conjugate. B) Man$_9$ glycodendron bovine serum albumin (BSA) conjugate. C) bacteriophage Qβ–Man$_9$.[68]

R., Ito, Y., Sanders, R. W., Ogohara, C., Paulson, J. C., Feizi, T., Scalan, C. N., Wong, C., Moore, J. P., Olson, W. C., Ward, A. B., Poignard, P., Schief, W. R., Burton, D. R., and Wilson, I. A. (2011). A potent and broad neutralizing antibody recognizes and penetrates the HIV glycan shield. *Science*, **334**, 1097-1103.

[62] Ni, J., Song, H., Wang, Y., Stamatos, N. M., and Wang, L. X. (2006). Toward a carbohydrate-based HIV-1 vaccine: synthesis and immunological studies of oligomannose-containing glycoconjugates.*Bioconjugate Chem.*, **17**, 493–500.

[63] Wang, J., Li, H., Zou, G., and Wang, L. X. (2007). Novel template-assembled oligosaccharide clusters as epitope mimics for HIV-neutralizing antibody 2G12. Design, synthesis, and antibody binding study. *Org. Biomol. Chem.* **5**, 1529-1540.

[64] R. D. Astronomo, E. Kaltgrad, A. K. Udit, S. K. Wang, K. J. Doores, C. Y. Huang, R. Pantophlet, J. C. Paulson, C. H. Wong, M. G. Finn and D. R. Burton, 2010 Defining criteria for oligomannose immunogens for HIV using icosahedral virus capsid scaffolds. *Chem. Biol.* **17**, 357–370.

[65] Astronomo, R. D., Lee, H. K., Scanlan, C. N., Pantophlet, R., Huang, C. Y., Wilson, I. A., Blixt, O., Dwek, R. A., Wong, C. H., and Burton, D. R. (2008). A glycoconjugate antigen based on the recognition motif of a broadly neutralizing human immunodeficiency virus antibody, 2G12, is immunogenic but elicits antibodies unable to bind to the self glycans of gp120**.** *J. Virol.*, **82**, 6359–6368.

[66] Joyce, J. G., Krauss, I. J., Song, H. C., Opalka, D. W., Grimm, K. M., Nahas, D. D., Esser, M. T., Hrin, R., Feng, M., Dudkin, V. Y., Chastain, M., Shiver, J. W. and Danishefsky, S. J. (2008). An oligosaccharide-based HIV-1 2G12 mimotope vaccine induces carbohydrate-specific antibodies that fail to neutralize HIV-1 virions. *Proc. Natl. Acad. Sci. U. S. A.* **105**, 15684–15689.

[67] Kabanova, A., Adamo, R., Proietti, D., Berti, F., Tontini, M., Rappuoli, R., and Costantino, P. (2010). Preparation, characterization and immunogenicity of HIV-1 related high-mannose oligosaccharides-CRM 197 glycoconjugates. *Glycoconjugate J.* **27**, 501–513.

[68] Astronomo, R. D., and Burton, D. R. (2010). Carbohydrate vaccines: developing sweet solutions to sticky situations? *Nat. Rev. Drug Discovery*, **9**, 308-324.

Although most of these systems were able to induce a carbohydrate-specific immune response in animals, the IgG antibodies were unable to bind to gp120 or neutralize the virus. The difficulty of eliciting high titters of antibodies against the 2G12 epitope remains a still open challenge in search for synthetic carbohydrate-based vaccines against HIV.

High-mannose oligosaccharides are also implicated in HIV trans-infection process mediated by DC-SIGN. Multivalent systems based on dendrons,[69] bearing multiple copies of mannosides were prepared and studied in the binding with DC-SIGN. Our group has previously shown that gold glyconanoparticles coated with mannose oligosaccharides are able to inhibit HIV-1 up-take and infection of DCs through DC-SIGN.[70, 71]

Nowadays, nanotechnology plays a key role in the biomedical field.[72] Diagnostics, therapy, drug delivery and tissue engineering are the main biomedical areas in which the application of nanotechnology is creating a high expectation of health benefits.[73] Metallic nanoparticles display unique magnetic, electrical, optical, mechanical and chemical properties, which can be tuned by controlling the size, the shape and by varying the core materials.[74] The unique properties and utility of nanoparticles arise from a variety of attributes, including the similar size of nanoparticles to biomolecules (proteins and polynucleic acids).[75] The biomedical applications of metal nanoparticles

[69] Sánchez-Navarro, M., Rojo, J. (2010). Targeting DC-SIGN with carbohydrate multivalent systems. *Drug News and Perspectives*, **23**, 557-572.

[70] Martínez-vila, O., Hijazi, K., Marradi, M., Clavel, C., Campion, C., Kelly, C., and Penades, S. (2009). Gold manno-glyconanoparticles: multivalent systems to block HIV-1 gp120 binding to the lectin DC-SIGN. *Chem. Eur. J.* **15**, 9874–9888.

[71] Martinez-Avila, O., Bedoya, L. M., Marradi, M., Clavel, C., Alcami, J., and Penades, S. (2009). Multivalent manno-glyconanoparticles inhibit DC-SIGN-mediated HIV-1 trans-infection of human T cells. *ChemBioChem*, **10**, 1806–1809.

[72] Riehemann, K., Schneider, S. W., Luger, T. A., Godin, B., Ferrari, M., and Fuchs, H. (2009). Nanomedicine – challenge and perspectives. *Angew. Chem. Int. Ed.* **48**, 872–897.

[73] Boisselier, E., and Astruc, D. (2009). Gold nanoparticles in nanomedicine: preparations, imaging, diagnostics, therapies and toxicity. *Chem. Soc. Rev.* **38**, 1759–1782.

[74] Hodes, G. (2007). When small is different: some recent advances in concepts and applications of nanoscale phenomena. *Adv. Mater.* **19**, 639–655.

[75] De, M., Ghosh, P. S., and Rotello, V. M. (2008). Applications of nanoparticles in biology. *Adv. Mater.* **20**, 1-17.

started in the 1970s with the discovery of immunogold labelling by Faulk and Taylor.[76] Citrate reduction of Au(III) to Au(0) in water was introduced by Turkevitch et al. in 1951.[77] Although AuNPs can be stabilized by a large variety of molecules (surfactants, polymers, biomolecules, etc.),[78] the most robust AuNPs were disclosed by Giersig and Mulvaney to be stabilized by thiolates using the strong Au–S bond between the soft acid Au and the soft thiolate base.[79] Along this line, by far the most popular synthetic method using such sulphur coordination for AuNP stabilization is the Shiffrin–Brust biphasic synthesis using $HAuCl_4$, a thiol, tetraoctylammonium bromide and $NaBH_4$ in water–toluene yielding thiolate-AuNPs.[80] Nowadays, there are a large number of ways to synthesize gold nanoparticles (AuNPs) most of the time starting from commercial chloroauric acid ($HAuCl_4$).[81]

Multivalent drugs gold nanoparticles

In 2008 Bowman et al. prepared 2.0 nm diameter mercaptobenzoic acid coated gold nanoparticles conjugated to SDC-1721, a derivative of TAK-779, (Figure 11) a known CCR5 antagonist. [82]

Figure 11. Molecular structure of TAK-779 and SDC-1721.[82]

[76] Faulk, W. P., and Taylor, G. M. (1971). An immunocolloid method for the electron microscope. *Immunochemistry* **8**, 1081–1083.

[77] Turkevich, J., Stevenson, P. C., and Hillier, J. (1951). A study of the nucleation and growth processes in the synthesis of colloidal gold. *Discuss. Faraday Soc.* **11**, 55–75.

[78] Daniel, M. C. and Astruc, D. (2004). Gold nanoparticles: assembly, supramolecular chemistry, quantum-size-related properties, and applications toward biology, catalysis, and nanotechnology. *Chem. Rev.* **104**, 293–346.

[79] Giersig, M. and Mulvaney, P. (1993). Preparation of ordered colloid monolayers by electrophoretic deposition. *Langmuir*, **9**, 3408–3413.

[80] Brust, M., Walker, M., Bethell, D., Schiffrin, D. J., and Whyman, R. J. (1994). Synthesis of Thiol-derivatised Gold Nanoparticles in a Two-phase Liquid-Liquid System. *J. Chem. Soc., Chem. Commun.*, 801–802.

[81] Marradi, M., Martín-Lomas, M., and Penadés, S. (2010). Glyconanoparticles: polyvalent tools to study carbohydrate-based interactions. *Adv. Carb. Chem. Biochem.* **64**, 211-290.

[82] Bowman, M., Ballard, T. E., Ackerson, C. J., Feldheim, D. L., Margolis, D. M., and Melander, C. (2008). Inhibition of HIV fusion with multivalent gold nanoparticles. *J. Am. Chem. Soc.* **130**, 6896–6897.

Authors showed for the first time that gold nanoparticle coated with small molecule can be effective inhibitor of HIV fusion. The results demonstrate that therapeutically inactive monovalent small organic molecules may be converted into highly active drugs by simply conjugating them to gold nanoparticles. This is the only example of multimerization of an anti-viral drug on the surface of gold nanoparticles.

Gold Glyconanoparticles

Since 2000 our laboratory has been developing metallic nanoparticles, biofunctionalized with carbohydrates (glyconanoparticles, GNPs) to study carbohydrate-mediated interaction[83] and to explore their potential applications in the emerging area of nanomedicine.[84] GNPs consist of a metallic core with self-assembled monolayers of glycoconjugates covalently linked. GNPs and the methodology developed to prepare them (glyconanotechnology) have led to the development of multivalent, biocompatible and multifunctional gold, magnetic and semiconductor GNPs.[85, 86] Gold GNPs are multivalent tools extremely useful to study carbohydrate-mediated interactions.[87] GNPs are water soluble biofunctional gold nanoclusters with well defined composition and an exceptional small core size. They can display large number of molecules on a reduced surface (100 molecules on 2 nm diameter core gold) and allow the combination of different molecules in a controlled way.[88, 89]

[83] Barrientos, A. G., de la Fuente, J. M., Rojas, T. C., Fernández, A., and Penadés, S. (2003). Gold glyconanoparticles: synthetic polyvalent ligands mimicking glycocalyx-like surfaces as tools for glycobiological studies. *Chem. Eur. J.*, **9**, 1909-1921.

[84] García, I., Marradi, M., and Penadés S. (2010). Glyconanoparticles: multifunctional nanomaterials for biomedical applications. *Nanomedicine* **5**, 777–792.

[85] de la Fuente, J. M., and Penadés, S. (2006) Glyconanoparticles: types, synthesis and applications in glycoscience, biomedicine and material science. *Biochim. Biophys. Acta Gen. Subj.* **1760**, 636–651.

[86] Marradi, M., Martin-Lomas, M., and Penadés, S. (2010). Glyconanoparticles: polyvalent tools to study Carbohydrate-based interactions. *Adv. Carb. Chem. Biochem.* **64**, 211-290.

[87] de la Fuente, J. M., Barrientos, A. G., Rojas, T. C., Rojo, J., Cañada, J., Fernández, A., and Penadés, S. (2001). Glycosphingolipid clustering and interactions at the cell membrane can be modeled by gold glyconanoparticles prepared with biologically significant oligosaccharides. *Angew. Chem. Int. Ed.* **40**, 2258-2261.

[88] Ojeda, R., de Paz, J. L., Barrientos, A. G., Martin-Lomas, M., and Penadés S. (2007). Preparation of multifunctional glyconanoparticles as a platform for potential carbohydrate-based anticancer vaccines. *Carbohydrate Research* **342**, 448–459

[89] Marradi, M., Chiodo, F., García, I., and Penadés, S. (2013). Glyconanoparticles as multifunctional and multimodal carbohydrate systems. *Chem. Soc. Rev.* **42**, 4728-4745.

Aim of this work

GNPs represent an interesting multivalent tool in the study of the molecular basis of HIV infection because:

1) Most of the HIV-Env related binding (DC-SIGN, CD4, CCR5/CXCR4) was demonstrated to be multivalent,

2) GNPs can be covered with different selected molecules (peptide, carbohydrate, drug, etc…) that may interfere with concrete steps of HIV infection. These molecules can act together conferring synergy to the same binding event or they can have different role and work in sequential biological steps (i.e. targeting specific cells and subsequent release of active compounds).

Based on the versatility of glyconanotechnology methods, we have designed and prepared in this work gold GNPs incorporating significant molecules able to interfere in HIV-1 life cycle (Figure 12).
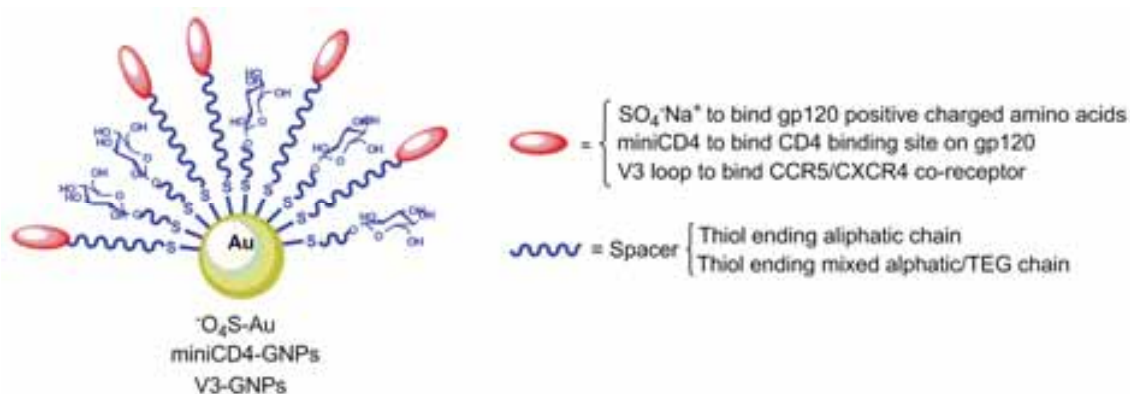
Figure 12. GNPs prepared in this thesis. Three groups of GNPs were prepared: GNPs covered with sulphates groups to bind gp120 positive charged amino acids, GNPs bringing miniCD4 miniprotein to bind to CD4 binding site on gp120 and GNPs with V3 loop peptides to bind to CCR5/CXCR4 co-receptors and to study as immunogen.

The selected molecules (sulphate and miniCD4 derivatives) are thought to reduce HIV entry into host cells by blocking specific regions of gp120, whereas a specific V3 peptide should block binding domains of HIV co-receptors. The multimerization of these molecules on GNPs was expected to increase their activity.

V3 loop in gp120 is able to elicit broadly neutralizing anti-V3 Ab (bNAb). We expected that multiple copies of V3 on GNPs will be also able to elicit anti V3 Ab. Previously, we showed that GNPs bearing multiple copies of a synthetic tetrasaccharide epitope

related to the *Streptococcus pneumoniae* and a T-helper peptide were able to stimulate the production of anti-carbohydrate Abs.[90]

Each chapter of this thesis is dedicated to the GNPs prepared with the selected molecules and the exploration of their properties as HIV anti-virals.

Chapter 1

One important step in HIV entry is the binding between V3 loop of gp120 and the host cell coreceptors CCR5 or CXCR4. V3 peptide is strongly positive charged and bind tyrosines sulfates of co-receptor N-terminal region. To neutralize HIV and block the entry, sulphated gold glyconanoparticles (SO_4-GNPs), able to bind positive charges on V3, were prepared and characterized. The interaction of SO_4-GNPs with gp120 was studied by surface plasmon resonance (SPR). To investigate the cell uptake of SO_4-GNPs, fluorescently labelled sulphated gold glyconanoparticles (SO_4-GNPs-FITC) were prepared and a preliminary study of cellular uptake in Raji cells was carried out. HIV-1 neutralization experiments were also performed in collaboration with Dr. Alcamí, (AIDS Immunopathogenesis Unit, Instituto de Salud Carlos III (ISCIII) Madrid), partner in the CHAARM project.

Chapter 2

HIV gp120 bind to CD4 in the first step of viral entry process. GNPs containing miniCD4 peptides, were prepared to compete with the binding of gp120 to cellular CD4 (miniCD4 from Dr. Loic Martin, Commisariat a l'Energie Atomique (CEA), partner in the CHAARM project). Three different miniCD4-GNPs were prepared: with only miniCD4, with cholesterol (miniCD4-GNP-Chol) and with sulphate linkers (miniCD4-GNP-SO_4). The structure of miniCD4 on the three GNPs was studied by circular dichroism (CD). SPR binding experiments to gp120 were also carried out. Moreover, HIV neutralization experiments were performed in the laboratory of Dr. Elisa Vicenzi (San Raffaele Hospital (HSR) Milan, Italy), partner in the CHAARM project.

Chapter 3

In the first two chapters GNPs that have HIV gp120 as target were presented. An alternative strategy is to prepare GNPs that bind and block HIV host cell receptors or coreceptors. In this chapter, the preparation and characterization of GNPs bearing V3 peptide (V3-GNPs) is presented. We have demonstrated that GNPs bearing only

---

[90] Gold nanoparticles as carriers for a synthetic *Streptococcus pneumoniae* type 14 conjugate vaccine. *Nanomedicine* (2012) 7(5), 651–662

glucose and carboxylic ending linkers are able to modulate the conformation of V3 peptide to obtain V3 constructs with well defined conformations. Depending on the experimental conditions, V3 peptide (that is essentially random coil) can assume a predominant α-helix or β-strand conformation in presence of GNPs as showed by circular dichroism (CD). V3-GNPs were also characterized by ^{1}HNMR, gel electrophoresis and Z-potential. The interaction of V3-GNPs with the anti-V3 antibody 447-52D was studied by SPR. HIV-1 neutralizing experiments with V3-GNPs were carried out. To study the immunogenic properties of V3 peptide on GNPs, Balb/c mice were immunized with V3β-GNP and antibody in mice sera were analyzed.

CHAPTER 1

Sulphated gold glyconanoparticles as anti-HIV agents

In the frame of CHAARM project

CHAPTER 1

Sulphated gold glyconanoparticles as anti-HIV agents

INTRODUCTION

HIV is spread predominantly through sexual transmission.[1] Right now, the best HIV prevention options for sexually active people is using condoms. However, for many people, especially for women, this option is not possible.

Microbicides are antimicrobial products formulated for application to the surface of the vagina and/or rectum for the prevention of HIV transmission during sexual intercourse.[2] They are considered to be one of the most promising preventive interventions on HIV infection.[3] It is believed that topical microbicides might be more effective than condoms in preventing HIV infection because they would be easier to use and women would not have to negotiate their use. Worldwide half of the people living with HIV are women. To be successful in reducing HIV transmission the ideal topical microbicide must have several characteristics:

- it must be safe and effective
- inexpensive and widely accepted
- available in both spermicidal and non-spermicidal formulations
- able to be used without partner knowledge.

Many compounds were studied as microbicides, for example: antibodies (b12, 2G12 and 2F5), chemokines (PSC RANTES), carbohydrate-binding proteins (cyanovirin-N and soluble DC-SIGN), peptide (T20), drugs (tenofovir), and polyanions (carraguard, cellulose sulfate and PRO2000).[4] Until now only drug and polyanions containing gels arrived until phase III clinical trial. Carraguard,[5] PRO2000 (0.5% buffer gel)[6] and

---

[1] http://aids.gov/hiv-aids-basics/prevention/prevention-research/microbicides/

[2] http://www.hptn.org/prevention_science/microbicides.asp

[3] http://www.niaid.nih.gov/topics/HIVAIDS/Research/prevention/Pages/topicalResearch.aspx

[4] J. D. Reeves, C. A. Derdeyn, *Entry Inhibitors in HIV Therapy.* Birkhauser Verlag. (2007).

[5] Skoler-Karpoff, S., Ramjee, G., Ahmed, K., Altini, L., Plagianos, M. G., Friedland, B., Govender, S., De Kock, A., Cassim, N., Palanee, T., Dozier, G., Maguire, R., and Lahteenmaki, P. (2008). Efficacy of Carraguard for prevention of HIV infection in women in South Africa: a randomised, double-blind, placebo-controlled trial. *Lancet.* **6**, 372, 1977-1987.

cellulose sulphate (6% vaginal gel)[7] have little or no effect on reducing a woman's risk of HIV infection. However, in 2010, a phase III clinical trial demonstrated that tenofovir gel appears safe and effective in preventing HIV infection.[8] Nevertheless, tenofovir gel reduced HIV acquisition by an estimated 39% overall, and by 54% in women with high gel adherence. The achievement of the 100% protection is still far, and HIV microbicides research is still necessary. It is widely accepted that one way could be to use a gel containing different molecules able to neutralize HIV virus.

In 2004 our laboratory began to work in HIV microbicides in the frame of the European Microbicides Project (EMPRO). EMPRO stopped in 2008 and a new European project on microbicides began: CHAARM (Combined Highly Active Anti-Retroviral Microbicides).[9] The experience of our laboratory in the preparation of gold glyconanoparticles (GNPs) as a platform to combine different molecules was the entry to participate in these projects. Our contribution to the CHAARM project consists in the preparation of new multivalent systems based on GNPs to block HIV infection by combining different microbicides on the gold surface. It is well known that polysulphated compounds are potent inhibitors of various enveloped viruses, [10] and most of the microbicides developed to neutralize HIV are sulphated polymers (carraguard, cellulose sulphate and PRO2000).

---

[6] Karim, S. S. A., Richardson, B. A., Ramjee, G., Hoffman, I. F., Chirenje, Z. M., Taha, T., Kapina, M., Maslankowski, L., Coletti, A., Profy, A., Moench, T. R., Piwowar-Manning, E., Mâsse, B., Hillier, S. L., and Soto-Torres, L., on behalf of the HPTN 035 Study Team. (2011). Safety and effectiveness of buffer gel and 0.5% PRO2000 gel for the prevention of HIV infection in women. *AIDS* **24**, 957–966.

[7] Van Damme, L., Govinden, R., Mirembe, F. M., Guédou, F., Solomon, S., Becker, M. L., Pradeep, Krishnan, A. K., Alary, M., Pande, B., Ramjee, G., Deese, J., Crucitti, T., and Taylor, D. (2008). Lack of effectiveness of cellulose sulfate gel for the prevention of vaginal HIV transmission. *N. Engl. J. Med.* **359**, 463-472.

[8] Karim, Q. A., Karim, S. S. A., Frohlich, J. A., Grobler, A. C., Baxter, C., Mansoor, L. E., Kharsany, A. B. M., Sibeko, S., Mlisana, K. P., Omar, Z., Gengiah, T. N., Maarschalk, S., Arulappan, N., Mlotshwa, M., Morris, L., Taylor, D., on behalf of the CAPRISA 004 Trial Group. (2010). Effectiveness and Safety of Tenofovir Gel, an Antiretroviral Microbicide, for the Prevention of HIV Infection in Women. *Science.* **329**, 1168-1174.

[9] http://chaarm.eu/

[10] (a) Witvrouw, M., Desmyter, J., and De Clercq, E. (1994). Antiviral portrait series: 4. Polysulfates as inhibitors of HIV and other enveloped viruses. *Antiviral Chem. Chemother.*, **5**, 345-359. (b) Scordi-Bello, I. A., Mosoian, A., He, C. J., Chen, Y. B., Cheng, Y., Jarvis, G. A., Keller, M. J., Hogarty, K., Waller, D. P., Profy, A. T., Herold, B. C., and Klotman, M. E. (2005). Candidate Sulfonated and Sulfated Topical Microbicides: Comparison of Anti-Human Immunodeficiency Virus Activities and Mechanisms of Action. *Antimicrob. Agents Chemother.*, **49**, 3607-3615.

The molecular basis of the HIV neutralization trough polyanions is strictly related with blocking the positive charged amino acids of gp120.[11] Positive charged amino acids of gp120 are mainly located in the V3 loop, and are responsible for the interaction with tyrosines sulphate present in the N-terminus of the CCR5 coreceptor of target cells.[12, 13] Kwong et al showed that positive charged regions point towards host cell membrane (Figure 1). Moreover, besides V3, there are other regions of gp120 containing multiple basic amino acids, the C-terminal region (amino acids 495-516) and discontinuous amino acids in regions 117-123, 207 and 419-444.
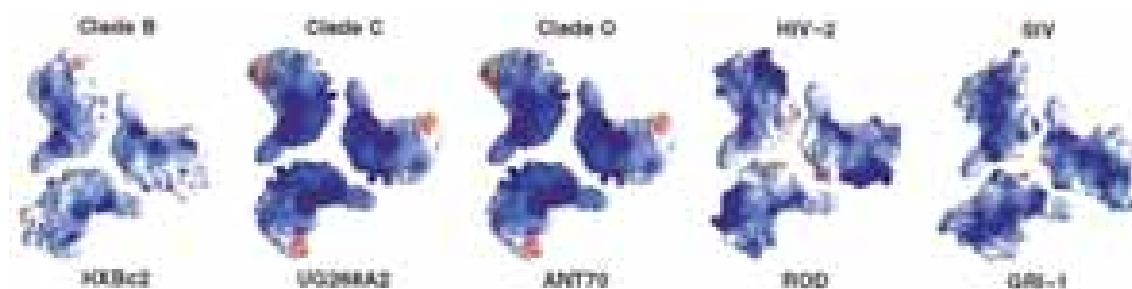
Figure 1. Electrostatic surface view of basic cell-facing surface of different gp120. Homology modeling was used to construct the corresponding structures of core gp120 for HIV-1 clades C and O as well as HIV-2 and SIV, starting with the crystal structure of HIV-1 clade B core gp120 modeled as the envelope oligomer. A positive charged (dark blue) surface can be seen in all isolates, although the precise charge distribution show variation.[14]

GNPs are 3D nanostructures with globular shape, and proteins similar size. We thought that GNPs decorated with ligands presenting sulphate group could interact with the positive charged regions of gp120 and inhibit virus infection by a mechanism similar to other sulphated molecules (natural and synthetic oligomers and polymers). In figure 2 is showed a gp120 trimeric model and a possible interaction with a negatively charged GNP.

---

[11] Moulard, M., Lortat-Jacob, H., Mondor, I., Roca, G., Wyatt, R., Sodroski, J., Lu, Z., Olson, W., Kwong, P. D., and Sattentau, Q. J. (2000). Selective polyanion interactions with basic surfaces on human immunodeficiency virus type 1 gp120. *J. Virol.* **74**, 1948-1960.

[12] Kwong, P. D., Wyatt, R., Robinson, J., Sweet, R. W., Sodroski, J., and Hendrickson, W. A. (1998). Structure of an HIV gp120 envelope glycoprotein in complex with the CD4 receptor and a neutralizing human antibody. *Nature*. **393**, 648-659.

[13] Rizzuto, C. D., Wyatt, R., Hernandez-Ramos, N., Sun, Y., Kwong, P. D., Hendrickson, W. A., and Sodroski, J. (1998). A conserved HIV gp120 glycoprotein structure involved in chemokine receptor binding. *Science* **280**, 1949-1953.

[14] Kwong, P. D., Wyatt R, Sattentau QJ, Sodroski J, Hendrickson WA. (2000). Oligomeric modeling and electrostatic analysis of the gp120 envelope glycoprotein of human immunodeficiency virus. *J. Virol.* **74**, 1961-1972.

GNPs posses an important advantage respect other multivalent systems. GNPs preparation gives the opportunity to place, in a controlled way, two or more kind of molecules on the same gold nucleus. In this way, the same GNPs can interact with different regions of the same target or with different target related to different biochemical processes.
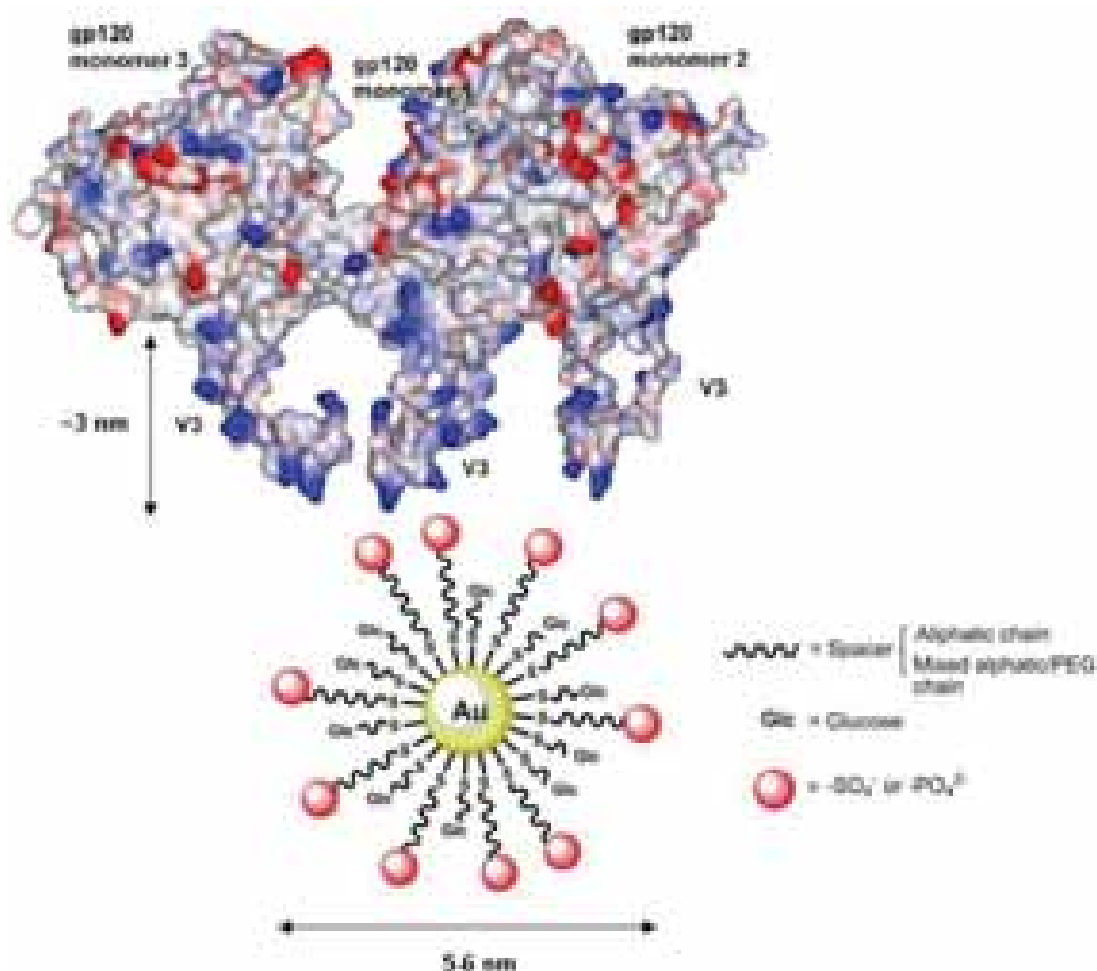
Figure 2. Electrostatic surfaces of a wild type gp120 model (Protein Data Bank ID: 2B4C). Side-view of the gp120 trimer with the V3 loops pointing towards the target cell membrane. The space between the gp120 monomers would normally be occupied by gp41. The solvent accessible surfaces are mapped with regions of negative (red) and positive (blue) electrostatic potential (charge). The positive charges of gp120 V3 loop can interact with negative charged surface of GNPs. Adapted from reference 15 and 16. [15, 16]

In the present work, a series of sulphated and phosphorylated gold glyconanoparticles (^-O_4S-Au and $^{2-}O_4P$-Au, respectively) were prepared and characterized (Figure 3).

---

[15] Huang, C., Tang, M., Zhang, M., Majeed, S., Montabana, E., Stanfield, R. L., Dimitrov, D. S., Korber, B., Sodroski, J., Wilson, I. A., Wyatt, R., and Kwong, P. D. (2005). Structure of a V3-containing HIV-1 gp120 core. *Science.* **310**, 1025-1028.

[16] Tyssen, D., Henderson, S. A., Johnson, A., Sterjovski, J., Moore, K., La, J., Zanin, M., Sonza, S., Karellas, P., Giannis, M. P., Krippner, G., Wesselingh, S., McCarthy, T., Gorry, P. R., Ramsland, P. A., Cone, R., Paull, J. R. A., Lewis, G. R., and Tachedjian, G. (2010). Structure activity relationship of dendrimer microbicides with dual action antiviral activity. *PLoS ONE* **5**, e12309-12324.
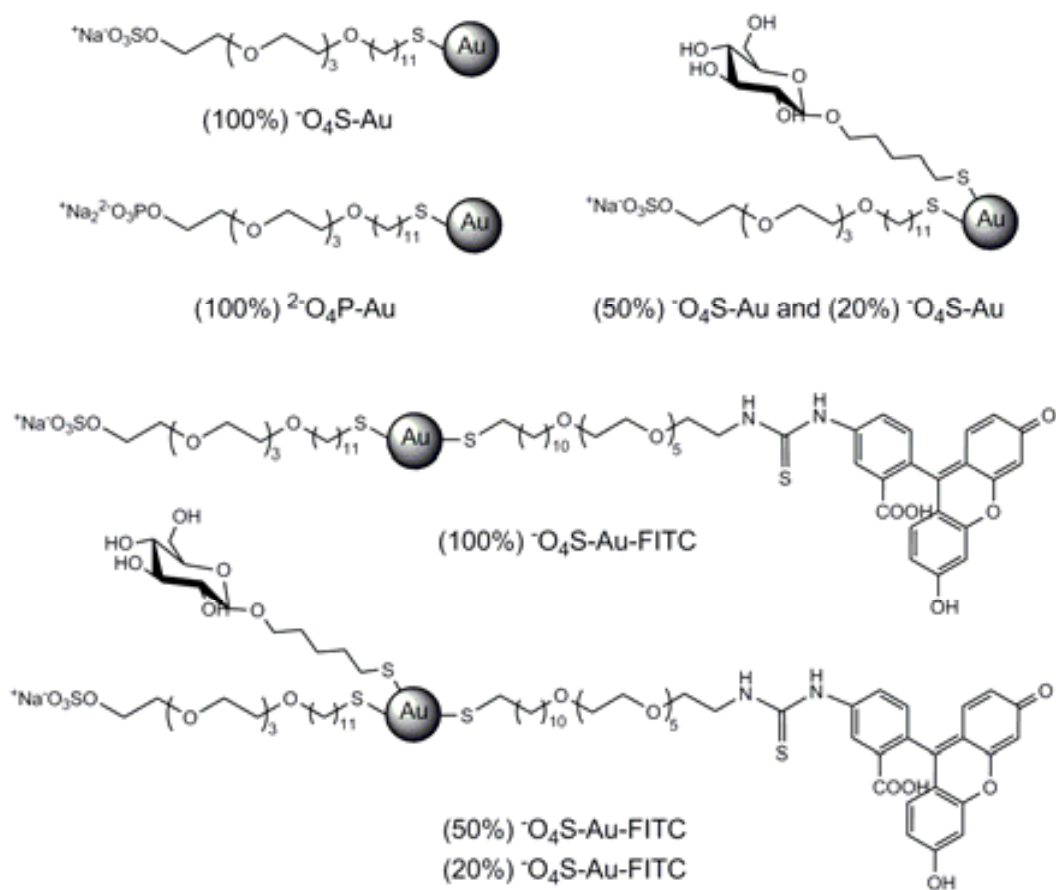
Figure 3. Negatively charged GNPs prepared in this work. The percentage that appears in bracket in the GNP name indicates the % of negatively charged ligand on the GNP. Gold nanoparticles completely covered with only thiol ending phosphate linker were prepared ((100%) $^{2-}O_4P$-Au). Sulphated GNPs covered with different density of a sulphated thiol ending linker (100%, 50% and 20%) and glucose conjugate were prepared. The corresponding fluorescent sulphated GNPs were also prepared with 5% of a fluorescein isothiocyanate linker (FITC).

The phosphorylated nanoparticles were prepared to be used as control nanoparticles. T. Dragic et al. demonstrated that despite the presence of negative charges, phosphorylated peptides derived from the N-terminal of CCR5 coreceptor are not able to inhibit HIV-1 (R5) entry as the sulphated peptides do.[17]

A series of gold nanoparticles bearing the negative charged sulphate (100% ^-O_4S-Au) or phosphate (100% $^{2-}O_4P$-Au) groups were prepared. A second series of sulphated GNPs ((50%) O_4S-Au and (20%) ^-O_4S-Au) with varying density was also prepared. The control of ligand density on GNPs was achieved by using the glucose conjugate to 5-

---

[17] Cormier, E. G., Persuh, M., Thompson, D. A. D., Lin, S. W., Sakmar, T. P., Olson, W. C., and Dragic, T. (2000). Specific interaction of CCR5 amino-terminal domain peptides containing sulfotyrosines with HIV-1 envelope glycoprotein gp120. *PNAS*, **97**, 5762–5767.

mercaptopentyl β-D-glucopyranoside (GlcC$_5$). GlcC$_5$ is used as inner component and give solubility and biocompatibility to GNPs. To follow uptake and internalization of the nanoparticles by cells a third series of sulphated GNPs bearing fluorescein was also prepared ((100%) $^-$O$_4$S-Au-FITC, (50%) $^-$O$_4$S-Au-FITC and (20%) $^-$O$_4$S-Au-FITC).

The interaction of these GNP with gp120 was studied by Surface Plasmon Resonance (SPR) and preliminary experiments were performed to study O$_4$S-Au uptake by cells,. Internalization of different density $^-$O$_4$S-Au-FITC by Raji cells was studied by flow cytometry and confocal microscopy. Viability cellular assays and HIV-1 neutralization experiments were also performed with different density $^-$O$_4$S-Au.

RESULTS AND DISCUSSION

Synthesis

The GNPs were prepared by using a well established procedure developed in our laboratory.[18] In this kind of preparation a thiol ending ligand is needed to cover the gold cluster formed. For the preparation of the GNPs showed in Figure 3 the appropriate thiol ending molecules have been synthesized (Figure 4).
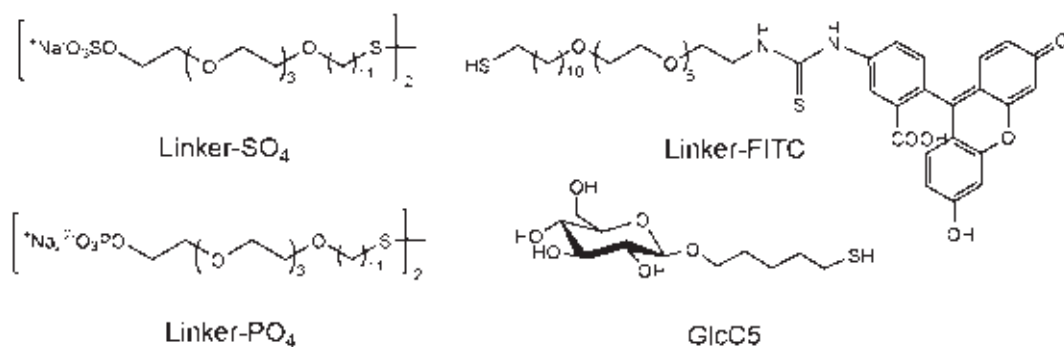
Figure 4. Thiol ending molecules used for the preparation of the GNPs presented in this chapter. Linker-SO$_4$ and Linker-PO$_4$, were used to prepare $^-$O$_4$S-Au and $^{2-}$O$_4$P-Au, respectively. Linker-FITC was used to give fluorescence to GNPs and GlcC$_5$ to control density on the GNPs.

All the ligands used in this work present three different parts: the active part (sulphate, phosphate, FITC or glucose), the spacer (or linker) and the thiol or disulphide. Thiols

---

[18] Barrientos, A. G., de la Fuente, J. M., Rojas, T. C., Fernández, A., and Penadés, S. (2003). Gold glyconanoparticles: synthetic polyvalent ligands mimicking glycocalyx-like surfaces as tools for glycobiological studies. *Chem. Eur. J.*, **9**, 1909-1921.

ord disulphides groups are necessary to create a stable bond with the gold cluster. The linkers are different: glucose was conjugate to the short aliphatic linker, while longer aliphatic/ethylenglycol mixed linker was used to prepare the charged ligands and the fluorescein conjugate. The aliphatic part of the linker guarantees the formation of an ordered and stable self assembled monolayer on gold. The length of the linker depends on the distance needed between the gold nucleus the active molecule. Tetraethyleneglycol was used to prepare longer linkers. Moreover, ethylenglycol moiety ensures flexibility, assists water solubility and defends against non-specific adsorption of other biomolecules and cells.[19]

Preparation of bifunctional linkers

The synthesis of sulphate ligand (Linker-SO$_4$) and phosphate ligand (Linker-PO$_4$) was performed following the reaction steps showed in Scheme 1.
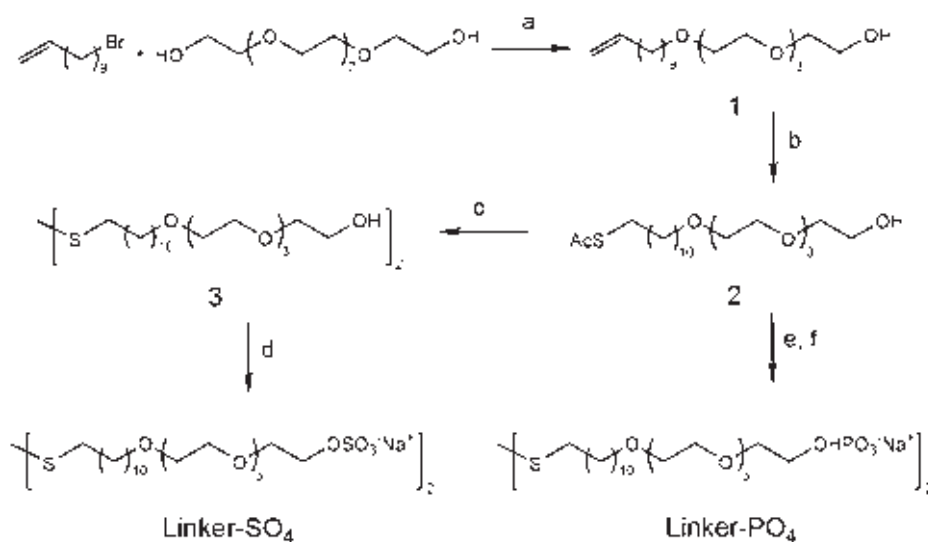
Scheme 1. Reagents and conditions. a) NaOH (50%), 100ºC, 16h, 69%. b) AcSH, AIBN, THFdry, reflux, 3h, 67%. C) (i) MeONa, MeOH, 15h (ii) amberlite IR-120, 85%. d) py·SO$_3$, DMF, 50ºC, 7h, 74%. e) (i) P(O)Cl$_3$, CH$_2$Cl$_2$, 25 ºC, 30 min (ii) dioxane-water, 25 ºC, 12 h. f) (i) MeONa, MeOH, 15h (ii) amberlite IR-120, 98%.

Both sulphate and phosphate linker preparations start with the synthesis of compound **1**. Compound **1** was prepared by nucleophilic substitution of 11-bromo-undecene with tetraethylenglycol (TEG) in presence of NaOH 50%. Addition of tioacetic group was

---

[19] Love, J. C., Estroff, L. A., Kriebel, J. K., Nuzzo, R. G., and Whitesides, G. M. (2005). Self-assembled monolayers of thiolates on metals as a form of nanotechnology. *Chem. Rev.* **105**, 1103-1169.

carried out by radical reaction on the double bond in presence of tioacetic acid with azobisisobutyronitrile (AIBN) as catalyst, to obtain compound **2**.

The sulphation of hydroxyl groups is a well established reaction.[20] Sulphation of hydroxyl group with HSO_3Cl in DMF or $Et_3N·SO_3$/ $Py·SO_3$ in DMF at 50ºC are usual procedure that give high yields. Both procedures work well for the sulphation of compound **2**. Three different deacetylation reactions were used to deprotect sulphated compound **2** (not showed in scheme 1): sodium methoxide in methanol (MeONa/MeOH), hydrazine acetate in ethanol ($AcOH·NH_2NH_2$/EtOH) and ethanol chloride solutions (EtOH/HCl). However, these deacetylation procedures partially hydrolyze the sulphate groups. For this reason deacetylation was carried out with MeONa/MeOH before sulphation to obtain compound **3**. The reaction was left stirring for 24 h until the complete formation of a disulphide moiety. For the sulphation of disulphide **3**, pyridinium sulphate complex ($Py·SO_3$) was used.

$GlcC_5$ was used to control density of sulphated linker and, at the same time, give solubility and biocompatibility of the GNPs. Because of the shorter linker, the glucose moiety remains inside of the organic shell of the GNPs giving more accessibility to the charged linker.

For the preparation of fluorescently labelled GNPs, fluorescein isothiocyanate (FITC) was conjugated to a longer spacer makes up of eleven carbons aliphatic and hexaethylenglycol chains, as already described.[21] A longer spacer was used because it has been reported that shorter linker cause quenching of the fluorescence due to the proximity to the gold nucleus. Linker-FITC was always used in 5% in the preparation of fluorescent GNPs. All molecules prepared present a thiol or disulfide group at the end of the spacer, which is a fundamental moiety for the formation of the self-assembled monolayers on GNPs.

GNPs preparation

The one-pot reaction was used to prepare the GNPs.[18] where the reduction of a gold salt in the presence of the thiol ligand induces the formation of a S-Au bond between the metallic core and the thiol linkers to give the thiol protected gold nanocluster. All the GNP preparations were performed in a mixture of $MeOH/H_2O/CH_3COOH$ (3:3:1) in

---

[20] a) Krylov, V. B., Ustyzhanina, N. E., Grachev, A., and Nifantiev, N. (2008). Efficient acid- promoted per-O-sulfation of organic polyols. *Tetrahedron Lett.* **49**, 5877-5879. b) Vongchan, P., Sajomsang, W., Subyen, D., and Kongtawelert, P. (2002). Anticuagulant activity of a sulphated chitosan. *Carbohydr. Res.* **337**, 1239-1242.

[21] Martinez-Avila, O., Hijazi, K., Marradi, M., Clavel, C., Campion, C., Kelly, C., Penades, S. (2009). Gold manno-glyconanoparticles: multivalent systems to block HIV-1 gp120 binding to the lectin DC-SIGN. *Chem. Eur. J.*, **15**, 9874-9888.

presence of NaBH$_4$ solution (1 N, 22 equiv), HAuCl$_4$ (0.025 M, 1 equiv) and a specific ratio of thiol/disulphide ligands (Scheme 2).
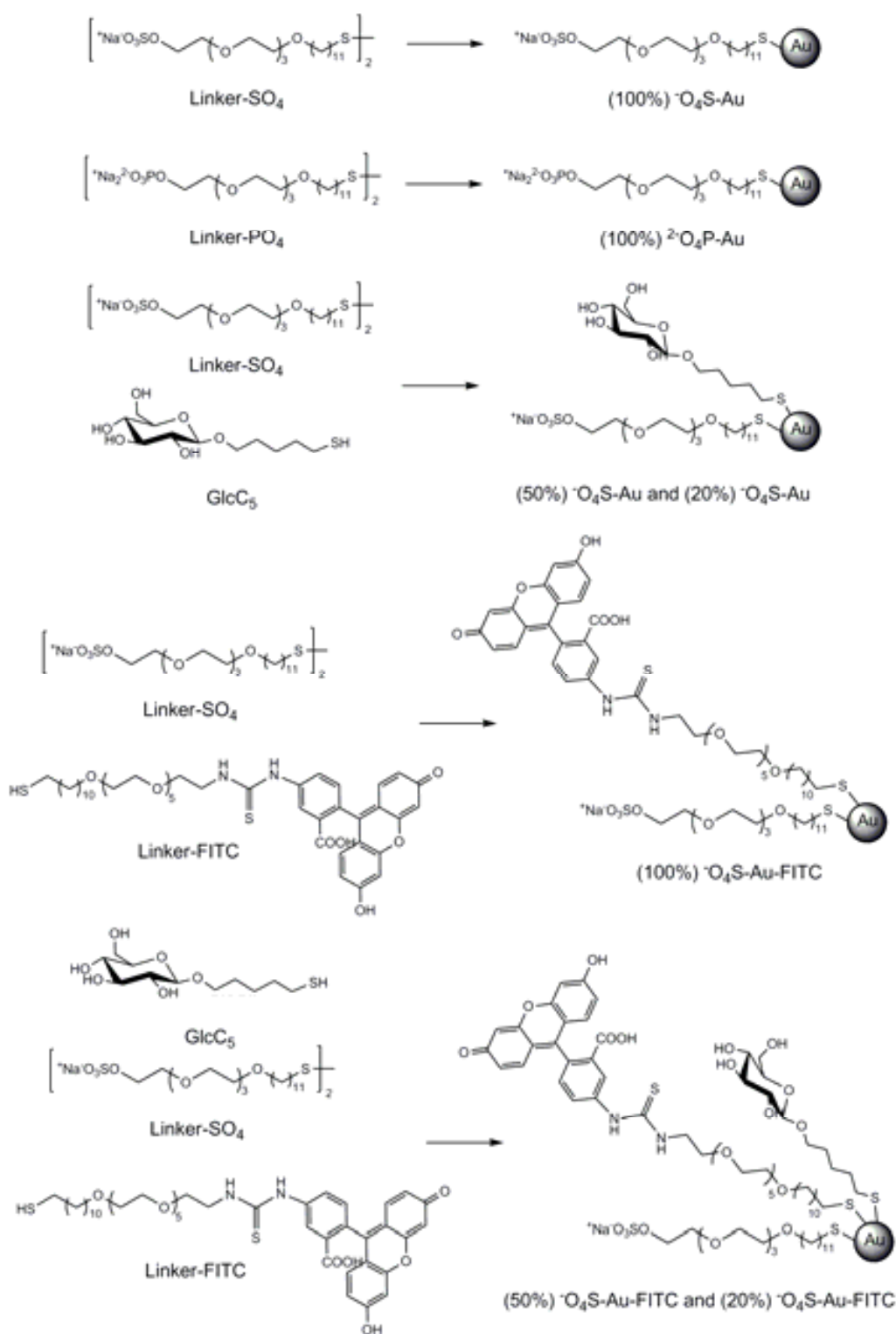
Scheme 2. Preparation of GNPs. All nanoparticles were prepared in the same conditions: HAuCl$_4$, NaBH$_4$, MeOH/H$_2$O/CH$_3$CO$_2$H (3:3:1), 25 °C, 2 h.

For the preparation of (50%) and (20%) ^-O_4S-Au, a 1:1 and 2:8 ratio of Linker-SO_4 and GlcC$_5$ was used, respectively. To prepare (100%) ^-O_4S-Au the Linker-SO_4 was used. For the preparation of (50%) and (20%) ^-O_4S-Au-FITC, mixtures of Linker-SO_4, Linker-FITC and GlcC$_5$ with ratios 5:0.5:4.5 and 2:0.5:7.5 were used, respectively. For the synthesis of (100%) ^-O_4S-Au-FITC a mixture of Linker-SO_4 and Linker-FITC in a 9.5:0.5 ratio was used.

All the GNPs were characterized by transmission electron microscopy (TEM), ^{1}HNMR, UV-vis and elemental analysis. Tipical GNP characterization is showed as an example in figure 5 ((50%) ^-O_4S-Au-FITC).
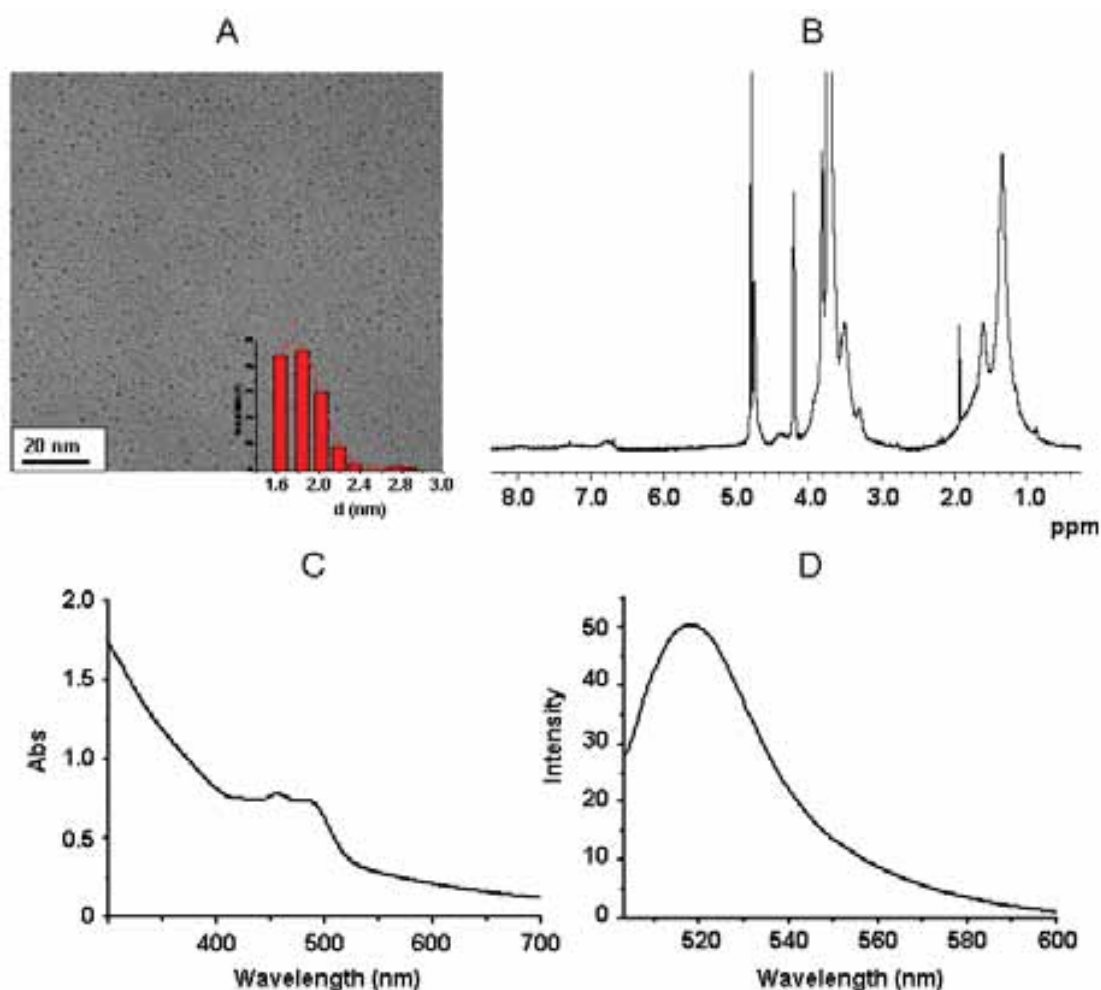
Figure 5. Characterization of (50%) ^-O_4S-Au-FITC. A) TEM picture (0.1 mg/ml in H_2O) shows the size of gold nucleus. This preparation gives nanoparticles with gold diameter around 2 nm. B) ^{1}HNMR (500 Mhz, 1 mg/ml D_2O) shows tipical protons broad signal of the organic shell around the gold. Three regions are detected (0.8-2.2 ppm, aliphatic protons; 2.8-4.6 ppm, CH_2-O, CH-OH and CH_2-SO_4; 6.8-8 ppm aromatic of FITC). C) UV-vis (0.1 mg/ml in H_2O) shows FITC assorbance. D) Fluorescence spectrum (0.1 mg/ml in H_2O) shows the emission of FITC.

(50%) ^-O_4S-Au-FITC present a narrow size distribution with average diameter of 1.7 ± 0.6. As usually occurs, the ^{1}HNMR of (50%) ^-O_4S-Au-FITC is characterized by broad

signals. The signal of the methylene in α position to the sulphate group is observed at 4.2 ppm). The anomeric proton of glucose (around 4.4 ppm) and the aromatic protons of FITC (6.8-7.4 ppm) were also detected. The presence of FITC in the GNPs was also confirmed by UV-vis (λ_{Abs}= 495 nm) and by fluorescence spectroscopy (λ_{em}= 520 nm). The average molecular weights and number of Linker-SO_4 or LinkerPO_4 per NP were calculated from the gold cluster size (as determined by TEM) and elemental analysis (Table 1).

Table 1. Physical features of GNPs prepared.

GNPs	d (nm)	N° gold atoms	N° of total chains	N° of SO_4 or PO_4 chains	Molecular formula	MW (kDa)
(100%) ^-O_4S-Au	1.7 ± 0.8	225	140	140	$Au_{225}(C_{10}H_{20}O_4S_2)_{140}$	109
(50%) ^-O_4S-Au	2.3 ± 0.5	586	272	160	$Au_{586}(C_{10}H_{20}O_4S_2)_{160}(C_{11}H_{22}O_6S)_{112}$	220
(20%) ^-O_4S-Au	2.6 ± 0.4	586	272	55	$Au_{586}(C_{10}H_{20}O_4S_2)_{55}(C_{11}H_{22}O_6S)_{217}$	202
(100%) $^{3-}O_4P$-Au	1.7 ± 0.4	225	140	140	$Au_{225}(C_{10}H_{20}O_4P_2)_{140}$	108
(100%) ^-O_4S-Au-FITC	1.7 ± 1.1	201	71	71	$Au_{201}(C_{10}H_{20}O_4S_2)_{67}(C_{44}H_{40}O_{11}N_2S_2)_4$	74
(50%) ^-O_4S-Au-FITC	1.7 ± 0.8	201	71	35	$Au_{201}(C_{10}H_{20}O_4S_2)_{33}(C_{11}H_{22}O_6S)_{33}(C_{44}H_{40}O_{11}N_2S_2)_4$	68
(20%) ^-O_4S-Au-FITC	1.8 ± 0.7	201	71	14	$Au_{201}(C_{10}H_{20}O_4S_2)_{14}(C_{11}H_{22}O_6S)_{62}(C_{44}H_{40}O_{11}N_2S_2)_4$	64

Number of gold atoms, molecular formulas and MW were calculated using the size of gold cluster obtained from TEM by measuring around 200 nanoparticles. Average number of gold atoms (N_{Au}) and total ligands (N_{TL}) per nanoparticle, as well as average molecular formulas and molecular weights (MW) were calculated from the size of gold cluster obtained by TEM as reported in the literature and confirmed by elemental analysis.[22] Average number of charged ligands (Linker-SO_4 or Linker-PO_4) per nanoparticle was determined by analysing the mixture of the ligands by ^{1}HNMR before and after the nanoparticles formation.

The (100%) ^-O_4S-Au displayed around 140 sulphated ligands in a gold cluster of 1.7 nm average diameter while (50%) ^-O_4S-Au was bigger in size (2.6 nm diameter) but approximately accommodated the same number of sulphated ligands, in addition to $GlcC_5$ as second ligand. Similarly to (50%) ^-O_4S-Au, the (20%) ^-O_4S-Au had an average gold cluster diameter of 2.3 nm, but displayed less sulfated ligands (~55), the rest being the inert component $GlcC_5$. TEM images of as-synthesized NPs also showed that are well dispersed. Low surface plasmon signal around 520 nm was observed in UV–vis spectra due to the small size of the NPs.

---

[22] Hostetler, M. J., Wingate, J. E., Zhong, C. J., Harris, J. E., Vachet, R. W., Clark, M. R., Londono, J. D., Green, S. J., Stokes, J. J., Wignall, G. D., Glish, G. L., Porter, M. D., Evans, N. D., and Murray, R. W. (1998). Alkanethiolate gold cluster molecules with core diameters from 1.5 to 5.2 nm: Core and monolayer properties as a function of core size. *Langmuir* **14**, 17-30.

The stability of the sulphate groups on the GNP were also studied. To determine whether the sulphate group could undergo hydrolysis in water (pH 6.5), a solution of (100%) ^-O_4S-Au (1 mg/ml) in D_2O was controlled every 8 hours for 5 days by ^1H NMR. No change was detected in the integral of methylene protons in alpha position of the sulphate group.

Interaction studies of GNPs

The interaction of the GNPs with gp120 was studied by SPR and by HIV neutralization assays.

SPR experiments

The binding of sulphated and phosphorylated NPs to gp120 was qualitatively evaluated by SPR using a ProteOn™ XPR36 system. Recombinant gp120 was covalently immobilized on the sensorchip by standard methodology at a level of 6000 RU and the substrates were injected at six different concentrations (2, 1, 0.5, 0.25, 0.125, and 0.0625 µg/ml) in TRIS buffered saline at 25 ºC (Figure 6).
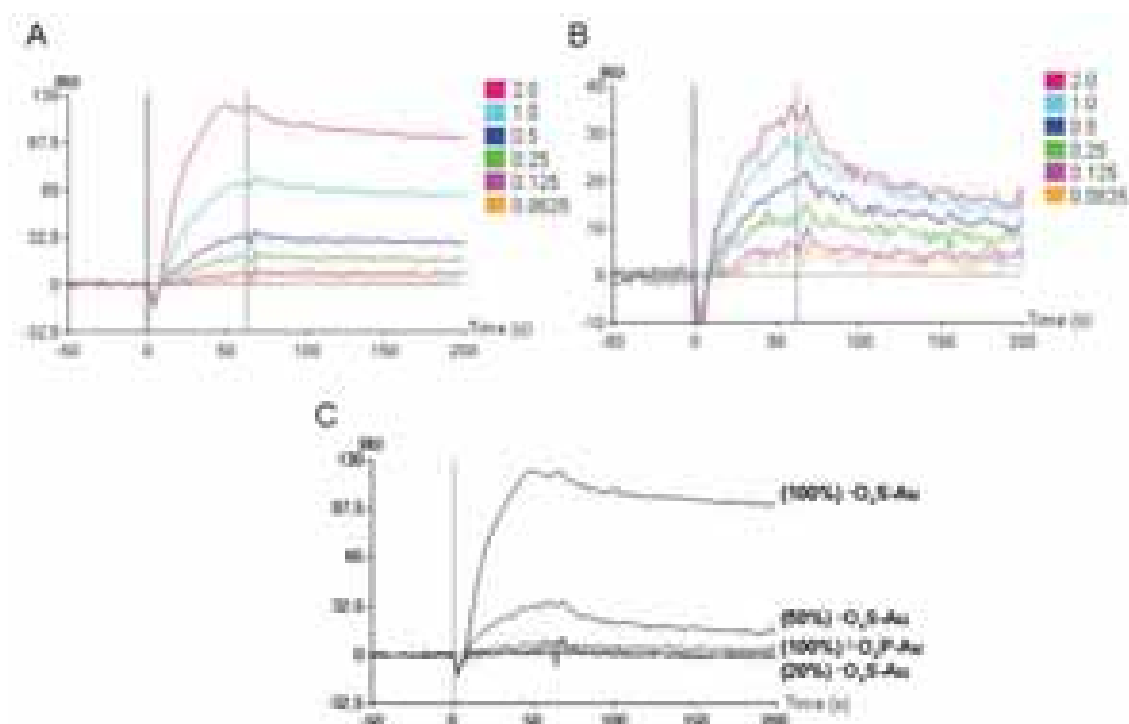
Figure 6. SPR experiments. Sensorgrams representing the dose-dependent binding of (100%) ^-O_4S-Au (A) and (50%) ^-O_4S-Au (B) to immobilized gp120. Six different concentrations in TRIS buffered saline (TRIS 10 mM, NaCl 150 mM, pH 7.4, 0.005% Tween 20) were tested (From 2 to 0.0625 µg/ml). C) Analyses of substrates' binding to gp120 at 2 µg/ml (sensorgrams of Linker-SO₄ and (20%) ^-O_4S-Au overlap at the baseline).

(100%) ^-O_4S-Au and (50%) ^-O_4S-Au showed dose dependent binding affinity to gp120 in this concentration range (Figure 6A and 6B), while (20%) ^-O_4S-Au did not give apparent binding at these concentrations (data not showed). Taking as a reference point the binding response unit (RU) at 30 seconds in the association phase of the sensorgrams, (100%) ^-O_4S-Au and (50%) ^-O_4S-Au gave 97 RU and 25 RU, respectively, at 2 µg/ml, which corresponds to 2.6 µM and 1.3 µM average concentration in terms of Linker-SO$_4$, respectively. To ensure that the binding effect was due to the sulphate moieties, gold NPs in which the sulphate group of (100%) ^-O_4S-Au is formally substituted by a phosphate group, (100%) $^{2-}O_4P$-Au, were also tested. The phosphate group was chosen because, in spite of its anionic character, it is known to have poor anti-HIV activity with respect to the sulfate.[17] No significant binding of (100%) $^{2-}O_4P$-Au to gp120 was detected at 2 µg/ml (<5 RU). These data discard an unspecific effect of the gold core and the linker, demonstrating that the sulphate group is essential to achieve efficient binding. No detectable binding to gp120 was observed with the free Linker-SO$_4$, as disulphide, which presents two sulphate units (2 µg/ml corresponding to 4.2 µM in terms of sulfate ligands).

Cellular experiments

The cytotoxicity of ^-O_4S-Au and ^-O_4S-Au-FITC
The cytotoxicity of O$_4$S-Au and fluorescent O$_4$S-Au-FITC was tested using the MTT or MTS assay. MTS assay (3-(4,5-dimethylthiazol-2-yl)-5-(3-carboxymethoxyphenyl)-2-(4-sulfophenyl)-2H-tetrazolium) is a more recent alternative to MTT.[23] The MTS assay measures the reducing potential of the cells using a colorimetric reaction (scheme 3). Viable cells will reduce the MTS reagent to a colored formazan product giving a purple color.[24] MTS, in presence of phenazine methosulfate (PMS), produces a water-soluble formazan that has an absorbance maximum at 490-500 nm in phosphate buffer. It is advantageous over MTT in that the reagents MTS + PMS are reduced more efficiently than MTT, and the product is water-soluble, decreasing toxicity to cells detected with an insoluble product. These reductions take place only when mitocondrial reductase is active, and therefore conversion is often used as a measure of viable (living) cells (Scheme 2).

---

[23] Cory, A., Owen, T., Barltrop, J., and Cory, J. (1991). Use of an aqueous soluble tetrazolium/formazan assay for cell growth assays in culture. *Cancer communications* **3**, 207-212.

[24] Mosmann, T. (1983). Rapid colorimetric assay for cellular growth and survival: application to proliferation and cytotoxicity assays. *J. Immunol. Methods* **65**, 55-63.
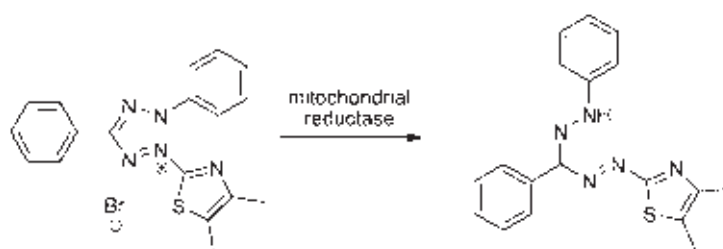
Scheme 2. Reduction of MTS by mitochondrial reductase.

MTS cytotoxicity test was used to evaluate the viability with non adherent Raji cells (human B lymphocyte; Burkitt's lymphoma). ^-O_4S-Au (fluorescent and no fluorescent) were incubated 24 h at 37ºC with Raji cells (10^4 cells) at five different concentrations (50 µg/ml the highest concentration). Absorbance was measured at 490 nm with a Microplate reader (Dynatech MR7000 instruments). The relative cell viability (%) related to control wells containing cell culture medium without nanoparticles was calculated by $[A]_{test}/[A]_{control}$ x 100. No cytotoxicity was detected at the evaluated concentrations (Figure 7A and 7B).
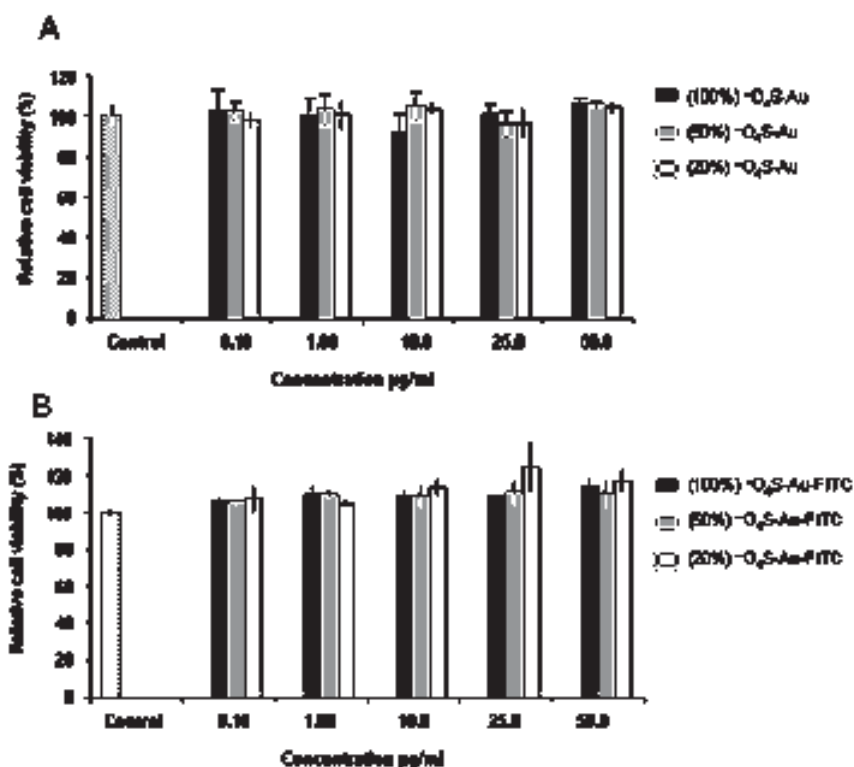
Figure 7. Relative cell viability of with Raji cells in the presence of different concentrations of ^-O_4S-Au (A) and ^-O_4S-Au-FITC (B). GNPs were incubated 24 h at 37ºC, under CO_2 (5%) atmosphere. Data are average of 4 measurements ± standard deviation (SD).

44

To ensure that NPs antiviral activity was not due to toxicity, cell viability of MT-2 cells was measured in the same conditions of the neutralization assay, but no virus was added to the cell culture. GNPs and Lnker-SO_4 were tested up to a concentration of 100 µg/ml and were compared to untreated controls. No toxicity was found and only mild toxic effect was observed with (100%) ^-O_4S-Au at 100 µg/ml (70% of cell viability) (Figure 8).
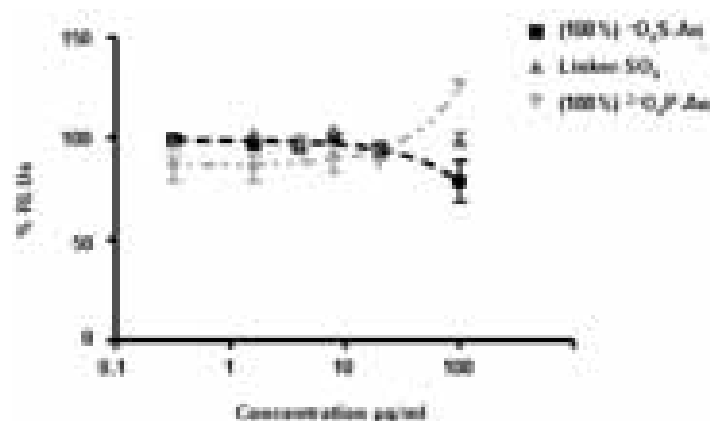
Figure 8. Citotoxicity of Linker-SO_4, ^-O_4S-Au and $^{2-}O_4P$-Au at different concentrations in MT-2 cells.

After 48 hours, CellTiter Glo reagent (Promega) was added to cell culture following the manufacturer instructions and cell viability was evaluated by luminometry. None of the compounds tested showed cell toxicity even at concentrations of 100 µg/ml.

Study of the uptake SO_4-NPs with Raji cells

Most of the new biofunctional nanomaterial has been designed for applications in cellular systems. Because of that an important issue is the study of their behaviour (cytotoxicity, uptake, exocitosis, etc,) in these systems. One of the aims of this work is to intervene with these GNPs in cellular systems related to the infection of HIV (antigen presenting cells and cellular line models). Then, cellular viability and uptake of GNPs with Raji cells were studied.

Uptake of ^-O_4S-Au-FITC by means of flow cytometry

It is very important to understand what happen when GNPs interact with cells, because they are a relative new biofunctional nanomaterial tools. Flow cytometry and confocal microscopy were used to study the uptake of ^-O_4S-Au-FITC to Raji cells.

Uptake kinetics was performed to study a time dependent internalization of (100%), (50%) and (20%) ^-O_4S-Au-FITC in Raji cells. Raji cells were incubated with 25 µg/ml of nanoparticles for 9 h at 37 °C. Flow cytometry measurements were carried out every

hour (except the first two measurements, 30'). The fluorescence intensity increases with time of incubation following the same profile for all ^-O_4S-Au-FITC and getting saturation around 9 h (Figure 9).
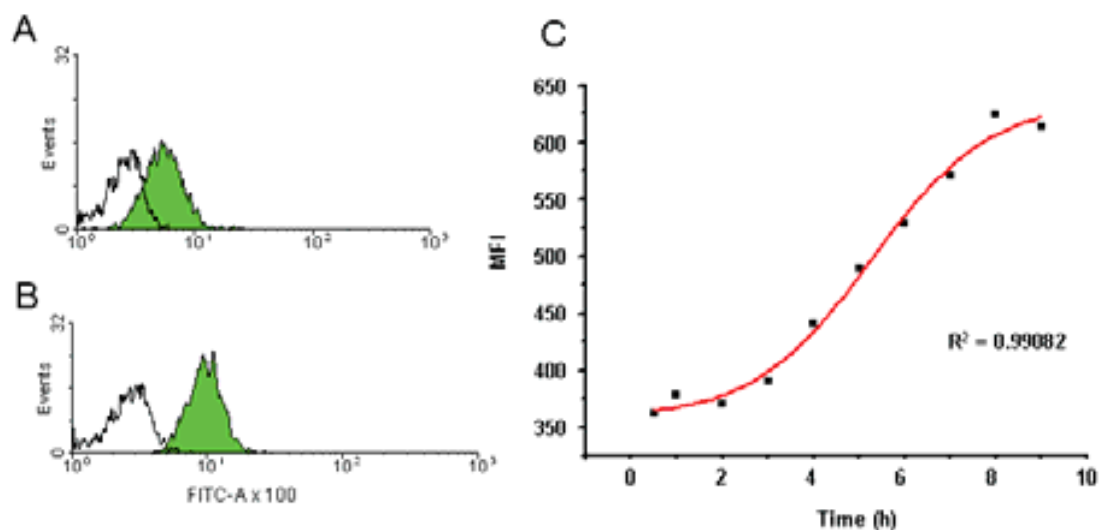
Figure 9. Flow cytometry uptake kinetic study of (50%) ^-O_4S-Au-FITC (25 µg/ml) in Raji cells. A) Flow cytometry data after 30' and B) after 9h. C) Uptake kinetic of (50%) ^-O_4S-Au-FITC

Localization of ^-O_4S-Au-FITC by confocal microscopy

Because flow cytometry does not discriminate between membrane-bound and internalized fluorophore,[25] confocal microscopy study was also performed to check where nanoparticles are located into cells. Raji cells were incubated with ^-O_4S-Au-FITC (25 µg/ml) for 8h at 37°C. After incubation cells were washed 2 times with PBS buffer and then fixed with 2% formaldehyde solution before microscopy experiments. By Z-stack experiments GNPs containing glucose ((50%) and (20%) ^-O_4S-Au-FITC) were detected in the cytoplasm, while most of the (100%) ^-O_4S-Au-FITC remains localized on the cellular membrane (Figure 10).

---

[25] Richard, J. P., Melikov, K., Vives, E., Ramos, C., Verbeure, B., Gait, M. J., Chernomordik, L. V., and Lebleu, B. (2003). Cell-penetrating peptides. A reelavuation of the mechanism of cellular uptake. *J. Biol. Chem.* **278**, 585-590.
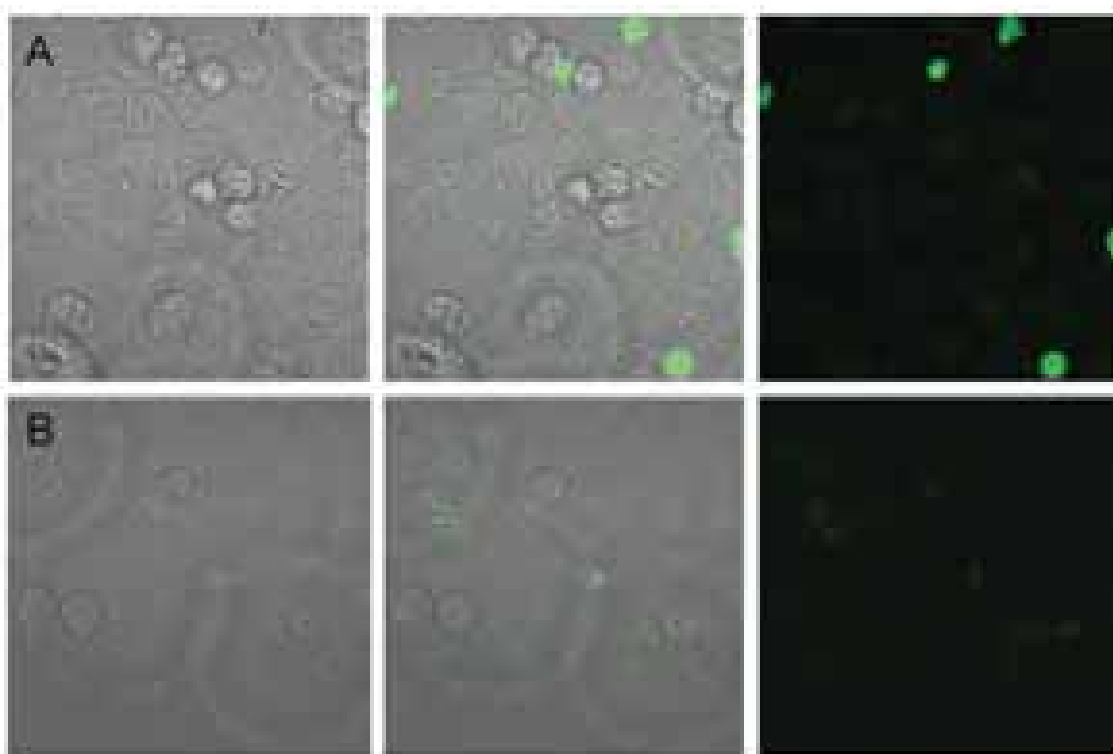
Figure 10. Internalization of 25 µg/ml of GNPs in Raji cells at 37ºC for 8h: A) (50%) $^-O_4$S-Au-FITC and B) (100%) $^-O_4$S-Au- FITC. The figure shows three different pictures for each GNPs. From left to right: bright field, superimposed bright/ fluorescence and fluorescence image.

Sulphated GNPs are not well internalized into the cell studied (Figure 10A and 10B). It seems that (50%) and (20%) $^-O_4$S-Au- FITC, internalize a bit more into the cells while (100%) $^-O_4$S-Au- FITC probably remains more confined on cell membrane but is not able to cross the membrane. Most of the cells present low intensity of fluorescence and only few and irregular-shaped cells show high intensity of fluorescence. Probably, they are no-healthy cells (figure 10A). No fluorescence was detected in the control (Raji cells without nanoparticles). The above results can be considered as a preliminary experiment and a more deep study has to be carried out to investigate the fate of these GNPs in cellular systems.

Neutralization experiments

Encouraged by the SPR screening, Linker-SO_4 and sulphated NPs were tested as anti-HIV systems in cell-based experiments. To evaluate their antiviral activity, MT-2 cells were infected with the X4 tropic NL4.3 Renilla HIV-1 recombinant virus in the presence or absence of the tested compounds. In this neutralization assay, inhibition of HIV-1 infection of MT-2 cells was assessed by use of a recombinant virus carrying the Renilla reporter genes.13 Briefly, NL4.3 Renilla HIV-1 recombinant virus was pre-incubated

47

with different concentrations of the tested compounds for 30 min. Afterwards, viral supernatants were used to infect target MT-2 cells. Viral replication was assessed 48 h post-infection by luciferase activity in cell lysates. The obtained results (Figure 11) indicate that the degree of sulphate density on the gold surface has an important effect on the inhibition of HIV-1 infection of MT-2 cells.
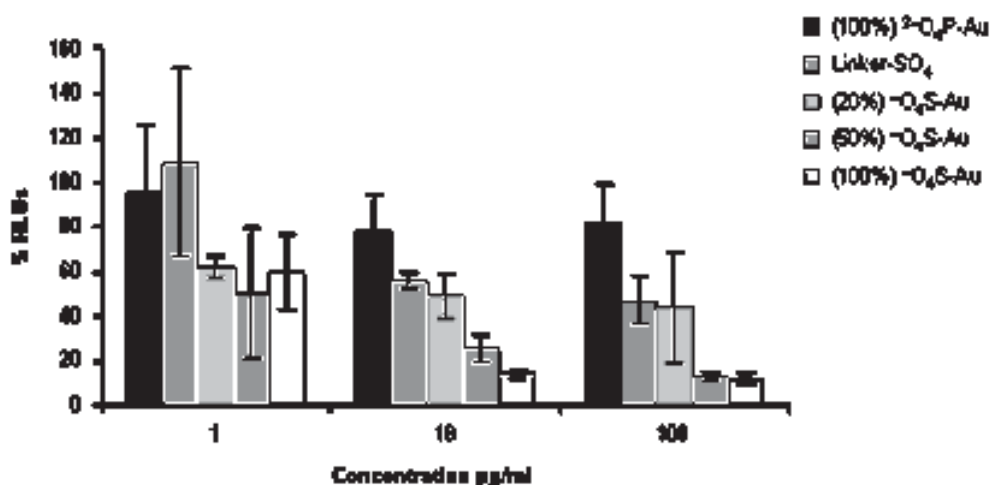
Figure 11. HIV neutralization assays. Inhibition of recombinant virus NL4.3 Renilla HIV-1 (X4) infection of MT-2 cells at different concentrations of tested compounds (Linker-SO_4 and (100%), (50%) and (20%) ^-O_4S-Au). $^{2-}O_4P$-Au was used as a negative control. Results are expressed as percentages of infection related to untreated control. Data represent the mean of three independent experiments ± SEM (Standard Error of the Mean).

Gold nanoparticles (100%) and (50%) ^-O_4S-Au, were more active than (20%) ^-O_4S-Au at concentrations of 10 µg/ml and higher. In this range of concentrations, (20%) ^-O_4S-Au and Linker-SO_4 displayed a similar behaviour. In the same assay, (100%) $^{2-}O_4P$-Au were unable to significantly inhibit viral replication even at 100 µg/ml, demonstrating that the inhibitory effect of (100%) and (50%) ^-O_4S-Au was neither due to the gold core of the nanoparticles nor to the aliphatic-tetraethyleneglycol moiety of the ligands. The inactivity of (20%) ^-O_4S-Au at the concentrations tested shows that glucose moieties do not contribute to antiviral activities of (50%) ^-O_4S-Au. The IC50 values are showed in Table2. As shown in Table 2, (100%) and (50%) ^-O_4S-Au inhibited HIV-1 infection with an IC50 of 1.29 and 2.32 µg/ml respectively.

Table 2 Half maximal inhibitory concentrations (IC50) of Linker-SO$_4$, $^-$O$_4$S-Au and $^-$O$_4$P-Au against HIV-1 exposed MT-2 cells in comparison with PRO 2000

Compound	MW (KDa)	N$_{TL}$[a]	N$_{CL}$[b]	IC50 (µg/mL)	IC50 (µM)	IC50 (µM)[c]
Compound 1	0.963	2	2	11.97	12.4	24.8
(100%)$^-$O$_4$S-Au	108	140	140	1.29	0.012	1.68
(50%)$^-$O$_4$S-Au	216	272	136	2.32	0.011	1.46
(20%)$^-$O$_4$S-Au	202	272	55	> 10	> 0.050	> 2.7
(100%)$^{2-}$O$_4$P-Au	108	140	140	> 100	> 0.93	> 130
PRO 2000	5	-	21[d]	1.9[e]; 0.43[f]	0.38[e];0.086[f]	7.98;1.81

[a] Number of total ligands per compound. [b] Number of charged ligands per compound. [c] IC50 expressed in charged ligands. [d] Taken from the NIH website (NIAID - Division of AIDS-HIV - Therapeutics Database). [e] Taken from Ref. 9a; PM-1 cells and HIV-1 RF (X4) were used. [f] Taken from Ref 9b; U87.CD4.CXCR4 cells and HIV-1 HxB2 (X4) were used.

Linker-SO$_4$ and (20%) $^-$O$_4$S-Au were not able to reach an IC50 at the concentrations tested. This trend is in agreement with the results obtained by SPR. In order to better rationalize the results, the IC50 values were also expressed in terms of molar concentration of each compound and further transformed into molarity of charged ligands (Table 2). (100%) and (50%) $^-$O$_4$S-Au afforded IC50 in the nanomolar range in NPs concentration and in the low micromolar range in terms of sulphated ligands.

The high degree of sulphation and molecular weight of the NPs,[26] and the higher local concentrations of the ligands compared to the disulphide Linker-SO$_4$,[27] may origin the increased anti-HIV activity that results from attaching the sulphated ligand to the gold nanocluster. The anti-viral activity of (100%) and (50%) $^-$O$_4$S-Au is comparable to that reported for PRO 2000. In similar assays, Shattock[28] and Sattentau[29] reported that

[26] (a) Witvrouw, M., Desmyter, J., De,Clercq, E. (1994). Antiviral portrait series: 4. Polysulfates as inhibitors of HIV and other enveloped viruses. *Antivir. Chem. Chemother.* **5**, 345-359. (b) Scordi-Bello, I. A., Mosoian, A., He, C. J., Chen, Y. B., Cheng, Y., Jarvis, G. A., Keller, M. J., Hogarty, K., Waller, D. P., Profy, A. T., Herold, B. C., Klotman, M. E. (2005). Candidate sulfonated and sulfated topical microbicides: comparison of anti-human immunodeficiency virus activities and mechanisms of action. *Antimicrob. Agents Chemother.* **49**, 3607-3615.

[27] Mammen, M., Choi, S. K., Whitesides, G. M. (1998). Polyvalent interactions in biological systems: implications for design and use of multivalent ligands and inhibitors. *Angew. Chem. Int. Ed.* **37**, 2755-2794.

[28] Fletcher, P. S., Wallace, G. S., Mesquita, P. M. M., Shattock, R. J. (2006). Candidate polyanion microbicides inhibit HIV-1 infection and dissemination pathways in human cervical explants. *Retrovirol.* **3**, 46-58.

[29] Gantlett, K. E., Weber, J. N., Sattentau, Q. J. (2007). Synergistic inhibition of HIV-1 infection by combinations of soluble polyanions with other potential microbicides. *Antivir. Res.* **75**, 188-197.

PRO 2000 has IC50 values of 1.9 µg/ml and 0.43 µg/ml, respectively. The differences in IC50 values are mainly related to the cell and virus types used. Expressed in molarity, these values are in the same order of magnitude of what we found for (100%) and (50%) ^-O_4S-Au in our experiments (Table 2). (100%) and (50%) ^-O_4S-Au thus proved to be potent inhibitors of X4 HIV. This also indicates that a 50% density of the sulphated ligand on the gold platform is enough to obtain a significant anti-HIV effect.

The HIV neutralization experiments showed in Figure 11 were performed with an X4 HIV virus. Most of the works reported in literature with polysulphates molecules were studied in inhibition experiments with X4 virus. This is because X4 virus has a more positive charged V3 loop then R5 and the effect of the polysulphates is better detected. To study the inhibition broadness of our ^-O_4S-Au, MT2 cells were infected with JR Ren (R5) virus in presence of (50%) ^-O_3SO-Au (Figure 12).
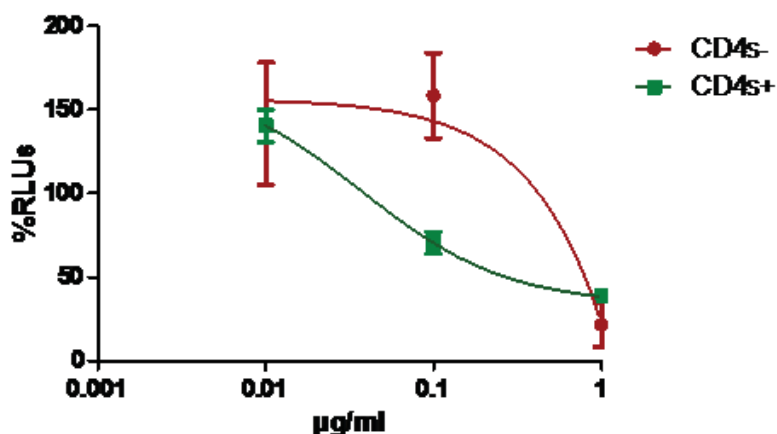
Figure 12. HIV neutralization assays Inhibition of recombinant virus JR Ren (R5) infection of MT-2 cells at different concentrations of (50%) ^-O_4S-Au in the presence (green) or absence (red) of sCD4. Results are expressed as percentages of infection related to untreated control. Data represent the mean of three independent experiments ± SEM (Standard Error of the Mean).

To better understand the molecular mechanism of the inhibition of ^-O_4S-Au, MT2 cells were also infected with JR Ren (R5) virus preincubated with soluble CD4 (sCD4). sCD4 induce a conformational change in gp120 that better expose the positive charged V3 loop.[30] These data showed that the (50%) ^-O_4S-Au is able to neutralize also R5 virus. Moreover, the data of figure 12 showed that in the presence of sCD4, 0.1 ug/ml of (50%) ^-O_4S-Au is able to neutralize HIV infection, but not effect is observed in the absence of sCD4 at the same concentration. This experiment confirms that ^-O_4S-Au bind preferentially the positive charged amino acids located in the V3 loop.

---

[30] Wyatt, R., and Sodroski, J. (1998). The HIV-1 envelope glycoproteins: fusogens, antigens, and immunogens. *Science*, **280**, 1884-1888.

CONCLUSION AND PERSPECTIVE

In conclusion, multivalent gold nanoparticles coated with sulphated ligands can be considered a novel alternative to the known anti-HIV systems for targeting the adsorption/fusion process of the virus infection. Depending on the ligand density, these NPs can bind gp120 with high affinity as shown in SPR-based experiments and neutralize the *in vitro* HIV direct infection of T-lymphocytes in the nanomolar range. We demonstrate that a 50% percentage density of sulphated ligands on ~2 nm nanoparticles is enough to achieve anti-HIV activities, which are comparable to those obtained with NPs completely coated with sulphated ligands, opening up the possibility of tailoring other anti-HIV molecules on the same gold cluster. The sulphated NPs are stable and well dispersible in water or physiological buffers, and not cytotoxic to MT-2 cells. Since many pathogens (especially enveloped viruses) suffer polysulphate-mediated inhibition in their early steps of infection, these Au-NPs may be potentially applied for the prevention of other infectious agents. In pursuit of microbicide candidates, more potent and/or less toxic agents may rise from combining different anti-HIV systems. Sattentau observed that cocktails of polyanions and other antiretroviral agents with microbicidal effect can act synergistically.[29] The next generation of sulphated GNPs could include galactose molecules that are able to bind V3 tip conserved region and probably enhance the antiviral activity of ^-O_4S-Au.

The possibility of simultaneously tailoring on the same gold nanoplatform both sulphated ligands and other active molecules, which target different stages of the HIV life cycle makes gold nanoparticles an appealing scaffold for the development of new multifunctional anti-HIV systems.

Experimental part

General Information

All chemicals were purchased as reagent grade from Sigma-Aldrich unless otherwise stated and were used without further purification. Reactions were monitored by thin layer chromatography (TLC) with silica gel 60 F_{254} aluminium sheets (Merck) and visualized by UV irradiation (254 nm) and/or staining with *p*-anisaldehyde solution [anisaldehyde (25 ml), H_2SO_4 (25 ml), EtOH (450 ml) and CH_3COOH (1 ml)] or 10% H_2SO_4 solution in EtOH, followed by heating at over 200℃. Size-exclusion column chromatography was performed on Sephadex™ LH-20 (GE Healthcare). Purification of compounds by flash column chromatography on silica gel (FCC) was performed on a Biotage Sp4 HPFC™ automated flash chromatography system (Biotage AB, Uppsala

Sweden) or by conventional flash chromatography using silica gel 60 (0.063-0.200 mm, 0.015-0.040 mm; Merck). UV-Vis spectra were carried out with a Beckman Coulter DU 800 spectrometer. ^{1}H and ^{13}C NMR spectra were recorded on a Bruker AVANCE (500 MHz) spectrometer. Chemical shifts (δ) are given in ppm relative to the residual signal of the solvent used. The values of coupling constants (J) are given in Hz. Splitting patterns are described by using the following abbreviations: br, broad; s, singlet; d, doublet; t, triplet; m, multiplet. Infrared spectra (IR) were recorded from 4000 to 400 cm^{-1} with a Nicolet 6700 FT-IR spectrometer (Thermo Spectra-Tech). The mass spectrometric data were obtained from a Waters LCT Premier XE instrument with a standard ESI source by direct injection. The instrument was operated with a capillary voltage of 1.0 kV and a cone voltage of 200 V. Cone and desolvation gas flow were set to 50 and 500 L/h, respectively; source and desolvation temperatures were 100 ºC. The exact mass was determined using glycocholic acid (Sigma) as an internal standard (2 M+Na^{+}, m/z = 953.6058).For transmission electron microscopy (TEM) examinations, a single drop (10 μL) of the aqueous solution (*ca.* 0.1 μg/ml in milliQ water) of the gold nanoparticles was placed onto a copper grid coated with a carbon film (Electron Microscopy Sciences). The grid was left to dry in air for several hours at room temperature. TEM analyses were carried out in a Philips JEOL JEM-2100F working at 200 kV. Surface plasmon resonance (SPR) measurements were carried out using a ProteOn XPR36 Protein Interaction Array System with research-grade GLC sensor chips and all reagents were supplied by Bio-Rad (Bio-Rad Laboratories, Inc.).

Recombinant Proteins. Recombinant gp120 from HIV-1 CN54 clone (repository reference ARP683) was obtained from the Programme EVA Centre for AIDS Reagents, NIBSC, UK, supported by the EC FP6/7 Europrise Network of Excellence, AVIP and NGIN consortia and the Bill and Melinda Gates GHRC-CAVD Project and was donated by Prof. Ian Jones (Reading University, UK).

Synthesis and characterization of the bifunctional ligands

Undecen-1-en-11-yl tetra(ethylene glycol) (1)

 A mixture of tetraethylenglycol (TEG) (35.6 g, 183.5 mmol) and NaOH (50%) (2.7 ml, 43.7 mmol) were stirred for 30 min at 100 ºC. The reaction was cooled to room temperature and 11-Br-undecene (10.2 g, 43.7 mmol) was added. The reaction was heated at 100ºC and left overnight under stirring. The mixture was diluted with CH$_2$Cl$_2$ (20 ml), washed with water (40 ml) and extracted with hexane (3 x 40 ml). The hexane fractions were collected, dried over Na$_2$SO$_4$, filtered and the solvent

evaporated at reduced pressure. The crude product (16 g) was purified by flash column chromatography on silica gel (EtOAc) to give compound 1 (10.46 g, 69%) as a yellow oil.

Rf = 0.31 (EtOAc). **^{1}H RMN** (CDCl$_3$, 500 MHz) 1.26-1.36 (m, 12H); 1.57-1.65 (m, 2H); 2.01 (dd, J = 14.4, 6.9 Hz, 2H). 3.12 (bs, 1H), 3.43 (t, J = 6.8 Hz, 2H); 3.54-3.67 (m, 14H); 3.68-3.73 (m, 2H); 4.90 (dd, J = 10.2, 9.1, 1H), 4.97 (ddd, J = 17.1, 3.4, 1.6, 1H); 5.78 (ddt, J = 16.9, 10.2, 6.7, 1H).

1-(Thioacetylundec-11-yl)tetra(ethylene glycol) *(2)*

To a solution of 1 (9.6 g, 27.7 mmol) in dry THF, AcSH (10.49 g, 138 mmol) and AIBN (cat.) were added. The mixture was stirred under reflux for 3 hours. The reaction was diluted with 30 ml of EtOAc and pH neutralised with a saturated solution of NaHCO$_3$. The organic phase was washed with brine, dried over Na$_2$SO$_4$ and the solvent removed at reduced pressure. The residue was purified by flash column chromatografy on silica gel (EtOAc:hexane 9:1 to EtOAc) to obtain compound 2 as a colourless oil (7.8 g, 67%). **Rf** = 0.28 (EtOAc). **^{1}H RMN** (CDCl$_3$, 500 MHz) 1.25-1.36 (m, 14H); 1.53-1.67 (m, 4H); 2.12 (s, 3H); 2.65 (t, J = 7.3 Hz, 2H); 3.26 (t, J = 6.8 Hz, 2H); 3.55-3.71 (m, 16H).

3,6,13,16-tetraoxa-9,10-dithiaoctadecane-1,18-diol *(3)*

Sodium methoxide (5.1 mg, 0.094 mmol, 0.2 eq.) was added to a stirred solution of compound 2 (200 mg, 0.47 mmol, 1 eq.) in MeOH (4 ml). After 15 hours at room temperature, the oxidation of the thiol intermediate into the corresponding disulphide 7 was *in situ* completed. The solution was treated with Amberlite IR-120, filtered and the solvent removed at reduced pressure. Purification by FCC afforded compound 3 as a white solid (150 mg, 0.20 mmol, 85%).

R_f = 0.43 (EtOAc/MeOH = 9/1). ^{1}H NMR (500 MHz, CDCl$_3$): δ 3.72 (br t, 2H, C*H*$_2$OH), 3.68-3.56 (m, 14H, 7xOCH$_2$), 3.44 (t, 2H, J = 6.8 Hz, CH$_2$CH$_2$C*H*$_2$O), 2.66 (t, 2H, J = 7.4 Hz, CH$_2$S), 2.63 (br signal, 1H, CH$_2$O*H*), 1.69-1.63 (m, 2H, C*H*$_2$CH$_2$S), 1.59-1.54 (m, 2H, CH$_2$C*H*$_2$CH$_2$O), 1.37-1.26 (m, 14H, CH$_2$(C*H*$_2$)$_7$CH$_2$); ^{13}C NMR (125 MHz, CDCl$_3$): δ 72.5 (t, 1C), 71.5 (t, 1C, CH$_2$CH$_2$*C*H$_2$O), 70.6-70.0 (t, 6C, 6xOCH$_2$), 61.7 (t, 1C, CH$_2$OH), 39.2 (t, 1C, CH$_2$S), 29.5-29.2, 28.5 and 26.0 (t, 9C, CH$_2$(*C*H$_2$)$_9$CH$_2$); IR (KBr): ṽ 3331, 2921, 2855, 1466, 1350, 1114 cm^{-1}; HRMS (m/z): [M+Na]$^+$ Calculated for C$_{38}$H$_{78}$NaO$_{10}$S$_2^+$: 781,4929; Found: 781.3861.

Sodium 3,6,13,16-tetraoxa-9,10-dithiaoctadecane-1,18-diyl disulfate (Linker-SO$_4$)
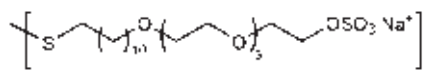
Sulphur trioxide pyridine complex (517 mg, 3.2 mmol, 8 eq.) was added in three portions to a stirred solution of compound 3 (150 mg, 0.2 mmol, 2 eq.) in DMF (4.5 ml). After 6 hours at 50 °C, the solvent was removed at reduced pressure. The mixture was dissolved in MeOH/H$_2$O 1:1 and the pH was adjusted to neutrality with NaOH 1N. The product was purified by Sephadex LH-20 column (MeOH/H$_2$O = 1/1) to afford Linker-SO$_4$ as a white solid (142 mg, 0.147 mmol, 74%).

R$_f$ = 0.34 (EtOAc/MeOH 9/1); ^{1}H NMR (500 MHz, D$_2$O): δ 4.22-4.20 and 3.84-3.82 (4H, AA´ and XX´ parts of an AA´XX´ system centred in δ 4.02: OCH$_2$C*H*$_2$OSO$_3$ and OC*H*$_2$CH$_2$OSO$_3$, respectively), 3.75-3.64 (m, 12H, 6xOCH$_2$), 3.52 (t, 2H, *J* = 6.8 Hz, CH$_2$CH$_2$C*H*$_2$O), 2.75 (t, 2H, *J* = 7.0 Hz, CH$_2$S), 1.78-1.74 (m, 2H, C*H*$_2$CH$_2$S), 1.66-1.58 (m, 2H, CH$_2$C*H*$_2$CH$_2$O); 1.53-1.44 (m, 2H, C*H*$_2$CH$_2$CH$_2$S), 1.43-1.34 (m, 12H, CH$_2$(C*H*$_2$)$_6$CH$_2$CH$_2$O); ^{13}C NMR (125 MHz, D$_2$O): δ 71.1 (t, 1C, CH$_2$CH$_2$*C*H$_2$O), 69.8-69.6 (t, 6C, 6xOCH$_2$), 69.0 (t, 1C, *C*H$_2$CH$_2$OSO$_3$), 67.5 (t, 1C, CH$_2$OSO$_3$), 39.0 (t, 1C, CH$_2$S), 29.9-29.3, 28.7 and 26.1 (t, 1C, CH$_2$CH$_2$CH$_2$S) (t, 9C, CH$_2$(*C*H$_2$)$_9$CH$_2$); IR (KBr): ṽ 3446, 2919, 2850, 1652, 1470, 1235, 1127, 1084, 1032, 943 cm^{-1}; HRMS (m/z): [M+Na]$^+$ Calculated for C$_{38}$H$_{76}$Na$_3$O$_{16}$S$_4$$^+$: 985,3704; Found: 985.3950.

Sodium 3,6,13,16-tetraoxa-9,10-dithiaoctadecane-1,18-diyl diphosphate (Linker-PO$_4$)
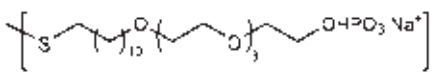
A solution of compound 2 (200 mg, 0.47 mmol, 1 eq.) in dry CH$_2$Cl$_2$ (2.5 ml) was dropwise added at 25 °C to a vigorously stirred solution of phosphorus oxychloride (215 µL, 2.35 mmol, 5 eq.) in dry CH$_2$Cl$_2$ (2.5 ml) under nitrogen atmosphere. After the addition, the resulting reaction mixture was stirred for 30 minutes and then the solvent was evaporated. The intermediate chlorophosphate was dissolved in dioxane (1 ml) and the solution was dropwise added at 25 °C to a vigorously stirred mixture of dioxane (1 ml) and water (0.5 ml). This mixture was stirred overnight (12 hours) and then the solvent was evaporated. The resulting residue (reddish oil) was purified by FCC to afford Linker-PO$_4$ as a hygroscopic white solid (231 mg, 0.46 mmol, 98%).

R$_f$ = 0.35 (AcOEt/MeOH/H$_2$O = 10/5/2); ^{1}H NMR (500 MHz, CD$_3$OD/D$_2$O = 1/1): δ 3.99 (br signal, 2H, CH$_2$OPO$_3$), 3.71-3.54 (m, 14H, 7xOCH$_2$), 3.44 (t, 2H, *J* = 6.7 Hz, CH$_2$CH$_2$C*H*$_2$O), 2.82 (t, 2H, *J* = 7.2 Hz, C*H*$_2$SAc), 2.29 (s, 3H, SAc), 1.57-1.48 (m, 4H, CH$_2$C*H*$_2$CH$_2$O and C*H*$_2$CH$_2$SAc), 1.37-1.20 (m, 14H, CH$_2$(C*H*$_2$)$_7$CH$_2$); ^{13}C NMR (125 MHz, CD$_3$OD/D$_2$O = 1/1): δ 198.8 (s, 1C, Ac), 72.2 (t, 1C, CH$_2$CH$_2$*C*H$_2$O), 71.4-70.6 (t,

7C, 7xOCH$_2$), 65.6 (t, 1C, CH$_2$OPO$_3$), 31.0 (q, 1C, SAc), 30.5-30.3, 30.0, 29.9, 29.6 and 26.9 (t, 10C, CH$_2$SAc and CH$_2$(CH$_2$)$_9$CH$_2$); IR (KBr): ṽ 3433, 2921, 2852, 1695, 1467, 1350, 1244, 1110, 1086, 961 cm^{-1}; HRMS (m/z): [M+Na]$^+$ Calculated for C$_{21}$H$_{43}$NaO$_9$PS$^+$: 525.2258; Found: 525.2281.

5,5'-Dithio bis (pentyl β-D-glucopyranoside) (GlcC5)
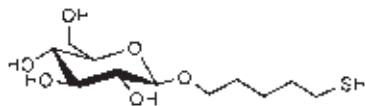
 Sodium methoxide (0.182 g, 3.38 mmol, 1 equiv.) was added to a methanolic solution of the 5-Thioacetylpentyl tetra-*O*-acetyl-*β*-D-glucopyranoside[31S] (1.66 g, 3.37 mmol, 1 equiv.), at RT. The solution was stirred for 2 h and then neutralized with Amberlite IR-120, filtered and evaporated to afford GlcC5 as a yellow oil, mixture of thiol and disulfide (0.895 g, 3.17 mmol, 94%). ^{1}H NMR (500 MHz, CD$_3$OD): δ=4.27 (d, *J*=7.7 Hz, 1H; H-1), 3.94-3.86 (m, 2H; H-6, OC*H*$_2$CH$_2$), 3.68 (dd, *J*=5.1, 11.9 Hz, 1H; H-6), 3.59-3.54 (m, 1H, OC*H*$_2$CH$_2$CH$_2$), 3.37 (t, *J*=8.4 Hz, 1H; H-3), 3.32-3.26 (m, 2H; H-4, H-5), 3.19 (t, *J*=8.4 Hz, 1H; H-2), 2.72 (t, *J*=7.2 Hz, 0.3H; CH$_2$SS), 2.52 (t, *J*=7.2 Hz, 1.7H; CH$_2$SH), 1.72 (t, *J*=7.3 Hz, 2H), 1.64 (t, *J*=7.3 Hz, 2H), 1.53-1.47 ppm (m, 2H); ^{13}C NMR (CD$_3$OD, 500 MHz): δ=104.2 (d; C-1), 77.98, 77.95, 75.0 (d; C-2), 71.5, 70.6 (t; O*C*H$_2$CH$_2$CH$_2$), 62.7 (t; C-6), 39.6 (t; CH$_2$SS), 34.9, 30.1, 25.8 (t; OCH$_2$CH$_2$*C*H$_2$), 24.9 ppm (t; *C*H$_2$SH). IR (neat) 2929.2, 2864.0, 1430.3, 1371.1, 1160.1, 1071.0, 1013.6, 894.6 cm^{-1}. HRMS: *m/z*: calcd. for C$_{11}$H$_{22}$O$_6$SNa$^+$ [*M*+Na]$^+$: 305.1029; found: 305.1021; calcd. for C$_{22}$H$_{42}$O$_{12}$S$_2$Na$^+$ [2*M*+Na]$^+$: 585.2015; found: 585.2010.

Synthesis and characterization of gold nanoparticles

General Procedures. To obtain nanoparticles (100%) $^-$O$_4$S-Au and (100%) $^{2-}$O$_4$P-Au, an aqueous solution of tetrachloroauric acid (Strem Chemicals) (0.025 M, 1 eq.) was added to a solution of Linker-SO$_4$ or Linker-PO$_4$ (0.012 M, 6 eq.) in MeOH/H$_2$O/CH$_3$COOH (3:3:1). An aqueous solution of NaBH$_4$ (1 M, 22 eq.) was then portion-wise added and the mixture was shaken for 2 hours at 25 ºC. The solvent was evaporated at reduced pressure. The residue was washed with ethanol, re-dissolved in the minimum quantity of milliQ water, loaded into 5-10 cm segments of SnakeSkin® pleated dialysis tubing (Pierce, 3500 MWCO) and purified by dialysis against distilled water (3 L of water, recharging with fresh water every 6 hours over the course of 72

[31S] T. Buscas, E. Söderberg, P. Konradsson, B. Fraser-Reid, *J. Org. Chem.* **2000**, *65*, 958-963.

hours). The nanoparticles were obtained as brown powder after lyophilization. The size distribution of the gold nanoparticles was evaluated from several TEM micrographs by means of an automatic image analyser. On the basis of the gold diameter obtained by TEM, the average number of gold atoms and molecular formula of the nanoparticles were calculated according to a previous work and confirmed by elemental analysis. To obtain NPs (50%) $^-O_4$S-Au and (20%) $^-O_4$S-Au, an aqueous solution of tetrachloroauric acid (Strem Chemicals) (0.025 M, 1 eq.) was added to MeOH/H_2O/CH_3COOH (3:3:1) solution containing a mixture of Linker-SO_4 in different ratios with GlcC$_5$ (1:1 for (50%) $^-O_4$S-Au and 9:1 for (20%) $^-O_4$S-Au). The overall molarity of organic ligands (0.012 M) and the other steps were maintained as above.

(100%) $^-O_4$S-Au
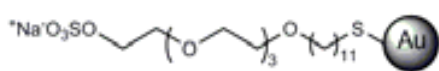
 Starting from Linker-SO_4 (15 mg, 0.0156 mmol), HAuCl$_4$ (208 µl, 25 mM) and NaBH$_4$ (117 µl, 1 M), (100%) $^-O_4$S-Au was obtained as brown amorphous powder (3.4 mg).

TEM (average diameter and number of gold atoms): 1.7 ± 0.8 nm, 225; ^{1}H NMR (500 MHz, D_2O): δ 4.24-4.18 (br signal, 2H, CH_2OSO_3), 3.85-3.79 (br signal, 2H), 3.78-3.63 (br m, 12H, 6xOCH_2), 3.51 (br t, 2H, J = 6.5 Hz), 2.74 (br signal, 2H, CH_2S), 1.80-1.69 (br m, 2H), 1.66-1.57 (br m, 2H), 1.54-1.29 (br m, 14H); IR (KBr): ν 3447, 2921, 2850, 1655, 1464, 1242, 1199, 1130, 1091, 1014, 944 cm^{-1}; UV-Vis (H_2O, 0.1 mg ml^{-1}): no surface plasmon signal was observed; Elemental analysis: Calculated (%) for Au$_{225}$(C$_{19}$H$_{39}$O$_8$S$_2$)$_{140}$: C 29.40, H 5.06, S 8.26; Found: C 30.73, H 5.75, S 8.48.

(50%) $^-O_4$S-Au
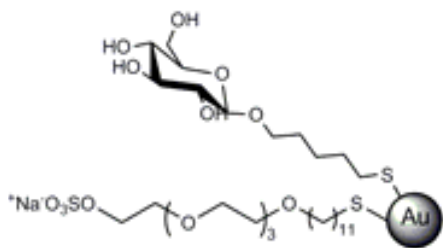
 Starting from Linker-SO_4 (15 mg, 0.0156 mmol), GlcC5 (4.6 mg, 0.016 mmol), HAuCl$_4$ (416 µl, 25 mM) and NaBH$_4$ (229 µl, 1 M), (50%) $^-O_4$S-Au was obtained as brown amorphous powder (4.4 mg).

TEM (average diameter and number of gold atoms): 2.6 ± 0.4 nm, 586; ^{1}H NMR (500 MHz, D_2O): δ 4.40 (br signal, ~1H, CH_2OSO_3), 4.18 (br signal, 1H, H-1 glucose), 3.99-3.21 (br m, ~16H), 2.72 (br signal, CH_2S), 1.87-1.24 (br m, 1H, 15H); IR (KBr): ν 3438, 2921, 2855, 1631, 1462, 1252, 1082, 1026, 933 cm^{-1}; UV-Vis (H_2O, 0.1 mg ml^{-1}): no

surface plasmon signal was observed; Elemental analysis calculated (%) for $Au_{586}(C_{19}H_{39}O_8S_2)_{136}(C_{11}H_{21}O_6S)_{136}$: C 22.67, H 3.8, S 6.05, found: C 25.32, 4.54, S 6.34.

(20%) ^-O_4S-Au
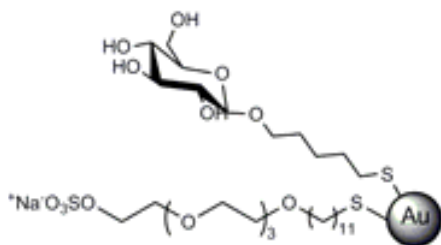
Starting from Linker-SO_4 (5 mg, 0.0052 mmol), GlcC5 (13.2 mg, 0.047 mmol), $HAuCl_4$ (700 µl, 25 mM) and $NaBH_4$ (0.383 µl, 1 M), (20%) ^-O_4S-Au was obtained as brown amorphous powder (5.2 mg).

TEM (average diameter and number of gold atoms): 2.3 ± 0.5 nm, 586; ^{1}H NMR (500 MHz, D_2O): δ 4.47 (br signal, ~0.25H, CH_2OSO_3), 4.21 (bs, H-1 glucose), 4.00-3.20 (br m, 12H), 1.86-1.25 (br m, ~10.5H), CH_2S not detected; IR (KBr): ν 3419, 2921, 2854, 1629, 1381, 1228, 1074 cm^{-1}; UV-Vis (H_2O, 0.1 mg ml^{-1}): no surface plasmon signal was observed; Elemental analysis: Calculated (%) for $Au_{586}(C_{19}H_{39}O_8S_2)_{55}(C_{11}H_{21}O_6S)_{217}$: C 20.43, H 3.35, S 5.20, found: C 20.36, H 3.42, S 5.35.

(100%) $^{2-}O_4P$-Au
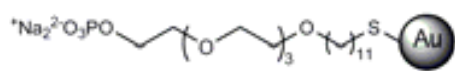
Starting from Linker-PO_4 (15.2 mg, 0.0151 mmol), $HAuCl_4$ (201 µl, 25 mM) and $NaBH_4$ (408 µL, 1 M), (100%) $^{2-}O_4P$-Au was obtained as brown powder (3.6 mg).

TEM (average diameter and number of gold atoms): 1.7 ± 0.4 nm, 225; ^{1}H NMR (500 MHz, D_2O): δ 3.94 (br signal, 2H, CH_2OPO_3), 3.77-3.65 (m, 14H, 7xOCH_2), 3.56 (br t, 2H, $CH_2CH_2CH_2O$), 2.91 (br signal, 2H, CH_2S), 1.79-1.68 (br m, 2H, CH_2CH_2S), 1.63-1.55 (m, 2H, $CH_2CH_2CH_2O$), 1.50-1.40 (m, 2H, $CH_2CH_2CH_2S$), 1.39-1.28 (m, 12H, $CH_2(CH_2)_6CH_2CH_2O$); IR (KBr): ν 3431, 2921, 2852, 1635, 1460, 1351, 1105, 1029, 962 cm^{-1}; UV-Vis (H_2O, 0.1 mg ml^{-1}): no surface plasmon signal was observed; Elemental analysis: Calculated (%) for $Au_{225}(C_{19}H_{40}O_8PS)_{140}$: C 29.40, H 5.19, S 4.13; Found: C 29.87, H 5.47, S 4.46.

(100%) ^-O_4S-Au-FITC
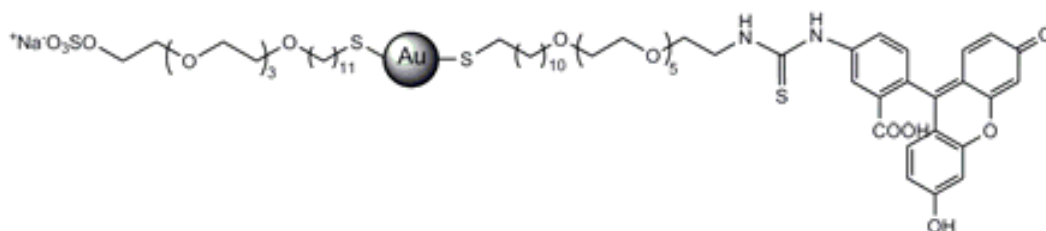
Starting from Linker-SO$_4$ (3.67 mg, 0.0076 mmol, 12 mM, 2.7 eq), Linker-FITC (0.34 mg, 0.0004 mmol, 0.3 eq), HAuCl$_4$ (106 µl, 25 mM, 0.027 mmol, 1 eq) and NaBH$_4$ (2.22 mg, 0.059 mmol, 1 M), (100%) $^-$O$_4$S-Au-FITC was obtained as brown amorphous powder (1.63 mg).
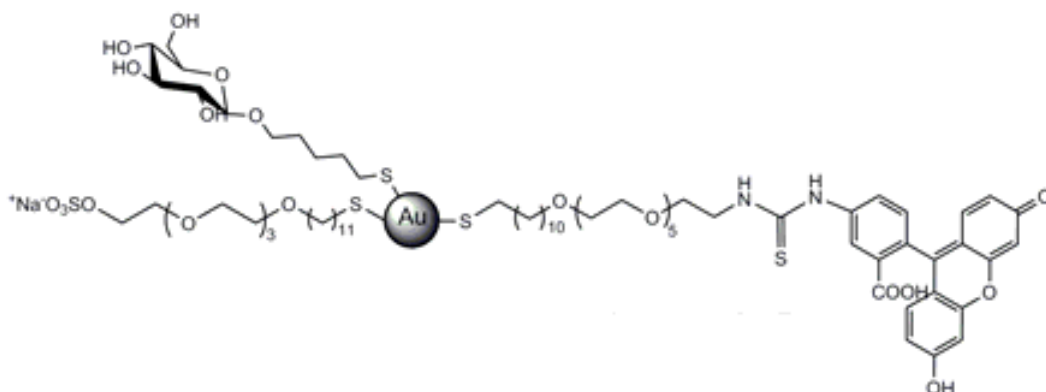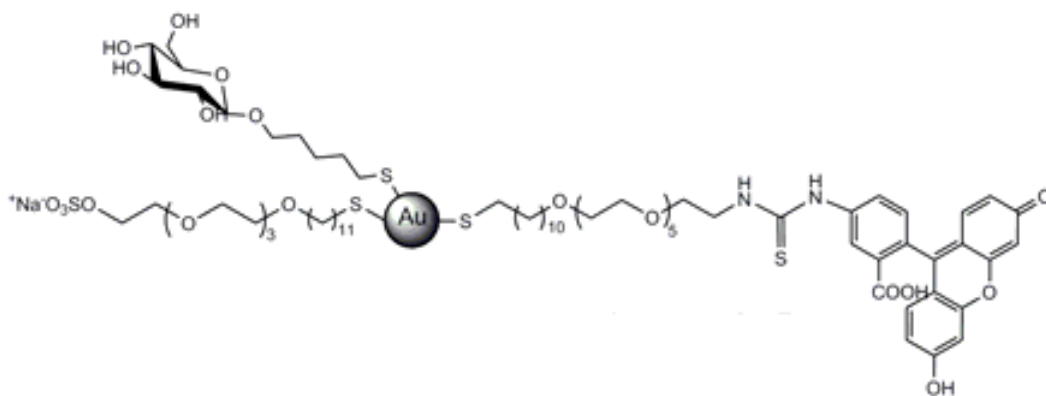
TEM (average diameter and number of gold atoms): 1.9 ± 1.1 nm, 201.

^{1}H RMN (D$_2$O, 500 MHz) δ=0.95-2.2 (bm, 14H); 3.1-4.05 (bm, 18H); 4.03 (bs, 2H, CH$_2$OSO$_3$); 6.5-7.1 (H-aromatic FITC).

UV-vis (H$_2$O, 0.1 mg/ml) λ=496

Fluorescence λ$_{ex}$=480; λ$_{em}$=520

(50%) $^-$O$_4$S-Au-FITC

Starting from Linker-SO$_4$ (1.93 mg, 0.004 mmol, 12 mM), GlcC5 (1 mg, 0.0036 mmol), Linker-FITC (0.34 mg, 0.0004 mmol), HAuCl$_4$ (106 µl, 25 mM, 0.027 mmol, 1 eq) and NaBH$_4$ (2.22 mg, 0.059 mmol, 1 M), (50%) $^-$O$_4$S-Au-FITC was obtained as brown amorphous powder (1.26 mg).

TEM (average diameter and number of gold atoms): 1.7 ± 0.6 nm, 201.

^{1}H RMN (D$_2$O, 500 MHz) δ=0.95-2.2 (bm, 18H); 3.1-4.05 (bm, 22H); 4.21 (bs, 2H, CH$_2$OSO$_3$); 4.4 (bs, H-1 glucose); 6.6-7.3 (H-aromatic FITC).

UV-vis (H$_2$O, 0.1 mg/ml) λ=496

Fluorescence λ$_{ex}$=480; λ$_{em}$=520

(20%) $^-$O$_4$S-Au-FITC

Starting from Linker-SO$_4$ (0.77 mg, 0.0016 mmol, 12 mM), GlcC5 (1.7 mg, 0.006 mmol), Linker-FITC (0.34 mg, 0.0004 mmol), HAuCl$_4$ (106 µl, 25 mM, 0.027 mmol, 1 eq) and NaBH$_4$ (2.22 mg, 0.059 mmol, 1 M), (20%) $^-$O$_4$S-Au-FITC was obtained as brown amorphous powder (1.05 mg).

TEM (average diameter and number of gold atoms): 1.8 ± 0.7 nm, 201.

^{1}H RMN (D$_2$O, 500 MHz) δ=0.95-2.1 (bm, 18H); 3.06-3.92 (bm, 23H); 4.18 (bs, 2H, CH$_2$OSO$_3$); 4.4 (bs, H-1 glucose); 6.6-7.4 (H-aromatic FITC).

UV-vis (H$_2$O, 0.1 mg/ml) λ=496

Fluorescence λ$_{ex}$=480; λ$_{em}$=518

Stability of SO$_3$-GNPs

In order to determine if sulphate group could undergo hydrolysis in water (pH 6.5), a solution of 5 mg of (50%) $^-$O$_4$S-Au in D$_2$O was checked every 8h for 5 days by ^{1}HNMR (500 MHz). No change was detected in the integral of methylene protons in α position of sulphate groups for all the time of the analysis.

SPR Experiments

The binding of compounds 1, and charged nanoparticles (in here, analytes) to gp120 was studied by SPR using a ProteOn XPR36 Protein Interaction Array System with research-grade GLC sensor chips (compact polymer layer containing easily activated carboxylic groups). Gp120 was immobilized on a GLC sensor chip using the standard amine coupling chemistry according to the manufacturer's instructions.

A GLC sensor chip was equilibrated with ProteOn PBS/Tween buffer (phosphate buffered saline, pH 7.4, 0.005% Tween 20). The carboxylic groups of two different channels on the chip surface were activated at 25 °C by injecting 30 µl (contact time: 60 sec; flow rate: 30 µl/min) of a 1 vol/vol mixture of EDAC (16 mM) and Sulpho-NHS (4 mM). Channel 1 was further injected with 120 µL (240 sec; 30 µl/min) of a gp120 solution in acetate buffer (50 µg/ml, 10 mM, pH 4) at 25 °C to obtain an immobilization

level of 6000 Response Units (RU). Only PBS/Tween was flown into channel 2, which was used as a reference surface. Finally, the surfaces of both channels were saturated by 100 µl (200 sec; 30 µl/min) of ethanolamine HCl (1 M, pH 8.5). Simultaneous binding of six different concentrations of each analyte to gp120 was studied. Each analyte was diluted at 2, 1, 0.5, 0.25, 0.125, and 0.0625 µg/ml in tris(hydroxymethyl)aminomethane (TRIS) buffered saline (TRIS 10 mM, NaCl 150 mM, pH 7.4) containing 0.005% of Tween 20, and injected at 25 ºC in both channels (contact time: 60 s; dissociation time: 100 s; flow rate: 100 µl/min). The binding profiles (sensorgrams) were obtained by an automatic subtraction of the reference surface signals from the gp120-activated surface signals. The sensor surface between runs was regenerated with a short pulse of 0.1 M HCl.

Cellular Experiments

Cytotoxicity experiments

Raji cells (10^4 cells per well, 80µL per well) were incubated with 20 µl per well of $^-O_4$S-Au and $^-O_4$S-Au-FITC solution at different concentration (50; 25; 10; 1; 0.1 µg/ml) and incubated 20h at 37ºC. MTS solution (20 µL of 5 mg/ml; final concentration 1 mg/ml) were added to each well and incubate 4 h at 37ºC. Absorbance was measured at 490 nm with a Microplate reader (Dynatech MR7000 instruments). The relative cell viability (%) related to control wells containing cell culture medium without nanoparticles was calculated by $[A]_{test}/[A]_{control}$ x 100.

Flow cytometry experiments

For flow cytometry experiments was used a BD Canto II flow flow cytometer (Becton Dickinson). Raji cells ($10·10^5$ cells in 2 ml) were incubated at 37 ºC with $^-O_4$S-Au-FITC solution (25 µg/ml). At different time (30 min, 1h, 2h, 3h, 4h, 5h, 6h, 7h, 8h and 9h) aliquot of 200 µl were washed 2 times with PBS buffer (500 µl), centrifuged, resuspend in 300 µL of PBS and the fluorescence measured in Flow cytometer (λ_{ex}=488; filter: long pass 502 nm and band pass 530/30 nm).

Fluorescence microscopy experiments

Images were acquired on a Confocal laser scanning microscopy Zeiss LSM 510 META equipped with 63X and 100X magnification oil lens and excitation wavelengths of 488 nm for FITC. Raji cells (10^5 cells in 200 µl) were incubated for 8 h at 37 ºC with $^-O_4$S-Au-FITC solution (25 µg/ml). Cells were washed twice with PBS, centrifuged and

formaldehyde/PBS (200 µL 2%) were added and incubated for 15 min at RT. Cells were washed twice with PBS, centrifuged and resuspended in 40 µl of PBS.

HIV neutralization experiments

The neutralization experiments were carried out by Dr. L.M Bedoya in the laboratory of Dr. Alcami.

Cells and viruses. MT-2 cells (American Type Culture Collection) were cultured in RPMI 1640 medium containing 10% (v/v) fetal bovine serum, 2 mM L-glutamine, penicillin (50 IU/ml) and streptomycin (50 µg/ml) (all Whittaker M.A. Bio-Products). MT-2 cells were cultured at 37 °C in a 5% CO_2 humidified atmosphere and splinted twice a week. 293 T cells were cultured in DMEM medium containing 10% (v/v) fetal bovine serum, 2 mM L-glutamine, penicillin (50 IU/ml) and streptomycin (50 µg/ml) (all Whittaker M.A. Bio-Products). 293T cells were cultured at 37 °C in a 5% CO_2 humidified atmosphere and splinted twice a week.

Plasmids. The pNL4.3-Renilla (X4 tropic) was generated by replacing the nef gene on the proviral clone (pNL4.3) by the Renilla reporter gene.

Production of recombinant viruses and neutralization assays. Recombinant virus stocks were obtained from calcium phosphate transfection of plasmid pNL4.3-Renilla on 293T cells. Stocks were then stored at -80ºC until use. Previously to neutralization assays, infectivity of recombinant viruses were evaluated by infecting MT-2 cells with serial dilutions of viral stocks. Neutralization assay of HIV was then performed by pre-treating viral stocks with different concentrations of compounds. After 30 minutes of incubation at 37 °C in 5% CO_2, pre-treated viral stocks were used to infect MT-2 cells, and maintained in culture at 37 °C in 5% CO_2. HIV replication was evaluated 48 hours post-infection following "Renilla luciferase assay system" (Promega) manufacturer procedures. Briefly, cells were lysed and relative luminescence units (RLUs) were obtained in a luminometer (Berthold Detection Systems) after the addition of substrate to cells extracts.

CHAPTER 2

Multivalent and multifunctional miniCD4 gold glyconanoparticles and their interaction with HIV envelop protein

In the frame of CHAARM project

# CHAPTER 2

Multivalent and multifunctional miniCD4 gold glyconanoparticles and their interaction with HIV envelop protein

INTRODUCTION

The aim of the work described in this part of the thesis is to intervene in HIV entry process into host cells that present CD4 receptor and CCR5 or CXCR4 on the membrane. The interaction of HIV gp120 with CD4 represents the initial step of virus entry into target cells (Figure 1).[1, 2, 3]
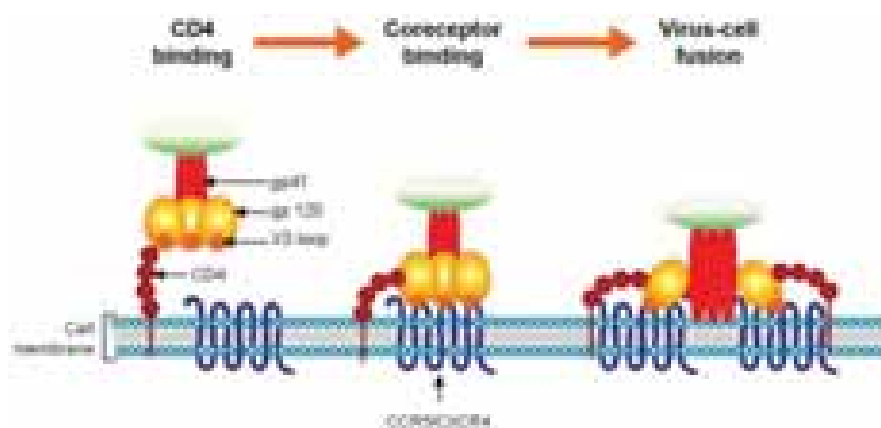
Figure 1. Cartoon of HIV entry process. Envelope protein (Env) is formed by three gp120 non covalently bonded to three gp41. In the first step CD4 receptor bind to gp120 and induce a conformational change in the protein that expose the third variable loop (V3). V3 bind the chemokine receptors (CCR5 or CXCR4) that induce a second conformational change in Env that expose gp41 until the contact with the host cell membrane. In the last step gp41 form a fusion pore in the membrane and allow the viral genetic material to enter in the cell.[4]

[1] Dalgleish, A. G., Beverley, P.C. L., Clapham, P. R., Crawford, D. H., Greaves, M. F., and Weiss, R. A. (1984). The CD4 (T4) antigen is an essential component of the receptor for the AIDS retrovirus. *Nature* **312**, 763-767.

[2] Klatzmann, D., Champagne, E., Chamaret, S., Gruest, J., Guetard, D., Hercend, T., Gluckman, J., and Montagnier, L. (1984). T-lymphocyte T4 molecule behaves as the receptor for human retrovirus LAV. *Nature* **312**, 767-768.

[3] Maddon, P. J., Dalgleish, A. G., McDougal J. S., Clapham, P. R., Weiss, R. A., and Axell, R. (1986). The T4 gene encodes the AIDS virus receptor and is expressed in the immune system and the brain. *Cell* **47**, 333-348.

[4] Moebius, K., Eichler, J. (2009). HIV-derived peptide mimics. *Drug Discov. Today: Technologies* **6**, e19-e25.

CD4 (cluster of differentiation 4) is a transmembrane glycoprotein found on the surface of immune cells such as T helper cells, monocytes, macrophages, and dendritic cells (DCs).[5, 6] CD4 is composed of four extracellular domains (D1-D4), a short cytoplasmatic tail and a single transmembrane helix.[7] gp120 bind the CD4 D1 domain, which forms a stable eight-stranded beta-sheet.[8] The 22 residues of CD4 that interact with 26 amino acids of gp120 are located in the N-terminus of CD4 D1 (residues 21-64). CD4 binding site on gp120 is a conserved deep hydrophobic pocket. CD4 is able to arrange Phe43 (F43) side chain in the gp120 cavity and Arg59 (R59) side chain form a double H-bond with the gp120 Asp368 (D368) side chain, as shown in the crystal structure in Figure 2.[9]
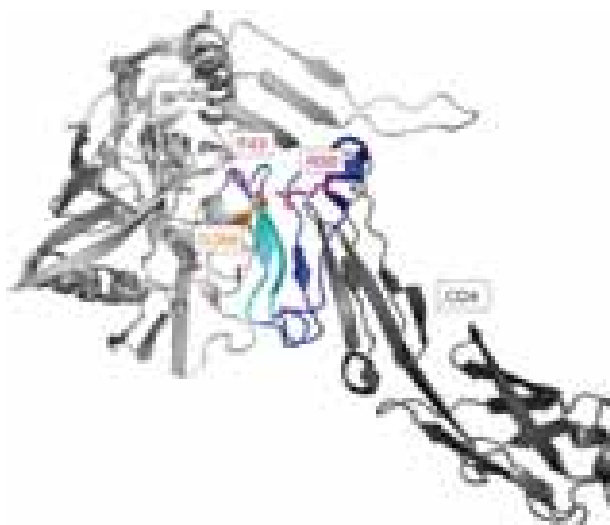
Figure 2. Structural details of the CD4–gp120 complex (pdb 1rzj). CD4 binds to gp120 interact with three important region of CD4: residues 22–33 and 49–64 (in blue) and residues 34–48 (in cyan). The most important residues for the binding with gp120 are Phe43 (F43) and Arg59 (R59), and the contact residue Asp368 of gp120 (D368).[10]

[5] Cruse, J. M., Lewis, R. E., and Wang, H. (2004). Immunology guidebook. Elsevier Academic Press.

[6] Lotze, M. T., and Thomson, A. W. (2001). Dendritic cells (2ND Ed.). Elsevier Academic Press.

[7] Ryu, S. Kwong, P. D., Truneh, A., Porter, T. G., Arthos, J., Rosenberg, M., Dai, X., Xuong, N., Axel, R., Sweet, R. W., and Hendrickson, W. A. (1990). Crystal structure of an HIV-binding recombinant fragment of human CD4. *Nature* 348, 419-426.

[8] Huang, C., Venturi, M., Majeed, S., Moore, M. J., Phogat, S., Zhang, M., Dimitrov, D. S., Hendrickson, W. A., Robinson, J., Sodroski, J., Wyatt, R., Choe, H., Farzan, M., and Kwong, P. D. (2004). Structural basis of tyrosine sulfation and V_H-gene usage in antibodies that recognize the HIV type 1 coreceptor-binding site on gp120. *Proc. Natl. Acad. Sci. U.S.A.* 2004, **101**, 2706–2711.

[9] Kwong, P. D., Wyatt, R., Robinson, J., Sweet, R. W., Sodroski, J., and Hendrickson, W. A. (1998). Structure of an HIV gp120 envelope glycoprotein in complex with the CD4 receptor and a neutralizing human antibody. *Nature* **393**, 648-659.

[10] Meier, J., Kassler, K., Sticht, H., and Eichler, J. (2012). Peptides presenting the binding site of human CD4 for the HIV-1 envelope glycoprotein gp120. *Beilstein J. Org. Chem.* **8**, 1858–1866.

CD4 binding induces conformational changes in the gp120 glycoprotein, and induce the exposure and/or formation of a binding site for interaction with specific chemokine receptors (CCR5 and CXCR4). Molecules able to inhibit CD4/gp120 binding are promising candidates for HIV-1 entry inhibitors, an upcoming class of AIDS therapeutics. During recent years, different CD4 mimetics were studied (small molecules and miniproteins).[11] In 1999, C. Vita *et al.* prepared for the first time a CD4 miniprotein (miniCD4) by using a scillatoxin as miniprotein scaffold. They substituted regions of scillatoxin miniprotein for CD4 residues: 36–47 β-hairpin and Arg-59 (Figure 3A). The obtained miniCD4 (CD4M33; Figure 3C) was able to bind the CD4 binding site on gp120 and to inhibits HIV-1 infection in cell assay better than soluble CD4.[12, 13]
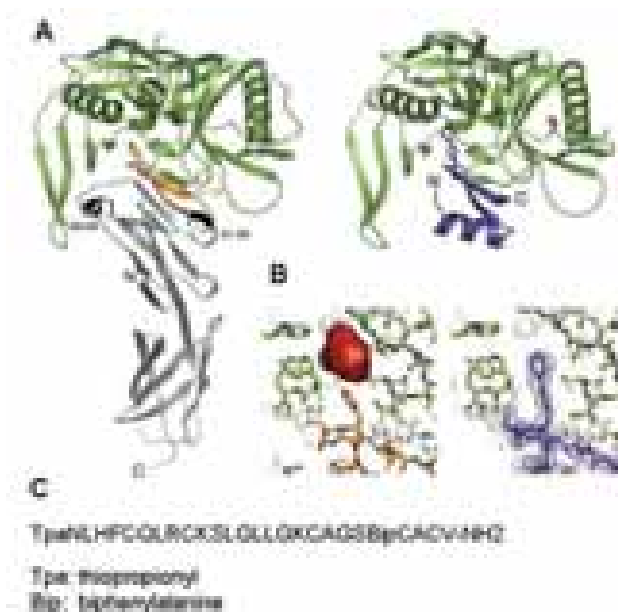
Figure 3. A) X-ray structure of gp120 core (green) complexed with CD4 (left) and CD4M33 miniCD4 (right). CD4 is shown in orange/gray and miniCD4 is shown in purple. (B) Close-up view of the CD4-gp120 binding site. The unusual interfacial cavity (red) between CD4 and gp120 is shown in the left panel. The right panel shows how the biphenyl side chain of miniCD4 better fill the hydrophobic cavity of gp120. C) Amino acid sequence of miniCD4 (CD4M33).[14]

---

[11] Madani, N., Scho, A., Princiotto, A. M., LaLonde, J. M., Courter, J. R., Soeta, T., Ng, D., Wang, L., Brower, E. T., Xiang, S., Kwon, Y., Huang, C., Wyatt, R., Kwong, P. D., Freire, E., Smith, A. B., and Sodroski, J. (2008). Small-molecule CD4 mimics interact with a highly conserved pocket on HIV-1 gp120. *Structure* **16**, 1689–1701.

[12] Vita, C., Drakopoulou, E., Vizzavona, J., S., Rochette, Martin, L., Ménez, A., Roumestand, C., Yang, Y., Ylisastigui, L., Benjouad, A., and Gluckman, J. C. (1999). Rational engineering of a miniprotein that reproduces the core of the CD4 site interacting with HIV-1 envelope glycoprotein. *Proc. Natl. Acad. Sci. USA* **96**, 13091-13096.

[13] Martin, L., Stricher, F., Missé, D., Sironi, F., Pugnière, M., Barthe, P., Prado-Gotor, R., Freulon, I., Magne, X., Roumestand, C., Ménez, A., Lusso, P., Veas, F., and Vita, C. (2003). Rational design of a CD4 mimic that inhibits HIV-1 entry and exposes cryptic neutralization epitopes. *Nat. Biotechnol.* **21**, 71-76.

[14] Huang, C., Stricher, F., Martin, L., Decker, J. M., Majeed, S., Barthe, P., Hendrickson, W. A., Robinson, J., Roumestand, C., Sodroski, J., Wyatt, R., Shaw, G. M., Vita, C., and Kwong, P. D., (2005). Scorpion-

Scillatoxin was selected because is a well-organized miniprotein, it contains 31 amino acids with three disulfide bonds and is formed by a short helix on one face and two antiparallel β-strands on the opposite face (similar to β-strands of CD4).[15] From the crystal structure of the CD4/gp120 complex, they found that Phe43 side chain of CD4 is not able to fill the CD4 binding site on gp120 cavity (red cloud on Figure 3B, left). Therefore, to better fill the gp120 hydrophobic cavity, the Phe43 was replaced by a biphenylalanine in the miniCD4 (Figure 3B, right and 3C). In an effort to improve the binding affinity of the first miniCD4 to gp120, C. Vita *et al.* prepared a new miniCD4 (M48-U1) in which the biphenylalanine43 is substituted by a phenylalanine with a cyclohexylmethoxy group on position 4 of the phenyl group (Figure 4).[16] M48-U1 is stable in strong denaturing conditions, including acidic pH, and they are relatively resistant to degradation by proteases, which favours the development of these compounds as anti-HIV drugs in general and as vaginal microbicides in particular.

TpaNLHFCQLRCKSLGLLGRCApTXCACV-NH2

Tpa: Thiopropionyl. p: D-proline. X: Phe(p-cyclohexylmetoxy)

X:
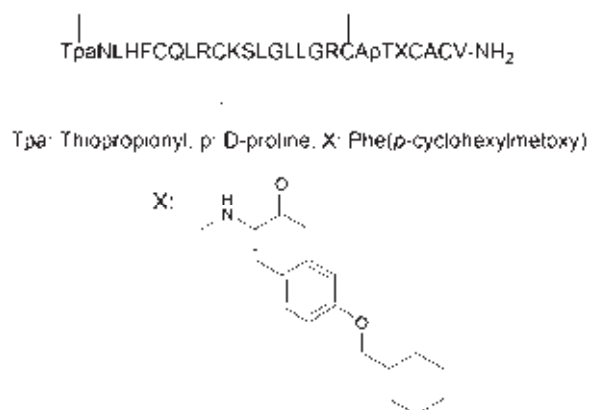
Figure 4. Amino acids sequence of last miniCD4 prepared (M48-U1). This miniCD4 was used in this work. Adapted from reference 16.

In vitro experiments showed that M48-U1 miniCD4 inhibits infection of cells by primary clinical HIV-1 isolates and exposes neutralization epitopes of the viral envelope. It was also studied as potential HIV microbicides using a so called transinfection assay with dendritic cells and CD4+ T-cells. In this experiment an EC50 around 79-105 nM was found. In the same article dimeric and tetrameric miniCD4 were also prepared. Higher

toxin mimics of CD4 in complex with human immunodeficiency virus gp120: crystal structures, molecular mimicry, and neutralization breadth. *Structure*, **13**, 755–768.

[15] Vita, C., Roumestand, C., Toma, F., And Ménez, A. (1995). Scorpion toxins as natural scaffolds for protein engineering. *Proc. Natl. Acad. Sci. USA* **92**, 6404-6408.

[16] Van Herrewege, Y., Morellato, L., Descours, A., Aerts, L., Michiels, J., Heyndrickx, L., Martin, L., and Vanham, G. (2008). CD4 mimetic miniproteins: potent anti-HIV compounds with promising activity as microbicides. *J. Antimicrobial Chemotherapy* **61**, 818-826.

activity was found for the dimeric miniproteins (EC50 between 15 and 30 nM), in contrast to the tetrameric miniproteins (EC50 between 107 and 377 nM).[16]

In the frame of CHAARM project we began a collaboration with Dr. L. Martin (CHAARM partner) who gave us the M48-U1 miniCD4 with the aim to increase its activity by multimerization on gold glyconanoparticles (GNPs). Taking into account the mechanism of HIV-1 entry mediated by CD4 and CCR5/CXCR4, three types of GNPs were designed (Figure 5).
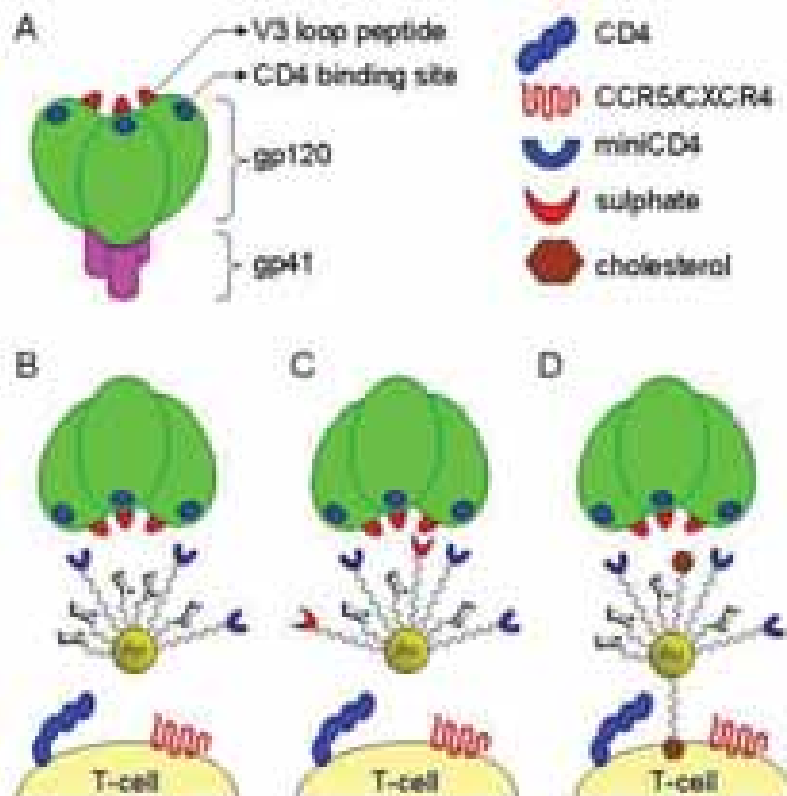
Figure 5. Cartoon representing: A) viral Env protein formed by trimeric gp120 no covalently bonded to trimeric gp41. B) miniCD4-GNP presenting multiple copies of miniCD4 would be able to bind simultaneously to more than one CD4 binding site on Env. C) miniCD4-GNP-SO4 covered with miniCD4 miniproteins and multiple copies of sulphate groups was designed to bind simultaneously to CD4 binding site and V3 loop. D) miniCD4-GNP-Chol bearing miniCD4 miniproteins and cholesterol molecules should anchor in the membrane regions (RAFT) of the host cells used by HIV to infect. In this way HIV would bind miniCD4-GNP-Chol and block HIV entry.

GNPs presenting multiple copies of miniCD4 should enhance its antiviral activity because miniCD4 binds to gp120 that is presented as a trimer in the viral Env protein... Multivalent miniCD4-GNPs could be able to simultaneously bind more than one CD4 binding site of Env, giving a stronger binding and thus higher neutralization activity (Figure 5B).

GNPs coated with miniCD4 and sulphate groups were also prepared (miniCD4-GNP-SO$_4$, Figure 5C). Baleux *et al.* showed that a miniCD4 conjugated to a short heparan sulphate dodecamer is able to bind gp120, induces the exposure of the coreceptor binding domain (V3 loop) and renders it available for interaction with the sulphate oligosaccharide.[17] The linkage between the miniCD4 and the heparan sulphate derivative provides strong cooperative effects, resulting in low-nanomolar antiviral activity. Very recently, by using similar strategy, they obtained better results by conjugating miniCD4 to a peptide that contain sulpho-tyrosine and p-carboxymethyl phenylalanine.[18]

We also prepared GNPs incorporating miniCD4 and cholesterol (miniCD4-GNP-Chol). We expected that the presence of cholesterol enhances the antiviral strength of miniCD4-GNPs by anchoring miniCD4-GNP-Chol to the cell membrane (Figure 5D). Ingallinella *et al.* have demonstrated that an anti-HIV peptide become more active when a cholesterol tail was linked to the peptide.[19] This was possible because cholesterol is a good lipid anchor for cholesterol-enriched lipid rafts that play also an important role in HIV fusion.[20, 21, 22] Lipid rafts are particularly enriched in transmembrane proteins and receptors, and these include CD4, the primary receptor for HIV. We used the same strategy of Ingallinella *et al.* to increase the potency of miniCD4 by targeting lipid raft with cholesterol directly linked to the GNP. The aim was to synthesize a multivalent artificial receptor localized in the region of the cellular membrane that HIV uses to entry into host cells.

In this chapter, the preparation and characterization of the three miniCD4-GNPs is presented (Figure 6). In the preparation of miniCD4-GNP, miniCD4 were coupled to a GNP decorated with GlcC5 and a carboxyl ending linker (miniCD4-GNP, Figure 6A). In the search of a possible synergy effect, and inspired by the work of Baleux, a second

---

[17] Baleux, F., Loureiro-Morais, L., Hersant, Y., Clayette, P., Arenzana-Seisdedos, F., Bonnaffé, D., and Lortat-Jacob, H. (2009). A synthetic CD4–heparan sulfate glycoconjugate inhibits CCR5 and CXCR4 HIV-1 attachment and entry. *Nat. Chem. Biol.* **5**, 743-748.

[18] Connell, B. J., Baleux, F., Coic, Y., Clayette, P., Bonnaffé, D., and Lortat-Jacob H. (2012). A synthetic heparan sulfate-mimetic peptide conjugated to a mini CD4 displays very high anti-HIV-1 activity independently of coreceptor usage. *Chem. Biol.* **19**, 131-139.

[19] Ingallinella, P., Bianchi, E., Ladwa, N. A., Wang, Y., Hrin, R., Veneziano, M., Bonelli, F., Ketas, T. J., Moore, J. P., Miller, M. D., and Pessi, A. (2009). Addition of a cholesterol group to an HIV-1 peptide fusion inhibitor dramatically increases its antiviral potency. *Proc. Natl. Acad. Sci. USA* **106**, 5801–5806.

[20] Aloia, R. C., Jensen, F. C., Curtain, C. C., Mobley, P. W., and Gordon, L. M. (1988). Lipid composition and fluidity of the human immunodeficiency virus. *Proc Natl Acad Sci USA* **85**, 900–904.

[21] Aloia, R. C., Tian, H., and Jensen, F. C. (1993). Lipid composition and fluidity of the human immunodeficiency virus envelope and host cell plasma membranes. *Proc Natl Acad Sci USA* **90**,.5181–5185.

[22] Ono, A., and Freed, E. O. (2005). Role of lipid rafts in virus replication. *Adv Virus Res* **64**, 311–358.

GNP decorated with miniCD4 and sulphate linkers was prepared (miniCD4-GNP-SO$_4$, Figure 6B).
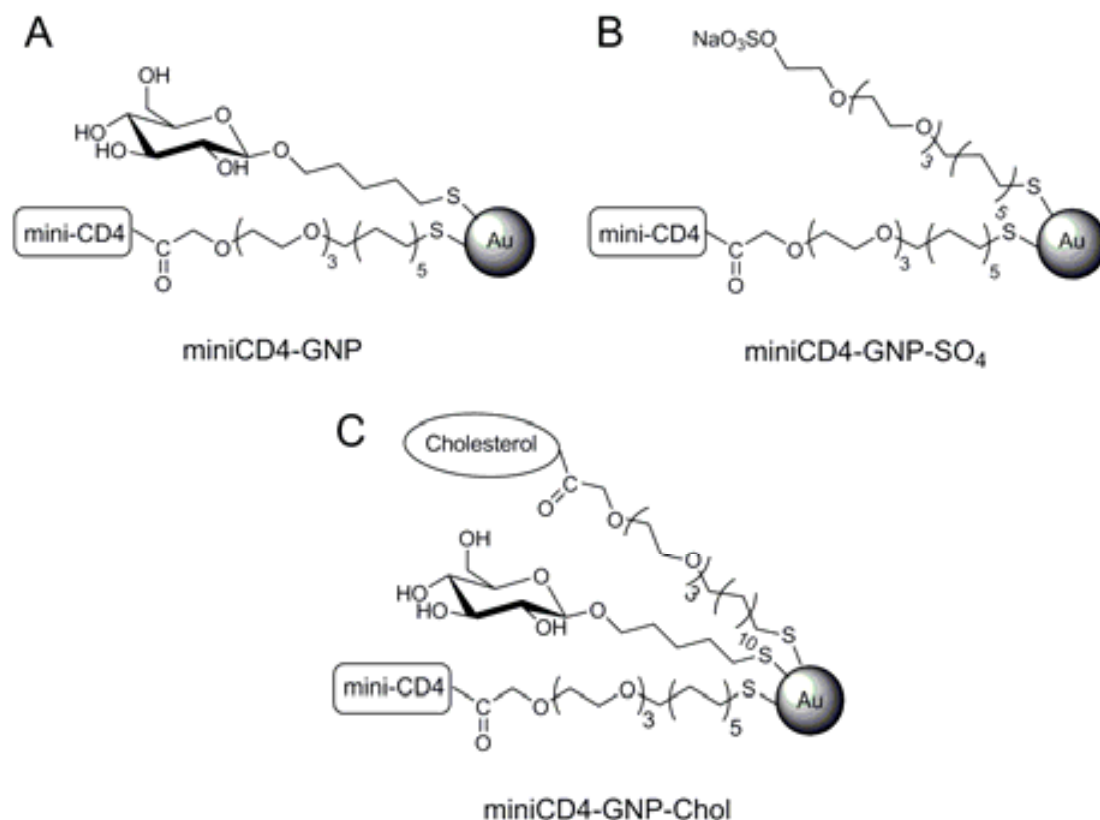
Figure 6. Schematic representation of the three miniCD4-GNPs designed and prepared. A) miniCD4-GNP is covered with 50% of GlcC5, 50% of Linker-CO$_2$H and 4 miniCD4 covalently linked to carboxylic groups. B) miniCD4-GNP-SO$_4$ is covered with 50% of Linker-SO$_4$, 50% of Linker-CO$_2$H and 4 miniCD4 covalently linked to carboxylic groups. C) miniCD4-GNP-SO$_4$ is covered with 50% of Linker-CO$_2$H, 45% of of GlcC5, 5% of Linker-Chol and 4 miniCD4 covalently linked to carboxylic groups.

We have already demonstrated that GNPs bearing sulphate groups (GNP-SO$_4$) are able to inhibit HIV infection in cells.[23] Now, looking for stronger antiviral effect, we covered GNPs with both miniCD4 and sulphate groups.

The third GNP incorporates miniCD4 in combination with cholesterol (miniCD4-GNP-Chol, Figure 6C) to anchor the GNP to the cell membrane.

The 3D structure of miniCD4 is essential for its activity, therefore we have studied the conformation of the miniCD4 on the GNPs by circular dichroism (CD) and compared with the conformation of the free miniCD4. To check that the miniCD4 after coupling with GNPs did not loose its capacity to bind gp120, the binding affinity of miniCD4-

---

[23] Di Gianvincenzo, P., Marradi, M., Martínez-Ávila, O. M., Bedoya, L. M., Alcamí, J., and Penadés, S. (2010). Gold nanoparticles capped with sulphated-ended ligands as anti-HIV agents. *Bioorg Med Chem Lett.* **20**, 2718-2721.

GNPs to gp120 was evaluated by surface plasmon resonance (SPR) experiments.. Moreover, the potency of miniCD4-GNPs to neutralize HIV-1, experiments was performed in the laboratory of Dr. Elisa Vicenzi (HSR, Milan, Italy), a partner in the CHAARM project.

Results and discussion

GNPs preparation and characterization

For the preparation of the miniCD4-GNPs we have previously synthesized three different GNPs (Scheme 1).
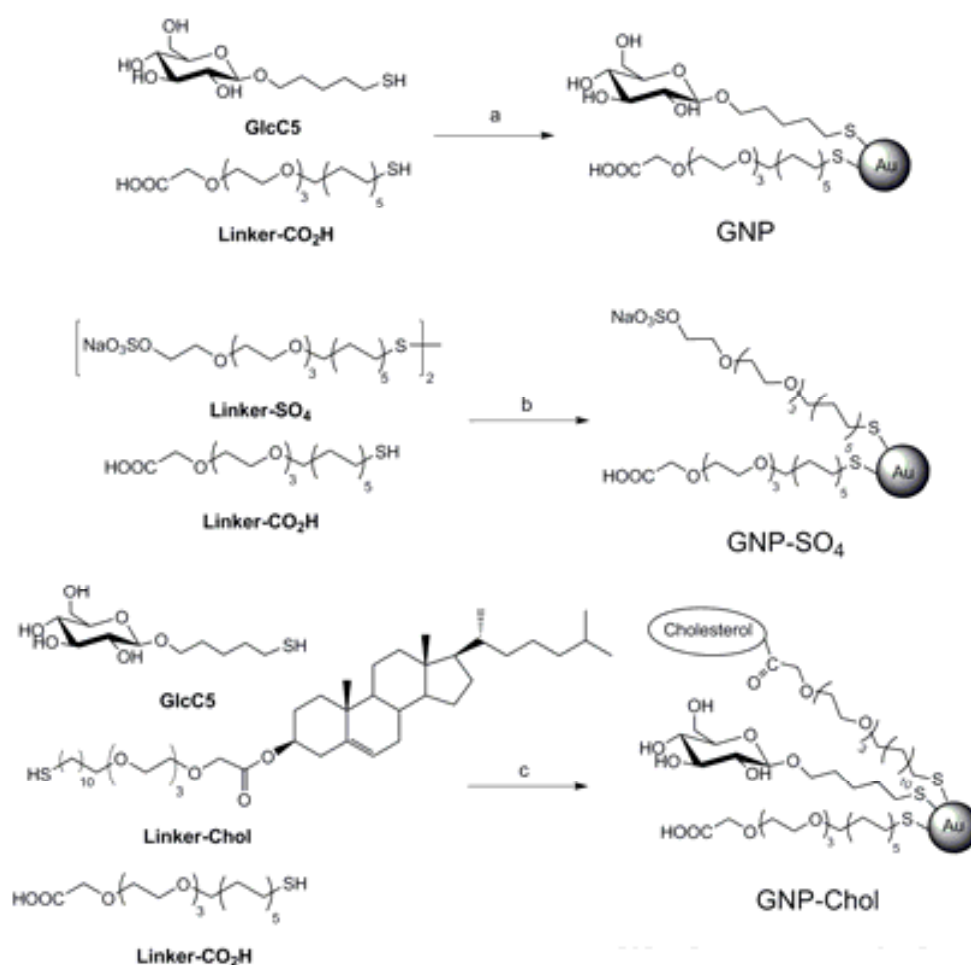
Scheme 1. Preparation of GNPs. Reagents and conditions. a) and b) HAuCl$_4$, NaBH$_4$, MeOH /H$_2$O/CH$_3$CO$_2$H (3:3:1), 25 °C, 2 h. c) HAuCl$_4$, NaBH$_4$, MeOH/H$_2$O/CH$_3$CO$_2$H (4:2:1), 25 °C, 2 h.

One of them (GNP) is covered with 50% of 5-(thio)pentyl β-D-glucopyranoside (GlcC$_5$) and 50% of a bifunctional tetramethylenglycol-C$_{11}$ aliphatic linker ending in a carboxylic group at the ot (Linker-CO$_2$H). The GNP-SO$_4$ is coated by 50% of Linker-CO$_2$H and

50% of Linker-SO$_4$ already described in chapter 1. The GNP-Chol is coated by 50% of Linker-CO$_2$H, 45% of GlcC$_5$ and 5% of a cholesterol derivative (Linker-Chol). The carboxylic groups present in the three GNPs are required to conjugate the miniCD4 to GNPs by the formation of a peptidic bond with the only lysine present on the miniCD4. GlcC$_5$, is used to give solubility, biocompatibility and to control the ligands density on the GNP surface. The synthesis of Linker-SO$_4$ was already described in chapter 1. Synthesis of Linker-CO$_2$H was already described[24] and is reported in the experimental part of this chapter. The preparation of the cholesterol ending linker (Linker-Chol) was carried out following the procedure illustrated in Scheme 2.
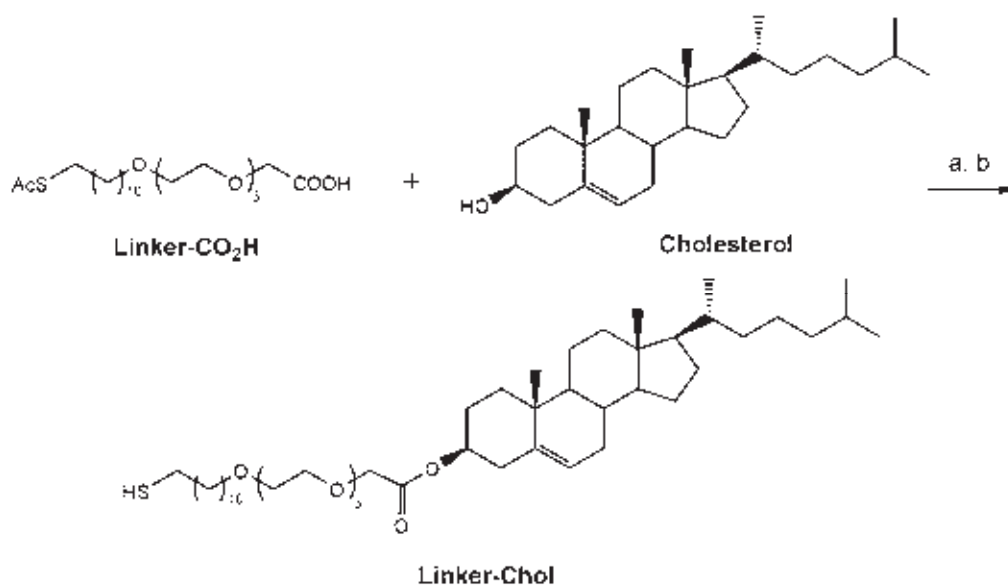
Scheme 2. Preparation of compound Linker-Chol. Reagents and conditions. a) EDC, DMAP, DCM, R.T. 20h, 52%. b) NH$_2$NH$_2$Ac, MeOH/DCM (1:1), R.T. 24h, 40%.

Commercially available cholesterol was conjugated to Linker-CO$_2$H through an ester bond between the carboxylic group of Linker-CO$_2$H and the hydroxylic group of cholesterol. Carboxyl group of Linker-CO$_2$H was deprotonated with DMAP and activated with EDC in DCM dry. Cholesterol was added to the mixture and left under stirring 20 hours at room temperature. The crude was purified in an automatic flash column chromatography (Biotage SP4, FCC) and the tioacetylated Linker-Chol was obtained with 52% yield. Thiol deprotection with MeONa/MeOH gives also hydrolysis of the ester group. A modified procedure used by A. Endo et al.[25] was used in a second

[24] García, I., Gallo, J., Genicio, N., Padro, D., and Penadés, S. (2011). Magnetic glyconanoparticles as a versatile platform for selective immunolabelling and imaging of cells. *Bioconjugate Chem.* **22**, 264–273.
[25] Endo, A., Yanagisawa, A., Abe, M., Tohma, S., Kan, T., and Fukuyama, T. (2002). Total Synthesis of Ecteinascidin 743. *J. Am. Chem. Soc.* **124**, 6552-6554.

attempt. Deprotection was carried out in MeOH/DCM (1:1) by treatment with NH_2NH_2Ac at room temperature for 24h. Linker-Chol was obtained with 40% yield.

GNPs were prepared using a one-pot reaction well established in our laboratory.[26] The reduction of a $HAuCl_4$ (0.025 M, 1 equiv) in presence of $NaBH_4$ (1 N, 22 equiv) induces the formation of an S-Au bond between the metallic core and the thiol linkers (Scheme 1). All the reactions were performed in a mixture of $MeOH/H_2O/CH_3COOH$. For the preparation of GNP and GNP-SO_4 a 1:1 ratio of Linker-CO_2H/GlcC$_5$, and Linker-CO_2H/ Linker-SO_4 was used, respectively. After 2 hours shaking, the solvent was removed at reduced pressure and the brown/black solid was washed with MeOH or EtOH to eliminate unreacted products. GNPs were dissolved in the minimum quantity of milliQ water, loaded into a segment of SnakeSkin® pleated dialysis tubing (Pierce, 3500 MWCO) and purified by dialysis against distilled water. For the preparation of GNP-Chol, a mixture of Linker-CO_2H/GlcC$_5$/Linker-Chol (ratio 48:48:4) was dissolved in $MeOH/H_2O/CH_3COOH$ (4:2:1). $HAuCl_4$ and $NaBH_4$ were added, and the reaction was left shaking 24 hours at RT. After EtOH wash and dialysis all GNPs were freeze dried. TEM, UV-vis and ^{1}HNMR analysis of GNP (with only GlcC$_5$ and Linker-CO_2H) are presented in Figure 7 as an example of characterization.
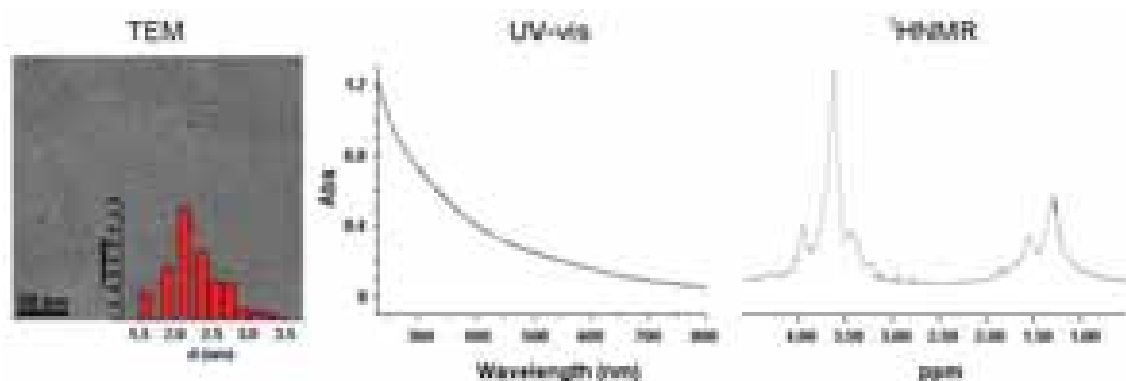
Figure 7. Usual GNP characterization: TEM, UV-vis spectra and ^{1}HNMR spectra of GNP.

The size distribution of all GNPs was evaluated from TEM micrographs by means of an automatic image analyser. On the basis of the gold diameter obtained by TEM, the average number of gold atoms, and the molecular formula of the nanoparticles were calculated according to a previous work (Table 1). For GNP and GNP-SO_4 the ratio between different compounds on the nanoparticles was determined by ^{1}HNMR of the respective washings (around 50% of each ligand was found). In the case of GNP-Chol, was not possible to determine with good accuracy the low amount of cholesterol

[26] Barrientos, A. G., de la Fuente, J. M., Rojas, T. C., Fernández, A., and Penadés, S. (2003). Gold glyconanoparticles: synthetic polyvalent ligands mimicking glycocalyx-like surfaces as tools for glycobiological studies. *Chem. Eur. J.*, **9**, 1909-1921.

lingand in the washings. For this reason 0.5 mg of GNP-Chol were treated with I_2 in H_2O to completely remove the organic molecules from the gold nucleus. The insoluble naked gold nanoparticles were removed by filtration and ^{1}HNMR was performed on the soluble fraction containing organic ligands. From ^{1}HNMR was found that Linker-CO_2H was present in 50%, $GlcC_5$ in 45% and Linker-Chol in 5%. Average MW and diameter of each GNPs are showed in Table 1.

Table 1. Physical features of GNPs prepared.

GNPs	d (nm)	N° gold atoms	N° of total chains	Molecular formula	MW (KDa)
GNP	2.1 ± 0.5	225	124	$Au_{225}(C_{19}H_{37}O_6S)_{60}(C_{11}H_{21}O_6S)_{64}$	86
GNP-SO_4	1.8 ± 0.4	201	106	$Au_{201}(C_{19}H_{39}O_8S_2)_{53}(C_{19}H_{37}O_6S)_{53}$	86
GNP-Chol	1.9 ± 0.7	225	127	$Au_{225}(C_{19}H_{37}O_6S)_{65}(C_{11}H_{21}O_6S)_{58}(C_{46}H_{82}O_6S)_4$	89

Number of gold atoms, molecular formulas and MW were calculated using the size of gold cluster obtained by TEM. [27] Data confirmed by elemental analysis.

Preparation of miniCD4-GNPs

For the preparation of miniCD4 functionalized GNPs, the previously prepared GNPs (Scheme 1), were coupled to miniCD4 M48U1, (received from Dr Loic Martin CEA, Commissariat à l' énergie atomique, partner in the CHAARM project) through a peptidic bond between carboxylic group of the GNP and the amine group of the lysine present in the peptide. This type of linkage was choose to prevent any modification of the miniCD4 binding site. Indeed lysine is located on the α-helix region of miniCD4 and its side-chain point in opposite direction respect the binding site of the gp120. GNPs were dissolved in PBS (1 mg/ml) and 1-ethyl-3-(-3-dimethylaminopropyl) carbodiimide hydrochloride (EDC) and N-hydroxysuccinimide (NHS) were added. The mixtures were left under shaking 1 h and a solution of miniCD4 (1 mg/ml in PBS) was added. Coupling reactions were left under shaking 24 h at RT. MiniCD4-GNPs were filtered and washed with HCl (5 mM) and H_2O on Amicon filters (30 KDa MWCO). Washings were collected to determine the amount of miniCD4 coupled to the GNP.

---

[27] Hostetler, M. J. Wingate, J. E., Zhong, C. J., Harris, J. E., Vachet, R. W., Clark, M. R., Londono, J. D., Green, S. J., Stokes, J. J., Wignall, G. D., Glish, G. L., Porter, M. D., Evans, N. D., and Murray, R. W. (1998). Alkanethiolate gold cluster molecules with core diameters from 1.5 to 5.2 nm: Core and monolayer properties as a function of core size. *Langmuir* **14**, 17-30.

Characterization of miniCD4-GNPs

After coupling all the three miniCD4-GNPs were characterized by ^{1}HNMR to check the presence of miniCD4 on GNPs (Figure 8). The ^{1}HNMR of miniCD4-GNP show a broad signal between 0.7-0.9 ppm indicating the presence of miniCD4 on the GNP (CH_3 of miniCD4 leucine's). Less intense signals related to the peptide were also detected around 3 ppm and between 6.8-7.4 ppm (aromatic region).
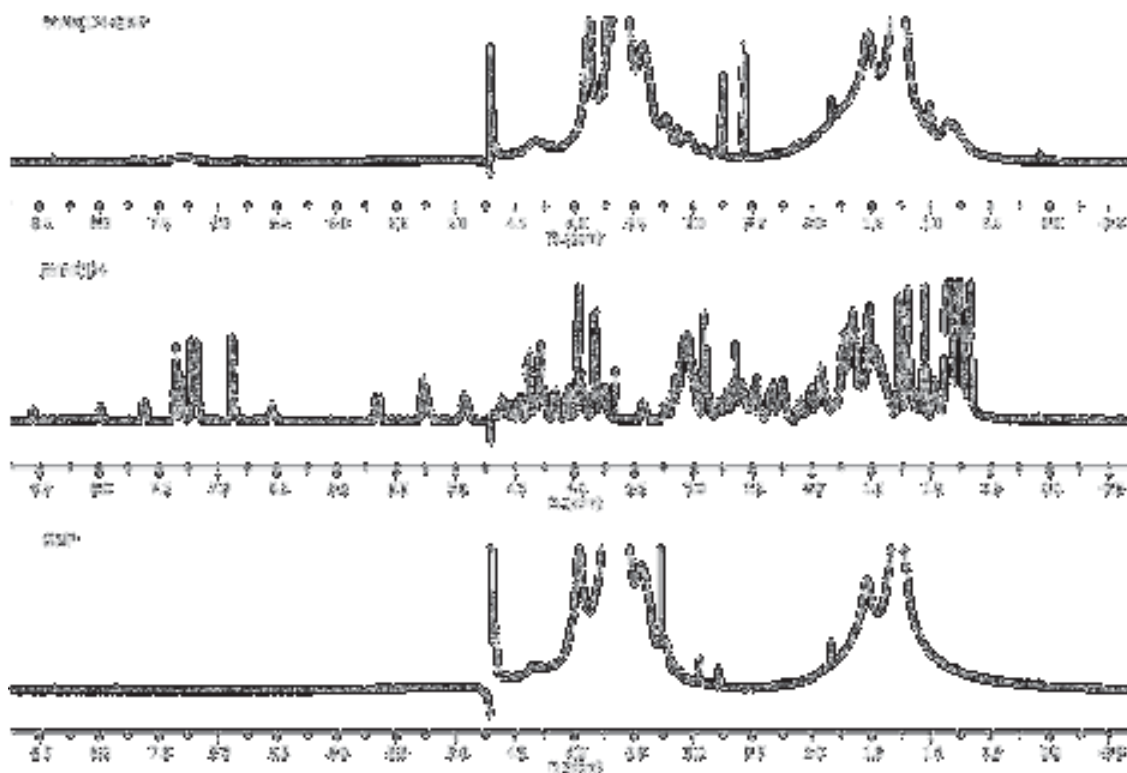
Figure 8. ^{1}HNMR characterization of miniCD4-GNP (500 MHz, D_2O). Comparison between ^{1}HNMR spectra of GNP, miniCD4 and miniCD4-GNP.

The amount of miniCD4 on the miniCD4-GNP was determined analyzing the washings that should contain the miniCD4 no coupled to GNPs by Bradford test. Was found that around 4 miniCD4 were coupled per GNP.

The miniCD4-GNPs were also characterized by CD (Figure 9). CD experiments are very important tools to study proteins-nanoparticles complexes because proteins and peptides often undergo conformational change after binding to charged nanoparticles.[28, 29] The CD spectra of miniCD4 and miniCD4-GNPs were performed at

---

[28] Aubin-Tam, M., and Hamad-Schifferli, K. (2005). Gold nanoparticle-cytochrome c complexes the effect of nanoparticle ligand charge on protein structure. *Langmuir* **21**, 12080-12084.

[29] Shang, L., Wang, Y., Jiang, J., and Dong, S. (2007). pH-Dependent protein conformational changes in albumin:gold nanoparticles bioconjugates: a spectroscopic study. *Langmuir* **23**, 2714-2721.

20 µM of miniCD4 in phosphate buffer 5 mM pH 7. Each CD spectrum was subtracted from buffer spectrum and secondary structure analysis of CD spectrum was performed by using the algorithm CDSSTR on DICHROWEB (http://www.cryst.bbk.ac.uk/cdweb/html/ home.html).[30, 31]
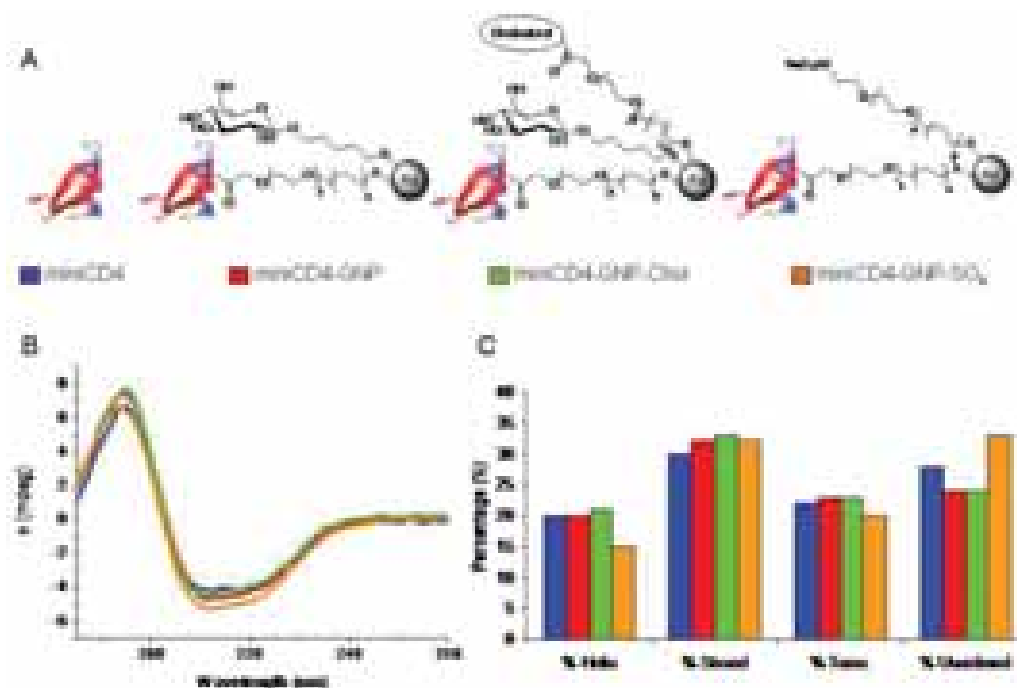
Figure 9. CD spectra of miniCD4 and miniCD4-GNPs. A) structure of miniCD4 and miniCD4-GNPs. B) CD spectra of miniCD4 and miniCD4-GNPs (20 µM in miniCD4, phosphate buffer 5 mM, pH 7). C) Secondary structure analysis of CD spectra performed by using the algorithm CDSSTR on DICHROWEB.

From CD data it is possible to conclude that there are no important changes in miniCD4 structure after coupling to GNPs. However, it seems that miniCD4 on GNP-SO$_4$ loose some α-helix characters, while the percentage of unordered/random coil increase. The proximity of an arginine in the α-helix region of miniCD4 and the negative charges of sulphates on GNP-SO$_4$, probably induce an interaction that partially unfolds the α-helix segment.

Interaction of miniCD4-GNPs with gp120

The interaction of miniCD4-GNPs and control GNPs with gp120 was studied in a preliminary screening with ProteOn biosensor. gp120 was immobilized on a GLC sensor chip using the standard amine coupling. The carboxylic groups of two different

[30] Whitmore, L. and Wallace, B. A. (2004) DICHROWEB, an online server for protein secondary structure analyses from circular dichroism spectroscopic data. *Nucleic Acids Res.* **3**, W668-673.

[31] Whitmore, L. and Wallace, B. A. (2008) Protein secondary structure analyses from circular dichroism spectroscopy: methods and reference databases. *Biopolymers* **89**, 392-400.

channels (channel 1 and 2) of the chip surface were activated by a mixture of EDAC (16 mM) and Sulpho-NHS (4 mM). Channel 1 was further injected with a gp120 solution in acetate buffer (50 µg mL^{-1}, 10 mM, pH 4) to obtain an immobilization level of 3300 Response Units (RU). Only PBS/Tween was flown thought channel 2, which was used as a reference surface. Six different concentrations (20, 10, 5, 2.5, 1.25, and 0.625 µg mL^{-1} in PBST containing 0.005% of Tween 20) of each miniCD4-GNP were injected over both channels.
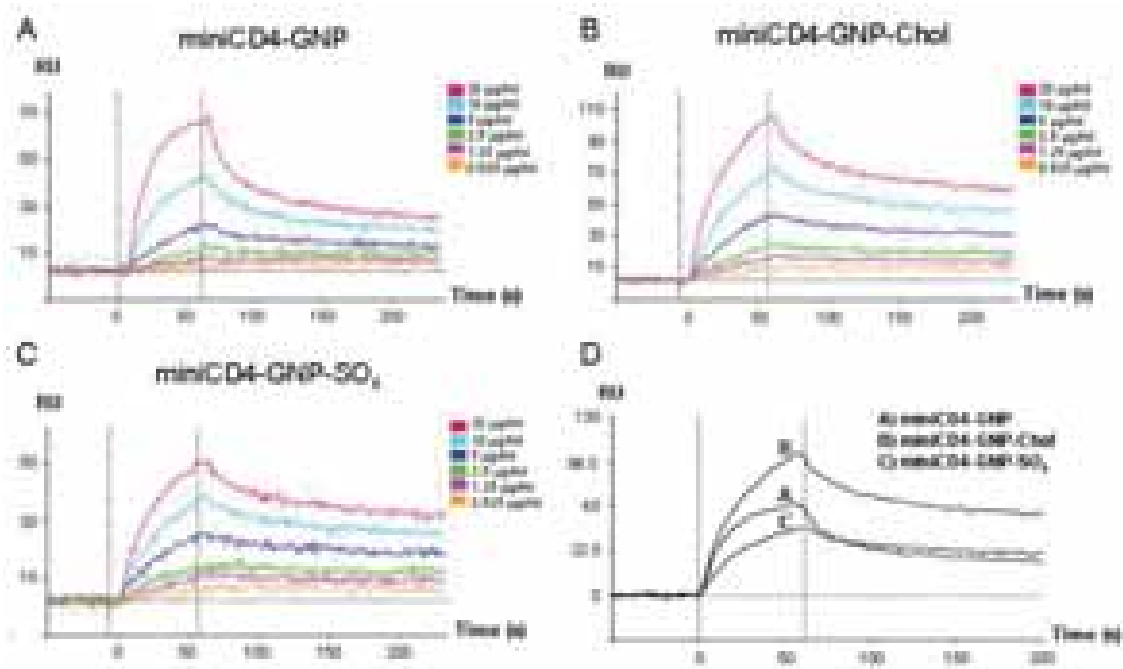
Figure 10. SPR experiments. Sensorgrams representing the dose-dependent binding of miniCD4-GNPs to immobilized gp120. Six different concentrations in PBST were tested for each GNP (20, 10, 5, 2.5, 1.25, and 0.625 µg/ml in ProteOn PBS/Tween buffer). A) miniCD4-GNP binding to gp120 B) miniCD4-GNP-Chol binding to gp120C) miniCD4-GNP-SO$_4$ binding to gp120 D) Sensogram with the highest concentration binding curve (20 µg/ml) of each miniCD4-GNP.

The binding profiles (sensorgrams) were obtained by an automatic subtraction of the reference surface signals from the gp120-activated surface signals (Figure 10). The sensor surface between runs was regenerated with a short pulse of 0.1 M HCl.

All miniCD4-GNPs bind gp120. From SPR data we can say that miniCD4 on GNPs do not loose the ability to bind gp120, probably because the lysine involved in the coupling with GNPs is located on the α-helix region of miniCD4 in opposite direction respect the binding site of the gp120. Kinetic analysis was performed with Langmuir model (Table 3).

Table 3. Kinetic data obtained from sensograms of figure 9 (Langmuir kinetic model).

	Ka (1/Ms)	Kd (1/s)	Rmax	Chi2
miniCD4-GNP	$1.67 \cdot 10^5$	$5.05 \cdot 10^{-3}$	57.5	6.55
miniCD4-GNP-SO$_4$	$2.25 \cdot 10^5$	$2.34 \cdot 10^{-3}$	43.9	2.16
miniCD4-GNP-Chol	$1.91 \cdot 10^5$	$2.72 \cdot 10^{-3}$	95.2	7.35

The differences in binding between the three miniCD4-GNPs. are not due to different molecular weight because, as showed in table 1, all the miniCD4-GNPs have a MW around 86 KDa. The best binding comes from miniCD4-GNP-Chol, probably because of the interaction of cholesterol with hydrophobic regions on gp120. Indeed, conserved regions of gp120 (C3 and C4) contain hydrophobic amino acids that influence the interaction of gp120 with gp41.[32] These hydrophobic regions lie adjacent to residues implicated in the CD4 binding site on gp120.

HIV neutralization assay

The potency of miniCD4-GNP, miniCD4-GNP-Chol, and miniCD4-GNP-SO$_4$ and the respective controls (GNP, GNP-Chol, and GNP-SO$_4$) to neutralize HIV were tested in the laboratory of Prof. Elisa Vicenzi (Figure 11). Two different neutralization experiments were performed. In one experiment, cells were incubated with miniCD4-GNPs before virus infection (Figure 11A) and another experiment, the virus was incubated with miniCD4-GNPs followed by incubation with cells (Figure 11B). Two HIV-1 virus were used in each neutralization experiment: Bal(R5) and IIIB(X4). TZMBL cell line stably transfected with CD4 and both CCR5 and CXCR4, were used in HIV-1 neutralization experiments. These cells contain a HIV-1 long terminal repeat-Luciferase cassette. The efficiency of virus infection was determined by measurement of Luciferase activity in cell lysates. The results are average of 2 independent experiments.[33]

---

[32] Helseth, E., Olshevsky, U., Furman, C., and Sodroski, J. (1991). Human Immunodeficiency Virus Type 1 gpl20 Envelope Glycoprotein Regions Important for Association with the gp4l Transmembrane Glycoprotein. *J. Virol.* **65**, 2119-2123.

[33] Trouplin, V., Salvatori, F., Cappello, F., Obry, V., Brelot, A., Heveker, N., Alizon, M., Scarlatti, G., Clavel, F., and Mammano, F. (2001). Determination of Coreceptor Usage of Human Immunodeficiency Virus Type 1 from Patient Plasma Samples by Using a Recombinant Phenotypic Assay. *J. Virol.* **75**, 251-259.
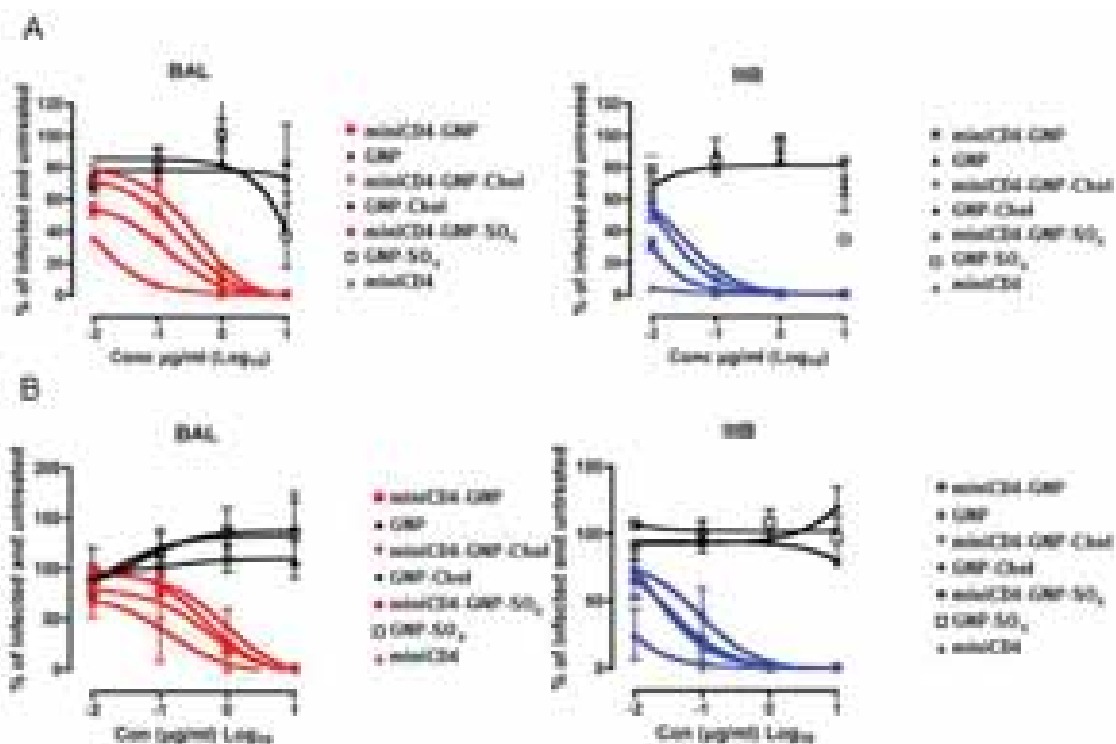
Figure 11. HIV neutralization experiments. A) incubation of cells with miniCD4-GNPs and then virus infection B) incubation of virus with miniCD4-GNPs and subsequent incubation with cells.

From data showed in figure 11, IC50 values were calculated and are presented in Table 2.

Table 2. IC50 values (nM in miniCD4) of HIV-1 neutralization experiments. Two experiments: cells+compounds and virus+compounds. For each experiment two different virus were used: Bal (R5 virus) and IIIB (X4 virus).

Compound	Cells + Compound		Virus + Compound	
	Bal	IIB	Bal	IIB
miniCD4-GNP	5.7	0.8	20.4	1.2
miniCD4-GNP-Chol	16.3	0.9	39.2	0.4
miniCD4-GNP-StO4	8.9	0.7	19.7	0.8
miniCD4	<3.3	0.3	47	<3.3

miniCD4-GNPs inhibit T-cell infection by IIIB virus better than Bal virus and do not present substantial difference in the two different experiments (cells+compound or virus+compound). With the data of these experiments, we can conclude that miniCD4-GNPs inhibit HIV-1 infection in a cell assay with similar potency to the free miniCD4. This result confirms that miniCD4 peptide does not loose its binding capacity on the

GNPs. However,, this result also indicates that the multivalence and multifunctionality of miniCD4-GNPs has not effect in the neutralization of the virus.

Conclusions

The first interaction that allow HIV virus to infect cells is the binding between CD4 and gp120. CD4 binding site in gp120 is highly conserved among different strain. Drugs able to block this interaction can be good candidates for AIDS therapy. In the last years small molecules and miniproteins able to block CD4/gp120 interaction and inhibit HIV infection have been developed.

In the frame of CHAARM project, we had the opportunity to collaborate with L. Martin, who developed a very strong inhibitor of CD4 binding, the miniCD4 M48-U1. It is well known that Env protein is trimeric and HIV entry into the host cells probably need more than one CD4/gp120 binding event. It was hypothesize that the multimerization of miniCD4 M48-U1 probably can enhance the potency of the miniprotein. In this chapter the preparation and the characterization of three different miniCD4-GNPs were presented. Around 4 miniCD4 per GNP were detected on GNPs after peptidic coupling between the lysine of miniCD4 and carboxylic groups of GNPs. The conformation of miniCD4 did not change once linked to the GNPs as showed by CD experiments. Only slightly deviation was found in the CD spectrum of miniCD4-GNP-SO$_4$.

The miniCD4 on the GNPs still binds to gp120 as determined by SPR experiments. HIV-1 neutralization assays do not showed improved IC50 values for the miniCD4-GNPs respect to the free miniCD4.

All together these results clearly show that miniCD4 was successfully linked on the GNPs without any loss of activity. Unfortunately, no multivalent effect were founded. The problem probably lies in the distance between the miniCD4 on the GNPs that do not perfectly match the distance between CD4 binding site on HIV Env. Future studies could be addressed to the preparation of multivalent miniCD4-GNPs with longer or shorter linkers.

Experimental part

General Information

All chemicals were purchased as reagent grade from Sigma-Aldrich unless otherwise stated and were used without further purification. Reactions were monitored by thin layer chromatography (TLC) with silica gel 60 F$_{254}$ aluminium sheets (Merck) and visualized by UV irradiation (254 nm) and/or staining with *p*-anisaldehyde solution

[anisaldehyde (25 mL), H_2SO_4 (25 mL), EtOH (450 mL) and CH_3COOH (1 mL)] or 10% H_2SO_4 solution in EtOH, followed by heating at over 200℃. Size-exclusion column chromatography was performed on Sephadex^{TM} LH-20 (GE Healthcare). Purification of compounds by flash column chromatography on silica gel (FCC) was performed on a Biotage Sp4 HPFC™ automated flash chromatography system (Biotage AB, Uppsala Sweden) or by conventional flash chromatography using silica gel 60 (0.063-0.200 mm, 0.015-0.040 mm; Merck). UV-Vis spectra were carried out with a Beckman Coulter DU 800 spectrometer. ^{1}H and ^{13}C NMR spectra were recorded on a Bruker AVANCE (500 MHz) spectrometer. Chemical shifts (δ) are given in ppm relative to the residual signal of the solvent used. The values of coupling constants (*J*) are given in Hz. Splitting patterns are described by using the following abbreviations: br, broad; s, singlet; d, doublet; t, triplet; m, multiplet. The mass spectrometric data were obtained from a Waters LCT Premier XE instrument with a standard ESI source by direct injection. The instrument was operated with a capillary voltage of 1.0 kV and a cone voltage of 200 V. Cone and desolvation gas flow were set to 50 and 500 L/h, respectively; source and desolvation temperatures were 100 ºC. The exact mass was determined using glycocholic acid (Sigma) as an internal standard (2 M+Na^{+}, m/z = 953.6058). For transmission electron microscopy (TEM) examinations, a single drop (10 µL) of the aqueous solution (*ca.* 0.1 mg mL^{-1} in milliQ water) of the gold nanoparticles was placed onto a copper grid coated with a carbon film (Electron Microscopy Sciences). The grid was left to dry in air for several hours at room temperature. TEM analyses were carried out in a Philips JEOL JEM-2100F working at 200 kV. Surface plasmon resonance (SPR) measurements were carried out using a ProteOn XPR36 Protein Interaction Array System with research-grade GLC sensor chips and all reagents were supplied by Bio-Rad (Bio-Rad Laboratories, Inc.).

Recombinant Proteins. Recombinant gp120 from HIV-1 CN54 clone (repository reference ARP683) was obtained from the Programme EVA Centre for AIDS Reagents, NIBSC, UK, supported by the EC FP6/7 Europrise Network of Excellence, AVIP and NGIN consortia and the Bill and Melinda Gates GHRC-CAVD Project and was donated by Prof. Ian Jones (Reading University, UK).

Synthesis

Preparation of 23-mercapto-3,6,9,12-tetraoxatricosan-1-oic acid (Linker-CO₂H)

1

2   **4**
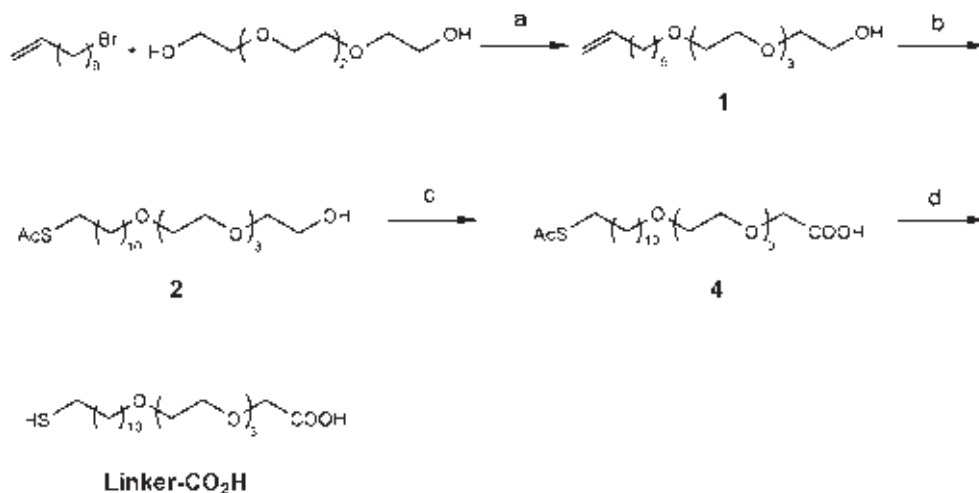
Linker-CO₂H

Preparation of Linker-CO$_2$H. Reagents and conditions. a) NaOH (50%), 100ºC, 16h. b) AcSH, AIBN, THFdry, reflux, 3h . C) (i) MeONa, MeOH, 15h (ii) amberlite IR-120.

Undecen-1-en-11-yl tetra(ethylene glycol) (1)

 A mixture of tetraethylenglycol (TEG) (35.6 g, 183.5 mmol) and NaOH (50%) (2.7 ml, 43.7 mmol) were stirred for 30 min at 100 ºC. The reaction was cooled to room temperature and 11-Br-undecene (10.2 g, 43.7 mmol) was added. The reaction was heated at 100ºC and left overnight under stirring. The mixture was diluted with CH$_2$Cl$_2$ (20 ml), washed with water (40 ml) and extracted with hexane (3 x 40 ml). The hexane fractions were collected, dried over Na$_2$SO$_4$, filtered and the solvent evaporated at reduced pressure. The crude product (16 g) was purified by flash column chromatography on silica gel (EtOAc) to give 1 (10.46 g, 69%) as a yellow oil.

Rf = 0.31 (EtOAc). ^{1}H RMN (CDCl$_3$, 500 MHz) 1.26-1.36 (m, 12H); 1.57-1.65 (m, 2H); 2.01 (dd, *J* = 14.4, 6.9 Hz, 2H). 3.12 (bs, 1H), 3.43 (t, *J* = 6.8 Hz, 2H); 3.54-3.67 (m, 14H); 3.68-3.73 (m, 2H); 4.90 (dd, *J* = 10.2, 9.1, 1H), 4.97 (ddd, *J* = 17.1, 3.4, 1.6, 1H); 5.78 (ddt, *J* = 16.9, 10.2, 6.7, 1H).

1-(Thioacetylundec-11-yl)tetra(ethylene glycol) (2)

 To a solution of 1 (9.6 g, 27.7 mmol) in dry THF, AcSH (10.49 g, 138 mmol) and AIBN (cat.) were added. The mixture was stirred under reflux for 3 hours. The reaction was diluted with 30 ml of EtOAc and pH neutralised with a

saturated solution of NaHCO$_3$. The organic phase was washed with brine, dried over Na$_2$SO$_4$ and the solvent removed at reduced pressure. The residue was purified by flash column chromatografy on silica gel (EtOAc:hexane 9:1 to EtOAc) to obtain 2 as a colourless oil (7.8 g, 67%). Rf = 0.28 (EtOAc). ^{1}H RMN (CDCl$_3$, 500 MHz) 1.25-1.36 (m, 14H); 1.53-1.67 (m, 4H); 2.12 (s, 3H); 2.65 (t, *J* = 7.3 Hz, 2H); 3.26 (t, *J* = 6.8 Hz, 2H); 3.55-3.71 (m, 16H).

22-(Thioacetyl)-2,5,8,11-tetraoxadocosan-1-oic acid (4)

 Compound 2 (1 g, 2.37 mmol) was dissolved in 5 ml acetone and Jones reagent was added drop by drop until red colour persisted. Then, the reaction was allowed to continue for 30 min and it was subsequently stopped with 2-propanol, diluted with ethyl acetate, washed twice with water, and dried in the rotatory evaporator. The purification was performed by column chromatography (CH$_2$Cl$_2$: MeOH 19:1) and product 4 was obtained as a syrup (69% yield). ^{1}H NMR (500 MHz, CDCl$_3$), δ 1.12-1.36 (m, 14H), 1.43-1.66 (m, 4H), 2.30 (s, 3H), 2.84 (t, *J* = 7.3 Hz, 2H), 3.40 (t, *J* = 6.8 Hz, 2H), 3.49-3.82 (m, 12H), 4.00 (s, 2H).

Linker-CO$_2$H

The protected product 4 (0.712 g, 1.8 mmol) was dissolved in 34 ml methanol and sodium methoxide (0.088 g, 1.6 mmol) was added. The solution was stirred for 6 hours and then the pH was neutralized with Amberlite IR120 H$^+$. The reaction was filtered, dried in the rotary evaporator and washed several times with diethyl ether. The final Linker-CO$_2$H was obtained as a mixture of thiol and disulfide (39:61). (82% yield). ^{1}H NMR (500 MHz, CDCl$_3$), δ 1.30-1.70 (m, 18H), 2.50 (t, *J* = 7.0 Hz, 2H thiol), 2.69 (t, *J* = 7.0 Hz, 2H disulfide) 3.50 (t, *J* = 14.0 Hz, 2H), 3.60-3.80 (m, 12H), 4.15 (s, 2H disulfide), 4.19 (s, 2H thiol). HR-MS (pos., ionization phase MeOH) m/z: 416.2213 [M + 2Na]$^{+2}$ (C$_{38}$H$_{72}$O$_{12}$S$_2$Na$_2$ requires 416.2209).

Linker-Chol
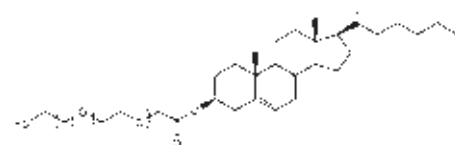
 Linker-CO$_2$H (73.3 mg, 0.168 mmol) and cholesterol (50 mg, 0.13 mmol) were dissolved in 8 ml of DCM dry. EDC (49.5 mg, 0.259 mmol) and DMAP (14.2 mg, 0.116 mmol) were added to the mixture and left under stirring 20h at RT. The solvent was removed under reduced pressure giving Linker-Chol crude as

yellow oil (250 mg). The product was purified in biotage sp4 FCC (Hexane/AcOEt) and product was obtained as an oil (54 mg, 52% yield).The protected product (25 mg, 0.031 mmol) was dissolved in DCM/methanol 1:1 (1 ml) and a solution of NH_2NH_2Ac in methanol (114 µl, 1M) was added. The solution was left under stirring over night at RT. The reaction was diluted with DCM and washed with 1 M HCl, $NaHCO_3$ sat. solution, NaCl sat. solution and dried over Na_2SO_4. The product was purified in biotage sp4 FCC (Hexane/AcOEt) and product was obtained as an oil (11 mg, 40% yield).The final Linker-Chol was obtained as a mixture of thiol and disulfide. ^{1}H NMR (500 MHz, $CDCl_3$), δ 0.67 (s, 3H), 0.86 (d, 6H), 0.91 (d, 3H), 0.92-2.2 (m, 50H), 2.34 (d, 2H), 2.53 (q, 2H), 3.43 (t, 2H), 3.57-3.72 (m, 12H), 4.69 (m, 1H), 5.38 (d, 1H). HR-MS (pos., ionization phase MeOH) m/z: 785.9154 $[M + Na]^+$.

GNPs preparation

General Procedures. To obtain nanoparticles, an aqueous solution of tetrachloroauric acid (Strem Chemicals) (0.025 M, 1 eq.) was added to a solution of a mixture of appropriate thiol ending linkers (0.012 M, 6 eq.) in $MeOH/H_2O/CH_3COOH$ (3:3:1). An aqueous solution of $NaBH_4$ (1 M, 22 eq.) was then portion-wise added and the mixture was shaken for 2 hours at 25 ºC. The solvent was evaporated at reduced pressure. The residue was washed with ethanol, re-dissolved in the minimum quantity of milliQ water, loaded into 5-10 cm segments of SnakeSkin® pleated dialysis tubing (Pierce, 3500 MWCO) and purified by dialysis against distilled water (3 L of water, recharging with fresh water every 6 hours over the course of 72 hours). The nanoparticles were obtained as brown powder after lyophilization. The size distribution of the gold nanoparticles was evaluated from several TEM micrographs by means of an automatic image analyser. On the basis of the gold diameter obtained by TEM, the average number of gold atoms and molecular formula of the nanoparticles were calculated according to a previous work[4S] and confirmed by elemental analysis.

GNP

Starting from Linker-CO_2H (38.1 mg, 0.097 mmol) and $GlcC_5$ (27.3 mg, 0.097 mmol), $HAuCl_4$ (2.59 ml, 25 mM) and $NaBH_4$ (1.4 ml, 1 M), GNP was obtained as brown amorphous powder (20.8 mg).

TEM (average diameter and number of gold atoms): 2.1 ± 0.5 nm, 225; ^{1}H NMR (500 MHz, D$_2$O): δ 4.4 (br s, ~1H), 4.2-3.2 (br m, ~26H), 2.1-0.6 (br m, ~22H); UV-Vis (H$_2$O, 0.1 mg/ml): very weak surface plasmon signal was observed at ~ 550 nm; Elemental analysis: Calculated (%) for Au$_{225}$(C$_{19}$H$_{37}$O$_6$S)$_{60}$(C$_{11}$H$_{21}$O$_6$S)$_{64}$: C 25.77, H 4.18, S 4.63, found: C 25.82, H 4.20, S 4.58.

GNP-SO$_4$
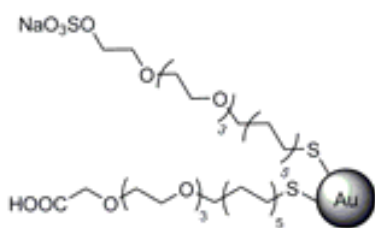
Starting from Linker-CO$_2$H (6.2 mg, 0.0157 mmol) and Linker-SO$_4$ (7.58 mg, 0.0157 mmol), HAuCl$_4$ (419 µl, 25 mM) and NaBH$_4$ (230 µl, 1 M), GNP-SO$_4$ was obtained as brown amorphous powder (3.12 mg).

TEM (average diameter and number of gold atoms): 1.8 ± 0.4 nm, 201; ^{1}H NMR (500 MHz, D$_2$O): δ 4.26 (br s, ~2H), 4.1-3.0 (br m, ~30H), 2.05-0.9 (br m, ~40H); UV-Vis (H$_2$O, 0.1 mg/ml): no surface plasmon signal was observed; Elemental analysis: Calculated (%) for Au$_{201}$(C$_{19}$H$_{39}$O$_8$S$_2$)$_{53}$(C$_{19}$H$_{37}$O$_6$S)$_{53}$: C 29.09, H 4.81, S 5.94, found: C 29.71, H 4.74, S 5.09.

GNP-Chol
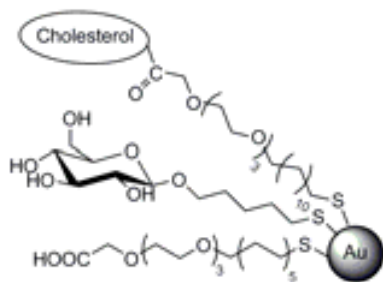
Starting from Linker-CO$_2$H (4.7 mg, 0.012 mmol), GlcC$_5$S (3.38 mg, 0.012 mmol), Linker-Chol (0.38 mg, 0.001 mmol), HAuCl$_4$ (330 µl, 25 mM) and NaBH$_4$ (180 µl, 1 M), GNP-Chol was obtained as brown amorphous powder (2.04 mg).

TEM (average diameter and number of gold atoms): 1.9 ± 0.7 nm, 225; ^{1}H NMR (500 MHz, D$_2$O): δ 4.31 (br s, ~3H), 3.90-3.10 (br m, ~90H), 2.65 (br s, 2H, CH$_2$S), 2.12-0.8 (br m, ~60H); UV-Vis (H$_2$O, 0.1 mg/ml): no surface plasmon signal was observed; Elemental analysis: Calculated (%) for Au$_{225}$(C$_{19}$H$_{37}$O$_6$S)$_{65}$(C$_{11}$H$_{21}$O$_6$S)$_{58}$(C$_{46}$H$_{82}$O$_6$S)$_4$: C 27.68, H 4.46, S 4.56, found: C 27.70, H 4.41, S 4.78.

miniCD4-GNPs preparation

In a typical experiment, 1.0 mg of lyophilized GNPs (GNP, GNP-SO_4 or GNP-Chol) was dissolved in 1 ml of PBS 10 mM. The carboxyl groups were activated by adding a solution of 1-ethyl-3-(-3-dimethylaminopropyl) carbodiimide hydrochloride (EDC) (0.12 mg, 0.001 mmol) and N-hydroxysuccinimide (NHS) (0.13 mg, 0.0007 mmol). This mixture was allowed to shake for 1h, and then 150 µl of miniCD4 (1 mg/ml) in PBS was added and the solution was left under shaking over night at RT. The mixture was filtered/centrifuged on amicon filters 30 KDa MWCO, washed once with HCl (5 mM) and three times with H_2O. The brown residue was recovered and freeze dried.

Circular Dichroism (CD) experiments

Experiments were performed on a Jasco 720 spectrophotometer using a quartz cuvette with a 1 mm path length. For all CD studies, scans were taken from 180 to 280 nm at a rate of 20 nm/min with a sample interval of 0.1 nm and an 8 sec response. Each experiments give a final spectrum which is the average of ten scans. All CD spectra were subtracted from blank.

SPR experiments

The binding of miniCD4-GNPs$^-$ to gp120 was studied by SPR using a ProteOn XPR36 Protein Interaction Array System with research-grade GLC sensor chips. Proteon sensor chip are built with an alginate polymer matrix bound to a thin gold film on a sensor prism.[34] gp120 was immobilized on a GLC sensor chip using the standard amine coupling chemistry according to the manufacturer's instructions. A GLC sensor chip was equilibrated with ProteOn PBS/Tween buffer (phosphate buffered saline, pH 7.4, 0.005% Tween 20). The carboxylic groups of two different channels of the chip surface were activated at 25 ºC by injecting 30 µl (contact time: 60 sec; flow rate: 30 µl/min) of a 1 vol/vol mixture of EDAC (16 mM) and Sulpho-NHS (4 mM). Channel 1 was further injected with 120 µL (240 sec; 30 µl/min) of a gp120 solution in acetate buffer (50 µg/ml, 10 mM, pH 4) at 25 ºC to obtain an immobilization level of 3300 Response Units (RU). Only PBS/Tween was flown into channel 2, which was used as a reference surface. Finally, the surfaces of both channels were saturated by 100 µl (200 sec; 30 µl/min) of ethanolamine HCl (1 M, pH 8.5). Simultaneous binding of six different concentrations of each analyte to gp120 was studied. Each analyte was diluted at 20,

---

[34] http://www.biorad.com/evportal/es/ES/evolutionPortal.portal?_nfpb=true&_pageLabel=SolutionsLanding Page&catID=LUSMBUHYP

10, 5, 2.5, 1.25, and 0.625 µg/ml in ProteOn PBS/Tween buffer, and injected at 25 ºC in both channels (contact time: 60 s; dissociation time: 100 s; flow rate: 100 µl/min). The binding profiles (sensorgrams) were obtained by an automatic subtraction of the reference surface signals from the gp120-activated surface signals. The sensor surface between runs was regenerated with a short pulse of 0.1 M HCl.

HIV-1 neutralization assays

TZMBL cell line is stably transfected with CD4 and both CCR5 and CXCR4. These cells contain a Luciferase reported gene that allows the detection of single cycle infection by colorimetric assay. The revelation is based on the expression of Luciferase induced by the newly synthesized Tat and is performed 30 h after the infection. Cells were seeded into 96-well flat bottomed plastic plates (Falcon) at $1x10^5$ cells/ml in 100 µl and were incubated in the presence or absence of the compound at 37℃ for 1h serial dilutions (from 10 to 0.01 µg/ml). Aliquots of IIIB or Bal viral stocks were then added and 48 h later, the efficiency of virus infection was determined by measurement of Luciferase activity in cell lysates.

CHAPTER 3

Secondary structures of a gp120 V3 loop peptide on negative charged glyconanoparticles and study of their interaction

In the frame of CHAARM project

CHAPTER 3

Secondary structures of a gp120 V3 loop peptide on negative charged glyconanoparticles and study of their interaction

INTRODUCTION

HIV virus gain entry into host cells by using envelope proteins (Env) that decorate the viral membrane. Env protein is formed by three transmembrane glycoproteins gp41 non-covalently bound to three gp120. Conformational change of gp120 induced by the binding to CD4 receptors allows the interaction of the exposed V3 loop (third variable region of gp120) peptide with the seven transmembrane proteins (7TM) co-receptor CCR5, responsible for HIV-1 transmission and early years of infection, or/and with the CXCR4, responsible for late infection stages (see Figure 4 in chapter 1).[1]

The V3 loop peptide is the major determinant of HIV tropism and coreceptor usage. Virus that use CCR5 (R5), also referred to as nonsyncytia-inducing or macrophage tropic (M-tropic) viruses, are those preferentially transmitted, whereas those using CXCR4 (X4), also termed syncytia-inducing or T cell line tropic (T-tropic) viruses, are those more associated with later stage disease and disease progression.[2] So-called R5X4 isolates are able to exploit both coreceptors. V3 peptide is the third of five variable regions present in gp120. Despite its name, it presents many constant features: a fixed size (30-35 aa), a conserved type II turn at its tip (GPGR/Q), a disulphide bond at its base, a net positive charge and three conserved *N*-linked glycosylation sites within or adjacent to the V3 loop (N295 or N301, N332, and N392).[3] Co-receptor selection was extensively studied and the "11/24/25 rule" was formulated: *a positively charged amino acid at position 11, 24, or 25 defines X4, otherwise R5*.[4] This rule gave an overall prediction value of 94% for 217 viruses whose tropism had been determined experimentally as either X4 or R5. V3 charge is not the only important

---

[1] Wyatt, R., and Sodroski, J. (1998). The HIV-1 envelope glycoproteins: fusogens, antigens, and immunogens. *Science*, **280**, 1884-1888.

[2] Connor, R. I., Sheridan, K. E., Ceradini, D., Choe, S., and Landau, N. R. (1997). Change in coreceptor use correlates with disease progression in HIV-1-infected individuals. *J. Exp. Med.* **185**, 621-628.

[3] Zolla-Panzer, S., (2004). Identifying epitopes of HIV-1 that induce protective antibodies. *Nat Rev. Imm.* **4**, 199-210.

[4] Cardozo, T., Kimura, T., Philpott, S., Weiser, B., Burger, H., and Zolla Pazner, S. (2007). Structural basis for coreceptor selectivity by the type 1 V3 loop. *AIDS Res. Hum. Retroviruses* **23**, 415-426.

factor for tropism determination. Indeed, the loss of an *N*-linked glycosylation site within the V3 region, in association with the high positive charge, can lead to the complete switch of the virus from the R5 to X4 phenotype.[5] In addition, it was proposed that the N-terminus of the coreceptor binds to the V3 base, while the V3 tip (or arch) interacts with the second extracellular loop of CCR5.[6]

The V3 loop of gp120 not only binds to co-receptors, but also to β-galactosylceramides (β-GalCer) patches and to heparan sulphate, facilitating the initial recruitment of virus to target cells.[7, 8] The amino acids of V3 loop recognized by a synthetic water soluble analog of β-GalCer correspond to the conserved core V3 sequence Gly-Pro-Gly-Arg-Ala-Phe.[9]

Because of its crucial role in HIV entry/fusion process, V3 peptide was widely studied as inhibitor of HIV infection.[10, 11, 12, 13, 14, 15] Since 1993 different modified or truncated V3

[5] Pollakis, G., Kang, S., Kliphuis, A., Chalaby, M. I. M., Goudsmit, J., and Paxton, W. A. (2001). N-linked glycosylation of the HIV type-1 gp120 envelope glycoprotein as a major determinat of CCR5 and CXCR4 coreceptor utilization. *J. Biol. Chem.* **276**, 13433-13441.

[6] Cormier, E. G., and Dragic, T. (2002). The crown and stem of the V3 loop play distinct role in human immunodeficiency virus type 1 envelope glycoprotein interactions with the CCR5 coreceptor. *J. Virol.* **76**, 8953-8957.

[7] Bhat, S., Spitalnik, S. L., Gonzalez-Scarano, F., and Silberberg, D. H. (1991). Galactosyl ceramide or a derivative is an essential component of the neural receptor for human immunodeficiency virus type 1 envelope glycoprotein gp120. *Proc. Nat. Acad. Sci. USA.* **88**, 7131–7134.

[8] Vivés, R. R., Imberty, A., Sattentau, Q. J., and Lortat-Jacob, H. (2005). Heparan sulfate targets the HIV-1 envelope glycoprotein gp120 coreceptor binding site. *J. Biol. Chem.* **280**, 21353–21357.

[9] Fantini, J., Hammache, D., Delezay, O., Yahi, N., Andre-Barres, C., Rico-Lattes, I., and Lattes, A. (1997). Synthetic soluble analogs of galactosylceramide (GALCER) bind to the V3 domain of HIV-1 gp120 and inhibit HIV-1-induced fusion and entry. *J. Biol. Chem.* **272**, 7245–7252.

[10] Nehete, P. N., Arlinghaus, R. B., and Sastry, K. J. (1993). Inhibition of human immunodeficiency virus type 1 infection and syncytium formation in human cells by V3 loop synthetic peptides from gp120. *J. Virol.* **67**, 11, 6841-6846.

[11] Yahi, N., Sabatier, J., Baghdiguian, S., Gonzalez-Scarano, F., and Fantini, J. (1995). Syhthetic multimeric peptides derived from the principal neutralization domain (V3 loop) of human immunodeficiency virus type 1 (HIV-1) gp120 bind to galactosylceramide and block HIV-1 infection in a human CD4-negative mucosal epithelial cell line. *J. Virol.* **69**, 320-325.

[12] Yahi, N., Fantini, J., Mabrouk, K., Tamalet, C., De Micco, P., Van Rietschoten, J., Rochat, H., and Sabatier, J. (1994). Multibranched V3 peptides inhibit human immunodeficiency virus infection in human lymphocytes and macrophages. *J. Virol.* **68**, 9, 5714-5720.

[13] Yahi, N., Fantini, J., Baghdiguian, S., Mabrouk, K., Tamalet, C., Rochat, H., Van Rietschoten, J., and Sabatier, J. (1995). SPC3, a synthetic peptide derived from the V3 domain of human immunodeficiency virus type 1 (HIV-1). *Proc. Natl. Acad. Sci.* USA, **92**, 4867-4871.

[14] Rabehi, L., Seddiki, N., Benjouad, A., Gluckman, J. C., and Gattengo, L. (1998). Interaction of human immunodeficiency virus type 1 envelope glycoprotein V3 loop with CCR5 and CD4 at the membrane of human primary macrophages. *AIDS Res. Hum. Retroviruses*, **14**, 1, 605-1615.

peptides were tested in HIV neutralization assays in order to determine the shorter and most potent sequence able to block virus infection. Some of these V3 peptides as mono- or multivalent presentation are summarized in Table 1. Authors of these works discovered the importance of the conserved tip region (Gly-Pro-Gly-Arg), the multivalent presentation, and the higher inhibitor potency of the circular constrained V3 peptide respect to the opened linear one.

Table 1. V3 peptide with different amino acids sequence studied as entry/fusion inhibitors.

Peptide	Inhibition	Conc.	Method	Ref.
RIHIGPGRAFVTIGK	100%	1 μg/ml	Rev Transcr Act	10
NNTRKSIRIQRGPGRAFVTIGK	100%	1 μg/ml	Rev Transcr Act	10
RAFVTIGK	73%	1 μg/ml	Rev Transcr Act	10
IKGPGRVYAT	66%	1 μg/ml	Rev Transcr Act	10
HIGPGRAFYTTGK	76%	1 μg/ml	Rev Transcr Act	10
GPGRAF	0%	5 μM	p24	11, 12, 13
[GPGRAF]₂KG	100%	5 μM	p24	11, 12, 13
[GPGRAF]₄KKG	100%	5 μM	p24	11, 12, 13
[GPG(R)₄AF]₂KKG	30%	5 μM	p24	11, 13, 12
[KKHIGPGRAF]₄KKG	100%	5 μM	p24	11, 13, 12
CTRPNNNTRKSIH GPGRAFYTTGEIIGDIRQAHC (disulfide)	% of inhibition of RANTES binding			14
RKSIRIQRGPGRAFVTIGKIGNMRQAHCNLS (disulfide)	100%	10 μM	MTT	15
CTRPNNNTRKSIRIQRGPGRAFYTIGKIGNMRQAHC (no peptide)	0%	20 μM	MTT	15

() S-S = synthetic peptide constrained (lysine dendrimer)

At the beginning of the 2000 the number of publications related to V3 as infection inhibitor drastically decreased. This was probably due to the success of the Highly Active Antiretroviral Therapy (HAART) introduced in the late 1990s. However, the scientific community did not loose its interest in V3 peptide. It is well known since 1989 that V3 is also highly immunogenic and considered the "principal neutralizing determinant" of HIV-1.[16] Indeed, anti-V3 antibodies are normally present in almost all HIV-1 infected individuals.[17, 18]

---

[15] Sakaida, H., Hori, T., Yonezawa, A., Sato, A., Isaka, Y., Yoshie, O., Hattori, T., and Uchiyama, T. (1998). T-tropic human immunodeficiency virus type 1 (HIV-1)-derived V3 loop peptides directly bind to CXCR4 and inhibit T-tropic HIV-1 infection. *J. Virol.* **72**, 9763-9770.

[16] Javaherian, K., Langlois, A., McDanal, C., Ross, K. L., Eckler, L. I., Jellis, C. L., Profy, A. T., Rushe, J. R., Bolognesi, D. P., Putney, S. D., and Matthews, T. (1989). Principal neutralizing domain of the human immunodeficiency virus type 1 envelope protein. *Proc. Natl. Acad. Sci.* USA **86**, 6768-6772.

[17] Carrow, E.W., Vujcic, L. K., Glass, W. L., Seamon, K. B., Rastogi, S. C., Hendry, R. M., Roulos, R., Nzila, N., and Quinnan, G. V. (1991). High prevalence of antibodies to the gp120 V3 region principal neutralizing determinant of HIV-MN in sera from Africa and the Americas. *AIDS Res. Hum. Retroviruses* **7**, 831-838.

[18] Vogel, T., Kurth, R., Norley, S. (1994). The majority of neutralizing Abs in HIV-1 infected patients recognize linear V3 loop sequences. Studies using HIV-1MN multiple antigenic peptides. *J. Immunol.* **153**, 1895-1904.

An effective immunogen should induce Abs able to neutralize a broad spectrum of virus in the many subgroups (clades) that make up the HIV family. X-ray crystal structure of human broadly neutralizing Abs in complex with different V3 peptides were studied and conserved structural elements were found in the so called HIV-1 V3 crown.[19] V3 crown contains around 13 amino acids which can be divided into the arch, the circlet, and the band (Figure 1).
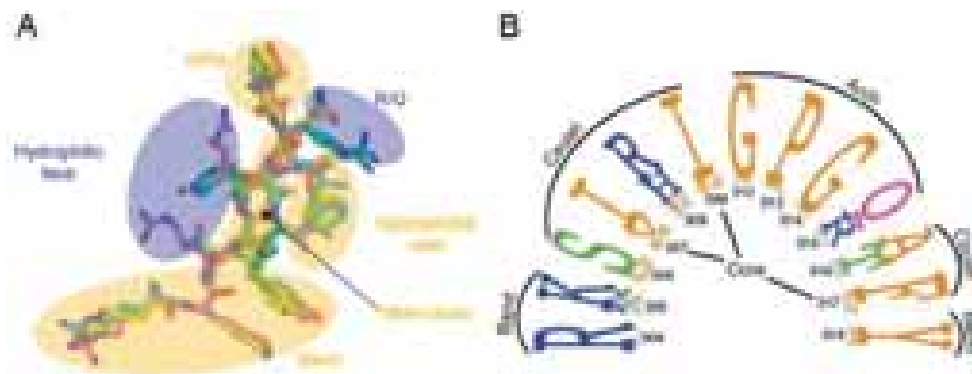
Figure 1. Conserved amino acids of V3 loop. A) In light orange the four conserved V3 segments: GPG turn of the arch, the hydrophobic core in the circlet, the band and the backbone (main chain interactions with mAbs). In blue the two variable regions that limit antibody cross-reactivity: the hydrophilic face in the circlet and the arginine/glutamine residue in the arch. B) The height of the amino acid letter is proportional to its frequency in HIV clades A, B and C. Figure 1 was taken from reference 19.

Broadly reactive anti-V3 mAbs bind to these conserved elements. The arch is the β-turn of the crown, consisting of the highly conserved Gly-Pro-Gly-Arg/Gln (GPGR/Q) motif. The circlet is the middle region of the V3 crown with a hydrophilic face and a hydrophobic face. Three residues on the hydrophobic face, residues 307 and 309 (very often two isoleucines) and 317 (often a phenylalanine), form the hydrophobic 'core' of the V3 crown. The hydrophilic face contains residue 308 (often an arginine or a histidine), N-terminal residue 306 (often a serine) and the C-terminal residue 316 (usually an alanine or a threonine). The band region is often formed by the positively charged residues 304 and 305 (an arginine and a lysine, respectively) and residue 318 (a tyrosine).

The structure of V3 peptides has been also extensively studied. Disulfide-bridged V3 loop, that is essentially random coil in H_2O solution, adopts α-helix conformation in TFE/water solution as showed by CD and 2D-NMR experiments.[20, 21]

---

[19] Jiang, X., Burke, V., Totrov, M., Williams, C., Cardozo, T., Gorny, M. K., Zolla-Pazner, S., and Kong, X. (2010). Conserved structural elements in the V3 crown of HIV-1 gp120. *Nat. Struct. Mol. Biol.* **17**, 955-961.

[20] Chandrasekhar, K., Profy, A. T., and Dyson, H. J. (1991). Solution conformational preferences of immunogenic peptides derived from the principal neutralizing determinant of the HIV-1 envelop glycoprotein gp120. *Biochemistry.* **30**, 9187-9194.

Wang et al reported the preparation and characterization of full-size cyclic HIV-1 V3 peptides carrying two N-glycans at amino acids N295 and N332.[22] They demonstrated by circular dichroism (CD) and by attenuated total reflection Fourier transformation infrared spectroscopy (ATR-FTIR) that the glycosylation has a tendency to enhance the β-turn structure.

The crystal structure of the human IgG broadly neutralizing monoclonal antibody 447-52D in complex with V3 peptide reveals that the V3 amino acids sequence Lys-Arg-Ile-His-Ile (KRIHI) form an extended β-strand followed by a β turn around GPGR (Figure 2).[23]
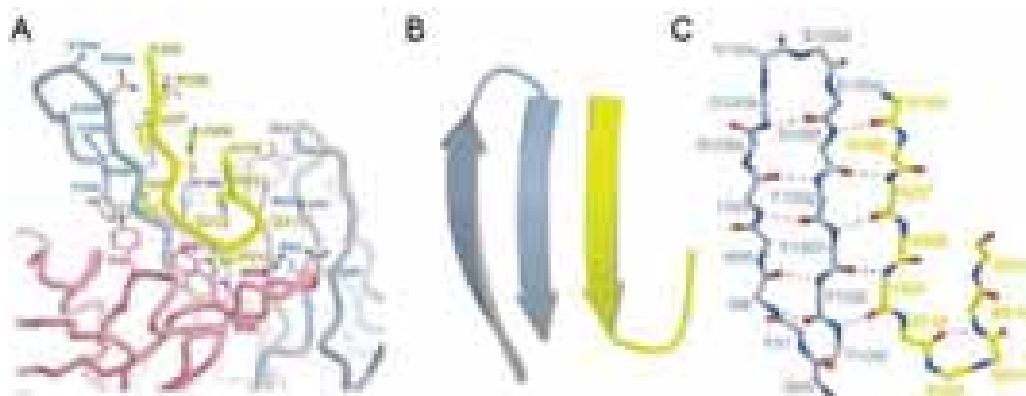
Figure 2. A) X-ray crystal structure of anti V3 antibody 447-52D Fab complexed with V3 peptide. The Fab light and heavy chains are colored in pink and blue, and V3 in yellow. B) and C) Main chains interaction of the CDR H3 of the Ab with Lys^{305}-Ile^{301} of V3 forms a mixed β-strand. Figure 2 was taken from reference 23.

The peptide β-strand forms extensive main chain interactions with the complementary determining region (CDR H3) of the Ab resulting in a three-stranded mixed β sheet, with an up/down/down topology. The crystal structures of V3 with other anti-V3 mAb

---

[21] Vranken, W. F., Budesinsky, M., Fant, F., Boulez, K., and Borremans, F. A. M (1995). The complete consensus V3 loop peptide of the envelope protein gp120 of HIV-1 shows pronounced helical character in solution. *FEBS Lett.* **374**, 117-121.

[22] Li, H., Li, B., Song, H., Breydo, L., Baskakov, I. V., and Wang, L. (2005). Chemoenzymatic synthesis of HIV-1 V3 glycopeptides carryng two N-glycans and effects of glycosylation on the peptide domain. *J. Org. Chem.* **70**, 9990-9996.

[23] Stanfield, R. L., Gorny M. K., Williams, C., Zolla-Pazner, S., and Wilson, I. A. (2004). Structural rational for the broad neutralizion of HIV-1 by human monoclonal antibody 447-52D. *Structure*, **12**, 193-204.

showed similar binding mode with the presence of a β-strand in the N-terminal of V3.[24] [25]

In 2005, Kwong et al. were able to determine the structure of V3 in the complex formed by an HIV-1 gp120 core, CD4 receptor and X5 antibody.[26] They found that V3 is almost 50 Å long (from the disulfide to its tip) and, in this complex, V3 protrudes 30 Å from gp120 core and consists of three different regions: a conserved base, a flexible stem and a β-hairpin tip. Two years later, the X-ray structure of a tyrosine-sulphated Ab (412d) in complex with gp120 and CD4 was solved (Figure 3A and 3B).[27]
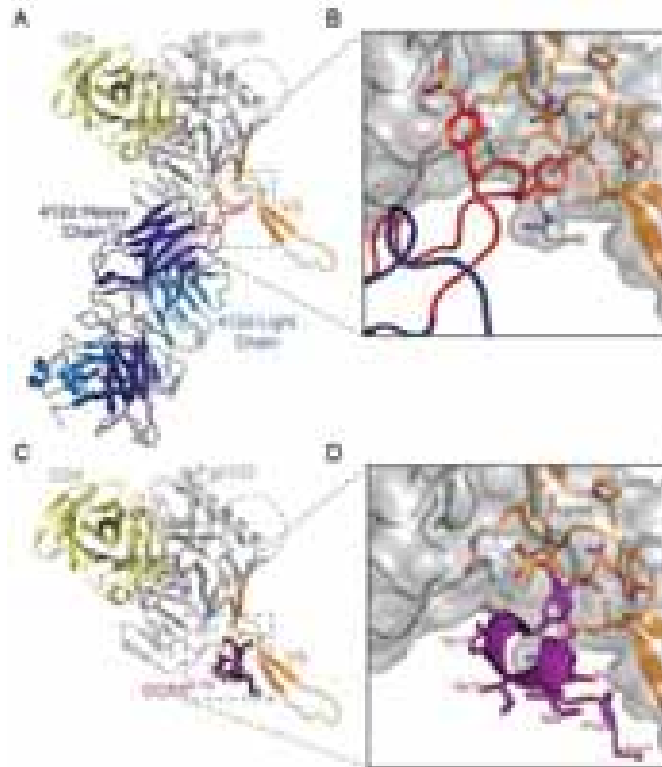
Figure 3. X-ray crystal structure of a gp120 bearing the complete V3 loop. A) Crystal structure of gp120 co-crystalized with soluble CD4 (sCD4) and an anti-V3 antibody. B) Close-up view, with gp120 in gray, sulfotyrosines of 412d red and V3 orange. C) Molecular docking of the interaction of the N terminus of CCR5 with HIV-1 gp120-CD4. D) Close-up, with gp120 in gray, CCR5 purple and V3 orange. From reference 27

---

[24] Stanfield, R. L., Gorny M. K., Zolla-Pazner, S., and Wilson, I. A. (2006). Crystal structure of human immunodeficiency virus type 1 (HIV-1) neutralizing antibody 2219 in complex with three different V3 peptides reveal a new binding mode for HIV-1 cross-reactivity. *J. Virol.* **80**, 6093-6105.

[25] Burke, V., Burke, V., Williams, C., Sukumaran, M., Kim, S., Li, H., Wang, X., Gorny, M. K., Zolla-Pazner, S., and Kong, X. (2009). Structural basis of the cross-reactivity of genetically related human anti-HIV-1 mAbs: implications for design of V3-based immunogens. *Structure* **17**, 1538-1546.

[26] Huang, C., Tang, M., Zhang, M., Majeed, S., Montabana, E., Stanfield, R. L., Dimitrov, D. S., Korber, B., Sodroski, J., Wilson, I. A., Wyatt, R., and Kwong P. D. (2005). Structure of a V3-containing HIV-1 gp120 core. *Science*, **310**, 1025-1028.

[27] Huang, C., Lam, S. N., Acharya, P., Tang, M., Xiang, S., Hussan, S. S., Stanfield, R. L., Sodroski, J., Wilson, I. A., Wyatt, R., Bewley, C. A., and Kwong P. D. (2007). Structures of the CCR5 N terminus and of a tyrosine-sulfated antibody with HIV-1 gp120 and CD4. *Science*, **317**, 1930-1934.

Molecular docking of the CCR5 N terminus NMR structure with the x-ray structure of gp120/CD4 complex was performed (Figure 3C and 3D) and was found that both the binding of gp120 with the Ab and with CCR5 N-terminus convert the flexible V3 loop into a rigid β-hairpin.

Very recently a novel anti HIV-1 mAb (PGT 128) able to recognize two different $Man_{8/9}GlcNAc_2$ glycans (N301 and N332) as well as the C-terminal of the V3 loop was isolated.[28] Authors co-crystallized PGT 128 Fab with a glycosylated gp120 outer domain containing a truncated V3 loop (Figure 4). The truncated V3 loop adopts a β-strand conformation in the complex with PGT 128. The binding is primarily mediated through backbone interactions that are tolerant of side-chain variation, as seen for the V3 crown-specific antibody 447-52D.
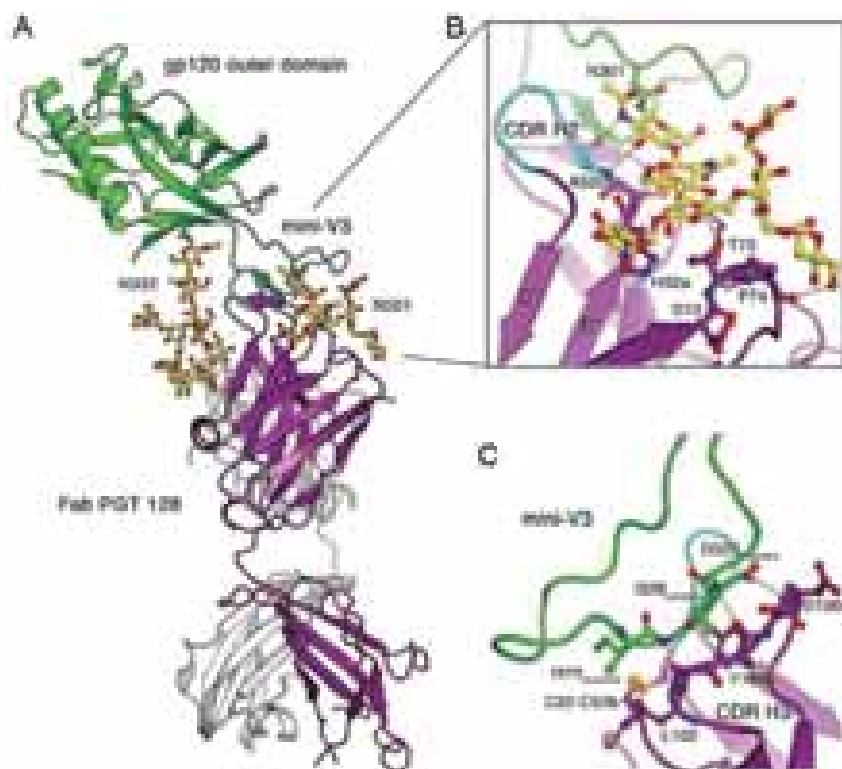
Figure 4. A) X-ray crystal structure of glycosylated gp120 with Ab PGT128 Fab fragment (gp120 in green, glycans in yellow and Ab gray and purple). B) Close-up view of the interaction of oligomannosides with the Ab. C) Close-up view of the binding of truncated V3 peptide with CDR H3 of the Ab. From reference 28.

Because of V3 peptide flexibility, unconstrained V3 peptides used as immunogens induce a broad distribution of antibodies, many of which will not recognize the native

---

[28] Pejchal, R., Doores, K. J., Walker, L. M., Khayat, R., Huang, P., Wang, S., Stanfield, R. L., Julien, J., Ramos, A., Crispin, M., Depetris, R., Katpally, U., Marozsan, A., Cupo, A., Maloveste, S., Liu, Y., Mcbride, R., Ito, Y., Sanders, R. W., Ogohara, C., Paulson, J. C., Feizi, T., Scalan, C. N., Wong, C., Moore, J. P., Olson, W. C., Ward, A. B., Poignard, P., Schief, W. R., Burton, D. R., Wilson, I. A. (2011). A potent and broad neutralizing antibody recognizes and penetrates the HIV glycan shield. *Science*, **334**, 1097-1103.

conformation of V3 region in gp120. Many efforts have been done to found the correct V3 conformation and amino acids sequence able to elicit anti-V3 neutralizing antibodies (NAbs). To mimic the native V3 secondary structure cyclic constrained V3 peptides were prepared. Disulfide bridges between two cysteines were used to reproduce V3 structure in gp120. Constrained V3 peptides were conjugated to immunostimulant proteins such as keyhole limpet hemocyanin (KLH), pseudomonas exotoxin (PE),[29] truncated murine leukemia virus gp70 (MuLV),[30] cholera toxin (CTB)[31] or the fourth conserved domain of gp120 (C4)[32] (Figure 5). All the results showed that constrained V3 peptides elicit a HIV-1 neutralizing response.
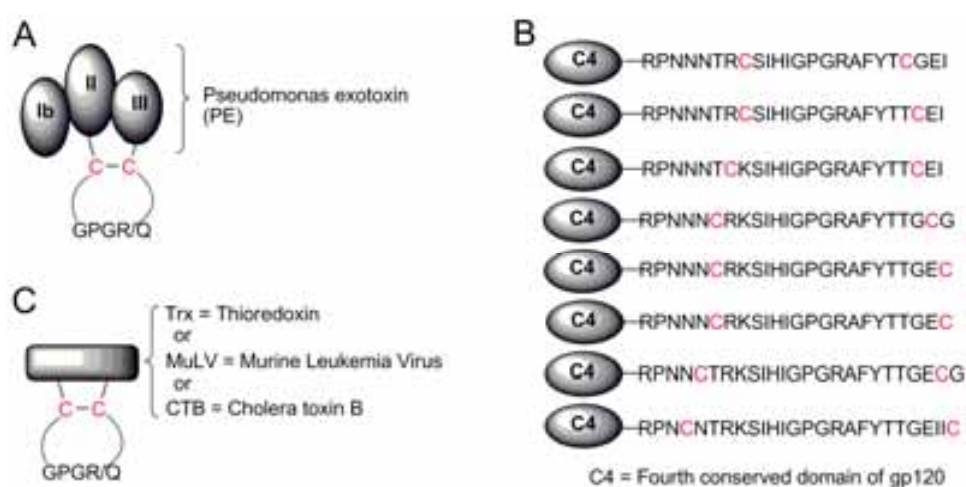
Figure 5. Constrained V3 peptide linked to immunostimulating proteins. A) V3 conjugated to Pseudomonas exotoxin. B) Different V3 peptides conjugated to the fourth-conserved region of gp120. C) V3 conjugated to thioredoxin, murine leukemia virus and cholera toxin B. Disulfide bonds are between cysteines colored in red. Adapted from reference 29 and 32.

Another important topic to take into account in the design of immunogens is the multivalent presentation, which can contribute to increase the potency of the

---

[29] FitzGerald, D. J., Fryling, C. M., Mckee, M. L., Vennari, J. C., Wrin, T., Cromwell, M. E., Daugherty, A. L., and Mrsny, R. J. (1998). Characterization of V3 loop-*Pseudomonas* exotoxin chimeras. *J. Biol. Chem.* **273**, 9951-9958.

[30] Zolla-Pazner, S., Cohen, S., Pinter, A., Krachmarov, C., Wrin, T., Wang, S., and Lu, S. (2009). Cross-clade neutralizing antibodies against HIV-1 induced in rabbits by focusing the immune response on a neutralizing epitope. *Virology* **392**, 82–93.

[31] Totrov, M., Jiang, X., Kong, X., Cohen, S., Krachmarov, C., Salomon, A., Williams, C., Seaman, M. S., Cardozo, T., Gorny, M. K., Wang, S., Lu, S., Pinter, A., and Zolla Pazner, S. (2010). Structure-guided design and immunological characterization of immunogens presenting the HIV-1 gp120 V3 loop on a CTB scaffold. *Virology* **405**. 513–523.

[32] Moseri, A., Tantry, S., Sagi, Y., Arshava, B., Naider, F., and Anglister, J. (2010). An optimally constrained V3 peptide is a better immunogen than its linear homolog or HIV-1 gp120. *Virology* **401**, 293-304.

immunogenic response. It is well known that viral Env is formed by three gp120/gp41. Moreover, the binding of Env to CD4 and coreceptors is cooperative, requiring three CD4 binding events, multiple CCR5 (from 4 to 6) and multiple cluster of gp120/gp41 to effectively form a fusion pore.[33, 34] It has also been suggested that repetitive presentation of an epitope on the immunogen can induce a stronger immune response, probably because such immunogens can trigger oligomerization of B-cell receptors recognizing the epitope.[35, 36, 37] To study the efficacy of multivalent presentation, linear oligomers of V3 peptides,[38] V3 peptide coupled to multimeric proteins[39] or lysine dendrimers,[40] and micelles formed by lipid V3 conjugate were prepared.[41, 42] Some of those V3 conjugates are shown in Figure 6.

[33] Kuhmann, S. E., Platt, E. J., Kozak, S. L. and Kabat, D. (2000). Cooperation of multiple CCR5 coreceptors is required for infections by human immunodeficiency virus type 1. *J. Virol.* **74**, 7005-7015.

[34] McReynolds, K. D., and Gervay-Hague, J. (2007). Chemotherapeutic interventions targeting HIV interactions with host-associated carbohydrates. *Chem. Rev.* **107**, 1533-1552.

[35] Kiessling, L. L., Gestwicki, J. E., and Strong, L. E (2000). Synthetic multivalent ligands in the exploration of cell-surface interactions. *Curr. Opin. Chem. Biol.* **4**, 696-703.

[36] Cruz, L. J., Iglesias, E., Aguilar, J. C., Cabrales, A., Reyes, O., and Andreu, D. (2004). Different immune response of mice immunized with conjugates containing multiple copies of either consensus or mixotope version of the V3 loop peptide from human immunodeficiency virus type 1. *Bioconjug. Chem.* **15**, 1110-1117.

[37] Totrov, M., Jiang, X., Kong, X., Cohen, S., Krachmarov, C., Salomon, A., Williams, C. Seaman, M. S., Cardozo, T., Gorny, M. K., Wang, S., Lu, S., Pinter, A., and Zolla-Pazner, S. (2010). Structure-guided design and immunological characterization of immunogens presenting the HIV-1 gp120 V3 loop on a CTB scaffold. *Virology* **405**, 513–523.

[38] Javaherian, K., Langlois, A. J., Larosa, G. J., Profy, A. T., Bolognesi, D. P., Herlihy, W. C., Putney, S. D., and Matthews, T. J. (1990). Broadly neutralizing antibodies elicited by the hypervariable neutralizing determinant of HIV-1. *Science*, **250**, 1590-1593.

[39] Totrov, M., Jiang, X., Kong, X., Cohen, S., Krachmarov, C., Salomon, A., Williams, C., Seaman, M. S., Cardozo, T., Gorny, M. K., Wang, S., Lu, S., Pinter, A., and Zolla Pazner, S. (2010). Structure-guided design and immunological characterization of immunogens presenting the HIV-1 gp120 V3 loop on a CTB scaffold. *Virology* **405**. 513–523.

[40] Hewer, R., and Meyer, D. (2003). Peptide immunogens based on the envelope region of HIV-1 are recognized by HIV/AIDS patient polyclonal antibodies and induce strong humoral immune responses in mice and rabbits. *Mol. Immunol.* **40**, 327-335.

[41] Azizi, A., Anderson, D. E., Torres, J. V., Ogrel, A., Ghorbani, M., Soare, C., Sandstrom, P., Fournier, J., and Diaz-Mitoma, F. (2008). Induction of broad cross-subtype-specific HIV-1 immune responses by a novel multivalent HIV-1 peptide vaccine in cynomolgus macaques. *J. Immunol.* **180**, 2174-2186.

[42] Riedel, T., Ghasparian, A., Moehle, K., Rusert, P., Trkola, A., and Robinson, J. A. (2011). Synthetic virus-like particles and conformationally constrained peptidomimetics in vaccine design. *ChemBioChem*, **12**, 2829 – 2836.
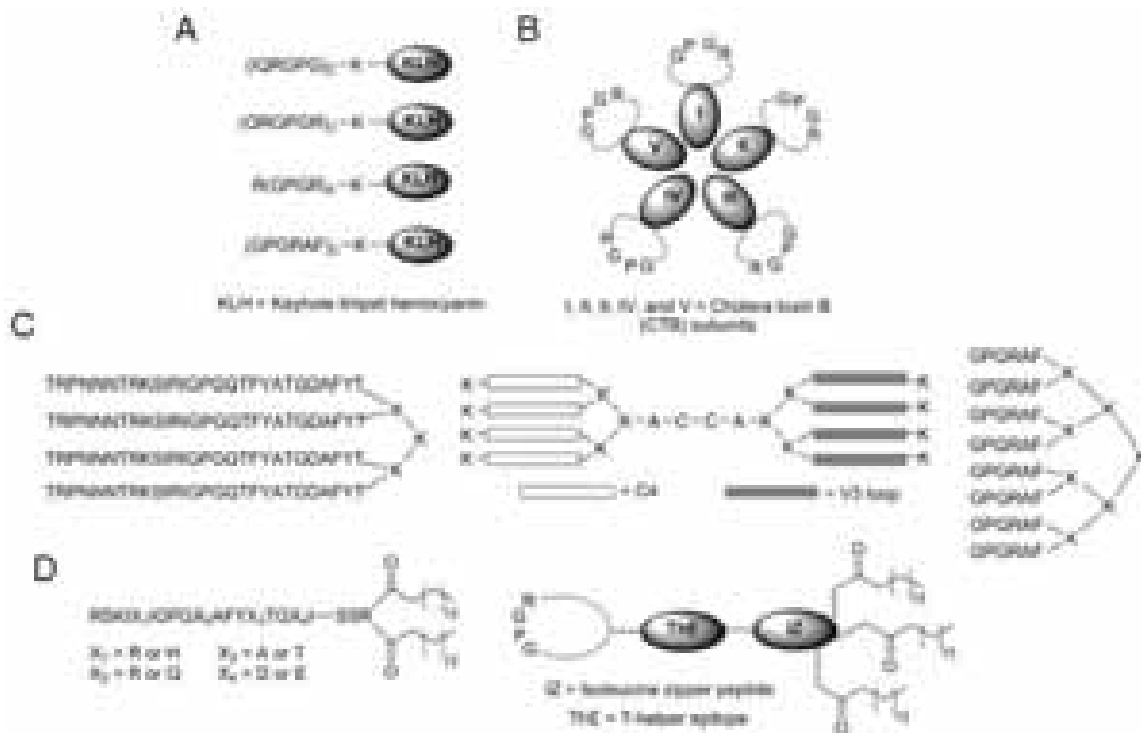
Figure 6. Multivalent V3 constructs used for immunization study. A) Linear oligomer based on the V3 tip coupled to KLH protein. B) Multivalent V3 peptide coupled to cholera toxin B. C) V3 peptides coupled to lysine dendrimers. D) V3 lipid derivates used to prepare micelles. Adapted from reference 36 and 40.

Although these constructs are able to induce an immune response in animals, the sera neutralize only T-cell line adapted virus or narrow range of primary isolates. The reason of this weak immune response probably lies in the conformation of V3 peptide that was not determined in these V3 based immunogens (proteins, dendrimers and liposomes).

In conclusion, to construct new and potent V3-based HIV entry inhibitors or immunogens, a constrained V3 peptide containing conserved amino acids should be used and, if possible, presented in a multivalent way (at least 3 peptides, as in the trimeric Env). A second important point to be taken into account is that the coupling of V3 to a molecular carrier or scaffold may significantly change its conformation. Thus, an extensive conformational study of the V3-constructs should be also performed.

In this chapter, we address the multimerization of V3 peptide on negative charged gold glyconanoparticles (GNPs). Initially, our aim was to enhance the potency of the monomeric V3 as entry inhibitors. However, along the preparation of the V3-GNPs, we observed significant conformational changes of V3 depending on the experimental conditions used, so that it was necessary to analyze these changes to well characterize

the V3-GNP constructs. It is well known that the interaction of charged peptides with charged vesicles or nanoparticles (NPs) can induce a conformational change in the peptides due to electrostatic interactions between opposite charges. It has been observed that both positive and negative charged NPs can induce a helical structure in random coil peptide when the charged amino acids are spaced by two or three no charged aminoacids,[43][44] and this is the case of the V3 loop.

To multimerize the V3 peptide, we have prepared three different negative charged glyconanoparticles (GNP1, GNP2, and GNP1-FITC) bearing carbohydrates conjugates, a carboxyl group ending linker, and a fluorescein derivate (Figure 7).
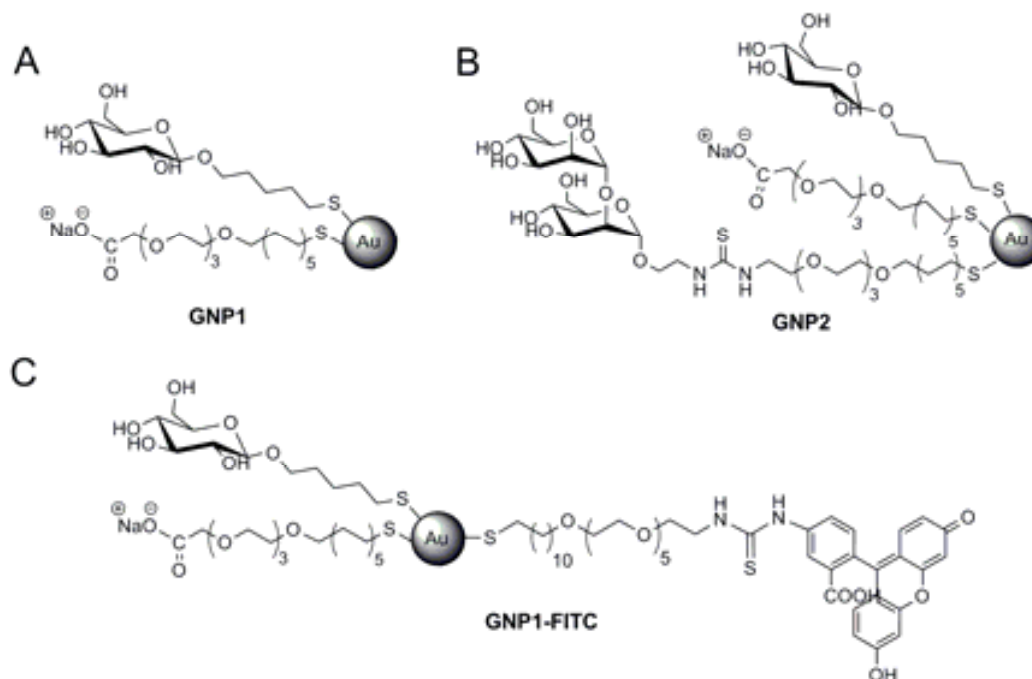
Figure 7. Gold glyconanoparticles (GNPs) used in this work. A) GNP1 is covered with 50% of glucose conjugate (GlcC$_5$) and 50% of carboxyl linker (Linker-CO$_2$H). B) GNP2 is covered with 40% of GlcC$_5$, 50% of Linker-CO$_2$H and 10% dimannose conjugate. C) GNP1-FITC is covered with 40% of GlcC$_5$, 50% of Linker-CO$_2$H and 5% of a fluorescein isotiocianate linker (Linker-FITC). The number of each molecules depends on the number of gold surface atoms.

GNP1 is covered with 50% density of glucose conjugate (GlcC$_5$) and 50% of carboxyl linker (Linker-CO$_2$H), GNP2 is covered with 40% of GlcC5, 50% of Linker-CO$_2$H and 10% dimannose conjugate (Figure 7B). The fluorescently labelled GNP1-FITC is

---

[43] Verma, A., Nakade, H., Simard, J. M., and Rotello, V. M. (2004). Recognition and stabilization of peptide α-helices using templatable nanoparticle receptors. *J. Am. Chem. Soc.* **126**, 10806-10807.

[44] Lundqvist, M., Nygren, P., Jonsson, B., and Broo, K. (2006). Induction of structure and function in a designed peptide upon adsorption on a silica nanoparticles. *Angew. Chem. Int. Ed.* **45**, 8169-8173.

covered with 45% of $GlcC_5$, 50% of $Linker-CO_2H$ and 5% of a thiol ending linker conjugate to a isothiocianate fluorescein derivate (Linker-FITC).

The positive charged V3 peptide used in our experiments is a 35-aminoacid cyclic constrained peptide containing all the conserved elements (bands, circlets and arch) determined by Zolla-Pazner (Figure 8A).[19]

The conformation of V3 peptide is determinant for its biological activity. Structural data related to our V3 peptide are summarized in Figure 8.
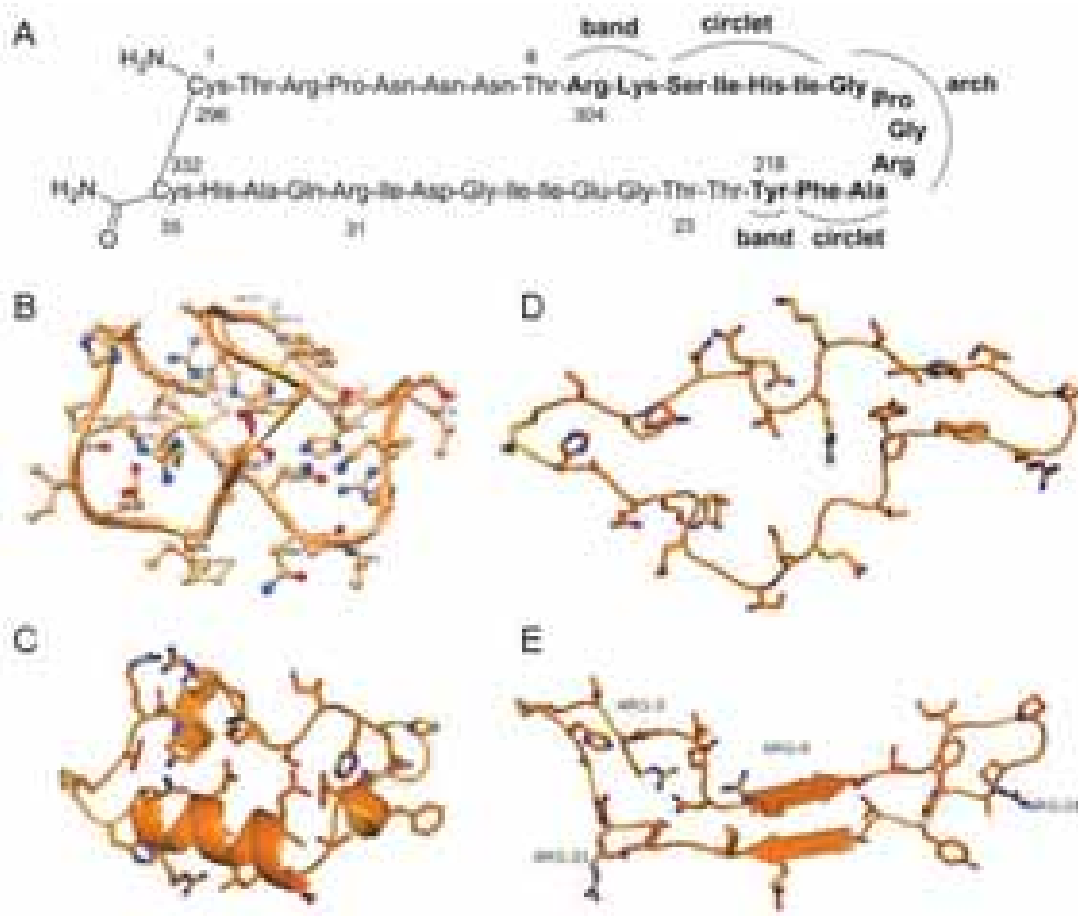
Figure 8. V3 peptide amino acid sequence and structures. A) Cyclic V3 peptide, formed by 35 amino acids, containing the crown conserved region. Two different numeration are showed: the outer numeration from Cys^1 to Cys^{35} (peptide alone) and the inner numeration from Cys^{296} to Cys^{332} (peptide in gp120) B) V3 peptide random coil structure based on homology modelling and ^{1}HNMR spectroscopy C) V3 peptide with α-helix structure determined by ^{1}HNMR of V3 in 20% TFE/H_2O (PDB 1CE4) D) V3 peptide with a β-strand conformation determined by X-ray structure of gp120 in the complex with CD4 and X5 Ab (PDB 2B4C) E) V3 peptide with a β-strand conformation determined by X-ray structure of gp120 in the complex with CD4 and the anti V3 Ab 412d (PDB 2QAD). Figure 8 was taken/adapted from reference 46, 21, 26 and 27.

In water solution V3 does not have a well-defined secondary structure except for a transient β-turn formed by the GPGR tip (arch) segment (Figure 8B).[45] [46] However in less polar solvent (20% TFE/H_2O) the C-terminal amino acids region Thr^{23}-Arg^{31} is predominantly helical (Figure 8C). Two beta strand conformation have been identified in two different crystal structure of gp120 with the complete V3 loop complexed with CD4 and an Ab (Figure 8D, PDB 2B4C and Figure 8E, PDB 2QAD).[26] [27] In the structure of figure 8D, the β-strand extends from its N-terminus (Cys^{296}) to Arg^{298} and from Ser^{306} to Gly^{312} which terminates in a Gly-Pro-Gly-Arg β-turn (residues 312 to 315). After the turn, the returning density is less well defined, indicative of some disorder. V3 peptide in the crystal structure of figure 8E present short antiparallel β-sheet in the cysteines region (similar to V3 in PDB 2B4C), and antiparallel β-sheet in the regions: Thr^{303}-Ile^{307} and Thr^{318}-Ile^{322}. The β-strand conformation of V3 peptide is very important for the interaction with anti-V3 Abs and probably also with CCR5 co-receptor.

In the work presented in this chapter, we demonstrate that our charged GNPs are able to modulate the conformation of V3 peptide to obtain V3 constructs with predominant α-helix (V3α-GNP) or β-strand (V3β-GNP) conformation, depending on the preparation conditions, as showed by circular dichroism (CD). The influence of V3 conformation in the interaction of V3-GNPs with the anti-V3 mAb 447-52D and with the CCR5 coreceptor was studied by surface plasmon resonance (SPR). The corresponding fluorescent GNPs (V3α-GNP1-FITC and V3β-GNP-FITC) were prepared. from the GNP1-FITC to follow, by flow cytometry, the uptake by CCR5/CXCR4 overexpressing cells. Cytotoxicity and HIV neutralization activity of GNP1, V3α-GNP1, V3β-GNP1 and V3β-GNP2 were also evaluated with Peripheral Blood Mononuclear Cells (PBMC). Finally, we see a great potential in the V3β-GNP1 construct as immunogens and have began the study of their potential.to produce anti-V3 antibodies in mice.

---

[45] Chandrasekhar, K., Profy, A. T., and Dyson, H. J. (1991). Solution conformational preferences of immunogenic peptides derived from the principal neutralizing determinant of the HIV-1 envelope glycoprotein gp120. *Biochem.* **30**, 9187-9194.

[46] Andrianov, A. M., Anishchenko, I. V., and Tuzikov, A. V. (2011). Discovery of novel promising targets for anti-aids drug developments by computer modeling: application to the HIV-1 gp120 V3 loop. *J. Chem. Inf. Model.* **51**, 2760–2767.

Results and Discussion

Because of the net positive charge of V3 peptides, we decided to use GNPs bearing carboxyl groups as a platform to multimerize V3 peptide and to modulate its conformation by exploring different experimental conditions. In addition to the carboxyl ending linkers, the nanoparticles incorporate a glucose conjugates or/and a dimannose terminal disaccharides (Manα1-2Manα) of the high-mannose glycans of the gp120.

We select a V3 peptide that contains the conserved elements founded in the 13 amino acid sequence of the crown (corresponding to amino acids 304 to 318 in the gp120). The 35 amino acids V3 peptide is cyclic because of the disulfide bond between two terminal cysteines and it has a net positive charge at neutral pH. The positive charge is given by the basic aminoacids present in the peptide: 4 arginines, 1 lysine and 2 histidines.

To study the structure of V3 before and after the interaction with GNPs, circular dichroism spectroscopy (CD) was used. CD is a non-destructive technique for rapid determination of the secondary structure of proteins and peptides. Depending on the regular arrays of amide polypeptide bonds, such as α-helix or β-strands, a characteristic spectrum is obtained. Proteins that contain α-helical structure present CD spectra with negative bands at 222 nm and 208 nm and a positive band at 193 nm and proteins with well-defined antiparallel β-strand show negative bands at 218 nm and positive bands at 195 nm, whereas disordered proteins (random coil) have very low ellipticity above 210 nm and a negative band around 197 nm.[47, 48, 49, 50]

Preparation and characterization of GNPs

For the preparation of glyconanoparticles GNP-1, GNP-2 and GNP1-FITC, 5-(thio)pentyl β-D-glucopyranoside (GlcC$_5$), the mannose disaccharide conjugate, 23, 23'-dithiobis[*N*-(ethyl-α-D-mannopyranosyl-(1→2)-α-D-mannopyranosyl),*N*'-(3,6,9,12-tetraoxa tricosanyl) thiourea] (Manα1-2Man), the carboxylic thiol ending linker, 22-mercapto [2,5,8,11-tetraoxadocosan]-1-oic acid (Linker-CO$_2$H) and the fluorescein thiol

---

[47] Greenfield, N., and Fasman, G. D. (1969). Computed circular dichroism spectra for the evaluation of protein conformation. *Biochemistry*. **8**, 4108-4116.

[48] Manavalan, P., and Curtis Johnson, W. (1983). Sensitivity of circular dichroism to protein tertiary structure class. *Nature*. **305**, 831-832.

[49] Sonnichsen, F. D., Van Eyk, J. E., Hodges, R. S., and Sykes, B. D. (1992). Effect of trifluoroethanol on protein secondary structure: an NMR and CD study using a synthetic actin peptide. *Biochemistry*. **31**, 8790-8798.

[50] Greenfield, N. J. (2006). Using circular dichroism spectra to estimate protein secondary structure. *Nat. protoc*. **1**, 2876-2890.

ending linker derivate Bis[N-fluorescein-N'-(29-mercapto-3,6,9,12,15,18-hexaoxa-nonacosanil) tiourea] (Linker-FITC) were employed (Scheme 1).
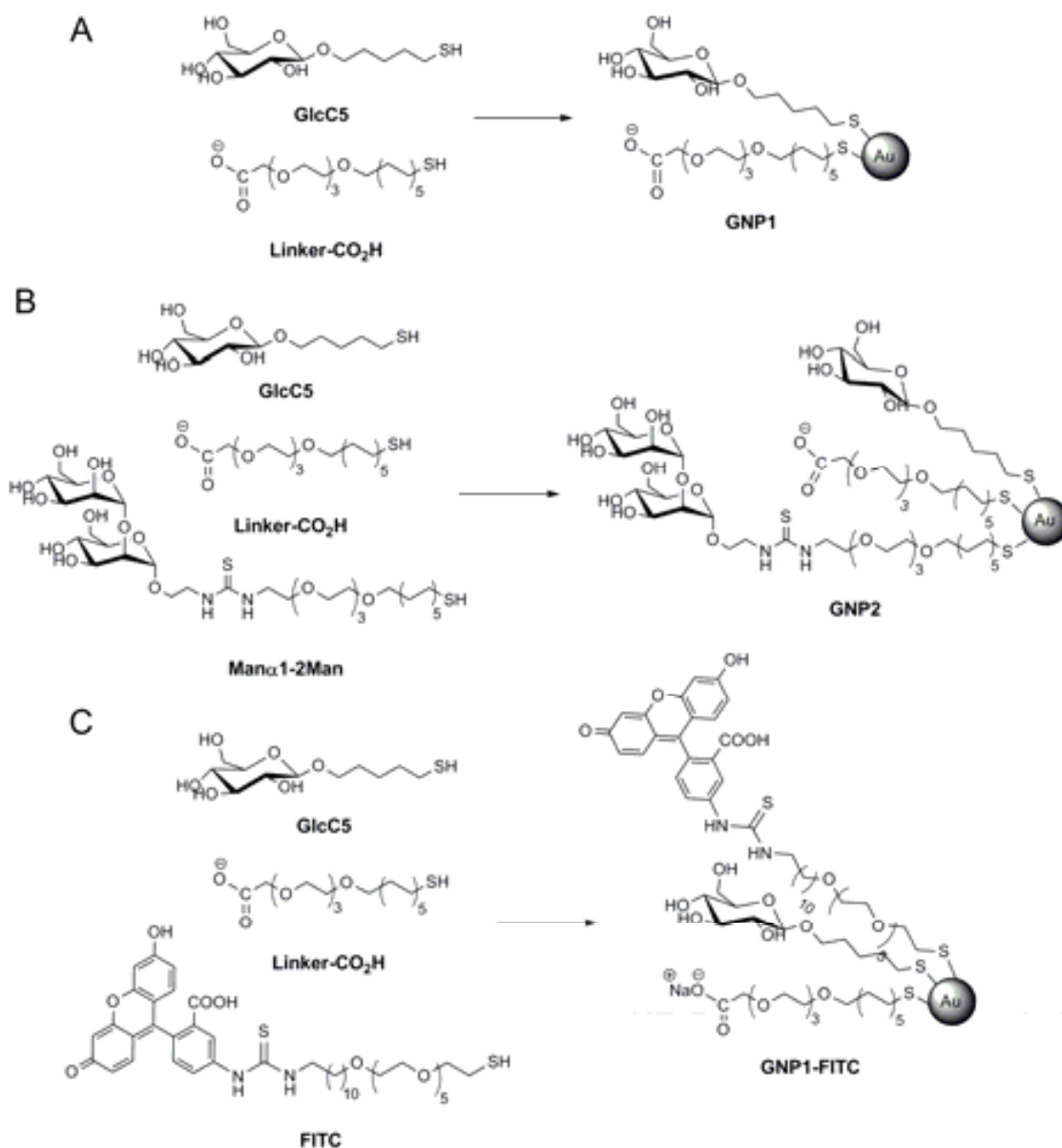
Scheme 1. Preparation of GNP1 and GNP2 and GNP1-FITC. All the GNPs were prepared dissolving the corresponding thiol derivates in a mixture of MeOH/H_2O/AcOH, in presence of $HAuCl_4$ and $NaBH_4$. All reactions were left under shaking for 2h at room temperature (RT). A) In GNP1 preparation GlcC$_5$ and Linker-CO_2H were mixed in 1:1 proportion. B) GNP2 was prepared using a mixture of GlcC$_5$:Linker-CO_2H:Manα1-2Man in ratio 4:5:1. C) For the preparation of GNP1-FITC a mixture of GlcC$_5$:Linker-CO_2H:Linker-FITC 4.5:5:0.5 was used.

The synthesis of thiol ending molecules used for the preparation of the GNPs was described elsewhere.[51] [52] To give solubility and biocompatibility to the GNPs, GlcC$_5$

[51] Martinez-Avila, O., Hijazi, K., Marradi, M., Clavel, C., Campion, C., Kelly, C., and Penadés, S. (2009). Gold Manno Glyconanoparticles: Multivalent systems to block HIV-1 gp120 binding to the lectin DC-SIGN+. *Chem. Eur. J.* **15**, 9874-9888.

was used as inner component. Linker-CO$_2$H was employed to give negative charge to the GNPs. Mannose disaccharide conjugate (Manα1-2Man) was used to mimic the terminal disaccharide of the high-mannose glycans around V3 in the gp120. Linker-FITC was used to prepare fluorescent GNPs to study cellular uptake by flow cytometry. GNPs were prepared and characterized by using the procedures developed in our laboratory.[53] Briefly, an aqueous solution of tetrachloroauric acid was added to a MeOH/H$_2$O/AcOH solution of a mixture of thiol ending molecules. In the case of GNP1, GlcC$_5$ and Linker-CO$_2$H were mixed in 1:1 proportion, GNP2 was prepared using a mixture of GlcC$_5$:Linker-CO$_2$H:Manα1-2Man in ratio 4:5:1, while for GNP1-FITC a mixture of GlcC$_5$:Linker-CO$_2$H:Linker-FITC 4.5:5:0.5 was used. Each mixture was reduced with an excess of NaBH$_4$ and the suspension was vigorously shaken for 2 h at room temperature (RT). The supernatant was removed and the residue was dissolved in milliQ water, purified by dialysis or centrifugal filtration, and characterized by ^{1}H-NMR spectroscopy, transmission electron microscopy (TEM), and ultraviolet spectroscopy (UV). GNPs obtained were water soluble and well dispersed with a gold nucleus diameter of around 2 nm as found by TEM.

Preparation and characterization of V3-GNPs

The V3 peptide selected for the preparation of V3-GNPs is the 35 aminoacids cyclic peptide that contains the conserved elements founded in the 13 amino acids sequence of the crown (corresponding to amino acids 304 to 318 in the gp120) and it has a net positive charge at neutral pH with isoelectric point (IP) around 9.5.

V3-GNPs were prepared in phosphate buffer (4 or 40 mM) and at different pH (from 5.8 to 8). In a typical preparation GNPs (100 µl, 2 mg/ml in H$_2$O) were added to 100 µl of phosphate buffer solution (10 mM or 100 mM) and V3 peptide (55 µl, 2 mg/ml in H$_2$O) was added to obtain a final phosphate concentration of 4 or 40 mM. The brown solution was left under shaking over night at RT. No precipitate was detected. The mixture was diluted with mQ water and centrifuged on amicon filter (30 KDa MWCO) for 5 minutes at 3000 rpm and 10 °C. The residue and the washing were collected. The GNPs were lyophilized and the washing analyzed with Bradford test. No peptide was found in the washings, indicating that all V3 peptides added remain complexed to the GNP1

---

[52] He, S., Garcia, I., Gallo, J., and Penadés, S. (2009). A step-heating procedure for the synthesis of high-quality FePt nanostars. *CrystEngComm.* **11**, 2605-2607.

[53] Barrientos, A. G., de la Fuente, J. M., Rojas, T. C., Fernández, A., and Penadés, S. (2003). Gold glyconanoparticles: synthetic polyvalent ligands mimicking glycocalyx-like surfaces as tools for glycobiological studies. *Chem. Eur. J.*, **9**, 1909-1921.

(around 6 V3 peptides per GNPs). V3β-GNP1 was also prepared with double amount of V3 (V3β-GNP1b; 12 V3 per GNP1).

V3-GNPs were characterized by ^{1}H-NMR and agarose gel electrophoresis. In Figure 8, ^{1}H-NMR and agarose gel electrophoresis of GNP1 and V3β-GNP1 is presented (the other V3-GNPs present the same ^{1}H-NMR spectra and same agarose gel). Both experiments confirm the presence of the peptide on the GNP1. The ^{1}H-NMR spectrum of V3-GNP shows a broad signal around 0.9 ppm indicating the presence of methyl protons coming from the peptides. The rest of peptide signals (with lower intensity respect methyl protons) could not be assigned due to the broad signals of the GNP1 spectrum.
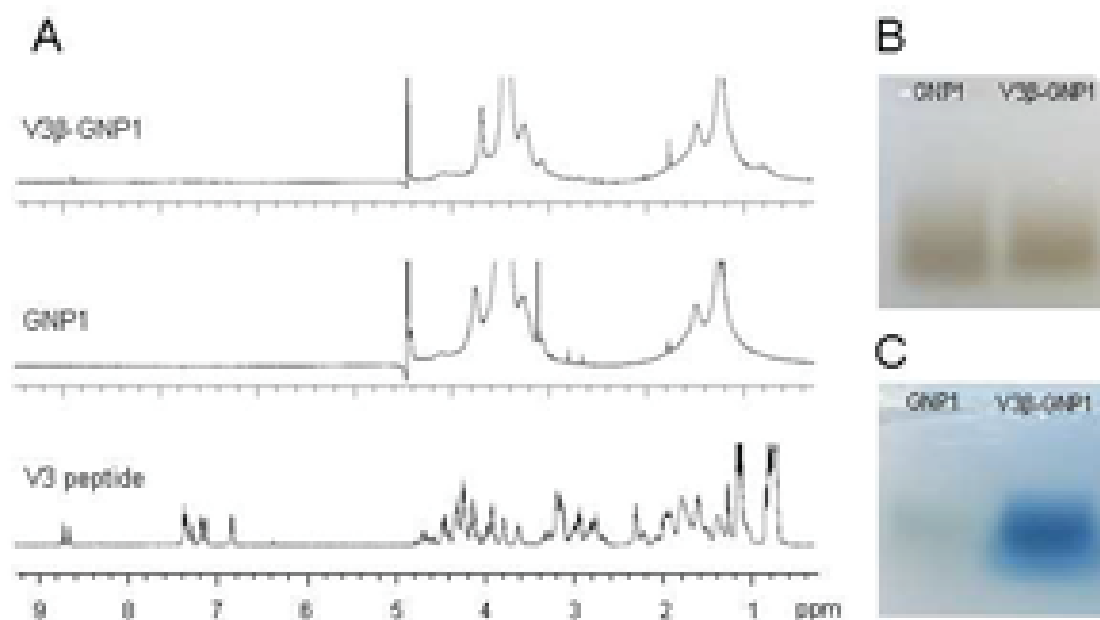
Figure 8. Characterization of V3-GNPs by ^{1}HNMR and agarose gel electrophoresis. A) Comparison of ^{1}HNMR of V3 peptide alone, GNP1 and V3β-GNP1. All ^{1}HNMR were perfomed in D_2O. B) Agarose gel electrophoresis of GNP1 and V3β-GNP1 (running buffer: Tris-Borate EDTA (88 mM Tris Base, 88 mM boric acid and 2 mM EDTA). C) Agarose gel electrophoresis of GNP1 and V3β-GNP1 after staining with SimplyBlue SafeStain (Invitrogen).

Agarose gel of GNP1 and V3β-GNP1 was performed with Tris-Borate EDTA (88 mM Tris Base, 88 mM boric acid and 2 mM EDTA) as running buffer (Figure 8B and 8C). GNP1 and V3β-GNP1 (2 mg/ml in H_2O) were mixed with 4 µl of TBE (5x), 2 µl of glycerol (30%) and loaded in the gel. The gel was run at 50V for 1 h (running buffer TBE 0.5x). The gel was stained for 1 h at room temperature with gentle shaking with SimplyBlue SafeStain (Invitrogen). The gel showed that GNPs with and without V3 run almost together (Figure 8B), but, after staining (Figure 8C), only V3-GNP1 shows the

typical blue colour of the presence of the peptide. GNP1 and V3β-GNP1 run almost together, indicating that the presence of the peptide did not significantly change the negative charge of the GNP as confirmed by z-potential experiments at different pH (Figure 9).
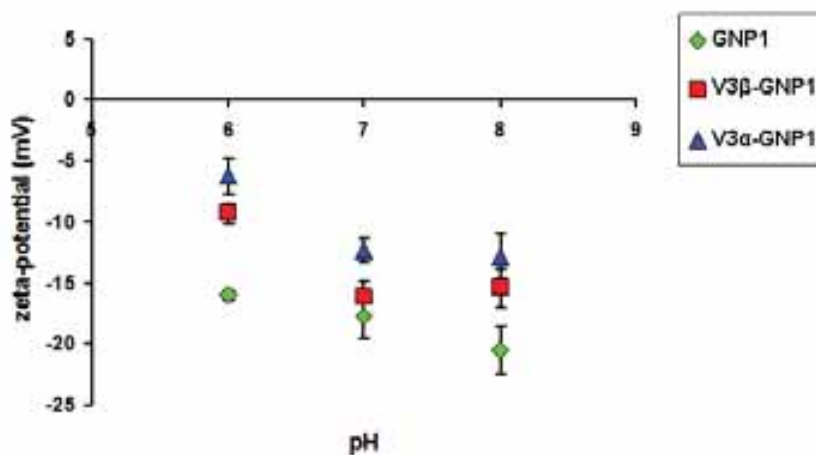
Figure 9. Dependence of V3-GNPs charge with the pH. Zeta potential of GNP1, V3β-GNP1 and V3α-GNP1 (100 ug/ml) in 10 mM phosphate buffer at different pHs. Data are the average of three experiments ± standard deviation (SD).

The TEM pictures of GNP1 and V3-GNP1 did not show size change of the gold clusters after the conjugation of V3 peptides to GNP1. It seems also that no aggregation of the V3 functionalized GNPs takes place (Figure 10)
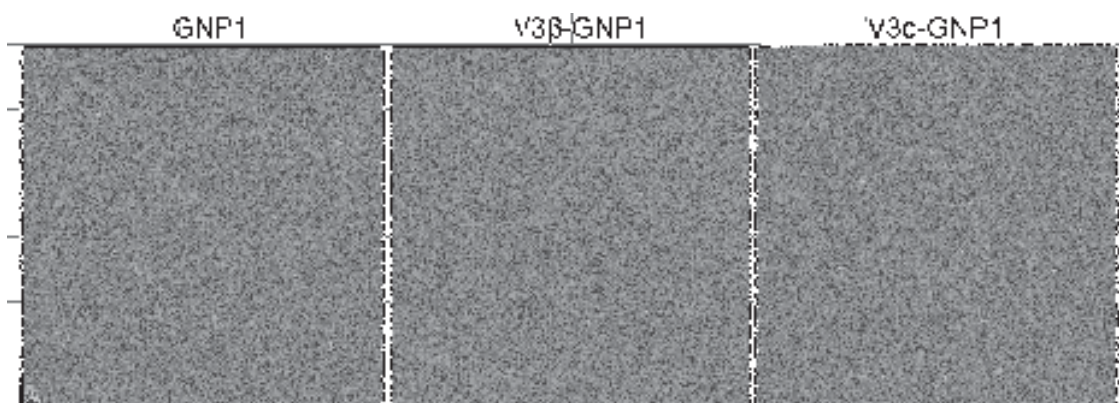
Figure 10. TEM pictures of GNP1, V3β-GNP1 and V3α-GNP1 (100 ug/ml) in H_2O.

Circular dichroism study of the interaction between GNP1 and V3

In water solution the conformation of V3 peptide is mainly random coil as indicates by NMR and electronic circular dichroism (CD) studies.[21] As showed before, β-strand conformation is preferentially adopted when V3 bind antibodies or coreceptor.

Circular dichroism is a well suited technique to study V3 conformation of V3-GNPs complexes because GNPs alone does not present any CD absorption. We found that,

by interacting with GNPs, the V3 conformation changes from random coil to predominant α-helix or β-strand depending on the experimental conditions. The CD spectra corresponding to the preparations of V3-GNP1 in different condition are showed in Figure 11.
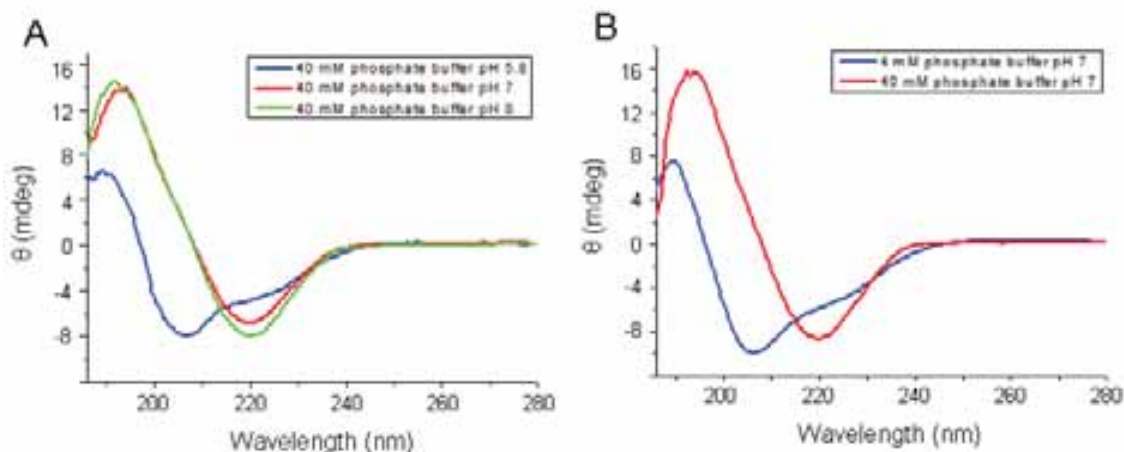
Figure 11. CD spectra of V3-GNPs prepared in different conditons. A) CD spectra of V3-GNP1 prepared at the same phosphate buffer concentration (40 mM), but different pH (from 5.8 to 8). B) CD spectra of V3-GNPs prepared at the same pH (pH 7), but different phosphate buffer concentration (4 and 40 mM).

At pH 5.8 or low concentration of phosphate buffer (4 mM), a typical α-helix CD spectrum was obtained with a maximun at 195 nm and minimum at 218 and 220 nm (Figure 11A and 11B, blue line), while at pH ≥ 7.0 or higher phosphate buffer concentration (40 mM), β-strand conformation with max. at 197 and min. around 219 nm (Figure 11A and 11B, red and green lines) was preferred.

The peptide conformational change is probably due to electrostatic interactions between the negatively charged GNPs and the positive charges of the peptide. From pH 5.8 to pH 8 the GNPs remain negatively charged, as demonstrated by z-potential measurements (Figure 9). Nevertheless, the net positive charge of V3 is influenced by both the pH and the concentration of phosphate buffer.[54, 55] At pH 5.8, V3 is more positively charged, than at pH> 7.0 (isoelectric point 9.54). At pH 5.8 all basic amino acid side chains, including histidines (pK_a=6), are protonated and can interact with the carboxylic groups of GNPs. The formation of V3α-GNP1 could be explained by comparing the positive charged amino acid sequence **K**SI**H**IGPG**R** of V3 and the one described by Broo *et al.*, in which a model peptide formed by positive charged amino

[54] Hofmeister, F. (1888). Zur Lehre von der Wirkung der Salze. [Title translation: About the science of the effect of salts.] *Arch. Exp. Pathol. Pharmakol.* **24**, 247-260.

[55] Collins, K. D. (2004). Ions from the Hofmeister series and osmolytes: effects on proteins in solution and in the crystallization process. *Methods*, **34**, 300-311.

acids spaced by two or three non-charged amino acids form an α-helix after interaction with negative charged silica NPs.[44]

The concentration of the phosphate (4 mM or 40 mM) also influence the conformation because phosphates are able to bind the positive charged amino acids of the V3 peptide. In addition, depending on the pH, phosphate present one negative charge $H_2PO_4^-$ (pH ≤6) or two negative charges HPO_4^{2-} (pH>7). The formation of the β-strand (V3β-GNP1) occurs with an increase of the pH and phosphate concentration. At pH ≥ 7.0 histidines (pK 6) are not protonated and phosphate (HPO_4^{2-}) is a dianion, resulting in a lower total positive charge of the peptide. The resulting V3β-GNP1 conformation is probably a balance of the influence of all the electrostatic interactions present.

Trying to understand the reasons of conformational changes observed in the interaction of V3 with the GNPs, a series of CD experiments varying pH, concentrations, solvent, ionic strength, and reaction time were also carried out with the free peptide and compared with the V3-GNP.

Influence of buffer, solvent, and ionic strength
Control experiments were carried out to evaluate the effect of phosphate and peptide concentration on the conformation of the free peptide. The CD spectra of free V3 at different concentrations of peptide and buffer were recorded and no change in the random coil conformation of the peptide was observed (Figure 12A and 12B). V3 peptide in 30% TFE presents the typical α-helix CD spectra (Figure 12C). It is well known that addition of trifluorethanol (TFE) to a peptide water solution can induces the formation of α-helix conformation.[56] A control experiment with the peptide bound to the GNPs was also carried out to investigate whether the phosphate in necessary to get the β-conformation or is the *ionic strength* which influence the peptide conformation. The V3 was added to a solution of GNP1 in 4 mM phosphate buffer (pH 7) containing NaCl 80 mM (ionic strength of a 35 mM phosphate buffer pH 7). The CD spectrum obtained is rather different to that of V3α-GNP1 or V3β-GNP1 and shows a weak min at 218 nm (Figure 12D, green line), indicating that an increase of phosphates concentration, but not of the ionic strength, is necessary to induce a predominant β-strand conformation on the V3 peptide.

[56] Myers, J. K., Pace, C. N., and Scholtz, J. M. (1998). Trifluoroethanol effects on helix propensity and electrostatic interactions in the helical peptide from ribonuclease T1. *Protein Sci.* **7**, 383–388.
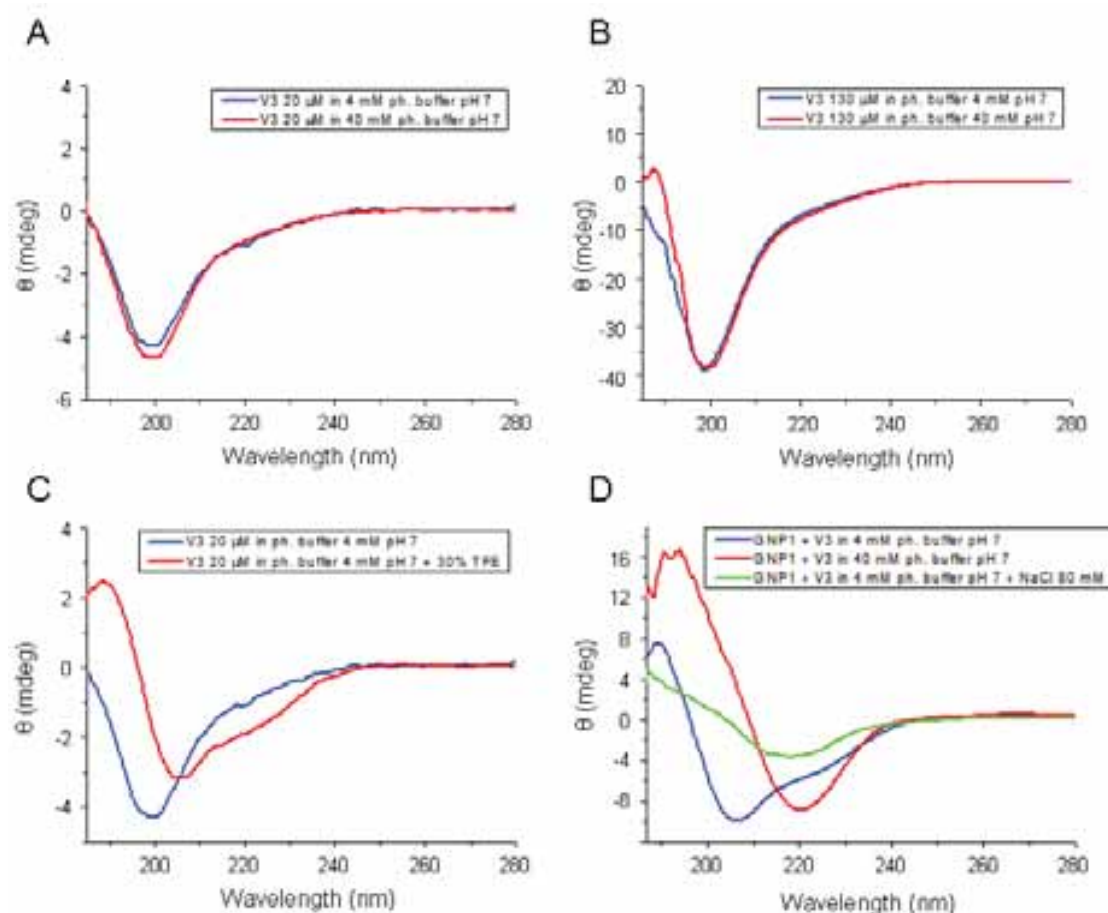
Figure 12. CD spectra of the V3 peptide and V3-GNP1 prepared in different conditons. A) Influence of phosphate buffer concentration. V3 peptide (20 µM) in 4 mM (blue) or 40 mM (red) phosphate buffer pH 7. B) Influence of phosphate buffer concentration. V3 peptide (130 µM) in 4 mM (blue) or 40 mM (red) phosphate buffer pH 7. C) Influence of TFE. V3 peptide (20 µM) in 4 mM phosphate buffer pH 7 in presence or not of 30% TFE. D) Influence of ionic strength. V3-GNPs prepared with 50 µM of V3 peptide in 4 mM phosphate buffer pH 7 (blue); V3-GNPs prepared with 50 µM of V3 peptide in 40 mM phosphate buffer pH 7 (red); V3-GNPs prepared with 50 µM of V3 peptide in 4 mM phosphate buffer pH 7 and NaCl (80 mM) (green); The different ionic strength between blue (4 mM phosphate buffer) and red (40 mM phosphate buffer) preparation due to different phosphate concentration was replaced by NaCl (80 mM).

To test the importance of negative charge of the carboxyl group and the influence of the glucose on the V3/GNP interactions, the peptide was also incubated with GNPs decorated only with the glucose linker (GlcC$_5$). No changes in the CD spectrum of random coil conformation of the peptide were detected (data not shown).

Influence of V3 peptide concentration and time on the conformation of V3-GNPs
We have also observed that the formation of V3β-GNP1 is concentration and time dependent. Titration of 4 mM phosphate solution (pH 7) of GNP1 with *increasing concentration* of V3 peptide (10 µL of 1 mg/ml water solution of peptide) along 8 hours

give a typical α-helix CD spectra with retention of the α-helix conformation (Figure 13A). In contrast, when the titration is carried out in 40 mM phosphate solution (pH 7) of GNP1, the formation of the α-helix was first observed, but after four additions of 0.0104 µmol of peptide (4 h), a conformational change from α-helix to β-strand was observed (Figure 13B). An isodichroic point, typical of a two state conformation transition, was observed at 212 nm.
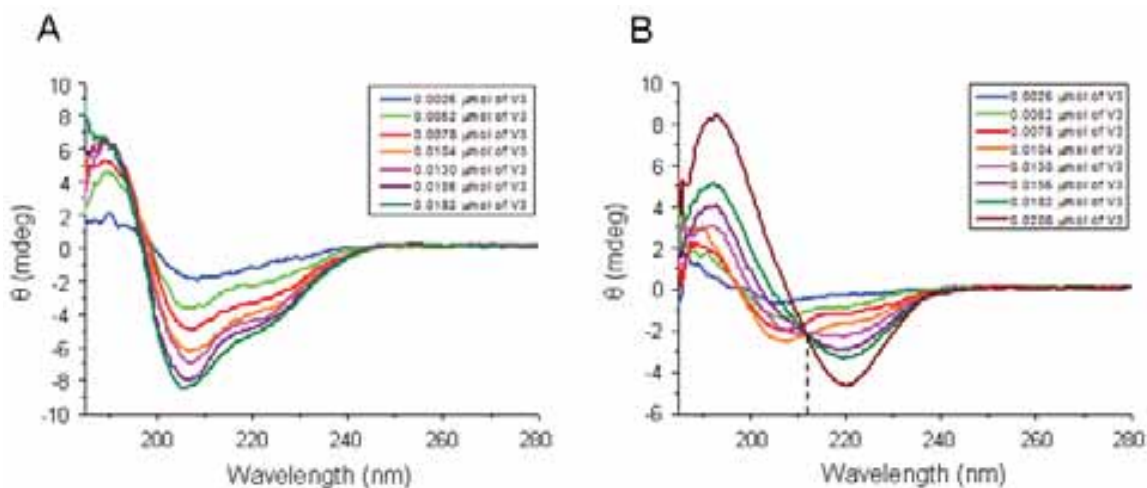
Figure 13. Titration of GNP1 with V3 peptide. A) GNP1 (0.00375 µmol, 0.0125 mM) was titrated in phosphate buffer (4 mM, pH 7) with V3 peptide (7 x 0.0026 µmol). B) GNP1 (0.00375 µmol, 0.0125 mM) was titrated in phosphate buffer (40 mM, pH 7) with V3 peptide (8 x 0.0026 µmol). From the 0.0104 µM peptide concentration on, an isodichroic point at 212 nm is observed (dotted line).

An isodichroic point at 208 nm is indicative of a transition from random coil to β-sheet, while at 204 nm indicates a transition from random coil to α-helix.[47] A similar isodichroic point (211 nm) was found by Zhang *et al.*[57] They observed that a 16 amino acids peptide with a β-sheet structure at ambient temperature undergoes an abrupt structural transition at high temperatures to form a stable α-helical structure.

The influence of the *reaction time* was also investigated by addition once of the total peptide concentration to the GNP1 solution under the conditions of α-helix (0.0182 µmol, buffer 4 mM, pH 7) or β-sheet formation (0.0208 µmol, buffer 40 mM, pH 7). CD spectra were recorded after 1h and 15 hours from the addition. In the conditions of V3α-GNP1 formation, no changes were detected with the time in the CD spectra (Figure 14A). However, in the preparation of V3β-GNP1, first the α-helix is formed after 1 h, but after 15 h the conformation changes to a prevalent β-strand (Figure 14B).

---

[57] Zhang, S., and Rich, A. (1997). Direct conversion of an oligopeptide from a beta-sheet to an alpha-helix: a model for amyloid formation. *Proc. Natl. Acad. Sci. U S A* **94**,,23-28.
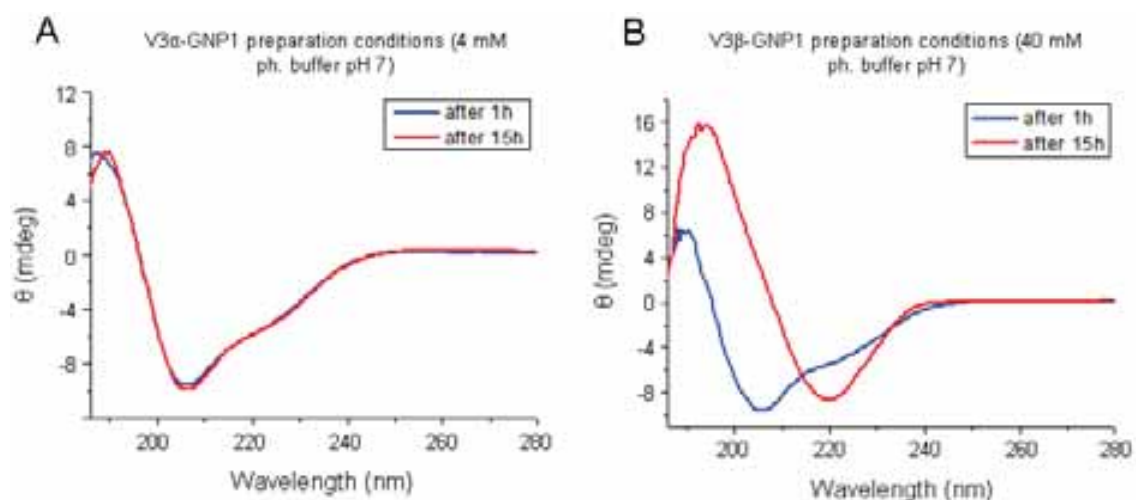
Figure 14. CD spectra of V3α-GNP1 and V3β-GNP1 at different reaction time. A) CD spectra of V3α-GNPs after 1h and 15 h addition of 0.0182 μM of V3 (4 mM phosphate buffer pH 7). B) CD spectra of V3β-GNPs after 1h and 15 h addition of 0.0208 μM of V3 (40 mM phosphate buffer pH 7).

This result indicates that at 40 mM phosphate concentration the V3 adopts first a α-helix that evolves with time to a more stable β-strand conformation. Other examples of conformational changes of peptides from random coil to α-helix or β-strand by varying conditions such as: pH, temperature and salts or peptide concentration have been already reported.[58, 59, 60, 61]

Influence of amino acid sequence on conformational behaviour.

We studied also the conformational changes of a model positive charged peptide. We select the positive charged peptide composed by the amino acid sequence KWGAKI-(KIGAKI)$_2$-NH$_2$ (pep18) and compare with V3. It is well known that pep18 changes its conformation from random coil to β-sheet after binding with small negatively charged phospholipid vesicles (~30 nm diameter) as showed by CD.[62]

---

[58] Mutter, M., Gassmann, R., Buttkus, U., and Altmann, K. H. (1991). Switch peptides: pH-induced α-helix to β-sheet transitions of bis-amphiphilic oligopeptides. *Angew. Chem. Int. Ed. Engl.* **30**, 1514-1516.

[59] Cerpa, R., Cohen, F. E., and Kuntz, I. D. (1996). Conformational switching in designed peptides: the helix/sheet transition. *Folding and Design*, **1**, 91–101.

[60] Zhang, S. (2002). Emerging biological materials through molecular self-assembly. *Biotechnol. Adv.* **20**, 321–339.

[61] Pagel, K., Wagner, S. C., Samedov, K., von Berlepsch, H., Bottcher, C., and Koksch, B. (2006). Random coils, β-sheet ribbons, and α-helical fibers: one peptide adopting three different secondary structures at will. *J. Am. Chem. Soc.* **128**, 2196-2197.

[62] Meier, M., and Seelig, J. (2008). Length dependence of the coil↔β-sheet transition in a membrane environment. *J. Am. Chem. Soc.* **130**, 1017-1024.

We have first studied by CD the conformation of the free pep18 by increasing concentration of phosphate buffer (H_2O pH 7, 4 mM pH 7 and 40 mM pH 7) and in presence of GNP1. In all preparations, the concentration of pep18 (56 µM, 0.5 mg/ml) was the same as in the V3 experiments. In contrast to the free V3, the presence of the phosphate was enough to observe a conformational change from random coil to β-strand (Figure 15A) with an isodichroic point around 208 nm, typical of this transition.
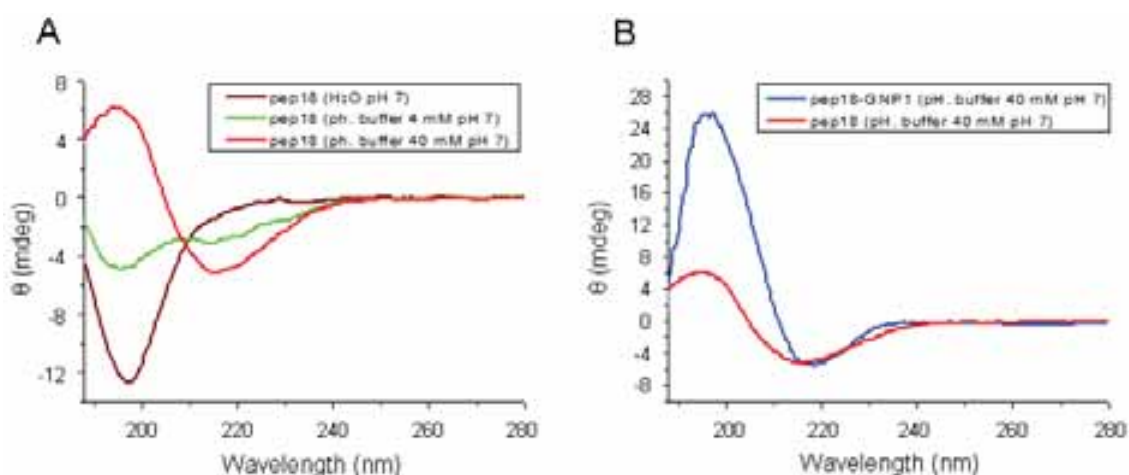
Figure 15. CD spectra of the peptide pep18 in different conditions. A) CD spectra of pep18 (56 µM) in H_2O pH 7 (brown line), in phosphate buffer 4 mM pH 7 (green line) and in phosphate buffer 40 mM pH 7 (red line). B) Comparison between CD spectra of pep18 (56 µM) in phosphate buffer 40 mM pH 7 (red line) and pep18 (56 µM) in phosphate buffer 40 mM pH 7 in presence of GNP1 (blue line).

Moreover, when pep18 (56 µM) was added to a 40 mM phosphate buffer solution in presence of GNP1 a more intense β-strand CD spectrum was observed (Figure 15B). The presence of both GNP1 and phosphate buffer (40mM) seems to induce a more extended β-strand region or aggregation of the peptide. The behaviour of pep18 presents significant differences compared with V3 peptide. In the presence of phosphate, pep18 move from random coil to β-strand, whereas the V3 remains random coil (see Figure 12A and 12B). In phosphate buffer 40 mM and in presence of GNP1 the conformation of pep18 remains β-strand along the time. After 15 h no changes in the CD spectrum were observed, while the conformation of the V3 changes from α-helix to β-strand.

These experiments show that both phosphate and negative charged GNP1 work together to modulate peptides conformation, but with different results depending on the positive charged peptide used.

Conformational stability of V3-GNP1

The previous experiments demonstrate that to modulate the conformation of V3 peptide, pH and phosphate concentration are very important, but once the V3α-GNP1 and V3β-GNP1 are formed the conformations remain stable in the different conditions. The V3α-GNP1 and V3β-GNP1 after purification and lyophilization were still stable. V3α-GNP1 and V3β-GNP1 (5 µM) were dissolved in phosphate buffer 5 mM and the stability in a range of different pHs and temperatures was studied by CD (Figure 16 and 17).
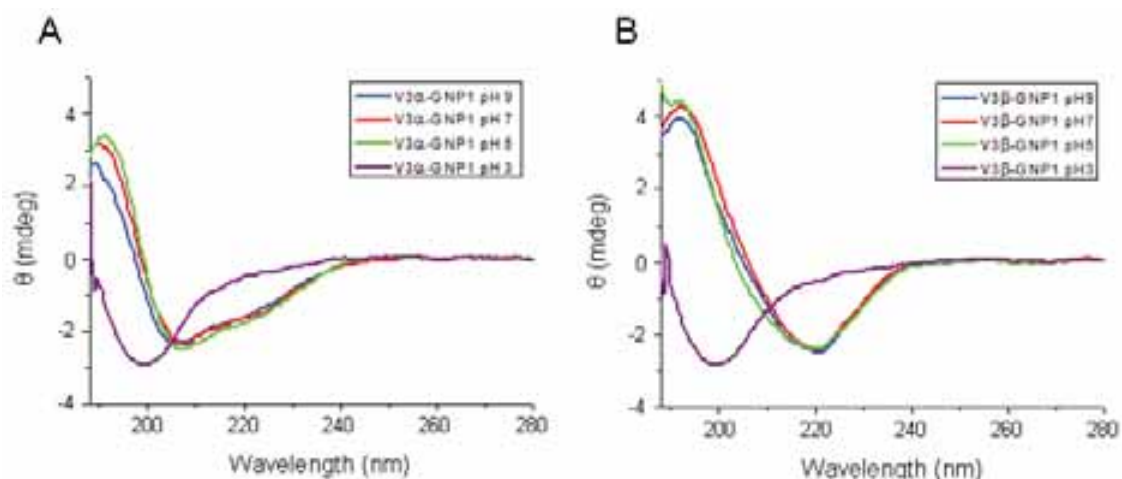
Figure 16. V3-GNP1 stability at different pH. CD spectra of (A) V3α-GNP1 and (B) V3β-GNP1 (5 µM) in phosphate buffer solution 5 mM at different pH (pH 3, purple; pH 5, green; pH 7 red; pH 9 blue).

Very slight changes were detected in the CD spectra of both GNPs between pH 5 and 9 (Figure 16A and 16B). However, at pH 3, GNP1 is not soluble and a black precipitate is formed. The CD spectra of the filtered off solutions showed the presence of V3 free peptide as random coil (Figure 16A and 16B, purple line). At this pH the carboxylic groups of the GNPs are protonated and the electrostatic interactions with V3 peptide basic amino acids disappear.

The V3α-GNP1 and V3β-GNP1 are also stable in a broad range of temperatures (Figure 17A and 17B). Increasing the temperature from 10ºC to 70ºC only slightly change in the CD spectra are observed, confirming the stability of both constructs, in contrast with the reversible transition of free peptides founded by Zhang.[57]
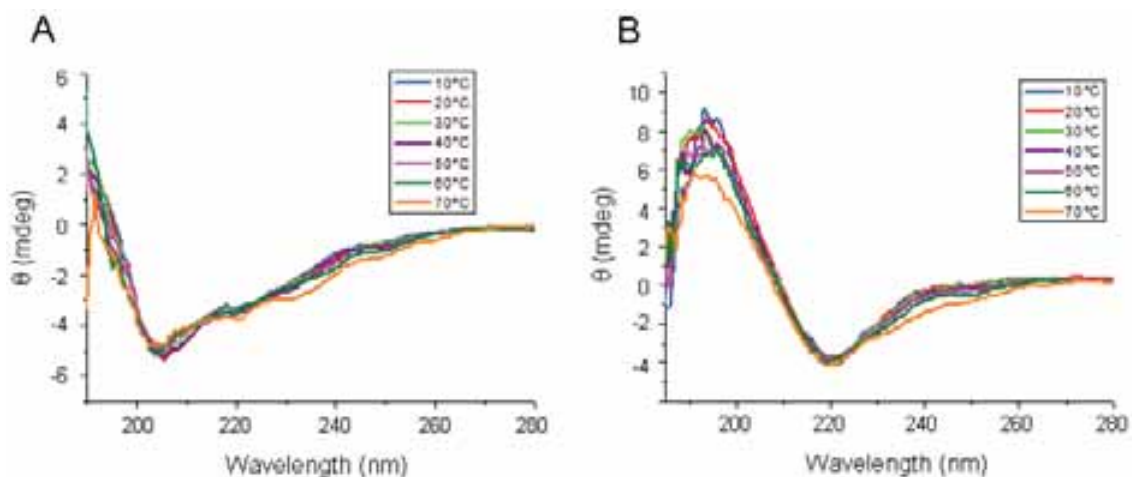
Figure 17. CD spectra of V3-GNPs at different temperatures (10-70ºC). A) V3α-GNP1 and B) V3β-GNP1 (10 µM) in phosphate buffer solution 5 mM.

Circular dichroism of the interaction between dimannoside containing GNP2 and V3

The V3 peptide in the native gp120 is characterized by the presence of three conserved *N*-linked oligomannosides within or adjacent to the loop in the positions N295 or N301, N332, and N392. The role of these oligommannosides in relation to V3 loop is not completely understood. However, it is well known that they play an important role in co-receptors selectivity,[5] in modulating V3 conformation[22] and in the immunological response related to V3 loop.[28] Indeed, very recently, a novel anti HIV-1 mAb (PGT 128) able to recognize two $Man_{8/9}GlcNAc_2$ glycans in position N301 and N332 as well as the C-terminal of the V3 loop was isolated. The fab fragment of Ab PGT 128 was crystallized with a glycosylated gp120 containing a truncated V3 loop that adopts a β-strand conformation in the binding with PGT 128 (see Figure 4).

GNP2 nanoparticles containing $GlcC_5$, linker-CO_2H and Manα1-2Man (GNP2) were prepared as showed in Scheme 1. The Manα1-2Man incorporated is the terminal disaccharide residue of $Man_9GlcNAc_2$ glycans of gp120 (see Introduction, Figure 3) and can influence the V3 conformation when interacting with the GNP2. GNP2 was characterized, and present very similar ^1H-NMR spectra UV-vis and TEM (around 2 nm) to GNP1.

To investigate the influence of the oligomannoside in the conformation of V3 we have prepared V3-GNP2 in the same conditions used for the preparation of V3β-GNP1 (6 eq. per GNP, in phosphate buffer 40 mM, pH 7). The resulting CD spectrum of V3β-GNP2 is similar to that of V3β-GNP1, the maximum shifts from 195 nm to around 200 nm and the minimum present a small shift from 220 to 202 nm (Figure 18). This small

difference between the two spectra may indicate a possible interaction between V3 peptides and the mannose oligosaccharides. However, to better understand the role of the oligomannosides new structures with more complex oligomannosides should be prepared in the future.
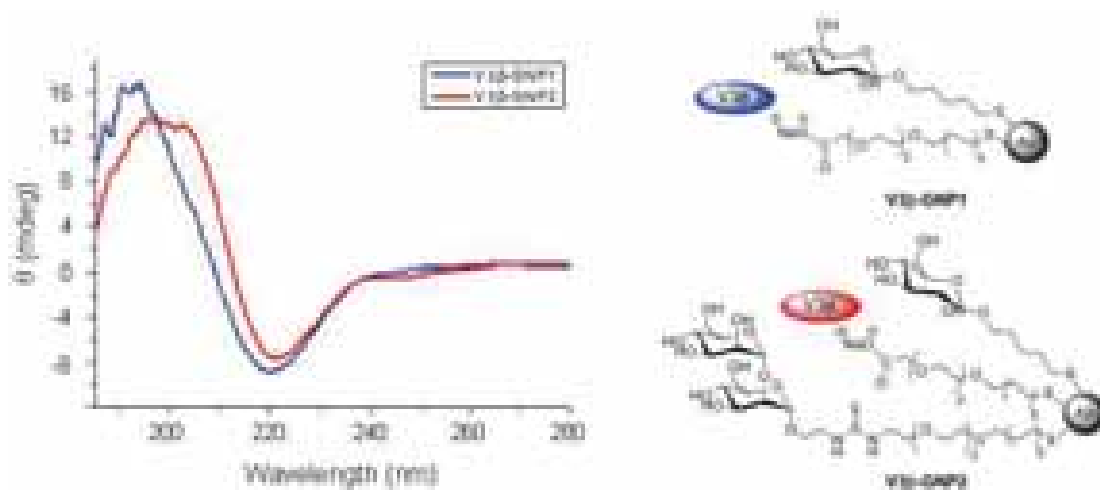
Figure 18. CD spectra of V3β-GNP1 and V3β-GNP2 prepared in the same conditions of pH and phosphate buffer concentrations.

Study of electrostatic interactions in the formation of V3α- and V3β-GNPs

The problem of protein-folding was first posed about one half-century ago.[63] Many factors contribute to protein folding: (i) hydrogen bonds, (ii) van der Waals interactions, (iii) backbone angle preferences, (iv) electrostatic interactions, (v) hydrophobic interactions (in proteins folded states the hydrophobic amino acids are predominantly located in the core and the polar amino acids are more commonly located on the protein's surface), (vi) chain entropy is also an important factor since the folding process implies a large loss in chain entropy. The structure adopted by peptides and proteins depend also on the sample preparation conditions such as solvent polarity, pH, salt concentration and so on. Medium-sized peptides with an intrinsic tendency to assume helical conformations in water often show a dramatic increase in helicity upon addition of relatively low concentrations of certain alcohols, of which the most efficient appears to be trifluoroethanol (TFE).[64]

---

[63] Dill, K. A., and MacCallum, J. L. (2012). The Protein-Folding Problem, 50 Years On. *Science* **338**, 1042-1046.
[64] Cammers-Goodwin, A., Allen, T. J., Oslick, S. L., McClure, K. F., Lee, J. H., and Kemp, D. S. (1996). Mechanism of stabilization of helical conformations of polypeptides by water containing trifluoroethanol. *J. Am. Chem. Soc.* **118**, 3082-3090.

The study of the origin of α-helix and β-strand conformational stability is important to understand protein-folding preferences. However, to unravel the molecular interaction that control the transformation from α-helix to β-strand remains today still a challenge.

We have tried to understand the origin of the conformational changes observed when the V3 peptide interacts with the GNPs in different conditions, but the complexity of the many affect makes the goal very difficult. Electrostatic interactions seem to be the driving force for the formation of the V3α- or V3β-GNPs. For example, Alzheimer peptide Aβ(1-40) displays a reversible random coil/β-strand transition at anionic membrane surface and unilamellar lipid vesicles.[65] As already mentioned, Seelig *et al.* demonstrated that also positive charged peptides like: KWGAKI-(KIGAKI)$_2$-NH$_2$ change from random coil to β-strand after interaction with small unilamellar vesicles.[62] Transitions between α-helix and β-strand influenced by solution conditions (pH, NaCl concentration, temperature, and peptide concentration) were also observed as reported by Kuntz *et al.* for the peptide Ac-ETATKAELLAKYEATHK-NH$_2$,[66] by Altmann *et al.*[67] for the peptide Ac-EAALEAALELAAELAA-NH$_2$ and by Zhang *et al.*[60] for the peptide DAR16-IV: DADADADARARARARA (positive charged peptides are depicted in blue and negative charged in red).

It was also found more recently that the interaction with nanoparticles also change the peptide conformations. Rotello et al showed that negative charged peptides (Ac-WAADAKADAADAAADAK-NH$_2$) can change from random coil to α-helix after binding to positive charged gold NPs.[43] Negative charged silica NPs induce α-helix formation in a positive charged random coil peptide (Ac-YARQQRAEARQQRAEARQQRAE ARQQRA-NH$_2$) as showed by Broo *et al.*[44] All these model peptides present in their sequence alternation of charged amino acids and no-charged amino acids, as the V3 cyclic peptide used in this work.

In an attempt to understand which regions of V3 interact with the negative charged GNPs, we have examined the spatial distribution of electrostatic charges for different conformations of V3 peptide (Figure 19). Electrostatic potential was calculated using the Adaptative Poisson-Boltzmann Solver (APBS) tools as implemented in the Pymol software (www.pymol.org). Electrostatic potential was mapped on the solvent

[65] Terzi, E., Holzemann, G., and Seelig, J. (1995). Self-association of β-amyloid peptide (1–40) in solution and binding to lipid membranes. *J. Mol. Biol.* **252**, 633–642.

[66] Cerpa, R., Cohen, F. E., and Kuntz, I. D. (1996). Conformational switching in designed peptides: the helix/sheet transition. *Folding & Design* **1**, 91–101.

[67] Mutter, M., Gassmann, R., Buttkus, U., and Altmann, K. H. (1991). Switch peptides: pH-induced α-helix to β-sheet transitions of bis-amphiphilic oligopeptides. *Angew. Chem. Int. Ed. Engl.* **30**, 1514-1516.

accessible surface; a blue color indicates regions of positive potential whereas red depicts negative potential values. Figure 19B shows the α-helix structure determined by ^{1}HNMR of V3 in 20% TFE/H_2O (PDB 1CE4) and the corresponding charge distribution.[21] Figure 19C represents the V3 peptide with a β-strand conformation as determined from the X-ray structure of gp120 complexed with CD4 and X5 Ab (PDB 2B4C).[26] Figure 19D shows the V3 peptide with a β-strand conformation as determined from the X-ray structure of gp120 complexed with CD4 and the anti-V3 Ab 412d (PDB 2QAD).[27]
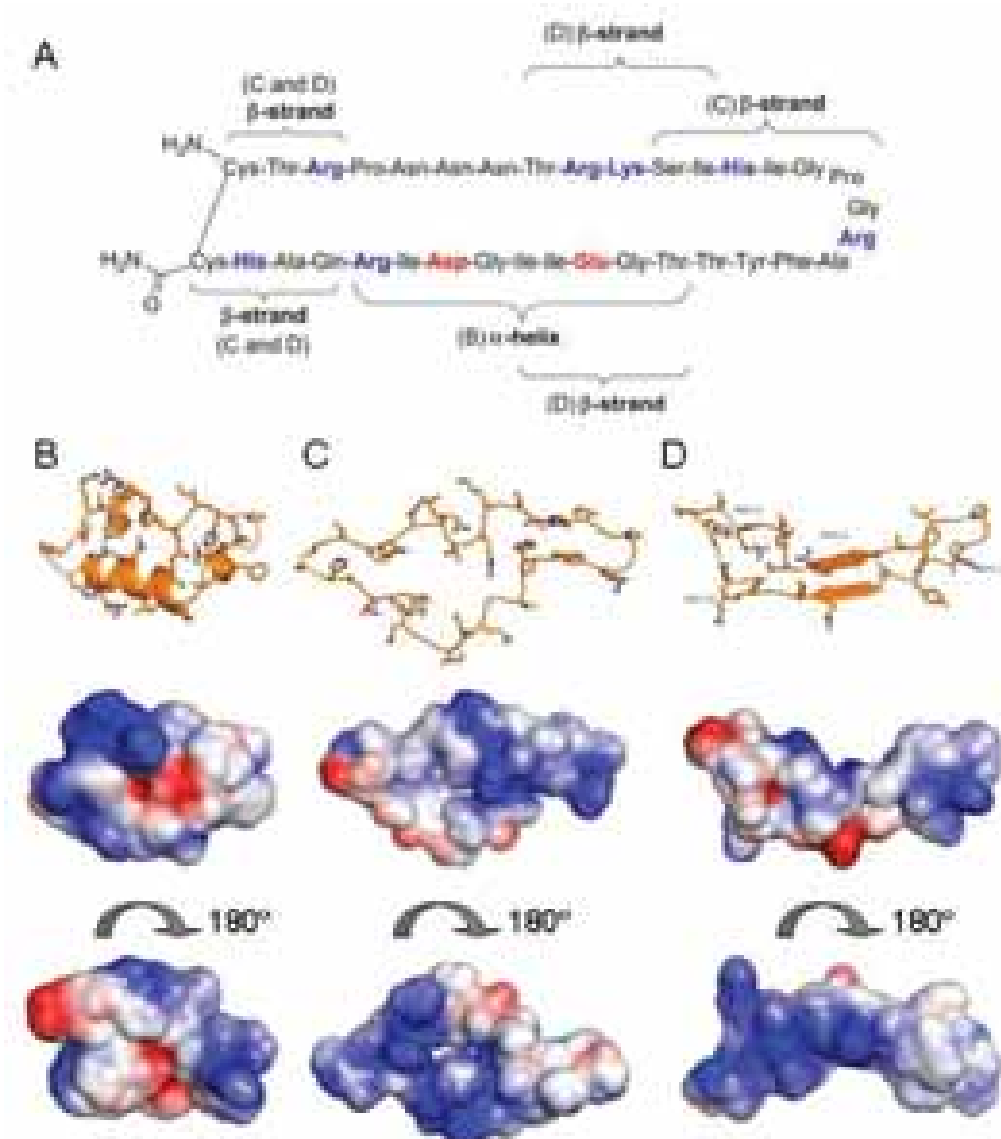
Figure 19. Representation of different V3 structure. A) Cyclic V3 peptide (positive charged peptides are depicted in blue and negative charged in red) B) V3 peptide with α-helix structure determined by ^{1}HNMR of V3 in 20% TFE/H_2O (PDB 1CE4)[21] C) V3 peptide with a β-strand conformation determined by X-ray structure of gp120 complexed with CD4 and X5 Ab (PDB 2B4C)[26] D) V3 peptide with a β-strand conformation determined by X-ray structure of gp120 complexed with CD4 and the anti V3 Ab 412d (PDB 2QAD).[27] Electrostatic potential was calculated using the Adaptative Poisson-Boltzmann Solver (APBS) tools as implemented in the Pymol software.

The α-helix shows a compact structure with the positive charges disperse along the surface. However, the electrostatic potential of V3 in β-strand conformation of figure 19D shows that the positive charged region is mostly confined in the opposite part of the arch. Both structures can interact with the negative charged GNP1, but it seems that in the V3β-GNP1 complex the GNP1 interact with the positive region far from the arch, leaving the V3 tip (GlyProGlyArg) free to bind to specific receptors as is the 447-52D Ab.[23] In the next section we will show SPR data that confirm the selectivity of this interaction.

Interaction of V3-GNPs with biological receptors

A series of experiments to evaluate the interaction of V3-GNPs with specific receptors were carried out to correlate the α-helix and β-strand conformations of V3, induced by GNPs, with its biological activity. The interaction of V3-GNPs with the broadly neutralizing anti-V3 Ab 447-52D and with the coreceptor CCR5 was first evaluated by surface plasmon resonance (SPR). The uptake of V3-GNPs by cells expressing coreceptors (CCR5 and CXCR4) were also performed. The ability of V3-GNPs to inhibit the virus infection in cell system was evaluated by HIV neutralization experiments. Finally, aiming at the exploration of GNPs as vaccine carriers, preliminary immunization experiments were performed in mice with the V3β-GNP1.

Interaction studies of V3-GNPs with anti-V3 Ab 447-52D and coreceptor CCR5 by SPR

In the introduction of this chapter we highlighted the works that establish the importance of V3 conformation in the interaction with anti-V3 Abs and with CCR5 coreceptor. These studies indicate that the β-strand conformation seems to be the preferred and active conformation in the interaction with specific Abs and coreceptors. We have shown that the interaction with GNPs modulates the conformation of the V3 peptide to obtain predominant α-helix or β-strand. We now explore the interaction of the V3-GNPs with the anti-V3 Ab 447-52D, specific for the conserved tip of the V3 loop, and with the coreceptor CCR5 by surface plasmon resonance (SPR) to correlate the conformation with the potency of the V3-GNPs to bind the receptors.

Binding of V3-GNPs with 447-52D Ab

An SPR study by using ProteOn XPR36 biosensor was performed in order to understand the relationship between V3 conformation and antibody binding activity. Standard amine coupling method was used to immobilize Ab 447-52D on research-

grade GLC Proteon sensor chip until 250 Resonance Units (RU). Binding of each analyte, control GNP1, free V3 peptide, V3α-GNP1, V3β-GNP1, V3β-GNP1b (with double amount of V3), and V3βGNP2 (with the dimannoside) to Ab 447-52D was studied at six different concentrations (0.2, 0.1, 0.05, 0.025, 0.0125, and 0.00625 mg/ml in PBS/Tween buffer). The binding profiles (sensorgrams) were obtained by an automatic subtraction of the reference surface signals from the 447-52D-activated surface signals (Figure 20). The channel surface between runs was regenerated with a short pulse of 0.1 M HCl.
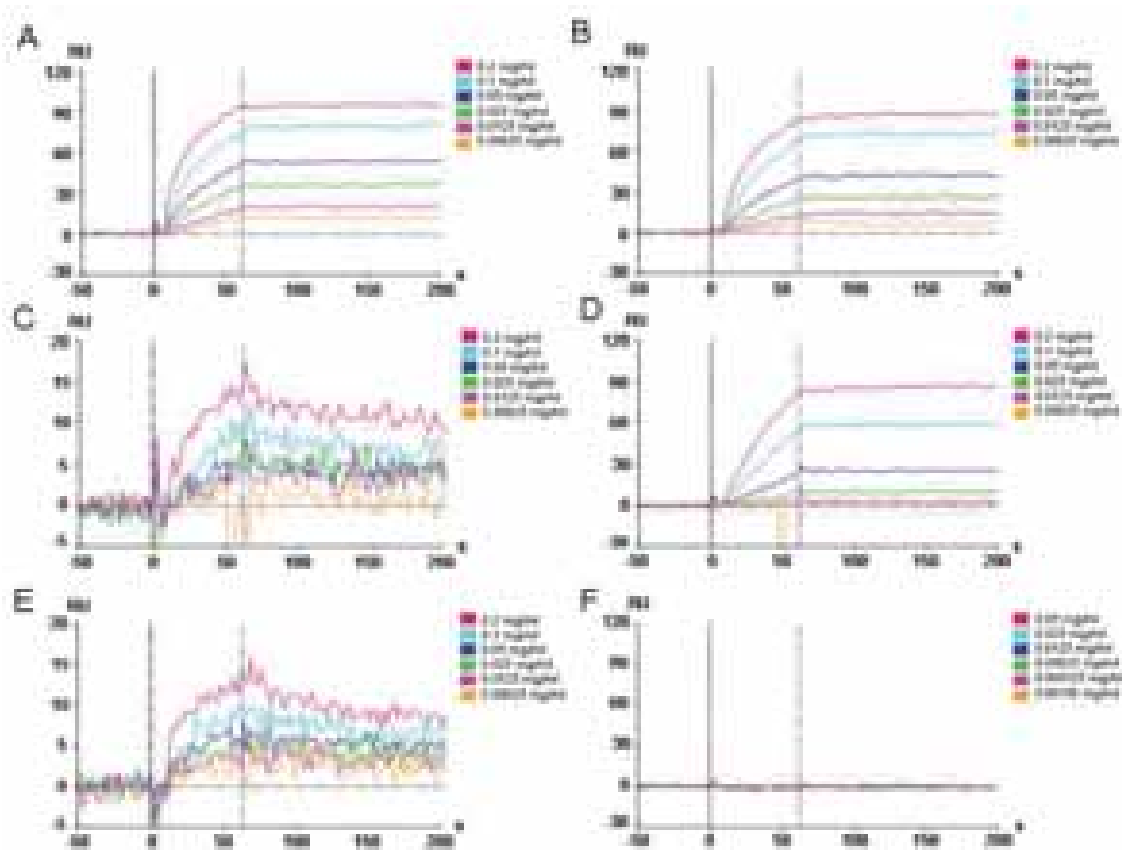
Figure 20. SPR experiments. Sensorgrams representing the dose-dependent binding of analytes to immobilized anti-V3 Ab 447-52D. A) V3β-GNP1; B) V3β-GNP1b; C) V3α-GNP1; D) V3β-GNP2; E) GNP1; F) V3 peptide. Six different concentrations were tested for V3-GNPs and GNP1 (0.2; 0.1; 0.05; 0.025; 0.0125; 0.00625 mg/ml) and six for the free peptide (0.05; 0.025; 0.0125; 0.00625; 0.003125; 0.00156; mg/ml). ProteOn PBS/Tween buffer was used to perform dilutions.

In all cases (except for V3 peptide) binding to the Ab occur in a concentration dependent manner. The strongest binding (highest RU) was obtained for the GNPs containing the V3 in the β-strand conformations (A, B, and D), while the V3α-GNP1 shows a weak binding similar to the control GNP1.

Sensograms corresponding to the highest tested concentration of V3β-GNP1, V3α-GNP1, GNP1 and V3 peptide were grouped in the same sensogram (Figure 21) for better comparison. Only V3β-GNPs strongly bind to Ab 447-52D in agreement with the crystallographic structure of the V3 peptide in complex with Ab 447-52D, where V3 peptides bind the Ab with a β-strand conformation (see Figure 2).[23] The binding of V3α-GNP1 and GNP1 to the antibody is the same and probably due to no-specific electrostatic interactions. Indeed, the Z-potential indicates that the V3α-GNPs (see Figure 9) is still negative charged. The difference between the specific interaction of V3β-GNP1 and the unspecific of V3α-GNPs may lie in the accessibility of the arch in the V3β-GNP1

Free V3 peptide binding to Ab was not detected despite the high concentrations used. This probably occurs because of its low molecular weight, and the low amount of Ab on the Proteon chip.

Figure 21. SPR experiments. mAb 447-52D was coupled to Proteon sensor chip using the recommended procedure until final 250 RU. A) Sensograms show the binding of V3 peptide (0.05 mg/ml) and GNP1, V3β-GNP1, V3β-GNP1b, V3α-GNP1 (0.2 mg/ml) to mAb 447-52D. B) Sensograms show the binding of V3β-GNP1 and V3β-GNP1b (0.2 mg/mL) to mAb 447-52D.

To study whether a higher number of V3 peptides per GNP was able to increase binding to 447-53D Ab, GNPs with double amount of V3 (V3β-GNP1b, 12 V3 per GNP1) was also tested. V3β-GNP1b is able to bind the Ab, however, no stronger interaction respect V3β-GNP1 was found (Figure 21). This is quite reasonable because each well oriented antibody on Proteon chip can bind two V3 peptides, and an excess of V3 peptides multivalently presented do not enhance the binding. Nevertheless, these data, does not exclude V3β-GNP1b from further biological experiments.

The binding of V3β-GNP2 covered with Man1-2Man disaccharides and V3 peptides with β-strand conformation with Ab was also studied. V3β-GNP2 is able to bind the Ab (Figure 23). Similar binding was observed with V3β-GNP1 and V3β-GNP2. The interaction of GNP2 without V3 peptides was also studied and no binding was observed.

The binding constants obtained from each group of 6 sensograms of Figure 20 are showed in table 2. The k_a of GNP1, V3α-GNP1, V3β-GNP1 and V3β-GNP1b has similar values (around 10^4). However, k_d is much lower for V3-GNP with β-strand conformation indicating a stronger binding. In the same way, V3-GNP with β-strand conformation has high Rmax values.

Table 2. Binding constants of GNP1, V3α-GNP1, V3β-GNP1 and V3β-GNP1b to anti-V3 antibody 447-52D.

	Ka (1/Ms)	Kd (1/s)	Rmax	Chi2
GNP1	$6.09 \ 10^4$	$2.13 \ 10^{-3}$	9.15	1.75
V3β-GNP1	$3.02 \ 10^4$	$1.19 \ 10^{-16}$	97.1	3.72
V3α-GNP1	$4.52 \ 10^4$	$1.82 \ 10^{-3}$	10.5	1.35
V3β-GNP1b	$2.91 \ 10^4$	$3.94 \ 10^{-18}$	95.8	4.71

In conclusion, SPR binding study showed that only GNPs bearing V3 peptide in β-strand conformation (V3β-GNPs) are able to strongly interact with Ab 447-52D. GNP1 and V3α-GNP1 bind weakly to the Ab. The strong binding of V3β-GNPs to the broadly neutralizing 447-52D Ab are a starting point to address the study of V3-GNPs as immunogens.

Binding of V3-GNPs with CCR5 coreceptor

The interaction of V3-GNPs with the coreceptor CCR5 was also studied by SPR. CCR5 is a membrane protein, which conformational features are difficult to reproduce in solution. The laboratory of S. Grzesiek (Biozentrum, Basel) has been able to efficiently express and stabilize the entire CCR5 [68] and set up an SPR experiment where the coreceptor is attached to a chip keeping its membrane conformation. Recombinant His-tagged CCR5 expressed in insect-cell was solubilised from cell membranes with a detergent mixture of cholesteryl hemisuccinate (CHS, 0.02%), CHAPS (0.1%), n-Dodecyl-β-D-maltopyranoside (DDM, 0.1%) and DOPC (50 nM). On a CM5 chip an antibody able to bind the 5His tag (Qiagen, Valencia, CA, USA) was immobilized, using amine coupling chemistry (9000 RU).[69] The His-tagged CCR5 solution was injected

---

[68] Nisius, L., Rogowski, M., Vangelista, L., and Grzesiek, S. (2008). Large-scale expression and purification of the major HIV-1 coreceptor CCR5 and characterization of its interaction with RANTES. *Protein Expression and Purification*, **61**, 155–162.

[69] Navratilova, I., Sodroski, J., and Myszka, D. G. (2005). Solubilization, stabilization, and purification of chemokine receptors using biosensor technology. *Anal. Biochem.* **339**, 271–281.

over the chip channel until 5000 RU. CCR5 was recognized by the conformation-dependent 2D7 antibody (mouse anti-human CD195, BD Pharmingen, Franklin Lakes, NJ, USA), which recognizes well-folded second extracellular loop (ECL2) of CCR5 (data not shown). Signals were processed with the Biacore T100 Evaluation Software using double referencing with both a reference channel (without CCR5) and blank injections (buffer only). The V3-GNPs and GNP1 were injected in the CCR5 and control channels. All GNPs gave strong and similar binding with CCR5. Attemps to regenerate this system (NaCl solution, 500 mM),, did not remove either V3-GNPs or GNP1 from CCR5 chip. Stronger condition (HCl or NaOH) would probably worked but they would remove also the CCR5. Looking into details the amino acids sequence of CCR5 we found that the "cytosolic face" of CCR5 contains a high number of positive charged amino acids that are probably responsible for the unspecific binding of any negative charged GNPs.[70]

Cellular experiments

To overcome the problems founded with the CCR5 in SPR experiments, we decided to directly study the V3-GNPs interaction with cellular lines that expresse the coreceptors. The selected cells were U87.CD4.CCR5, U87.CD4.CXCR4 and TZM-bl expressing both CCR5 and CXCR4.

Cellular uptake study of V3-GNP-FITC by flow cytometry

To confirm first the expresion of CCR5 and CXCR4, the selected cells, U87.CD4.CCR5, U87.CD4.CXCR4 and TZM-bl, were incubated with specific antibodies for each receptor: PE-labelled CD195 (clone2D7/CCR5) and PE-labelled anti-human CD184 (clone12G5/CXCR4).

---

[70] Oppermann, M. (2004). Chemokine receptor CCR5: insights into structure, function, and regulation. *Cell. Signaling,* **16**, 1201–1210.
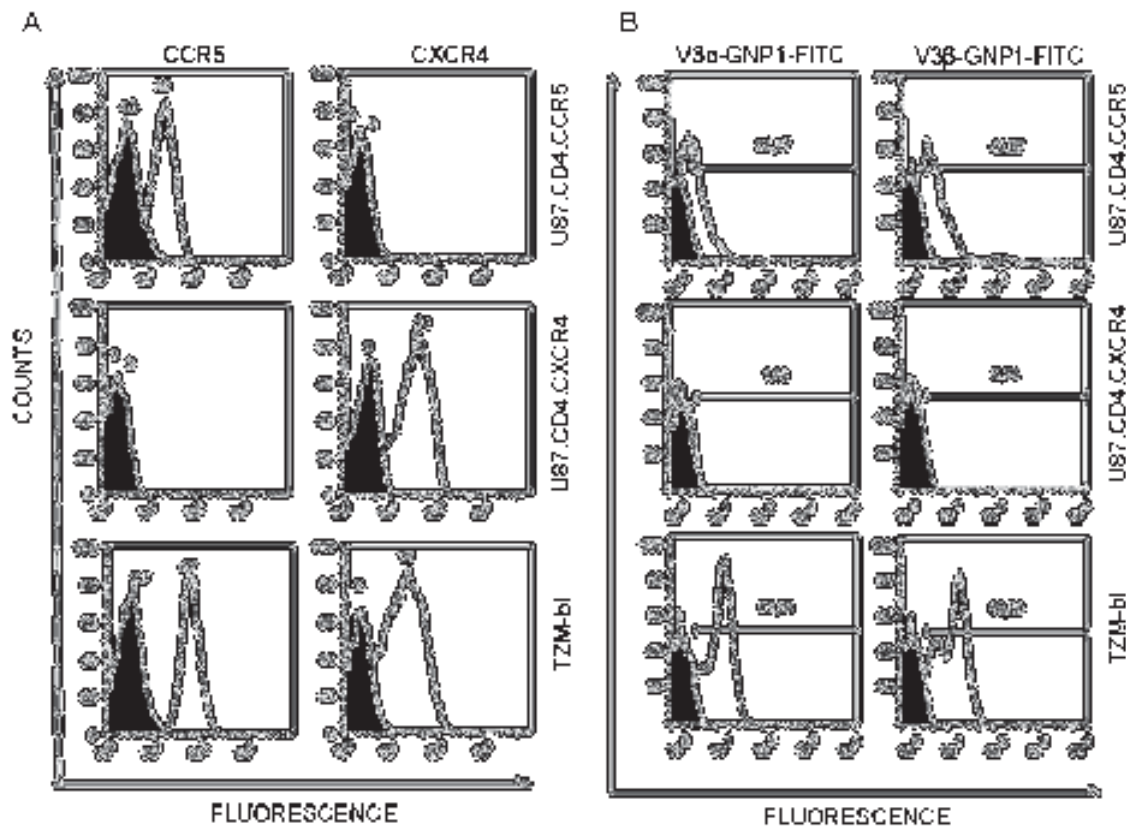
Figure 22. A) Expression of the CCR5 and CXCR4 coreceptors on U87.CD4.CCR5, U87.C4.CXCR4 and TMZ-bl. Cells were incubated with PE-labelled mAb specific for CCR5 or CXCR4 (empty histograms) and isotype controls (filled histograms). B) Uptake of V3-GNP1-FITC. Cells were incubated for 4h 30' with V3α-GNP1-FITC or V3β-GNP1-FITC at 25 µg/ml (empty histogram) or only with media (black histogram). The mean fluorescence intensity for each histogram is shown.

The results confirm that U87.CD4.CCR5 cells express CCR5, U87.C4.CXCR4 cells express CXCR4 and TMZ-bl cells express both coreceptors (Figure 22A).

To evaluate the receptor-mediated uptake of GNPs, cells were incubated with the fluorescently labelled V3α-GNP1-FITC or V3β-GNP1-FITC (25 µg/ml) at 37° C for 4h 30' (Figure 22B). The experiments showed that 31% of U87.CD4.CCR5 cells and 87% of TMZ-bl take V3α-GNP1-FITC up, while 45% of U87.CD4.CCR5 cells and over an 88% of TMZ-bl uptake V3β-GNP1-FITC. No uptake was found in cells expressing only CXCR4 coreceptor (U87.CD4.CXCR4). These results confirm that the V3 peptide used is selective for CCR5 receptor. U87.CD4.CCR5 cells preferentially uptake V3β-GNP1-FITC (45%) respect to V3α-GNP1-FITC (31%). TZM-bl cells uptake higher percentage of both V3-GNP1-FITC respect to U87.CD4.CCR5, probably because TZM-bl expresses higher amount of CCR5 (Figure 22A). The flow cytometry experiments indicate also that the viability of cells remains intact in the presence of the GNPs.

HIV-1 neutralization by V3-GNPs

The previous experiments confirmed that only cells expressing CCR5 were able to uptake V3-GNPs (Figure 22B). Due to the key role of CCR5 in HIV infection, it may be supposed that the interaction of V3-GNPs with this receptor would be able to block HIV entry and inhibit infection..

To test this mechanism, HIV neutralization experiments were performed in the laboratory of J. Alcamí (Instituto de Salud Carlos III, ISCIII, Madrid) by Dr. L. M. Bedoya. In HIV neutralization assay peripheral blood mononuclear cell (PBMCs) were treated with different concentrations of GNP1, V3-GNPs or V3 peptide alone. After 6 hours of incubation at 37 °C in 5% CO_2, viral stock was used to infect PBMCs, and maintained in culture at 37 °C in 5% CO_2. HIV replication was evaluated 48 hours post-infection following "Renilla luciferase assay system" (Promega) manufacturer procedures. Briefly, cells were lysed and relative luminescence units (RLUs) were obtained in a luminometer (Berthold Detection Systems) after the addition of substrate to cells extracts.[71] The results of the neutralization assay are showed in Figure 23.
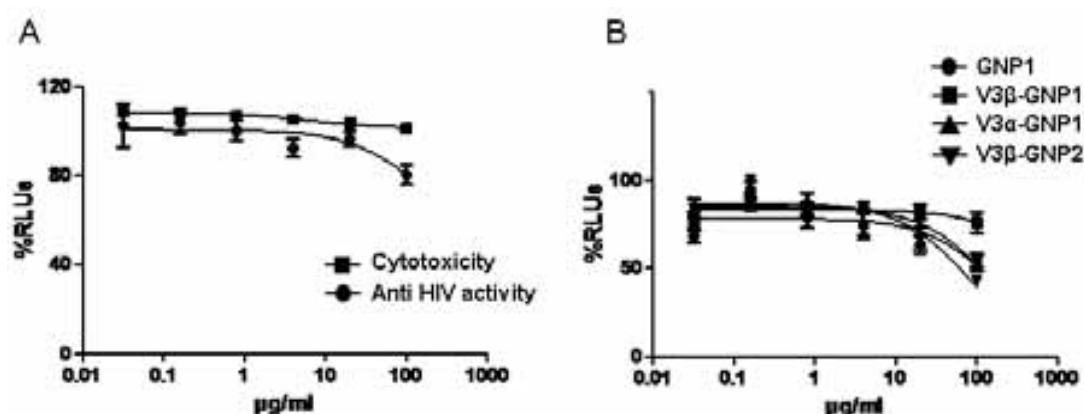
Figure 23. HIV neutralization assay. A) HIV neutralization assay and cytotoxicity of V3 peptide. B) HIV neutralization of GNP1 and V3-GNPs.

As showed in Figure 23A the peptide alone it is not cytotoxic and only a very slight inhibition of HIV infection at the highest concentration (100 µg/ml) was found. We thought that probably the multivalent presentation and/or the defined V3 conformation on the GNP1 could increase HIV neutralization activity. However, only at the highest concentration (100 µg/ml) a slightly better inhibition respect V3 free peptide was found (Figure 23B). Moreover, at 100 µg/ml neutralization activity of V3-GNPs is almost the same of GNP1 without the peptides, suggesting that the inhibition is probably due to the interaction of GNPs negative charges with gp120.

---

[71] Garcia-Perez, J., Sanchez-Palomino, S., Perez-Olmeda, M., Fernandez, B., and Alcami, J. (2007). A new strategy based on recombinant viruses as a tool for assessing drug susceptibility of human immunodeficiency virus type 1. *J. Med. Virol.* **79**, 127-137.

Cytotoxicity experiments

To ensure the viability of GNPs, cytotoxicity experiments were carried out with PBMCs in the same experimental conditions of the neutralization assay, but no virus was added to the cell culture. Compounds were tested at six different concentrations up to 100 µg/ml and were compared to untreated controls (Figure 24).
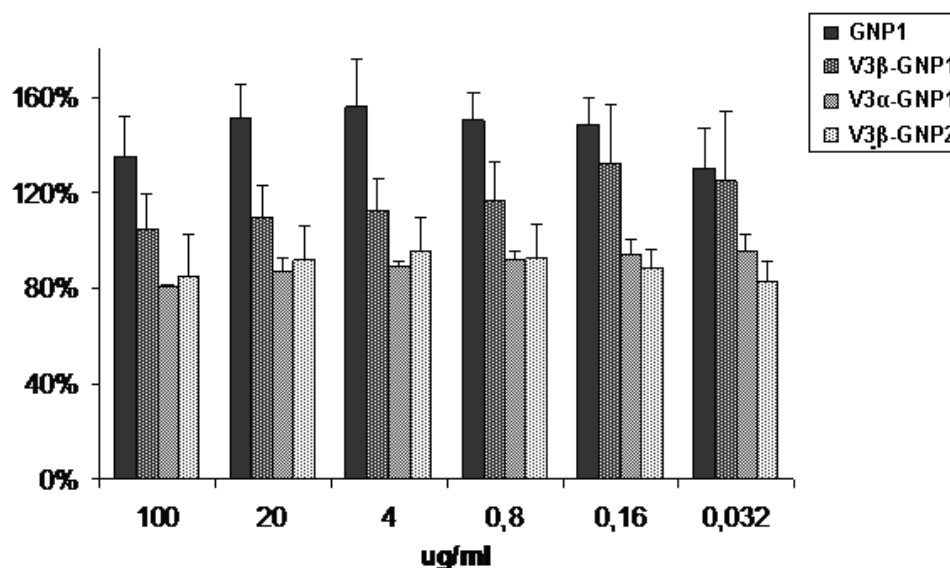
Figure 24. Cytotoxicity experiments of GNP1 and V3-GNPs with PBMCs.

After 48 hours, CellTiter Glo reagent (Promega) was added to cell culture following the manufacturer instructions and cell viability was evaluated by luminometry. No cell toxicity even at concentrations of 100 µg/ml was found for GNP1 and V3β-GNP1, however very slightly cytotoxicity was found for V3α-GNP1 and V3β-GNP2.

V3-GNPs as immunogens.

Anti-V3 Abs have been found in almost all HIV infected individual. However, these Ab are not able to eradicate de virus from patients. Many different V3-based immunogens have been prepared and studied as immunogens (see Figure 5 and 6). Although these constructs are able to induce an immune response in animals, the sera neutralize only T-cell line adapted virus or narrow range of primary isolates.

Immunogenicity of peptides is usually very poor because they are flexible and do not mimic well the conformational restraint of protein epitopes as well as they can undergo proteolysis in vivo. Coupling to highly immunogenic proteins is a general strategy to enhance humoral immune response of peptides. However, the coupling of the peptide to the carrier protein not always increase the immune response because of the peptide may be not accessible or it assumes an unpredictable not active conformation.

GNPs represent an alternative platform to conjugate peptides and limit their conformational mobility. We have previously shown that gold nanoparticles incorporating the repeating tetrasaccharide of the *Streptococcus pneumonia* capsular polysaccharide and a T-helper peptide were able to evoke anti-carbohydrate antibodies in mice that opsonise the bacteria in spleen infected cells.[72] Encouraged also by SPR results with Ab 447-52D, we thought that probably V3β-GNPs could elicit anti-V3 Abs in *in vivo* experiments.

Preliminary immunization study was performed only with V3β-GNP1 that gave the best binding with anti-V3 Ab 447-52D and with Balb/c mice as animal model. Three mice were immunized intracutaneously (MA) and three mice were immunized via intraperitoneal (MB). Every injection was performed with 50μg of V3β-GNP1 in presence of 10 μg of Monophosphoryl Lipid A (MPL) and 20μg of Quil-A as adjuvants. After 30 days, mice were boosted with other 50μg of V3β-GNP1 and after 40 days from the primary immunization, mice were sacrificed and sera collected for antibodies analysis.

To detect the presence of anti-V3 antibodies evoked in the mice immunised with V3β-GNP1, a GNPs-ELISA solid phase assay developed in our laboratory was used.[73]
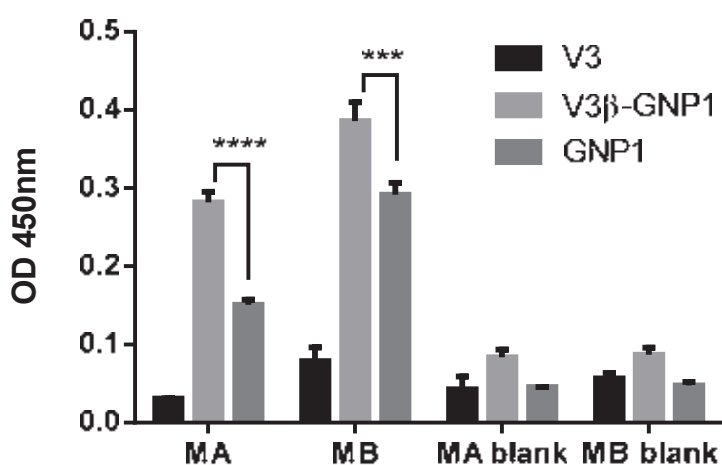
Figure 25. Specific IgGs from mice sera were detected by GNPs-ELISA. MA indicates mice sera immunized intracutaneously and MB indicates mice sera immunized via intraperitoneal. Sera were diluted 1:100 with PBS. IgGs sera were detected by OD at 450nm. A clear and significant IgGs response against V3β-GNP1 and GNP1, but not against the V3 peptide alone was detected. Control mice sera do not show presence of IgGs against V3β-GNP1 and GNP1.

---

[72] Gold nanoparticles as carriers for a synthetic *Streptococcus pneumoniae* type 14 conjugate vaccine. *Nanomedicine* (2012) 7(5), 651–662.

[73] F. Chiodo PhD thesis, Universidad del País Vasco, UPV/EHU, 2013.

In this GNP-ELISA test, GNPs were directly adsorbed on ELISA plate wells. Binding of IgGs from mice sera was tested against V3 peptide alone, V3β-GNP1 and GNP1 (Figure 25). mAb sera recognize V3β-GNP1 and GNP1, but not the free V3 alone. mAb sera recognize V3β-GNP1 with a significant difference to GNP1 suggesting the presence of specific anti-V3 antibody that recognize V3 in β-strand conformation. The interaction of mAb sera with GNP1 can be explained by unspecific interaction. It seems that immunization via intraperitoneal (MB) gave higher titer of IgGs than intracutaneous (MA) immunization. However, it seems that MA sera present higher ratio of specific Vs unspecific anti-V3 Ab respect MB sera. Control mice sera do not show the presence of IgGs against V3β-GNP1 nor GNP1.

Conclusions

Three different negatively charged GNPs were prepared to complex V3 peptides: GNP1 (covered with $GlcC_5$ and Linker-CO_2H), GNP2 (covered with GlcC5, Linker-CO_2H and the mannose disaccharide, Manα1-2Man) and a fluorescent GNP1 (covered with $GlcC_5$, Linker-CO_2H and a fluorescein linker, Linker-FITC). The V3 peptide that is almost random coil in water solution, changes its conformation after binding to GNPs, as demonstrated by CD experiments. V3 peptides on the GNP assume predominant α-helix (V3α-GNPs) or β-strand (V3β-GNPs) conformation depending of the preparation conditions. Phosphate concentration, pH, and reaction time were found to play an important role in V3-GNPs conformations. CD spectra of V3β-GNP1 and V3β-GNP2 are slightly different and suggest a possible interaction of dimannosides with V3 peptide.

The interaction of V3-GNPs with the anti-V3 Ab 447-52D and with the coreceptor CCR5 were studied by SPR. It is well known that mAb 447-52D recognizes the conserved GPGR tip of V3 and form a mixed β-strand with the KRIHI region of V3 by main chain hydrogen bonding.[23] SPR experiments showed that only V3β-GNPs are able to bind mAb 447-52D. V3α-GNPs gave the same binding affinity than the GNP-1 probably trough no specific interactions. Comparison of V3β-GNP1 and V3β-GNP2 showed similar binding with the Ab 447-52D in SPR experiments.

It is also known that N-terminal CCR5 interacts with the V3 base while the CCR5 second extracellular loop binds to V3 conserved tip. We tried to study the interaction of V3-GNPs with CCR5 by an SPR system set up by S. Grzesiek (Biozentrum, Basel). Unfortunately, the intracellular region of CCR5 contains many positive charged amino acids that are well exposed in this experiment and can interact with positive charged

molecules. In these conditions any specific V3/CCR5 binding was masked by unspecific electrostatic interactions.

Hence, we try to study V3-GNPs binding to CCR5 in cellular assays by using fluorescent labelled V3-GNPs (V3α-GNP1-FITC and V3β-GNP-FITC). The uptake of V3α-GNP1-FITC or V3β-GNP1-FITC on cells expressing CCR5 and or CXCR4 (U87.CD4.CCR5, U87.C4.CXCR4, and TMZ-bl) was studied. Only cells expressing CCR5 uptake V3-GNP1-FITC with little preference for V3β-GNP1-FITC.

HIV neutralization experiments with V3-GNP1 and GNP1 showed neutralization activity only at high concentration (100 ug/ml). Moreover, at this concentration, V3-GNP1 inhibition is comparable to GNP1. We can conclude that V3-GNPs are not a good system to block HIV entry.

A preliminary immunization study was performed with V3β-GNP1. mAb sera from both intracutaneous (MA) and intraperitoneal (MB) mice immunization recognize V3β-GNP1. New immunization experiments should be performed in order to understand the role played by GNP1 alone. Immunization experiments on rabbit will give higher sera amount allowing a more extensive Ab study.

Moreover, taking into account that oligomannose GNPs are able to bind lectins on the membrane of antigen presenting cells like dendritic cells (DCs). This process could facilitate the uptake of the V3-GNP2 to DCs encreasing immunogenicity of the peptide.

Experimental Part

General Information

All chemicals were purchased as reagent grade from Sigma-Aldrich, except chloroauric acid (Strem Chemicals), and were used without further purification. Reactions were monitored by thin layer chromatography (TLC) with silica gel 60 F_{254} aluminium sheets (Merck) and visualized by UV irradiation (254 nm) and/or staining with *p*-anisaldehyde solution [anisaldehyde (25 mL), H_2SO_4 (25 mL), EtOH (450 mL) and CH_3COOH (1 mL)] or 10% H_2SO_4 solution in EtOH, followed by heating at over 200℃. Size-exclusion column chromatography was performed on Sephadex^{TM} LH-20 (GE Healthcare). Purification of compounds by flash column chromatography on silica gel (FCC) was performed on a Biotage Sp4 HPFC™ automated flash chromatography system (Biotage AB, Uppsala Sweden) or by conventional flash chromatography using silica gel 60 (0.063-0.200 mm, 0.015-0.040 mm; Merck). UV-Vis spectra were carried out

with a Beckman Coulter DU 800 spectrometer. ^{1}H and ^{13}C NMR spectra were recorded on a Bruker AVANCE (500 MHz) spectrometer. Chemical shifts (δ) are given in ppm relative to the residual signal of the solvent used. The values of coupling constants (*J*) are given in Hz. Splitting patterns are described by using the following abbreviations: br, broad; s, singlet; d, doublet; t, triplet; m, multiplet. Infrared spectra (IR) were recorded from 4000 to 400 cm^{-1} with a Nicolet 6700 FT-IR spectrometer (Thermo Spectra-Tech). The mass spectrometric data were obtained from a Waters LCT Premier XE instrument with a standard ESI source by direct injection. The instrument was operated with a capillary voltage of 1.0 kV and a cone voltage of 200 V. Cone and desolvation gas flow were set to 50 and 500 L/h, respectively; source and desolvation temperatures were 100 ºC. The exact mass was determined using glycocholic acid (Sigma) as an internal standard (2 M+Na$^+$, m/z = 953.6058).For transmission electron microscopy (TEM) examinations, a single drop (10 µL) of the aqueous solution (*ca.* 0.1 mg mL^{-1} in milliQ water) of the gold nanoparticles was placed onto a copper grid coated with a carbon film (Electron Microscopy Sciences). The grid was left to dry in air for several hours at room temperature. TEM analyses were carried out in a Philips JEOL JEM-2100F working at 200 kV. Surface plasmon resonance (SPR) measurements were carried out using a ProteOn XPR36 Protein Interaction Array System with research-grade GLC sensor chips and all reagents were supplied by Bio-Rad (Bio-Rad Laboratories, Inc.).

Recombinant gp120 from HIV-1 CN54 clone (repository reference ARP683), monoclonal antibody 447-52D (repository reference ARP3219), and V3 peptide (repository reference EVA7041) were obtained from the Programme EVA Centre for AIDS Reagents, NIBSC, UK, supported by the EC FP6/7 Europrise Network of Excellence, AVIP and NGIN consortia and the Bill and Melinda Gates GHRC-CAVD Project and was donated by Prof. Ian Jones (Reading University, UK).

Synthesis

Synthesis and Characterization of Gold Nanoparticles
GNP1 was prepared as described in chapter 2 experimental part.

Preparation of **GNP2**. Linker carboxylate (3.93 mg, 0.09 mmol, 1.5 eq), GlcC$_5$ (2.82 mg, 0.09 mmol, 1.2 eq) and dimannose conjugate (1.3 mg, 0.002 mmol, 0.3 eq) were dissolved in 1.67 ml mixture of MeOH/H$_2$O/CH$_3$COOH (3:3:1) and added to a 0.27 ml solution of tetrachloroauric acid in water (25 mM, 0.01067 mmol, 1 eq). An aqueous solution of NaBH$_4$ (0.15 ml, 1 M, 22 eq.) was then portion-wise (4 x 37.5 µl) added and

the mixture was shaken for 2 hours at 25 ºC. The solvent was evaporated at reduced pressure. The black residue was washed three times with ethanol, re-dissolved in the minimum quantity of milliQ water, loaded into 5-10 cm segments of SnakeSkin® pleated dialysis tubing (Pierce, 3500 MWCO) and purified by dialysis against distilled water (3 L of water, recharging with fresh water every 6 hours over the course of 72 hours). The nanoparticles were obtained as brown powder after lyophilisation (2.7 mg). TEM (average diameter and number of gold atoms): 2.1 ± 0.5 nm, 225; ^{1}H NMR (500 MHz, D_2O): δ 4.40 (br signal, 1H), 4.1 (br signal, 1H), 3.8-3.2 (br m, ~16H), 1.87-1.24 (br m, 16H); UV-Vis (H_2O, 0.1 mg mL^{-1}): no surface plasmon signal was observed.

Preparation of **GNP1-FITC**

Starting from Linker-CO_2H (14.5 mg, 0.03 mmol), GlcC$_5$ (7.62 mg, 0.027 mmol), Linker-FITC (2.57 mg, 0.003 mmol), HAuCl$_4$ (800 µl, 25 mM) and NaBH$_4$ (440 µl, 1M), GNP1-FITC was obtained as brown amorphous powder (5.9 mg).

TEM (average diameter and number of gold atoms): 1.9 ± 0.4 nm, 225.

^{1}H RMN (D_2O, 500 MHz) δ 0.7-2.5 (bm, 32H); 2.8-4.1 (bm, 38H); 4.3 (bs, 2H); 6.6-7.0 (H-aromatic FITC).

UV-vis (H_2O, 0.1 mg/ml) λ=496

Fluorescence λ$_{ex}$=480; λ$_{em}$=520

Preparation of **V3β-GNPs**. A water solution of **GNP1** (1 ml, 2 mg/ml, 0.000025 mmol) was mixed with a phosphate buffer solution (1 ml, 100 mM, pH 7) and a water solution of V3 peptide (0.55 ml, 1 mg/ml, 0.00014 mmol) was added. The brown solution was left under shaking over night at RT. The mixture was diluted with 2.55 ml of distilled water and centrifuged on amicon filter (30 KDa MWCO), for 5 minutes, at 3000 rpm and 10 ºC. The residue and the washing were collected. The product was lyophilized and the washing analyzed with Bradford test. Around 5.5 V3 peptides per GNP were calculated because in the washing no peptide was detected.

Preparation of **V3α-GNPs**. A water solution of **GNP1** (1 ml, 2 mg/ml, 0.000025 mmol) was mixed with a phosphate buffer solution (1 ml, 10 mM, pH 5.8) and a water solution of V3 peptide (0.55 ml, 1 mg/ml, 0.00014 mmol) was added. The brown solution was left under shaking over night at RT. The mixture was diluted with 2.55 ml of distilled water and centrifuged on amicon filter (30 KDa MWCO), for 5 minutes, at 3000 rpm and 10 ºC. The residue and the washing were collected. The product was lyophilized and the washing analyzed with Bradford test. Around 5.5 V3 peptides per GNP were calculated because in the washing no peptide was detected.

Circular Dichroism (CD) experiments

Experiments were performed on a Jasco J815 spectrophotometer using a quartz cuvette with a 1-mm path length. For all CD studies, scans were taken from 180 to 280 nm at a rate of 20 nm/min with a sample interval of 0.1 nm and an 8 sec response. Each experiments give a final spectrum which is the average of ten scans. All CD spectra were subtracted from blank.

Agarose gel electrophoresis

1 g of agarose was dissolved in 100 ml of Tris-Borate EDTA buffer (88 mM Tris Base, 88 mM boric acid and 2 mM EDTA) and casted. Samples (2 mg/ml in H_2O) were mixed with 4 μl of TBE (5x), 2 μl of glycerol (30%) and loaded in the gel. The gel was run at 50V for 1 h (running buffer TBE 0.5x). For staining the gel was rinse in 100 ml ultrapure water 3 times for 5 min and stained for 1 h at room temperature with gentle shaking with SimplyBlue SafeStain (Invitrogen). For distaining the gel was washed with 100 ml water overnight.

Z-potential experiments

All zeta potential measurements were performed using a MALVERN Zetasizer Nano ZS. GNPs were tested at 100 μg/ml in phosphate buffer pH 6, pH 7 and pH 8 at 25ºC. Three rounds of assays were conducted and the average data are reported.

Spatial distribution of electrostatic charges

Electrostatic potential was calculated using the Adaptative Poisson-Boltzmann Solver (APBS) tools as implemented in the Pymol software (www.pymol.org). Hydrogen atoms and partial charges at pH 7 were computed in APBS plug in with PDB2PQR approach.[74] Electrostatic potential was calculated using APBS[75] for 150 mM ionic strength at with a protein dielectric of 2 and a solvent dielectric of 78.5 by using the a same grid of 300 x 300 x 150 ang. Electrostatic potential mapped on the solvent accessible surface; a blue color indicates regions of positive potential (>2 kT/e) whereas red depicts negative potential values (<-2 kT/e).

---

[74] Dolinsky, T. J., Nielsen, J. E., McCammon, J. A., and Baker, N. A. (2004). PDB2PQR: an automated pipeline for the setup, execution, and analysis of Poisson-Boltzmann electrostatics calculations. *Nucleic Acids Research* **32**, W665-W667.

[75] Baker, N. A., Sept, D., Joseph, S., Holst, M. J., and McCammon, J. A. (2001). Electrostatics of nanosystems: application to microtubules and the ribosome. *Proc. Natl. Acad. Sci. USA* **98**, 10037-10041.

SPR experiments

V3-GNPs and Ab 447-52D

The binding of GNPs and V3 peptide (in here, analytes) to mAb 447-52D was studied by SPR using a ProteOn XPR36 Protein Interaction Array System with research-grade GLC sensor chips (compact polymer layer containing easily activated carboxylic groups). mAb 447-52D was immobilized on a GLC sensor chip using the standard amine coupling chemistry according to the manufacturer's instructions. A GLC sensor chip was equilibrated with ProteOn PBS/Tween buffer (phosphate buffered saline, pH 7.4, 0.005% Tween 20). The carboxylic groups of two different channels on the chip surface were activated at 25 ºC by injecting 30 µl (contact time: 60 sec; flow rate: 30 µl/min) of a 1 vol/vol mixture of EDAC (16 mM) and Sulpho-NHS (4 mM). Channel 1 was further injected with 120 µL (240 sec; 30 µl/min) of a 447-52D solution in acetate buffer (50 µg/ ml, 10 mM, pH 4) at 25 ºC to obtain an immobilization level of 250 Response Units (RU). Only PBS/Tween was flown into channel 2, which was used as a reference. Finally, the surfaces of both channels were saturated by 100 µl (200 sec; 30 µl/min) of ethanolamine HCl (1 M, pH 8.5). Simultaneous binding of six different concentrations of each analyte to 447-52D was studied. Each analyte was diluted at 0.2, 0.1, 0.05, 0.025, 0.0125, and 0.00625 mg/ml in PBS/Tween buffer, and injected at 25 ºC in both channels (contact time: 60 s; dissociation time: 100 s; flow rate: 100 µl/min). The binding profiles (sensorgrams) were obtained by an automatic subtraction of the reference surface signals from the 447-52D-activated surface signals. The sensor surface between runs was regenerated with a short pulse of 0.1 M HCl. All binding experiments were repeated three times and the binding RUs were comparable taking into account the instrument error.

V3-GNPs and CCR5

The interaction of GNPs and V3 peptide to CCR5 coreceptor was assessed by SPR using a T100 Biacore instrument (GE Healthcare, Buckinghamshire, UK). The setup consisted of a CM5 chip on which an antibody against the 5His tag (20 mM Na-acetate pH 5.5; Qiagen, Valencia, CA, USA) was immobilized, using amine coupling chemistry (9000 RU). This antibody could capture, 5000 RU of recombinant His-tagged insect-cell expressed CCR5, solubilized from membranes using a detergent mixture of DDM, CHAPS, CHS, and DOPC at pH 7: this solution was injected over a surface constituted of amine-coupled anti-His-tag antibody. The capture of CCR5 was thus achieved through a 5His tag on its C-terminal (the intracellular part of the receptor). Experiments were performed at least twice using a flow rate of 50 ml/min during an association phase of 360 s. The buffer detergent mixture (20 mM HEPES pH 7, 150 mM NaCl, 0.1

mg/ml BSA, 0.1% DDM, 0.1% CHAPS, 0.02% CHS, and 50 nM DOPC) was present at all steps of the experiment; before, during and after injections. Signals were processed with the Biacore T100 Evaluation Software using double referencing with both a reference channel (without CCR5) and blank injections (buffer only).

Flow cytometry experiments

For the phenotyping studies, 100,000 cells were disassociated from the surface by incubating for 15min at 37ºC with cell disassociation solution (Sigma), blocked for 30 min at 20ºC with PBS containing 10% fetal bovine serum and 0.09% sodium azide and incubated for 45min at 20ºC with PBS containing 1% heat-inactivated FCS, 0.09% sodium azide and 20 µl PE-labelled mouse anti-human CD195 (clone3A9/CCR5), 5 µl CD195 (clone2D7/CCR5), 10 µl PE-labelled rat anti-human CD184 (clone1D9/CXCR4), 10 µl PE-labelled mouse anti-human CD184 (clone12G5/CXCR4), 3µl APC-labelled mouse anti-human CD4 orther corresponding isotype controls. Following two washes with PBS containing 1% heat-inactivated FCS, 0.09% sodium azide they were read in a Canto II flow cytometer (BDbioscience). All the antibodies were purchased from BDbioscience.

Employment of PE-labelled anti-human CD184 (clone1D9/CXCR4) showed proper CXCR4 expression only on U87.CD4.CXCR4 cells. Employment of PE-labelled CD195 (clone3A9/CCR5) showed no CCR5 expression on U87.CD4.CCR5 while when the anti-CCR5 antibody 3A9 clone was replaced by the 2D7 clone, U87.CD4.CCR5 showed CCR5 expression.

HIV-1 neutralization experiments

Cells and viruses. PBMCs were isolated from buffy coats of healthy donors and cultured in RPMI 1640 medium containing 10% (v/v) fetal bovine serum, 2mM L-glutamine, penicillin (50 IU/mL) and streptomycin (50 µg/mL) (all Whittaker M.A. Bio-Products, Walkerville, MD, USA) and pre-activated with IL-2 (300 U.I.; Chiron) and PHA (5 µg/mL; Sigma). Cells were cultured at 37ºC in a 5% CO_2 humidified atmosphere for 2 days with PHA and IL-2 and splinted every two or three days adding only IL-2 to assure cell survival.

Plasmids. The pJR-Renilla (R5 tropic) plasmid was generated by replacing the env gene on the proviral clone (pNL4.3- Renilla) by the env JR_{CSF} gene.

Production of recombinant viruses and neutralization assays. Recombinant virus stocks were obtained from calcium phosphate transfection of plasmid pJR-Renilla on 293T

cells. Stocks were then stored at -80ºC until use. Previously to neutralization assays, infectivity of recombinant viruses were evaluated by infecting cells with serial dilutions of viral stocks. Neutralization assay of HIV was then performed by pre-treating cell culture with different concentrations of compounds. After 6 hours of incubation at 37 ºC in 5% CO_2, pre-treated viral stocks were used to infect preactivated PBMCs, and maintained in culture at 37 ºC in 5% CO_2. HIV replication was evaluated 48 hours post-infection following "Renilla luciferase assay system" (Promega) manufacturer procedures. Briefly, cells were lysed and relative luminescence units (RLUs) were obtained in a luminometer (Berthold Detection Systems) after the addition of substrate to cells extracts.

Cytotoxicity.

The toxicity of the tested compounds was evaluated in the same conditions described for the neutralization assay in the absence of the virus. After 48 hours, CellTiter Glo reagent (Promega) was added to cell culture following the manufacturer instructions and cell viability was evaluated by luminometry.

GNPs ELISA

NUNC Maxisorp® ELISA plate wells were coated with 50 µL of GNPs (20 µg/mL), 50 µL of V3β-GNPs (20 µg/mL which contain 0.001 mM of V3 peptides) or 50µL of V3 peptide (0.001 mM). All solutions were prepared with coating buffer (50 mM Na_2CO_3, pH=9.7). After 2h at room temperature, solutions were removed and plate wells were washed with PBS (10 mM, pH=7.4; 2x200 µL). BSA solution (1% in PBS) was placed in each well (200 µL) and left for 30 minutes at room temperature. BSA solution was removed and 100 µL of 447-52D Ab (0.09 µg/mL) or 100µL of mice serum (1:100 in assay buffer: 0.5% BSA) were added and left under shaking 1 h at 500rpm. ELISA plate wells were washed with PBS (3x200µL) and 100 µL of anti-human horseradish peroxidase (0.8 µg/mL, life technologies, Novex® Goat anti-Human IgG-HRP) or 100 µL of anti-mouse horseradish peroxidase (0.8 µg/mL, life technologies, Novex® Rabbit anti-Mouse IgG-HRP) were added and left under shaking 1 h at 500rpm. Wells were washed with PBS (3x200µL) and 100 µL of substrate solution (3,3′,5,5′-Tetramethylbenzidine, TMB, in citric/acetate buffer, pH=4) were added. After 2 min at room temperature the reaction was stopped with 50 µL of H_2SO_4 (0.8 M) and the absorbance was measured at 450 nm in an ELISA plate reader. These experiments were performed in triplicate.

ANNEX

GNPs CHARACTERIZATION DATA

(20%)⁻O₃SO-Au
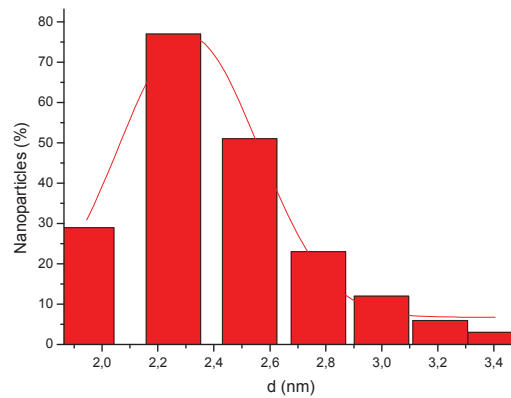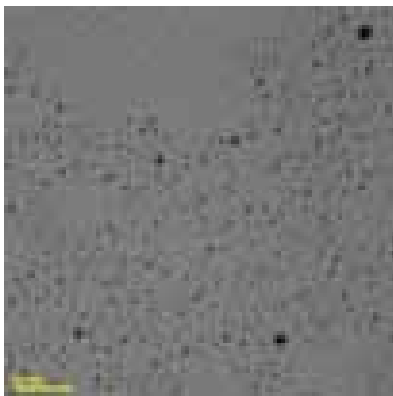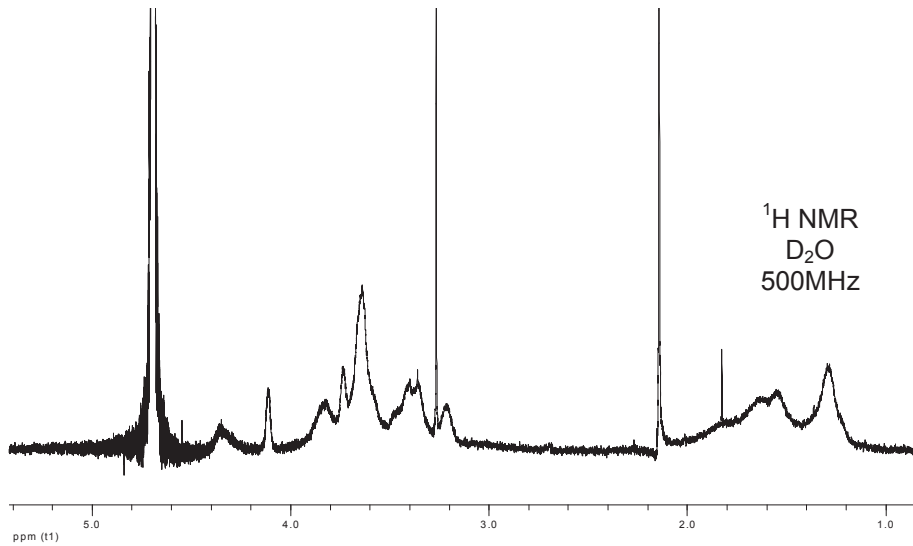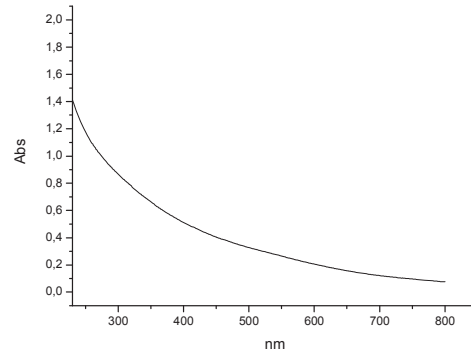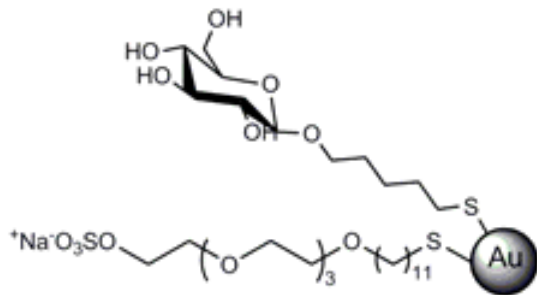
$(20\%)^-O_3SO\text{-}Au$

(50%)⁻O₃SO-Au
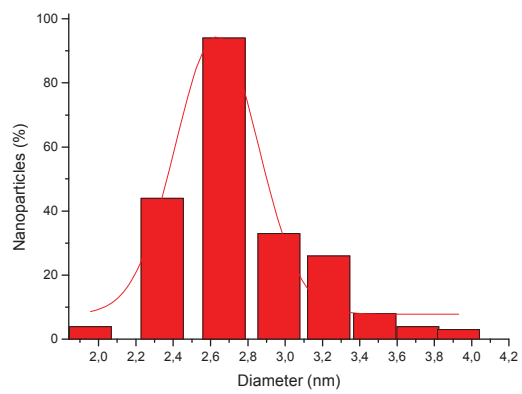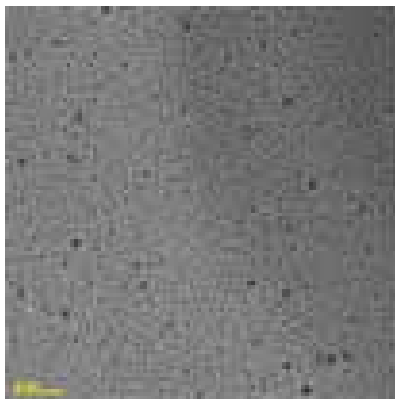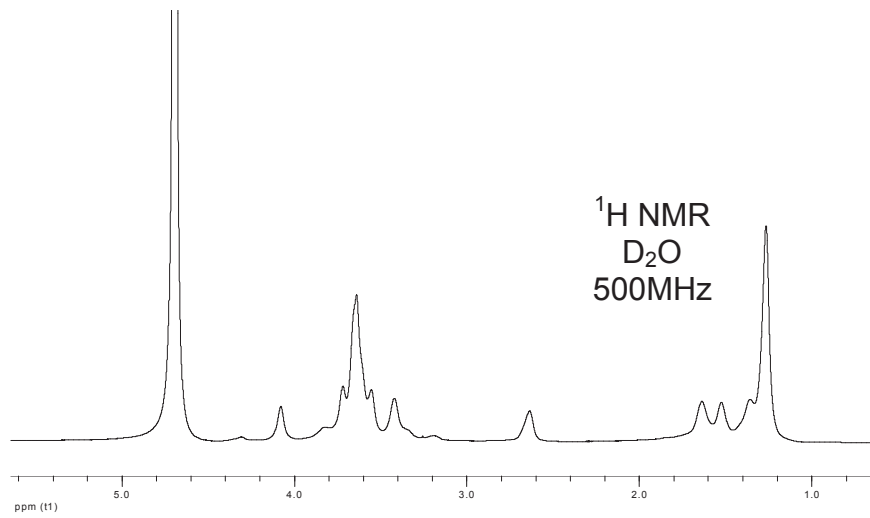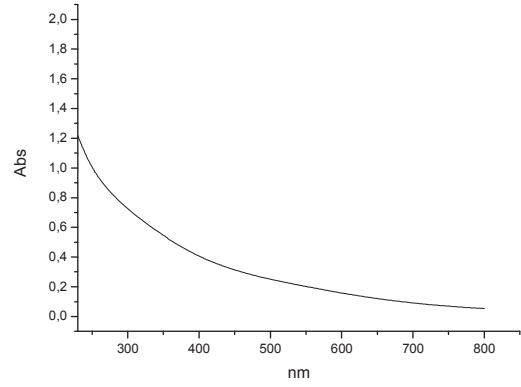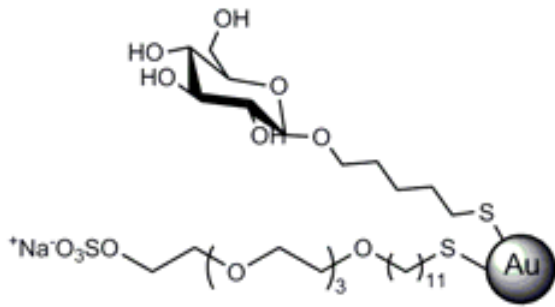
^{1}H NMR
D₂O
500MHz

(100%)⁻O₃SO-Au

$$(100\%)\ ^-O_3SO\text{-}Au$$

^{1}H NMR
D₂O
500MHz

(20%)⁻O₃SO-Au-FITC

^{1}H NMR
D$_2$O
500MHz

(50%)⁻O₃SO-Au-FITC

^{1}H NMR
D$_2$O
500MHz

(100%)⁻O₃SO-Au-FITC

^{1}H NMR
D$_2$O
500MHz

GNP

^{1}H NMR
D$_2$O
500MHz

GNP-Chol

^{1}H NMR
D$_2$O
500MHz

GNP-SO$_4$

NaO$_3$SO—(CH$_2$CH$_2$O)$_3$—...—S—
HOOC—CH$_2$—O—(CH$_2$CH$_2$O)$_3$—...—S—Au

^{1}H NMR
D$_2$O
500MHz

50 nm
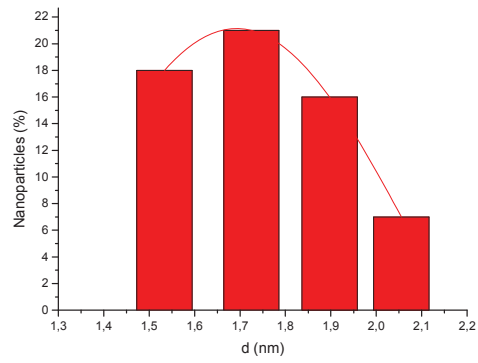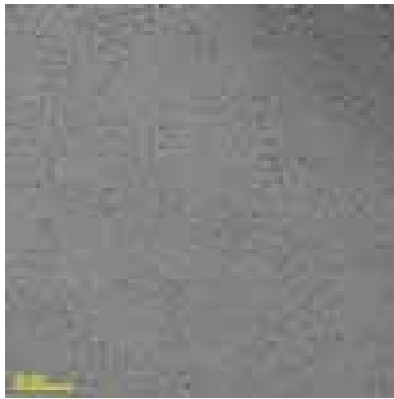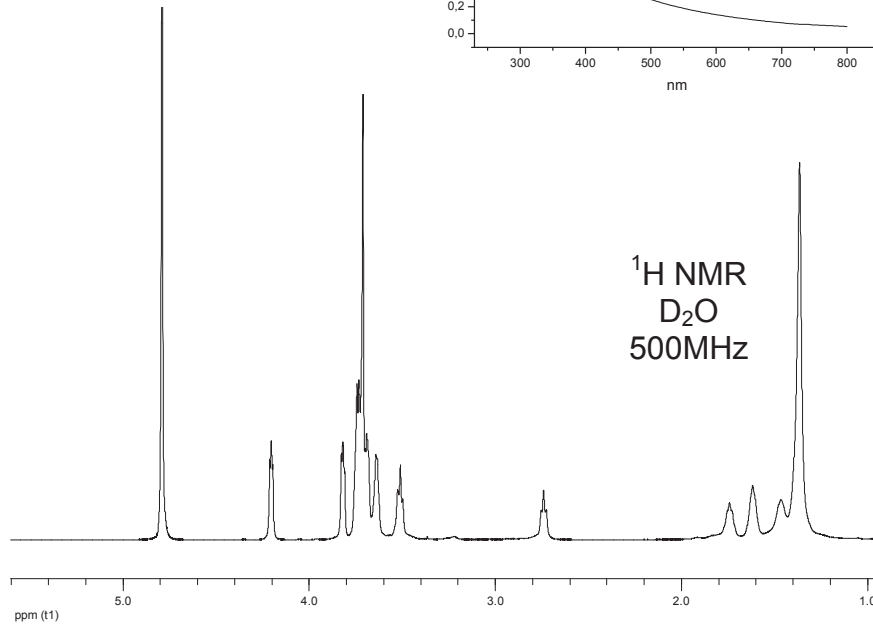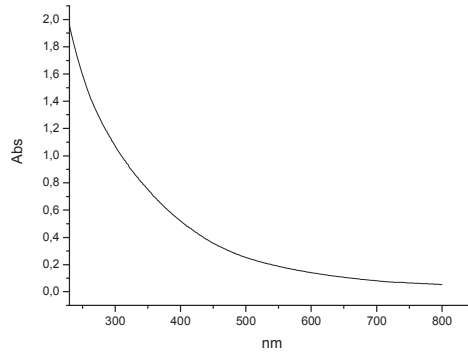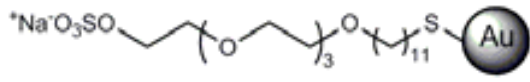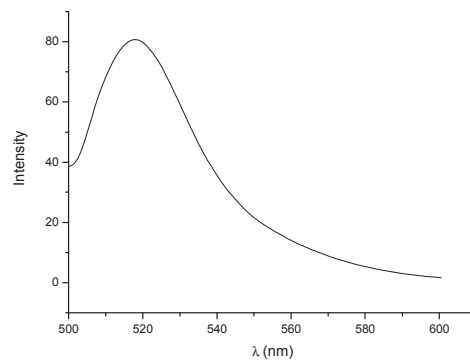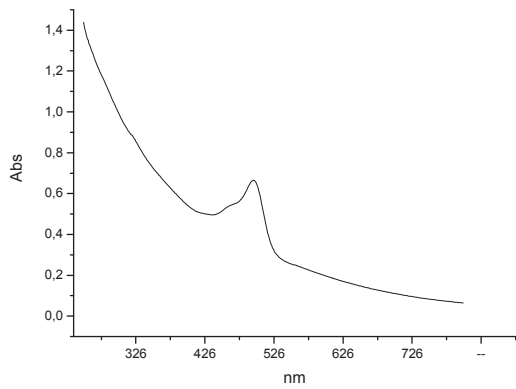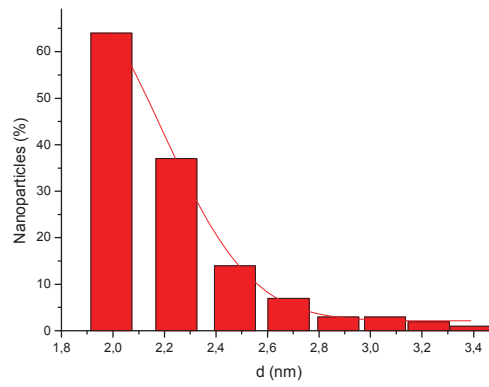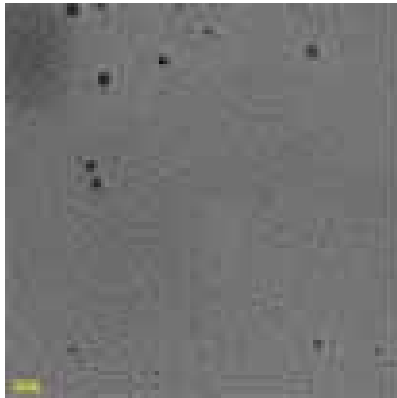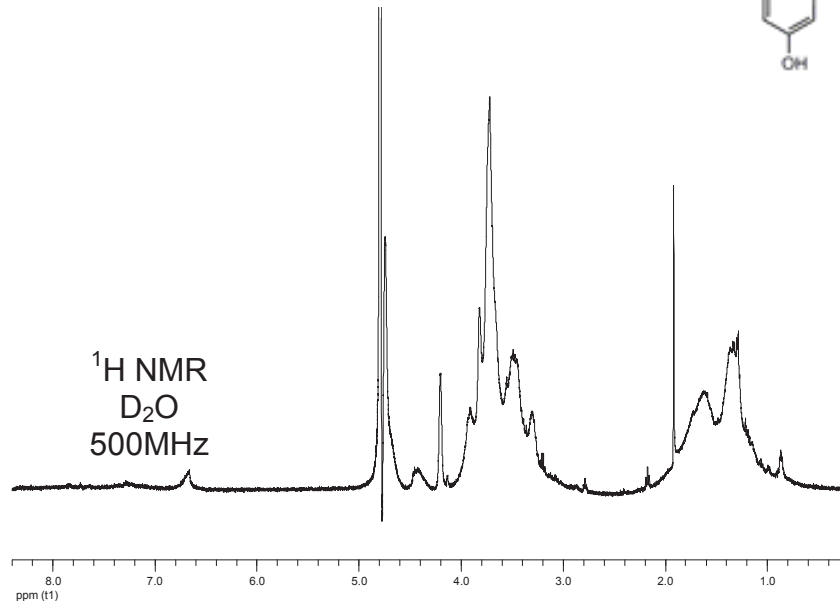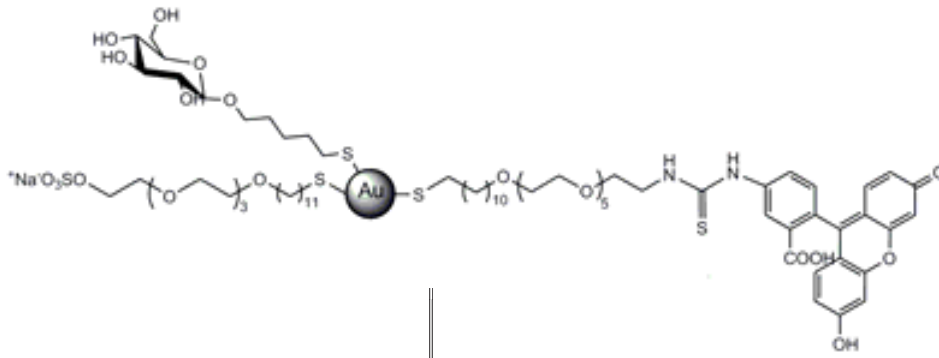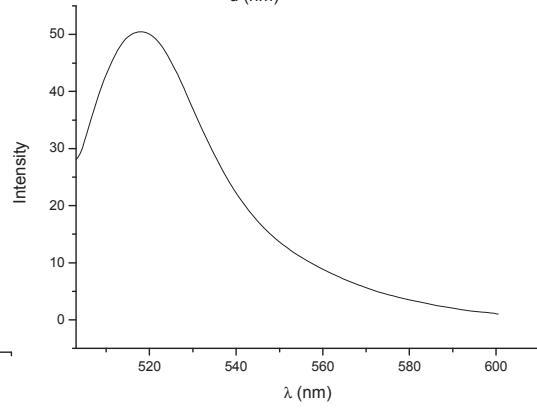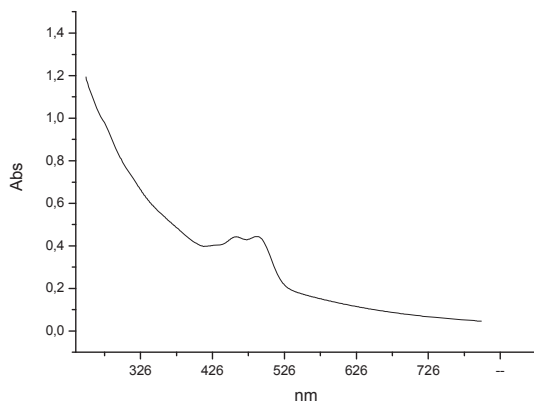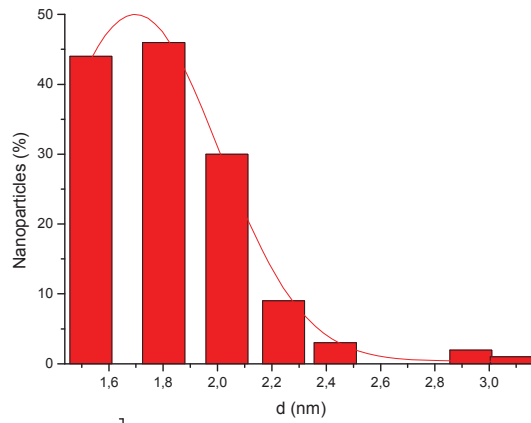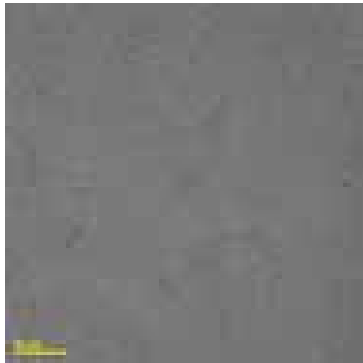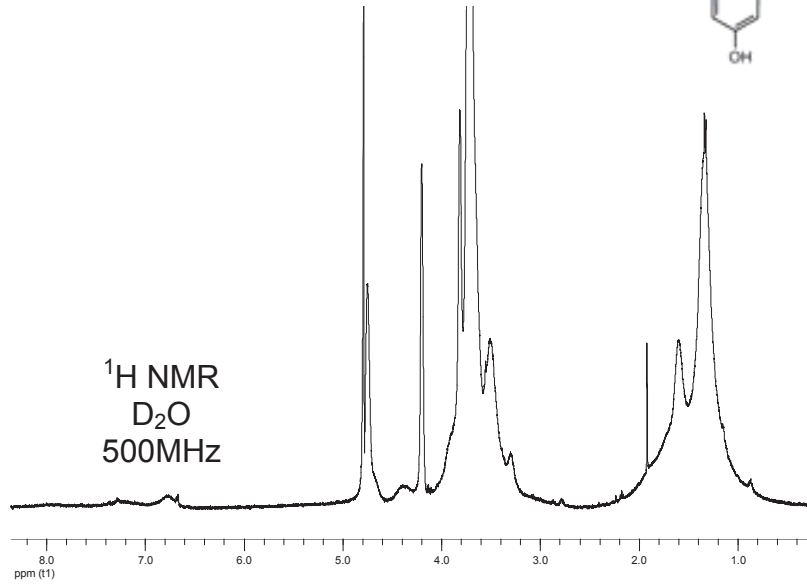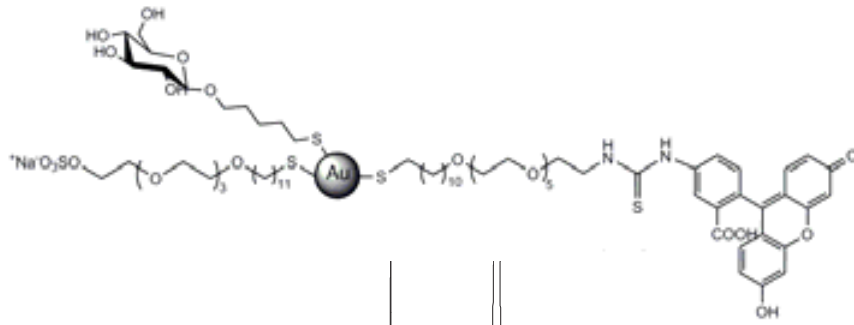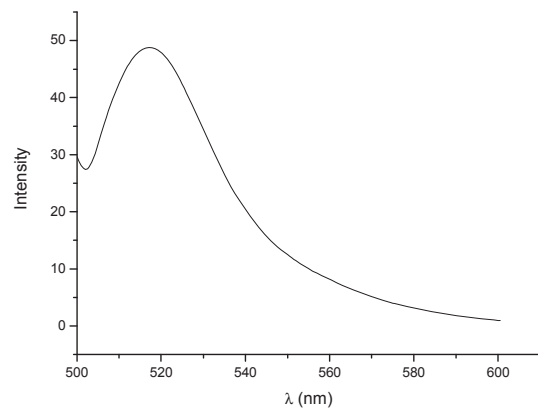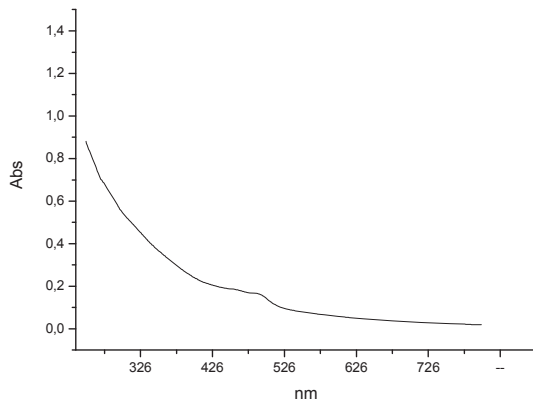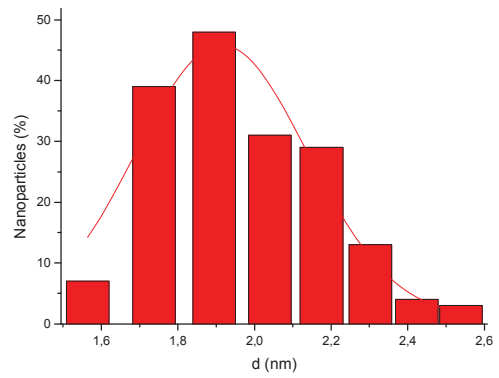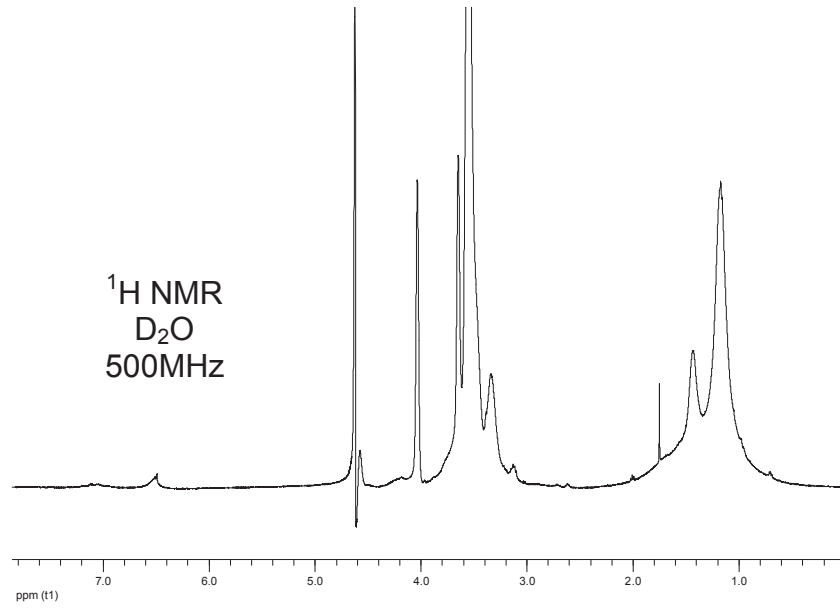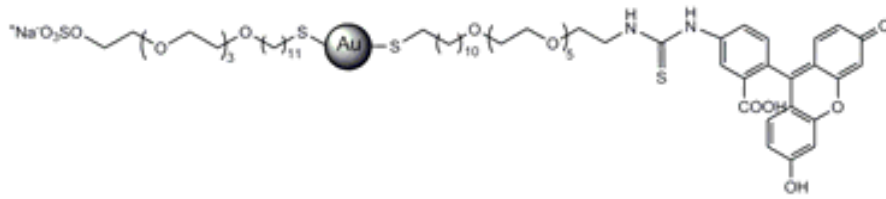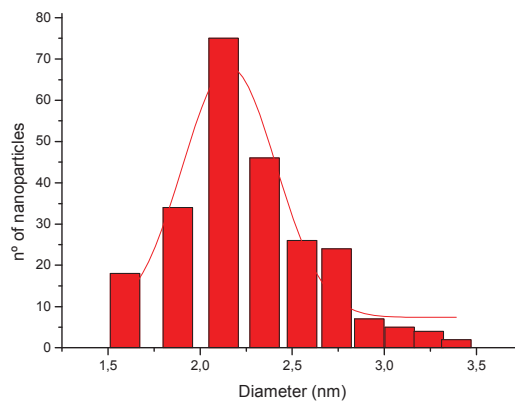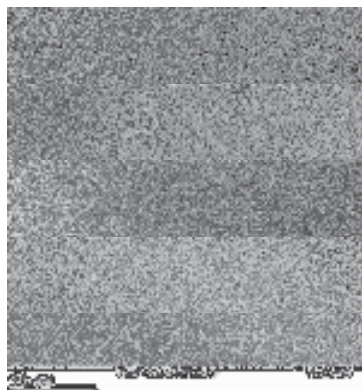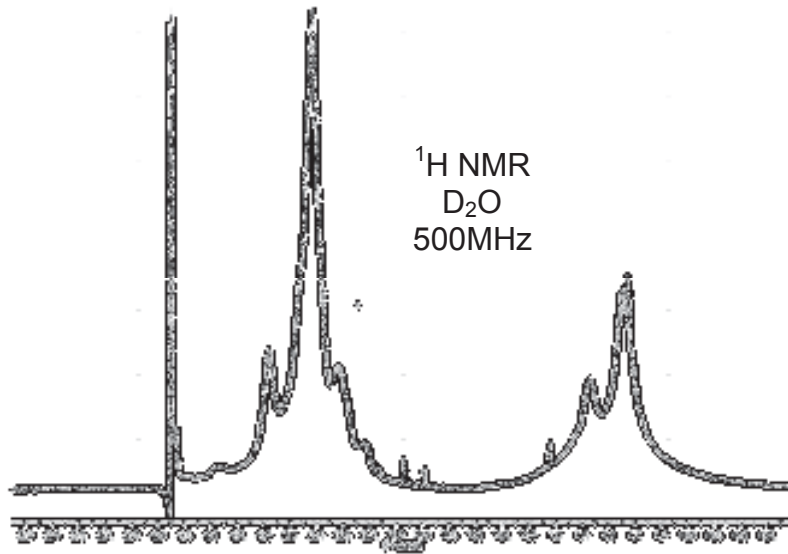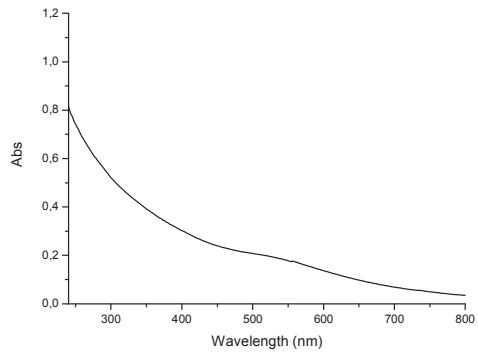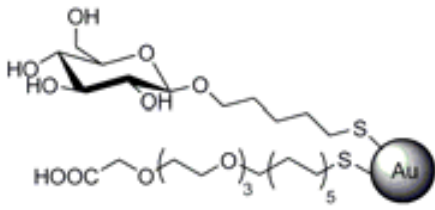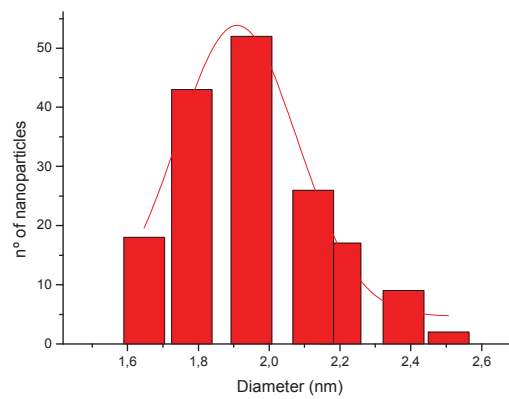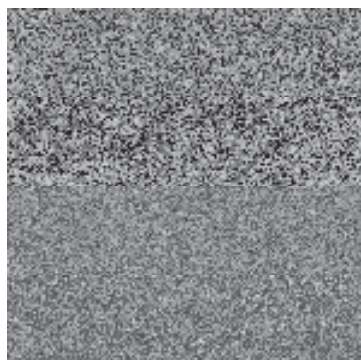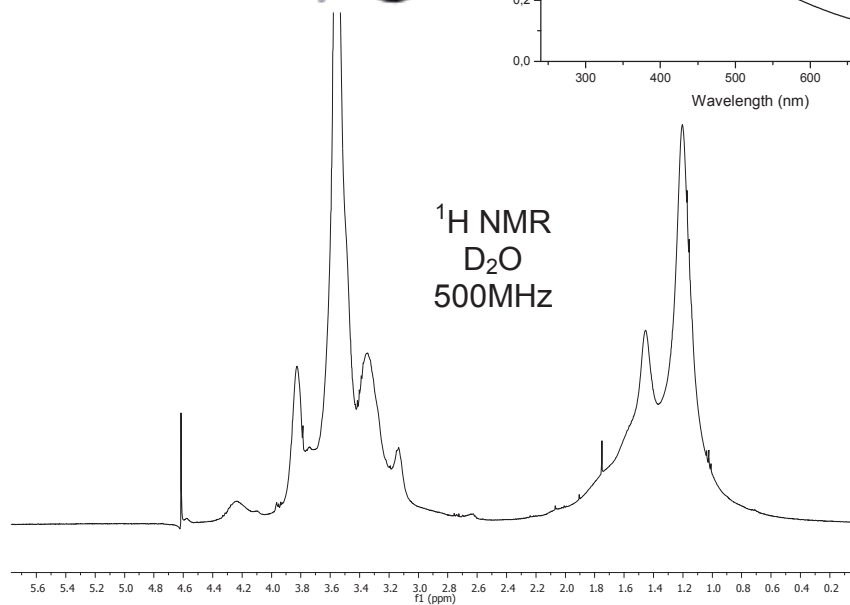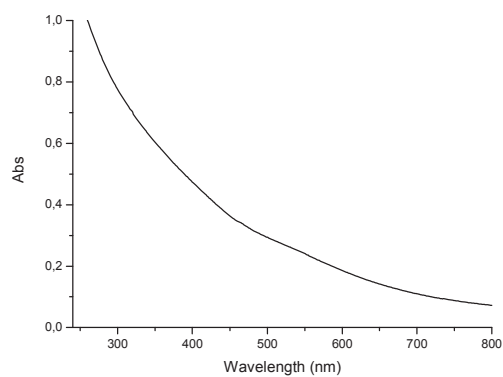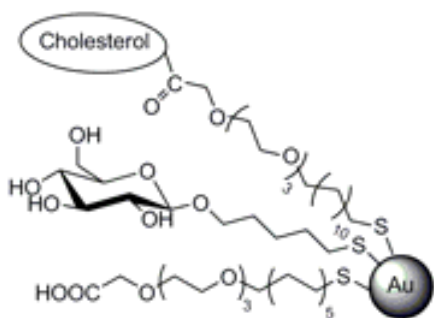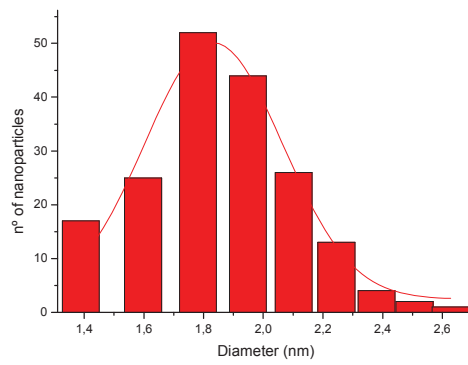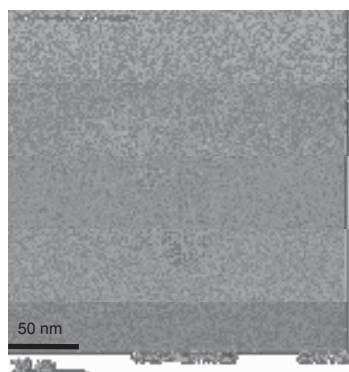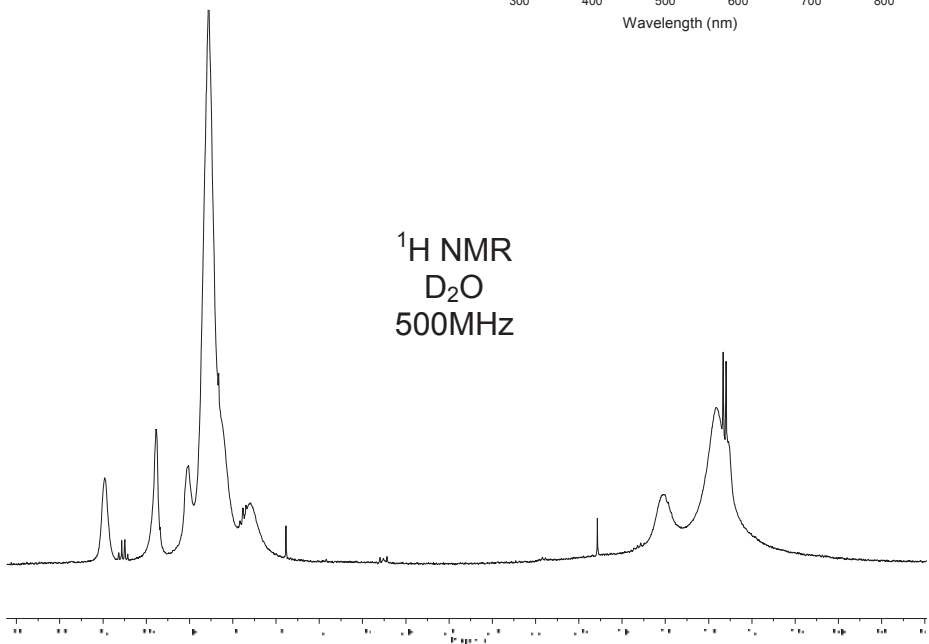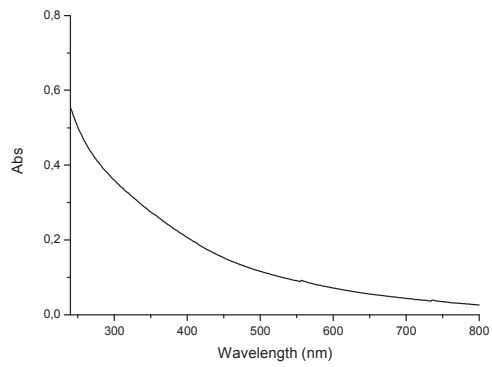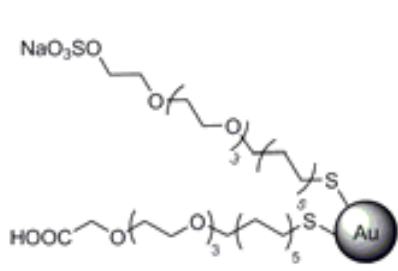
GNP1-FITC
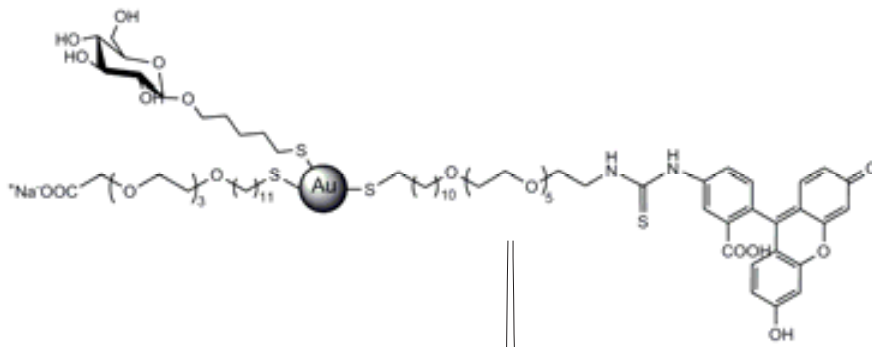
^{1}H NMR
D$_2$O
500MHz
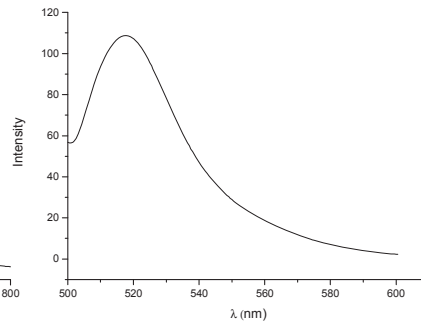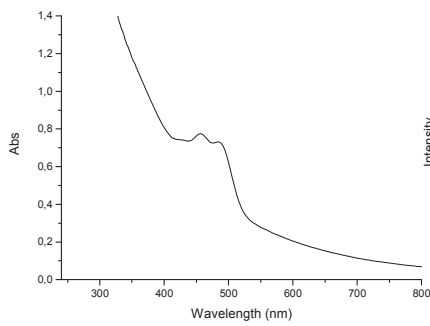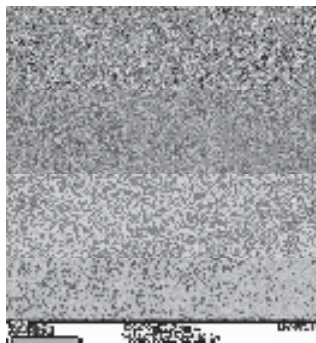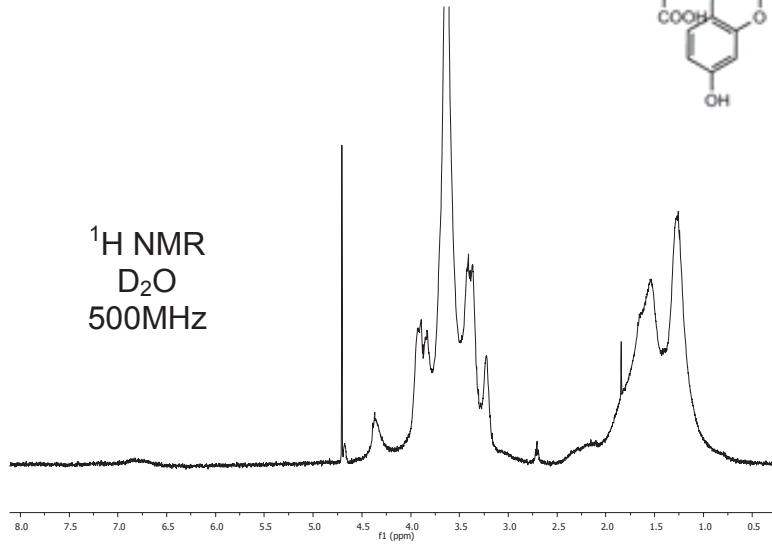
Paolo Di Gianvincenzo
Curriculum Vitae

Personal and contact details.

> Name   Paolo Di Gianvincenzo

> Date and Place of Birth   28 September, 1975, Milan, Italy.

> Nationality   Italian

> Address   Paseo de Francia 6, 1º
>   20012, Donostia-San Sebastián

> Telephone   Mobile   0034 691710507

> E-mail   ctrl_pol@hotmail.com

> Field of study   2306 (UNESCO code)

> Current position   Research technician/PhD student in "CICbiomaGUNE" research centre (Lab. of Glyconanotechnology, Paseo Miramón, 182; 20009 San Sebastián, SPAIN)

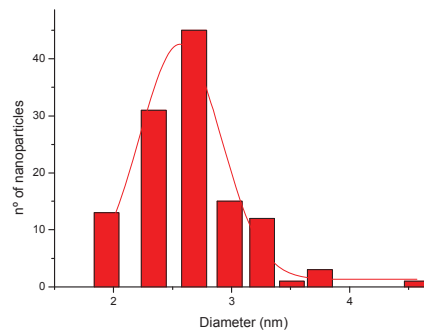> Present research area   Synthesis and characterization of gold glyconanoparticles (GNPs). Preparation of carbohydrate/peptide conjugated GNPs and binding study to target proteins. Application of GNPs as microbicides and/or vaccines candidates against HIV infection.

Scientific Education.

July 2009: Master degree in "Molecular biology and biomedicine", University of the Basque Country (UPV/EHU), Bilbao, under the supervision of Prof. Soledad Penades (Tutor: Felix Goñi).

June 2004: Postgraduated degree in "Synthetic Chemistry", at the University of Milan, Italy. Experimental thesis with title *"Synthesis of thiophene monomers for the preparation of block copolymers"* (Supervisor: Dr. A. Bolognesi).

March 2001: Degree in Chemistry at the University of University of Milan, (Italy). Experimental thesis in Organic Chemistry *"Biodegradation of polyclic aromatic hydrocarbons by Aspergillus terreus"* (Supervisors: Prof. B. M. Ranzi and Dr. A. Bernardi).

Research experience

2007-present. Research technician and PhD student in Biofunctional Nanomaterials Unit, CIC biomaGUNE (Donostia-San Sebastián). Research into the design and preparation of biofunctionalised gold glyconanoparticles as anti HIV-1 agents and vaccine, in the research group of Prof. Soledad Penadés.

2004-2007. Research grant in the Institute for Macromolecular Studies, ISMAC, CNR, Milan (Italy). Preparation and characterization of conducting polymers for optoelectronics, photonics and related devices. Work done in the laboratory of Dr. A. Bolognesi.

2002-2004. Research fellow in the Institute for Chemical and Biochemical Research, G. Ronzoni, Milan (Italy). Preparation and characterization of novel, sulfated oligosaccharides with antiangiogenic activity, in the group of Dr. A. Naggi.

1996-2002: In charge of test and evaluation of reliability of new kits for environmental toxicological analysis in Ecotox LDS srl, Pregnana Milanese (Italy).

Participation in funded research projects.

2010-present

Title:	Combined Highly Active Anti-Retroviral Microbicides (CHAARM)
Sponsor:	European Union under the 7th Framework Programme (FP7) for Research and Technological Development.
Centre	CIC biomaGUNE, San Sebastian, Spain
Duration	60 months
Main researcher	Prof. Soledad Penadés

2007-2009

Title:	European Microbicides Project (EMPRO)
Sponsor:	European Union under the 6th Framework Programme (FP6) for Research and Technological Development.
Centre	CIC biomaGUNE, San Sebastian, Spain
Duration	36 months
Main researcher	Prof. Soledad Penadés

2006-2007

Title:	Polymers and organic molecules for electronic and optoelectronic technology (Proteo)
Sponsor:	CARIPLO foundation
Centre	Institute for Macromolecular Studies, ISMAC, CNR, Milan (Italy)
Duration	24 months
Main researcher	Dr. A. Bolognesi

2004-2005

Title:	Teseo
Sponsor:	CARIPLO foundation
Centre	Institute for Macromolecular Studies, ISMAC, CNR, Milan (Italy)
Duration	24 months
Main researcher	Dr. A. Bolognesi

Congress

2012, Madrid, Spain. 26th International Carbohydrate Symposium. Poster title: Optical Activity of Gold (I) Glycoconjugate-Thiolate Complexes. G. Pourceau, P. Di Gianvincenzo and S. Penadés.

2011, Amsterdam, Netherlands. Frontiers of retrovirology. Poster title: Glyconanoparticles as a platform to multimerize peptides involved in HIV entry process. P. Di Gianvincenzo, B. Arnaiz, S. Ghezzi, E. Vicenzi, L. Martin and S. Penadés

2011, June, Salerno, Italy. 16th European Carbohydrate Symposium. Poster title: Gold Nanoparticles Coated with High Mannose-Type Oligosaccharides Mimic the Glycosylated Outer Domain of HIV. M. Marradi, P. Di Gianvincenzo, P. M. Enríquez-Navas, O. M. Martínez-Ávila, F. Chiodo, E. Yuste, J. Angulo and S. Penadés.

2010, March, Malaga, Spain. NanoSpain 2010. Poster title: Gold Nanoparticles Capped with Mannose Glycans Block HIV-1 gp120 Binding to Antibody 2G12 as Studied by Means of NMR and SPR Techniques. P. M. Enriquez Navas, P. Di Gianvincenzo, M. Marradi, O. Martínez-Ávila, J. Angulo and S. Penadés

2008, June, Barcelona, Spain. NanoBioEurope 2008. Poster title: SPR binding study between multivalent Manno-gold nanoparticles and the HIV-1 broadly neutralizing antibody 2G12. P. Di Gianvincenzo, M. Marradi, O. Martínez-Ávila and S. Penadés

2006, June, Arbatax (Tortoli), Italy. 5º Convegno Nazionale Materiali Molecolari Avanzati per fotonica ed elettronica. Talk title: Sintesi e caratterizzazione di copolimeri a blocchi per l'optoelettronica. P. Di Gianvincenzo, U. Giovanella and A. Bolognesi.

2005, September, Lisboa, Portugal. ICANS21 (21th International Conference on Amorphous and Nanocrystalline Materials). Poster title: The role of Al_2O_3 and SiO_2 gate dielectric surfaces on charge transport phenomena in P3HT based transistor. S. Ferrari, E. Peron, F. Persinotti, G. Tallarida, D. Natali, M. Caironi, L. Fumagalli, M. Sampietro, A. Angiulli, P, Di Gianvincenzo and A. Bolognesi.

2005, September, Naples, Italy. XVII Convegno Italiano di Scienza e Tecnologia delle macromolecole. Poster title: Poly(3-Alkylthiophene) as active layer in FET devices: Effect of side chain length. W. Porzio, S. Destri, M. Passini, A. Bolognesi, A. Angiulli, P. Di Gianvincenzo, D. Natali, M. Sampietro, M. Caironi and L. Fumagalli.

2005 June, Genoa, Italy. MMD Meeting (Matter, Materials and Devices). Poster title: Organic thin film transistor obtained using atomic layer Deposited Al_2O_3 as high-k dielectric. S. Ferrari, E. Peron, F. Persinotti, G. Scarel, D. Natali, M. Caironi, L. Fumagalli, M. Sampietro, A. Angiulli, P. Di Gianvincenzo and A. Bolognesi.

List of publications

1. G. Capotorti, P. Di Gianvincenzo, P. Cesti, A. Bernardi and G. Guglielmetti; *Biodegradation*, **2004**,*15*, 79-85 (Pyrene and benzo(a)pyrene Metabolism by an *Aspergillus Terreus* Strain Isolated from a Polycylic Aromatic Hydrocarbons Polluted Soil).

2. R. Cugola, U.Giovannella, P. Di Gianvincenzo, F. Bertini, M. Cattellani e S. Luzzati; *Thin Solid Films,* **2006**, *511-512*, 489-493 (Thermal characterization and annealing effects of polythiophene/fullerene photoactive layers for solar cells).

3. W. Porzio, S. Destri, M. Pasini, A. Bolognesi, A. Angiulli, P, Di Gianvincenzo, D. Natali, M. Sampietro, M. Caironi, L. Fumagalli, S. Ferrari, E. Peron, F. Persinotti; *Materials Science & Engineering C* , **2006**, *26*, 996-1001 (Oligo- and polymeric FET devices: Thiophene-based active materials and their interaction with different gate dielectrics).

4. A. Bolognesi, P. Di Gianvincenzo, U. Giovannella; Raniero Mendichi, Alberto Giacometti Schieroni *European Polymer Journal,* **2008**, *446*, 3, 793 (Polystyrene functionalised with EDOT oligomers).

5. L. Fumagalli, M. Binda, D. Natali, M. Sampietro, E. Salmoiraghi, P. Di Gianvincenzo, *Journal of Applied Physics,* **2008,** *104*, 84513 (Dependence of the mobility on charge carrier density and electric field in poly(3-hexylthiophene) based thin film transistors: effect of the molecular weight).

6. P. Di Gianvincenzo, M. Marradi, O. M. Martínez-Ávila, L. M. Bedoya, J. Alcamí, S. Penadés, *Bioorg. Med. Chem. Lett.*, **2010**, 20, 2718 (Gold nanoparticles capped with sulfate-ended ligands as anti-HIV agents).

7. M. Marradi, P. Di Gianvincenzo, P. M. Enriquez-Navas, O. M. Martínez-Ávila, F. Chiodo, E. Yuste, J. Angulo, and S. Penadés, *J. Mol. Biol.* **2011**, 410, 798 (Gold nanoparticles coated with oligomannosides of HIV-1 glycoprotein gp120 mimic the carbohydrate epitope of antibody 2G12).

8. P. Di Gianvincenzo, F. Chiodo, M. Marradi, and S. Penadés, *Methods in Enzi*mology. **2012**, 509, 21 (Gold *manno*-glyconanoparticles for intervening in HIV gp120 carbohydrate-mediated processes).

9. G. Pourceau, P. Di Gianvincenzo, L. del Valle-Carrandi, and S. Penadés, "On the Chiroptical properties of gold (I)-glycoconjugate-thiolate complexes" (manuscript in preparation).

10. P. Di Gianvincenzo, and S. Penadés, "Secondary structure of a gp120 V3 loop peptide on negative charged glyconanoparticles and study of their interaction" (manuscript in preparation).

Experimental skills

- Organic synthesis (including anhydrous and air-free conditions)
- Spectroscopy: UV-Vis absorption and emission, FT-IR, 1D- and 2D NMR, Circular dichroism.
- Purification techniques: flash chromatography, automated flash chromatography (Biotage SP4), HPLC.
- Bio-techniques: gel electrophoresis, ELISA, Surface Plasmon Resonance SPR (Biacore and ProteON),.
- Other: Isothermal titration calorimetry (ITC) and Z-potential.
- Computer skills: Microsoft Office, TopSpin Bruker, MesTrech/MestReNova software, , ChemDraw.

Languages

Italian   Native

Spanish   Fluent speaking and excellent writing and listening comprehension.

English   Fluent speaking and good writing and listening comprehension.